The Role of Mitochondria in Regulating the Senescence-Associated Secretory Phenotype during Cellular Senescence

James Edward Chapman

A thesis submitted for the degree of Doctor of Philosophy

Institute of Cellular Medicine

Faculty of Medicine

Newcastle University, UK

September 2019

Abstract

Senescent cells have been implicated in the ageing process and in the development of various age-related disorders. A key characteristic of senescent cells is the presence of dysfunctional mitochondria, which are crucial for the development of the SASP (Correia-Melo *et al.*, 2016). However, at this stage the underlying mechanisms by which mitochondria drive the SASP have not yet been completely elucidated.

In this thesis, I have discovered that mitochondria in senescent fibroblasts have an increased abundance of mitochondrial DNA (mtDNA) in the cytosol compared to young proliferating fibroblasts. Using super resolution microscopy, I discovered that a small subset of mitochondria in senescent cells display a recently identified phenomenon termed: limited mitochondrial outer membrane permeabilisation (miMOMP) (Ichim *et al.*, 2015). This subset of mitochondria show activation of pro-apoptotic BAX and BAK which cause a limited release of cytochrome c and caspase-dependent DNA damage in the absence of cell-death in senescent cells.

My data indicates that during senescence, miMOMP and the presence of BAX/BAK mitochondrial outer membrane pores allow the release of mtDNA to the cytosol. Consistent with a role for mitochondrial BAX/BAK and the release of mtDNA in cellular senescence, I found that both CRISPR/CAS9 deletion of BAX and BAK suppresses the SASP and the release of mtDNA during senescence, whilst maintaining the cell cycle arrest. Additionally, my data shows that cytosolic mtDNA binds to the DNA sensor cGAS, potentially activating the cGAS-STING pathway which has been previously implicated in SASP regulation (Dou *et al.*, 2017; Gluck *et al.*, 2017; Yang *et al.*, 2017). Moreover, genetic silencing of BAX/BAK *in vivo* prevents the upregulation of SASP related genes following the induction of senescence by irradiation. My data argue that the mitochondrial apoptotic pathway is a key SASP regulator.

Finally, I have demonstrated that pharmacological inhibitors of either BAX or cGAS lead to a robust suppression of the SASP, without impairing the cell cycle arrest. These small molecule inhibitors may therefore pose as potential candidates for senostatic therapies in offsetting the detrimental effects associated with the SASP.

Acknowledgements

First and foremost, I would like to thank my supervisors João Passos, Laura Greaves and Derek Mann for their continuous guidance and support throughout the PhD. Together they have strengthened my interest in science and furthered my development as a scientist.

Naturally, I would like to express my gratitude to my colleagues in the Passos lab. Not only have they shared their knowledge and helped me experimentally with my work but they have made my PhD an enjoyable experience. I'm sure collectively we will never forget the infamous Passos lab meetings on a Wednesday morning or the many lunch times which were spent discussing Portuguese cuisine. In particular, I would like to thank Jodie Birch who was always willing to help me in the early days and has continued to be a great friend and scientist. Stella Victorelli who has always been a lovely friend to have in the office and a constant source of inspiration for places to eat and things to do. Similarly, Anthony Lagnado has been an endless source of entertaining stories and a fun person to share an office with in my early days. It has been nice to share the journey with Hanna Salmonowicz who started at the same time as myself, together we have worked closely on many projects and I have thoroughly enjoyed her company and extravagant baking skills!

Throughout the PhD journey I have also shared many enjoyable memories and learnt a great deal from other students and members of the Campus for Ageing and Vitality. It has been wonderful to share a lab space with members of the Sanz and Korolchuk labs. As a consequences of this, I have shared many engaging scientific discussions and moments of comedy gold with Rhoda Stefanatos who has enlightened me with her exquisite knowledge of food. Along the way, Charlotte Graham has shared her excellent taste in music. I am also grateful to Elise Bennett without whom the lab would not run anywhere near as smoothly as it does, similarly, I am thankful to Lucy Sedlackova for sharing her mastery of Western Blots and Glyn Nelson for his exceptional knowledge of microscopy. In addition, I have shared many thought-provoking and stimulating lunch time conversations with Becca Reed, Filippo Scialo, Edward Fielder and George Kelly. It has also been a great learning experience and particularly enjoyable to share our lab meetings with Gavin Richardson, Emily Dookun and Anna Walaszczyk.

A small, but important note of dedication that I would like to make is to my ever faithful bike. Through rain, snow and the odd bit of sunshine it has never failed to transport me from Heaton

to the institute over the past 4 years, approximately 10,000 miles in total! For that I can only be truly grateful.

I would also like to give a special mention to Katie, who has supported me throughout the PhD. She has continuously pushed me to follow my heart and achieve things to the fullest of my potential. Similarly, it is important to acknowledge my family, as without them none of this would have been possible. Thank you.

Finally, I would like to extend my gratitude to the Medical Research Council and the Barbour Foundation for believing in and funding my work.

List of Abbreviations

53BP1	p53 Binding Protein 1
AAV	Adeno-associated Virus
ACMA	9-amino-6-chloro-2-methoxyacridine
AIF	Apoptosis Inducing Factor
AMPK	5' Adenosine Monophosphate-Activated Protein Kinase)
ATM	Ataxia-Telangiectasia Mutated
ATR	Ataxia Telangiectasia and Rad3-Related
BAD	BCL-2-associated Agonist of Cell Death
BAK	BCL-2 Homologous Antagonist Killer
BAX	BCL-2-associated X Protein
BCB	BAX Channel Blocker
BCL-2	B-Cell Lymphoma 2
BIP v5	BAX Inhibiting Peptide v5
CAD	Caspase Activated DNAse
CCF	Cytosolic Chromatin Fragment
CDKI	Cyclin-Dependent Kinase Inhibitors
cGAMP	Cyclic GMP-AMP
cGAS	Cyclic GMP-AMP Synthase
CHK1	Checkpoint-1
CHK2	Checkpoint-2
CRISPR	Clustered Regularly Interspaced Short Palindromic Repeats
DAMPs	Damage Associated Molecular Patterns
DAPI	4’,6-diamidino-2-phenylindole

DDR	DNA Damage Response
DRP1	Dynamin Related Protein 1
DSB	Double Stranded Break
ECAR	Extracellular Acidification Rate
ELISA	Enzyme Linked Immunosorbent Assay
FGF-2	Fibroblast Growth Factor 2
FIS1	Mitochondrial Fission Protein 1
FOXO4	Forkhead Box Protein 04
GM-CSF	Granulocyte-Macrophage Colony-Stimulating Factor
H3K9me3	Tri-methylation of Histone 3 Lysine 9
HSP	Heat Shock Protein
HUVEC	Human Umbilical Vein Endothelial Cell
IFN	Interferon
IKK	Inhibitor of Nuclear Factor Kappa-B Kinase
IL	Interleukin
INK-ATTAC	INK-Linked Apoptosis through Targeted Activation of Caspase
IP-10	IFN-γ inducible protein-10
IRF3	Interferon Regulatory Factor 3
MCP-1	Monocyte Chemoattractant Protein 1
miMOMP	Minority Mitochondrial Outer Membrane Permeabilisation
Mn-SOD	Manganese Super Oxide Dismutase
MOMP	Mitochondrial Outer Membrane Permeabilisation
MPTP	Mitochondrial Permeability Transition Pore
mtDNA	Mitochondrial DNA

MTORC1 Mammalian Target of Rapamycin Complex 1

NAC N-Acetyl-Cysteine

NADase CD38 NADase Cluster of Differentiation 38

NAMPT Nicotinamide Phosphoribosyltransferase

NLRP3 Nucleotide Binding Domain and Leucine-Rich Repeat Pyrin Domain Containing 3

OCR Oxygen Consumption Rate

P38 MAPK P38 Mitogen-Activated Protein Kinases

PAI2 Plasminogen-Activated Inhibitor-2

PARP Poly (ADP-ribose) Polymerase

PCNA Proliferating Cell Nuclear Antigen

PDGF-AA Platelet-Derived Growth Factor AA

PGC1-β Peroxisome Proliferator-Activated Receptor-Gamma Coactivator 1β

PI3Kδ Phosphatidyl 3-kinase-δ

PINK1 PTEN Induced Kinase 1

POT1 Protection of Telomeres 1

QC Quinacrine Dihydrochloride

ROS Reactive Oxygen Species

SAHF Senescence Associated Heterochromatin Foci

SASP Senescence Associated Secretory Phenotype

SA-β-Gal Senescence Associated β-Galactosidase

SIPS Stress-Induced Premature Senescence

SSB Single Strand Break

STING Stimulator of Interferon Genes

TAF Telomere Associated Foci

TBK1	TANK Binding Kinase 1
TERRA	Telomeric Repeat-containing RNA
TFAM	Transcription Factor A
TGF-β	Transforming Growth Factor-β
TIN2	TERF1-Interacting Nuclear Factor 2)
TNF	Tumour Necrosis Factor
TOM20	Outer Membrane Translocase Domain 20
TRF2	Telomeric Repeat Binding Factor 1
VEGF-A	Vascular Endothelial Growth Factor A
γH2AX	Phosphorylated Histone H2AX

Table of Contents

List of Tables

List of Figures

1. Chapter 1: Introduction

1.1. Cellular Senescence

Cellular senescence, which is generally characterized as an irreversible cell cycle arrest, has been defined as a classical hallmark of the ageing process. This phenomenon of persistent growth arrest was originally described by Hayflick and Moorhead in the 1960's when they observed that human fibroblasts in culture had a defined replicative limit (Hayflick, 1965). Although these cells remain indefinitely unable to divide, they are metabolically active and undergo several dramatic phenotypic changes. In the decades that have followed this initial observation, senescent cells have been implicated in a variety of key biological processes. Primarily, senescent cells avert the replication of cells that have sustained genomic damage, therefore they have a role in tumour suppression (Serrano *et al.*, 1997). Aside from tumour suppression, senescent cells function throughout the life course of an organism and have been demonstrated to engage in embryonic development and the wound healing process (Munoz-Espin *et al.*, 2013; Demaria *et al.*, 2014). These roles are of clear benefit to an organism, however, the accumulation of senescent cells, which has been shown to occur with age, has a detrimental effect and has been implicated as a driver of the ageing process and associated pathologies (Baker *et al.*, 2011; Xu *et al.*, 2015a; Baker *et al.*, 2016).

1.2. Mechanisms Responsible for the Induction of Senescence

Cellular senescence is a complex biological programme that occurs predominantly in response to cellular stresses and potentially functions as a mechanism to stop dysfunctional cells from proliferating. Its contribution to the ageing process has been postulated for a number of decades, therefore, extensive research has been undertaken to decipher the signalling pathways which promote and maintain the senescence response. Some of the main mechanisms involved in senescence are discussed in detail in this section.

1.2.1. DNA Damage

Throughout the life course of a cell it is constantly exposed to intra and extracellular stresses which can detrimentally affect the integrity of its genomic material (Menck and Munford, 2014). Extensive genomic damage has the capacity to inflict mutations on important sequences of DNA which can become tumorigenic and lead to aberrant proliferation. Therefore, cells are equipped with the ability to transiently arrest the cell cycle and subsequently repair DNA

damage through a variety of mechanisms. However, where cells have sustained severe or irreparable DNA damage they implement the senescence programme to prevent replication on a damaged template, and thus, prevent tumorigenesis (Campisi and d'Adda di Fagagna, 2007). It has been well established that DNA damage is an effective inducer of senescence, in particular double stranded breaks. A key source of molecular damage in senescent cells is associated with the production of ROS (reactive oxygen species). ROS are elevated in a number of models of senescence (replicative, stress-induced and oncogene induced) and have been shown to damage DNA directly, in the form of both single and double stranded DNA breaks (DSB) (Chen *et al.*, 1995b; Saretzki *et al.*, 2003; Passos *et al.*, 2010). Cells also can become senescent in response to hyperoxic conditions which promote intracellular damage via increased production of ROS (von Zglinicki *et al.*, 1995; Roper *et al.*, 2004). Interestingly, the role of ROS in senescence is multifaceted as they also play a role in maintaining a positive feedback loop whereby ROS induces short-lived DNA damage foci which maintain a constant stimulus. This continued initiation of damage engages the DNA damage response (DDR) and subsequently p21, which is a key senescence effector pathway for enforcing the cell cycle arrest and will be discussed later in this section (Passos *et al.*, 2010). Alongside ROS-mediated damage, a number of exogenous sources of DNA damage have been identified which can induce senescence; ionising radiation, UVB irradiation and chemotherapeutic agents such as actinomycin D, etoposide and doxorubicin (Di Leonardo *et al.*, 1994; Robles and Adami, 1998; Zhang *et al.*, 2002; Debacq-Chainiaux *et al.*, 2005). Cellular senescence that occurs in response to DNA damage is often referred to as stress-induced premature senescence (SIPS).

1.2.2. Telomere-dependent Senescence

Telomeres are protective fragments of DNA that are located at the end of linear chromosomes. They consist of a series of tandem 5'-TTAGGG-3' repeats which are stabilised by a protein complex collectively termed shelterin (de Lange, 2005). This complex consists of the proteins TRF1 and 2 (telomeric repeat binding factor 1 and 2) and POT1 (protection of telomeres 1), TIN2 (TERF1-interacting nuclear factor 2), tripeptidyl peptidase 1 and ras-related protein 1, together this complex forms a loop like structure termed the telomere loop (Griffith *et al.*, 1999; de Lange, 2005). This loop acts to prevent the ends of the functional DNA strands being identified as a DSB and thus being fused together by DNA repair mechanisms (Blackburn, 1991; Blackburn *et al.*, 2015). During DNA replication, DNA is lost during each division due to DNA polymerase being unable to completely synthesise the lagging strand of the DNA. This is referred to as the end replication problem and is responsible for the loss of between 50 and

200 base pairs following each replication. Therefore chromosomes are equipped with telomeres to ensure that functional DNA is not lost but rather the non-functional coding DNA repeats telomeres consist of, this process is referred to as telomere shortening (Olovnikov, 1971; Watson, 1972). In the context of senescence, this is of particular interest as it has been demonstrated that extensive rounds of replication lead to the induction of senescence (Hayflick, 1965). Since Hayflicks' initial observation of senescence, it has been firmly established that the phenomenon he described can be explained by telomere shortening, and is referred to as replicative senescence (Harley *et al.*, 1990). Mechanistically, extensive replication results in telomeres that become degraded to the point that their protective structure is impaired and they no longer perform their protective function, at this point, the DNA ends are recognised as a DSB and trigger a DDR which culminates in senescence (d'Adda di Fagagna *et al.*, 2003). Furthermore, it has been demonstrated experimentally that the overexpression of telomerase, an enzyme which extends telomeres, leads to an extension in lifespan of cultured human fibroblasts, thus highlighting a causal role of telomeres in driving the induction of senescence (Bodnar *et al.*, 1998).

Telomere shortening does not occur exclusively as a consequence of replication, there is now a body of evidence pinpointing the role of oxidative stress as a driver of telomere shortening. *In vitro*, it has been demonstrated that oxidative stress induced by mild hyperoxia increases the rate at which telomeres are shortened by approximately 5 fold, and this subsequently induces premature senescence which resembles replicative senescence (von Zglinicki *et al.*, 1995). To corroborate this, overexpression of antioxidants such as superoxide dismutase 3 reduces oxidative stress, slows the rate of telomere shortening and increases replicative lifespan in culture (Serra *et al.*, 2003). Consistently, the rate of telomere shortening can be slowed *in vitro* by other mediators that reduce mitochondrial-derived ROS such as the antioxidant MitoQ, nicotinamide as well as mild mitochondrial uncoupling (Saretzki *et al.*, 2003; Kang *et al.*, 2006; Passos *et al.*, 2007). Furthermore, dysfunctional mitochondria have been highlighted as contributing to telomere shortening (Liu *et al.*, 2002). This occurs predominantly due to the production of ROS, as treatment *in vitro* using a mitochondrial targeted antioxidant reduces telomere shortening and also leads to an extension of their replicative limit (Saretzki *et al.*, 2003). Similarly, the replicative capacity of fibroblasts can be extended by reducing ROS production following mild mitochondrial uncoupling, which has been shown to be as a consequence of reduced telomere shortening (Passos *et al.*, 2007). In addition to telomere shortening it has been highlighted that dysfunctional telomeres can be linked to the production

of inflammatory cytokines. Specifically it was discovered that exosomes containing noncoding telomere RNA transcripts [telomeric repeat-containing RNA (TERRA)] are secreted into the extracellular environment. These telomeric fragments can provoke the innate immune system to produce several cytokines which have been implicated in senescence (IL-6, TNF-α and IP-10) (Wang *et al.*, 2015). Therefore as both telomere dysfunction and the secretion of cytokines are features of senescence it is plausible that the two processes are interlinked, however, further study is required to confirm this.

It was mostly thought that the contribution of telomeres to senescence was solely associated with telomere shortening, however, recent work has demonstrated that during stress-induced senescence damage to telomeric regions occurs regardless of telomerase activity (Hewitt *et al.*, 2012). Furthermore, *in vivo* it has been found that in the liver and gut of mice telomere damage increases with age, irrespective of telomere length (Hewitt *et al.*, 2012; Jurk *et al.*, 2014). Similarly, telomere specific damage that occurs independently of length has been observed to increase in the hippocampal neurons and liver of baboons with increasing age (Fumagalli *et al.*, 2012). It has also been demonstrated that in cardiomyocytes length-independent damage which occurs at telomeres leads to a persistent DDR and subsequent activation of p16 and p21 to induce senescence (Anderson *et al.*, 2019).

Various studies have shown that DNA damage which occurs at telomeres (referred to as TAF; telomere associated foci) is less efficiently repaired compared to non-telomeric damage and in some cases is irreparable (Kruk *et al.*, 1995; Fumagalli *et al.*, 2012; Hewitt *et al.*, 2012). The lack of DNA damage repair is due to the TRF2/RAP1 mediated inhibition of DSB DNA repair, the purpose of this being to prevent telomere ends from being fused together. This occurs as TRF2/ ras-related protein 1 prevent non-homologous end joining of telomere ends by inhibiting the actions of DNA-Protein Kinase, furthermore this prevents the actions of ligase IV which also prevents end joining from occurring, together these mechanisms prevent the repair of double stranded telomeric damage (Bombarde *et al.*, 2010).

Furthermore, cells positive for TAF have been shown to accumulate with age in an assortment of organisms; mice, primates and humans (Herbig *et al.*, 2006; Hewitt *et al.*, 2012; Jurk *et al.*, 2014). Corroborating this, the presence of TAF positive cells has been noted to increase with age in an array of mouse tissues such as liver, intestine, lung, heart, muscle and bone (Hewitt *et al.*, 2012; Birch *et al.*, 2015; Farr *et al.*, 2017; Anderson *et al.*, 2019). With regards to senescence, it has been observed that the occurrence of TAF correlates with the presence of

other senescent markers in a number of diseases such as COPD, IPF and non-alcoholic liver disease (Birch *et al.*, 2015; Ogrodnik *et al.*, 2017; Schafer *et al.*, 2017). Finally, studies whereby senescent cells have been cleared using either the INK-ATTAC mouse model or senolytic treatment have demonstrated a reduction in the presence of TAF in hepatocytes, cardiomyocytes, neurons and the medial layer of the aorta (Roos *et al.*, 2016a; Ogrodnik *et al.*, 2017; Anderson *et al.*, 2019; Ogrodnik *et al.*, 2019). As such, the presence of TAF are considered a robust marker of senescent cells.

1.2.3. Oncogene-induced senescence

Oncogene-induced senescence was first described when it was observed that primary human and mouse cells could be permanently arrested in the G1 phase of the cell cycle following over expression of oncogenic ras (Serrano *et al.*, 1997). It has since been established that approximately 50 oncogenes have the capacity to induce senescence (Gorgoulis and Halazonetis, 2010). Oncogene-induced senescence has been observed both *in vitro* and *in vivo* to act as a potent tumour suppressor mechanism. Generally, in oncogene-induced senescence the senescence response is induced by launching a powerful DDR signal which occurs as a consequence of aberrant DNA hyper-replication, DNA replication stress and DNA DSBs (Bartkova *et al.*, 2006; Di Micco *et al.*, 2006). In models of oncogene-induced senescence where the DDR has been impaired, such as inhibition of the DDR component ATM (ataxia telangiectasia mutated) the induction of senescence is bypassed (Bartkova *et al.*, 2006). *In vivo*, this bypass is associated with an increased mean tumour size as well as exacerbated tumour invasiveness (Bartkova *et al.*, 2006). Another feature of oncogene-induced senescence is the derepression of INK4A and ARF (collectively referred to as CDKN2A locus). The CDKN2A locus codes for two key tumour suppressors p16 and ARF which are frequently upregulated and play an important role in enforcing the cell cycle arrest through a p53/p21 mediated mechanism (Kim and Sharpless, 2006). Typically, at the early stages of life the expression of the CDKN2A locus is very low, however, with advancing age it has been observed that expression is increased in an array of organs (Krishnamurthy *et al.*, 2004). Although at this stage, the cause of derepression is not well understood, current work has identified that the loss of the polycomb-group gene bmi-1 leads to derepression and consequently can regulates senescence induction (Jacobs *et al.*, 1999). More recently, it has been demonstrated during senescence that the polycomb group factor EZH2 (a histone H3 lysine-27 methyltransferase) is repressed (Ito *et al.*, 2018). This repression occurs from upstream WNT-MYC signalling and DNA damage

signalling through ATM. This is associated with a reduction in the presence of H3K27me3 marks which induces the expression of CDK2NA (Ito *et al.*, 2018).

1.3. Molecular Pathways which Regulate Cellular Senescence

During the induction of cellular senescence, cells typically respond to cellular stresses by mounting a DDR. The DDR subsequently feeds into activation of the p16-pRb and p53-p21 pathways, these two signalling pathways are crucial for initiating and maintaining the cell cycle arrest. Both the p16-Rb and p53-p21 pathways can induce senescence independently, generally, whether one or both pathways are engaged depends on the stimulus and cell type.

1.3.1. The DNA Damage Response

The DDR is a key feature in replicative, telomere-induced, stress-induced and oncogene-induced senescence (d'Adda di Fagagna *et al.*, 2003; Campisi and d'Adda di Fagagna, 2007; Hewitt *et al.*, 2012). Classically, the DDR responds to single stranded breaks (SSB) and DSBs of the DNA backbone, whereby it acts to halt cell cycle progression and recruit DNA repair machinery to allow repair of the DNA damage. If the damage is not severe then the DDR and subsequent cell cycle arrest is transient, however if the damage is severe or irreparable then a persistent DDR induces either senescence or apoptosis (d'Adda di Fagagna, 2008). It is clear that the nature and severity of the damage plays a role in dictating the decision between senescence and apoptosis, however, at this stage our understanding of the factors that determine cell fate are incompletely understood.

Following the induction of DNA damage, there are two key complexes which recognise the damage depending on type of lesion. SSBs such as those induced following replication stress or UV are detected by a DNA repair complex which consists of RAD17 and the replication proteins A and C (2-5) (Weiss *et al.*, 2002). Together, these proteins recruit a further complex to the site of damage, the 911 trimer complex which consists of RAD9, HUS1 and RAD1 (Cortez *et al.*, 2001; Weiss *et al.*, 2002). This complex triggers the recruitment and activation of ATR (Ataxia telangiectasia and Rad3-related) (Cortez *et al.*, 2001).

The second complex which predominantly responds to DSBs is the PARP-MRN complex (Poly (ADP Ribose) polymerase - MRE11-RAD50-NBS1 proteins), this complex locates at the damaged site and recruits ATM (Falck *et al.*, 2005). Recruitment of ATM triggers its auto phosphorylation, following activation ATM is also responsible for phosphorylating the histone

H2AX to γH2AX which also locates itself to the damaged site. γH2AX acts to further activate ATM and thus amplify its signal (Rogakou *et al.*, 1999; Falck *et al.*, 2005).

The activation of ATM (to DSBs) and ATR (to SSBs) following the recognition of damage by the aforementioned complexes leads to a cascade activation of further DDR components (Marechal and Zou, 2013). The predominant function being to recruit appropriate proteins which transduce the damage signal to allow optimal repair of the damage. This is facilitated by a number of mediators such as mediator of DNA damage checkpoint protein-1, 53BP-1, breast cancer type-1 susceptibility 1 protein and claspin (Huyen *et al.*, 2004). These proteins feed into and phosphorylate the proteins checkpoint-1 and 2 (CHK1, CHK2) following successive stimulation by either ATM or ATR. Following activation, CHK1 and CHK2 can then initiate the cell cycle arrest by acting on the effector proteins such as p53 and CDC25 (cell-division cycle 25) (d'Adda di Fagagna, 2008). CDC25A and CDC25C are phosphatases which regulate cell cycle progression through G1 to the S phase via activation of cyclin dependent kinases, however, when they are phosphorylated by CHK1 and CHK2 they become degraded and the cell cycle is halted (Mailand *et al.*, 2000). Similarly, activation of p53 by CHK2 and ATM instigates transcription of the cell cycle regulator, p21, which subsequently blocks progression of the cell cycle (Di Leonardo *et al.*, 1994; d'Adda di Fagagna, 2008).

1.3.2. The p53-p21 Signalling Axis

p53 is often referred to as the "guardian of the genome" due to its prominent role in tumour suppression. p53 is a transcription factor which responds to cellular stresses. Once active, it has the capacity to induce either a transient arrest, senescence or apoptosis depending on the nature of the stress (Murray-Zmijewski *et al.*, 2008). In healthy proliferating cells, p53 is negatively regulated by the E3 ubiquitin protein ligase human double minute 2 (HDM2) which inhibits its activation as well as targeting it for degradation. As such p53 activity is constitutively low in the absence of stress (Zilfou and Lowe, 2009). However in states of cellular stress, a number of DDR components such as ATM, ATR, CHK1 and CHK2 can phosphorylate p53, this prevents HDM2 mediated p53 degradation and consequently leads to p53 activation (Banin *et al.*, 1998; Tibbetts *et al.*, 1999; Chehab *et al.*, 2000). In the context of senescence, a key target gene of p53 is the cyclin-dependent kinase inhibitor (CDKI) p21. p21 prevents progression of the cell cycle by inhibiting cyclin dependent kinases and PCNA (proliferating cell nuclear antigen) and its upregulation is generally a key feature of senescent cells (Xiong *et al.*, 1993; Waga *et al.*, 1994; Herbig *et al.*, 2004; Passos *et al.*, 2010). It is important to note that p21 can be upregulated in non-senescent cells to transiently arrest progression of the cell cycle. For

example, it may be upregulated to allow for DNA repair to occur (Karimian *et al.*, 2016). Mechanistically, it has been demonstrated that genetic removal of p21 in mouse embryonic fibroblasts and human fibroblasts prevents the senescence response (Brugarolas *et al.*, 1995; Brown *et al.*, 1997). Similarly, when the p53-p21 axis is impaired by knockout of CHK2 the replicative capacity of human fibroblasts is increased following the failure of CHK2 to activate p53 and subsequently p21 (Gire *et al.*, 2004). Furthermore, *in vivo* when p21 is knocked out, senescence no longer occurs during the embryonic development process (Munoz-Espin *et al.*, 2013). Collectively, these studies implicate the importance of the p53-p21 axis in promoting the cell cycle arrest that is characteristic of cellular senescence.

1.3.3. The p16-pRB Signalling Axis

During the induction of senescence, the p53-p21 axis is generally the primary signalling pathway that is activated following a DDR. However, these stimuli can also engage the p16-pRb pathway independently of p53. Like p21, p16 is a CDKI which is located in the perinuclear cytoplasm. Following the activation of p16 it translocates to the nucleus where it halts cell cycle progression by binding to CDK4/5 and 6 which in turn prevents phosphorylation of the tumour suppressor gene retinoblastoma (Rb). Consequently, Rb is maintained in a state of hypophosphorylation and therefore remains associated with the transcription factor E2F1 in the cytoplasm, this prevents transcription of E2F1 target genes which are responsible for promoting cell cycle progression (Rayess *et al.*, 2012). Interestingly, the point at which the p16-pRB pathway is engaged varies between cell types. For example, in fibroblasts the activation of the p16-pRb pathway occurs secondary to the p53-p21 pathway, whereas epithelial cells have been demonstrated to become senescent through p16-pRb rather than p53-21 (Stein *et al.*, 1999; Jacobs and de Lange, 2004). The importance of p16 is highlighted by a number of studies which have determined that p16 expression is enhanced in cells induced to senesce following a number of stimuli, such as oxidative damage, irradiation, telomere dysfunction and activation of oncogenic ras (Serrano *et al.*, 1997; Meng *et al.*, 2003; Chen *et al.*, 2004a; Jacobs and de Lange, 2004). Furthermore, it has been observed that p16 positive cells accumulate in an array of tissues with advancing age (Krishnamurthy *et al.*, 2004; Waaijer *et al.*, 2012). Following the induction of senescence, levels of p16 are relatively low, however with time expression increases, conversely p21 expression peaks immediately following the induction of senescence and subsequently decreases with time (Alcorta *et al.*, 1996; Stein *et al.*, 1999). Following these observations, it has been postulated that that the p16-pRB functions as a secondary barrier to prevent cell cycle progression in human fibroblasts. To support this idea it has been

demonstrated that cells which express low levels of p16 during senescence can resume proliferation when p53 is inactivated, whereas, those which express high levels of p16 however do not resume replication when p53 is inactivated (Beausejour *et al.*, 2003).

The underlying mechanisms which lead to p16 activation are not completely elucidated. However, the p38 mitogenic-activated protein kinase (MAPK) can respond to signals from the DDR, and has been shown to be able to stimulate both the p53-p21 and p16-pRb signalling pathways (Debacq-Chainiaux *et al.*, 2010; Spallarossa *et al.*, 2010). Furthermore, p38MAPK has multifaceted roles in senescence and has been described as an important regulator of the DDR by promoting ROS production which stabilises the DDR by inducing short-term DNA damage foci (Passos *et al.*, 2010). P38MAPK has also been implicated as a regulator of the inflammatory profile exhibited by senescent cells (Freund *et al.*, 2011).

Interestingly, the role of tumour suppressors in the senescence inducing pathways varies between mice and human cells. It has been demonstrated in humans that activation of a DDR following telomere attrition or DNA damage leads to activation of the p53/p21 axis which inhibits CDK2-cycin E as well as CDK4/6-cyclinD which directly inhibits Rb to prevent cell cycle progression. In humans, Rb can also be inhibited by CDK4/6-cyclin D following the activation of p16. Thus the p53/21 and p16 pathways cooperate to provide two signalling networks which feed into Rb (Itahana *et al.*, 2004). It has been demonstrated that knockout of p21 or p53 can result in senescence bypass (Brown *et al.*, 1997; Wei and Sedivy, 1999), whereas p16 knockout alone cannot as Rb is still inhibited by p21 (Brookes *et al.*, 2002). Dual knockout of both p16 and p21 leads to a bypass of replicative senescence in human fibroblasts (Wei *et al.*, 2003b). As both pathways act downstream on Rb, studies have demonstrated that in human fibroblasts the senescence response can be bypassed by genetic knockout of Rb (Wei *et al.*, 2003a). In MEFs disruption of Rb genes is not sufficient to affect the senescence response (Sage *et al.*, 2000). This is because in murine cells, the p53/p21 axis does not lead to inhibition of Rb, only the p16 pathway does via CDK4/6-cyclin D. Therefore p53/p21 and p16 promote the cell cycle arrest by independent mechanisms (Itahana *et al.*, 2004). As such, in MEFs lacking p21 there is no bypass of senescence as observed in human fibroblasts (Brown *et al.*, 1997; Pantoja and Serrano, 1999). However, in MEFs it has been demonstrated that if one of the senescence modulating pathways is impaired (either the p53/p21 or the p16-Rb axis) then cells which have become senescent frequently become spontaneously immortalised following sustained culture (Dirac and Bernards, 2003; Odell *et al.*, 2010). As such the activity of both pathways is important to maintain an irreversible cell cycle arrest in mouse cells.

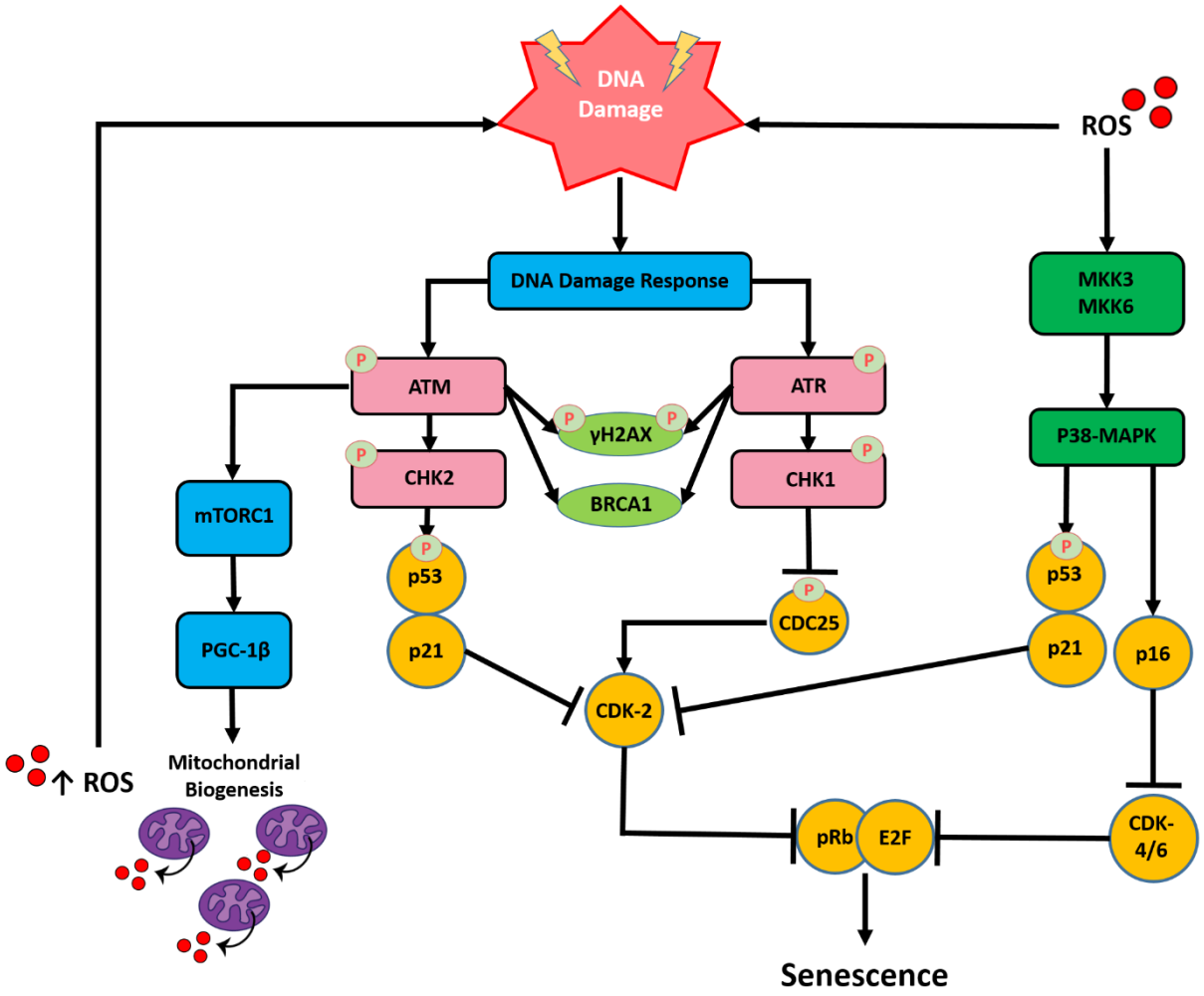

Figure 1.1 – Schematic overview of the DDR and signalling axis involved mediating senescence induction in human fibroblasts.

DNA damage occurs in response to a number of stimuli such as telomere shortening, genotoxic stress and ROS, this damage triggers a DDR. Damage to the genome promotes both ATM and ATR to be phosphorylated and subsequently activated, this leads to recruitment and phosphorylation of γH2AX at the site of DNA damage. ATM also triggers induction of senescence by CHK2 mediated phosphorylation of p53, which in turn inhibits CDK-2 and subsequently blocks pRb activation which promotes the cell cycle arrest. pRb activation is also blocked by activation of p16 which inhibits CDK-4 and CDK-6. Activation of p16 occurs in response to ROS mediated activation of the MAPK/ p38MAPK. ATM also promotes mitochondrial biogenesis through MTORC1 and PGC1-β. This leads to an exacerbated production of ROS which in turn can maintain the DDR by inducing short-lived foci.

1.4. The Senescent Phenotype

Senescent cells can be characterised phenotypically by a number of morphological changes. In addition to this they differ metabolically, as such, they display an array of fundamental changes with regards to gene expression, mitochondrial function and secretory profile. Collectively, these features are described as the senescent phenotype and will be discussed in depth in the forthcoming sections.

1.4.1. Morphological Changes

From a morphological perspective, senescent cells in culture can be clearly distinguished from their proliferating counterparts. Senescent cells undergo a vast increase in cellular volume, coupled with a flattening of both the nuclear region and cytoplasm, which is often observed to be vacuolised (Bayreuther *et al.*, 1988). Frequently, this nuclear region may be multi-nucleated and tends to have an associated loss of the nuclear envelope (Mehta *et al.*, 2007). Interestingly, *in vivo*, the morphology of senescent cells is generally not as distorted and reflects that of the tissue architecture.(Muñoz-Espín and Serrano, 2014).

1.4.2. Growth Arrest

The primary feature of senescence is the irreversible cell cycle arrest. Typically, analysis of senescent human fibroblasts and cells derived from mice reveals DNA content that is representative of the G1 phase of the cell cycle (Di Leonardo *et al.*, 1994; Herbig *et al.*, 2004). However, it is important to note that cells can undergo senescence at other stages of the cell cycle. For example, senescence that occurs in response to activation of oncogenes can arise in the G2 phase (Zhu *et al.*, 1998). Recent work has revealed that senescence is not restricted to mitotic cells. It has been discovered that post-mitotic and terminally differentiated cells such as cardiomyocytes and neurons which do not progress through the cell cycle can become senescent (Jurk *et al.*, 2012; Farr *et al.*, 2016; Anderson *et al.*, 2019). This abortion of cell cycle progression is facilitated by the upregulation of genes associated with the cell cycle arrest, crucially the CDKIs p16 and p21. The mechanisms responsible for the induction and maintenance of the growth arrest will be discussed in detail later.

1.4.3. Alterations in Gene Expression

In order for the senescent cells to sustain a stable cell cycle arrest it is critical that associated gene expression is altered to maintain this state. Therefore, analysis of genes that stimulate proliferation such as c-FOS, cyclin A, cyclin B and PCNA, are all repressed during the senescence programme (Seshadri and Campisi, 1990; Stein *et al.*, 1991; Pang and Chen, 1994).

To complement the repression of these genes, the expression of genes responsible for regulating cell cycle inhibition are upregulated. It has been well determined that the CDKIs p21 and p16 are responsible for the induction of the cell cycle arrest (Alcorta *et al.*, 1996; Herbig *et al.*, 2004). Furthermore, senescent cells display a secretory phenotype that consists primarily of inflammatory mediators. This can in part be attributed to enhanced expression of genes responsible for encoding secreted proteins that are observed as part of this inflammation, namely; extracellular matrix degrading proteins, growth factors and a number of pro-inflammatory cytokines (Shelton *et al.*, 1999).

1.4.4. Epigenetic Alterations

Senescent cells display a heterogeneous phenotype which can include a number of dynamic alterations to chromatin structure and the epigenetic landscape. The transcription of genes can be regulated by these processes. For example, genes can be silenced when chromatin is coiled and compacted into a heterochromatin state or they can be activated when chromatin exists in a loosely coiled state (euchromatin) which allows access of the transcriptional machinery. Condensed regions of heterochromatin can be identified by markers such as methylation of 5-methylcytosine in CpG dinucleotides and histone H3 on lysine 9 and 27 (H3K9me3 and H3K9me27), similarly, they can be identified by hypoacetylation of lysine on histones H3 and H4 (Grewal and Jia, 2007; Trojer and Reinberg, 2007). With regards to senescence, it has been observed that some senescent cell types display condensed regions of heterochromatin which are referred to as senescence-associated heterochromatin foci (SAHF) which can be recognised by punctate regions of DAPI staining (Narita *et al.*, 2003). Moreover, SAHF were found to be associated with recruitment of RB which is responsible for repressing E2F genes which are known to promote cell cycle progression, it was subsequently demonstrated that inactivation of RB family proteins /silencing of p16 prevented SAHF formation (Narita *et al.*, 2003). High mobility group A proteins have also been demonstrated to be integral in the development and structure of SAHF where they contribute to repression of cell cycle genes, in addition, HMGA proteins were shown to cooperate with p16 to stably repress E2F target genes in senescent cells, indeed silencing of HMGA2 led to a bypass of senescence (Narita *et al.*, 2006). Further study of SAHF has revealed that they are enriched in the transcriptionally repressive histone macroH2A, it has also been found that the formation of macroH2A containing SAHF is dependent on a histone complex consisting of HIRA and ASF1a which are known to promote the formation of transcriptionally inactive heterochromatin (Zhang *et al.*, 2005; Ye *et al.*, 2007). The E3 ubiquitin ligase adaptor SPOP has been demonstrated to be upregulated during

senescence and can promote senescence, furthermore, it has been implicated as a potential upstream regulator of SAHF development (Zhu *et al.*, 2015a). Recent work has unveiled that modifications in heterochromatin structure during senescence are underpinned by changes to the nuclear lamina which are associated with chromatin positioning and transcriptional regulation (Sadaie *et al.*, 2013; Chandra *et al.*, 2015). Specifically, it has been found that Lamin B1 a protein responsible for the structure underneath the inner nuclear membrane is downregulated in senescent cells as a consequence of autophagy mediated degradation (Freund *et al.*, 2012; Ivanov *et al.*, 2013; Sadaie *et al.*, 2013; Dou *et al.*, 2015). It has been shown that nuclear regions where Lamin B1 is depleted are associated with H3K9me3, corroborating this, the silencing of Lamin B1 promoted development of SAHF by instigating spatial relocalisation of perinuclear H3K9me3-positive heterochromatin (Sadaie *et al.*, 2013).

Collectively, these studies have highlighted that during senescence the formation of heterochromatin foci is a complex process which is associated with silencing of genes associated with the cell cycle which ultimately acts to reinforce a stable arrest of cellular proliferation.

1.4.5. Resistance to Apoptosis

Senescent cells have the ability to remain metabolically active despite no longer having the capacity to divide. Apoptosis is a process whereby cells are eliminated in a controlled manner. Senescence and apoptosis both occur in response to cellular stress, however, at this stage, it is not understood what dictates a cell to undergo senescence rather than apoptosis. However, there is some evidence suggesting that the level of stress plays a role in the designated response. For example, in cardiomyocytes derived from rats, a low level of the DNA intercalator doxorubicin culminates in senescence, contrastingly, a high dose results in apoptosis (Zhang *et al.*, 2009). Consistently, in human fibroblasts it has been demonstrated that etoposide (a topoisomerase II inhibitor that induces double strand breaks) and hydrogen peroxide (an inducer of oxidative damage) leads to senescence at low doses and apoptosis at higher doses (Chen and Ames, 1994; Chen *et al.*, 2000) (Probin *et al.*, 2006). Similarly, exposure to a low level of UVB irradiation which causes DNA damage renders cultured skin fibroblasts senescent, but a high dose leads to apoptosis (Debacq-Chainiaux *et al.*, 2005). However, aside from the level of stress, the type of cell seems to have a role in determining whether to undergo senescence or apoptosis in response to stress. In particular, fibroblasts and epithelial cells have a tendency to undergo senescence rather than apoptosis, for example, it has been demonstrated that the DNA damaging agent busulfan induces senescence in human fibroblasts, however, higher doses do not alter the

cell fate from senescence to apoptosis (Probin *et al.*, 2006). The same effect has been demonstrated in melanoma cells whereby temozolomide induces senescence but not apoptosis (Mhaidat *et al.*, 2007). Many cell types have the capacity to undergo both senescence and apoptosis, however, some cell types such as lymphocytes are more predisposed to undergo apoptosis rather than senescence (Campisi and d'Adda di Fagagna, 2007). Collectively, these data suggest that the nature and intensity of DNA damage in conjunction with the cell type play a crucial role in determining the cell fate. However at this stage, it is unclear whether differences associated with the intensity of damage are associated with the capacity for DNA repair to occur, or some inbuilt predisposition favouring senescence or apoptosis.

Interestingly, many types of cells that have undergone the senescence programme are resistant to apoptotic stimuli. For example, it has been demonstrated that senescent human fibroblasts can resist apoptosis in response to high doses of hydrogen peroxide, UVB and the withdrawal of serum which induce apoptosis in their proliferating counterparts (Wang, 1995; Chen *et al.*, 2000; Yeo *et al.*, 2000). This capacity to resist apoptosis has been attributed to the upregulation of anti-apoptotic BCL-2 proteins (B-cell lymphoma 2) (Wang, 1995; Chen *et al.*, 2000; Sanders *et al.*, 2013). Similarly, senescent keratinocytes have the capacity to resist UVB induced apoptosis (Chaturvedi *et al.*, 1999). However, although many cell types are resistant to apoptotic stimuli, some become more sensitive; such as endothelial cells. For example, fibroblasts become more resistant to apoptosis as passage number increases, conversely, HUVECs (human umbilical vein endothelial cell) become more sensitive with age (Hoffmann *et al.*, 2001). It has also been demonstrated that replicatively senescent porcine pulmonary artery endothelial cells undergo apoptosis more frequently than proliferating cells, this cell type has lower levels of anti-apoptotic BCL-2 proteins (Zhang *et al.*, 2002).

Alongside the BCL-2 proteins, there is evidence that p53 plays a role in determining whether a cell undergoes senescence or apoptosis. For example, in human fibroblasts treatment with hydrogen peroxide at a dose sufficient to induce apoptosis p53 expression was elevated compared to lower doses which lead to senescence (Chen *et al.*, 2000). In addition to this, it has been demonstrated that the kinetics of p53 expression are also important in determining cell fate. For example, low levels of γ-irradiation induce a transient rise in p53 expression leading to cell cycle arrest, a reduction in p53 leads to rescue of the cell cycle. However, if the degradation of p53 is blocked, the cell cycle does not resume and cellular senescence ensues (Purvis *et al.*, 2012). To support this notion, following mild oxidative stress induced DNA damage if p53 expression is stabilised by Nutlin-3a then the senescence programme is engaged

(Efeyan *et al.*, 2007). Furthermore, there is evidence suggesting that the capacity to stabilise p53 is diminished with age in splenocytes, this data indicates that with age damaged cells may not be able to stabilise p53 sufficiently to engage the apoptosis process, however can still induce senescence, hence a possible explanation as to why senescent cells accumulate with age (Feng *et al.*, 2007).

1.4.6. Markers Characteristic of Senescent Cells

First and foremost, it is important to note that there is no specific marker of senescence, therefore, it is essential to use several markers in conjunction to confidently identify senescent cells both *in vitro* and *in vivo*. The most prominent feature that distinguishes senescent cells from proliferating cells is the permanent cell cycle arrest. As such, prominent markers of senescence include proteins associated with enforcing this arrest, such as p16, ARF, p21, p15, p27 and p53 (Beausejour *et al.*, 2003). Alongside the upregulation of these proteins, there is also a loss of proliferative markers such as Ki67 and the incorporation of BrdU (5-bromodeoxyuridine) during progression through the cell cycle (Lawless *et al.*, 2010).

As senescence often occurs in response to cellular stress, a common feature of senescent cells is the evidence of DNA damage. Markers of DNA damage such as phosphorylated histone H2AX (γH2AX) and p53-binding protein-1 (53BP1) are frequently observed (Hewitt *et al.*, 2012). DNA damage which occurs specifically at telomeres referred to as TAF (telomere associated foci) has also been identified as an inducer of senescence and as such is a reliable marker of senescence (d'Adda di Fagagna *et al.*, 2003; Hewitt *et al.*, 2012). In addition, other markers of the DNA damage response such as phosphorylation of ATM (ataxia-telangiectasia mutated) and ATR (ataxia telangiectasia and Rad3-related) are often observed (d'Adda di Fagagna *et al.*, 2003). Aside from genomic DNA damage, senescent cells often display changes to the structure of their chromatin as discussed earlier. This is evident by the formation of senescence associated heterochromatin foci, which can be detected by dense staining areas of DAPI (4',6-diamidino-2-phenylindole). Also visible are areas enriched in histone modifications, such as methylation of Histone 3 Lysine 9. These modifications typically follow expression of p16 in cultured cells, however, they are not observed as frequently *in vivo (Kosar et al., 2011)*. Further changes to the nuclear region are evident in the loss of the nuclear envelope, typically lamin B1 is no longer present in senescent cells (Freund *et al.*, 2012). This loss has also been associated with the presence of nuclear fragments of DNA which are detectable in the cytoplasm of senescent cells (Ivanov *et al.*, 2013; Dou *et al.*, 2017; Gluck *et al.*, 2017; Yang *et al.*, 2017).

Perhaps the most widely used marker of senescence is the senescence associated β-galactosidase (SA-β-Gal). Senescent cells display increased biogenesis of lysosomes and consequently the enzyme, lysosomal β-galactosidase. As such, at pH 6.0 β-Gal activity is detectable and can be used for the detection of senescent cells both *in vitro* and *in vivo* by histochemistry. SA-β-Gal has been demonstrated to be detectable in an array of senescent cell types and was first described in 1995, where SA-β-Gal positive cells were demonstrated to increase with age in samples of human skin (Dimri *et al.*, 1995). It is important to note that there are several limitations with regards to the identification of senescent cells using SA-β-Gal, as it can be detected in confluent and starved cells as well as in immortalized cultures (Severino *et al.*, 2000).

1.4.7. The Senescence Associated Secretory Phenotype

A key characteristic of senescent cells is the senescence-associated secretory phenotype (SASP). The SASP is a complex pro-inflammatory response which consists of cytokines (interleukins (IL) 6 and 8) and chemokines (monocyte chemoattractant proteins and macrophage inflammatory proteins), growth factors (transforming growth factor-β (TGF-β)) and various proteases for degrading the extracellular matrix (Campisi and d'Adda di Fagagna, 2007).

It has been hypothesised that the evolutionary purpose of this secretory profile is to signal the immune system to clear away senescent cells: a process known as immunosurveillance. Indeed, there is evidence to support this notion as the SASP has been demonstrated to result in phagocytosis and cytotoxic-mediated killing of senescent cells (Kang *et al.*, 2011b). Furthermore, experimental work has revealed that the SASP limits the progression of liver fibrosis, as a consequence of removal of senescent hepatic stellate cells by natural killer cells both *in vitro* and *in vivo* (Krizhanovsky *et al.*, 2008). The SASP also has powerful autocrine and paracrine effects, there is clear evidence that it strongly reinforces the senescence phenotype through the secretion of IL-8 to prevent the damaged cell in question re-entering the cell cycle (Acosta *et al.*, 2008; Kuilman *et al.*, 2008). Another chemokine which forms part of the SASP is IP-10, its production is induced by IFN-γ. Once secreted, it can act on its receptor CXCR3 to activate NF-κB which has a binding site in the promoter of IP-10. This allows IP-10 to form a positive feedback loop to stimulate its own transcription which can re-inforce the SASP in a paracrine fashion (Perrott *et al.*, 2017)

Furthermore, it has been demonstrated that senescent cells can exert damage to neighbouring cells. Similarly, the SASP has been shown to be capable of inducing senescence in surrounding cells through a TGF-β/ROS/DNA damage mediated mechanism *in vitro*, similarly *in vivo*, there is evidence that where senescent cells occur they are often found in clusters, which potentially occur as a consequence of paracrine effects (Nelson *et al.*, 2012; Acosta *et al.*, 2013). It was also demonstrated experimentally that transplanting very low numbers of senescent cells into the knee joint *in vivo* was accompanied by reduced survival, this was not observed when non-senescent cells were transplanted (Xu *et al.*, 2018). This study indicated the role of senescent cells in shortening health and lifespan, potentially by inducing senescence in surrounding tissues. This frailty that occurred following the transplant of senescent cells could be attenuated by senolytic drugs (Xu *et al.*, 2018).

Taken together, it seems clear that the primary function of the SASP is to promote clearance and prevent the proliferation of damaged cells, which could in turn, lead to tumorigenesis. The SASP has been demonstrated to have another beneficial effect and that is during the wound healing process. Following acute injury, senescent fibroblasts and endothelial cells form, which promote myofibroblasts differentiation through the SASP, specifically through secretion of PDGF-AA (platelet-derived growth factor AA). These myofibroblasts aid the healing process and therefore demonstrate that senescence is required for optimal wound healing (Demaria *et al.*, 2014). Recent work has also established that the SASP plays an important role during embryonic development, through TGF-β/SMAD, the SASP promotes the induction of p21-mediated developmentally programmed senescence which is essential in the development of organelles which comprise the structure of the inner ear; mesonephros and endolymphatic sac. In this process, the SASP also promotes clearance of senescent cells through a TGF-β mediated mechanism of macrophage recruitment (Munoz-Espin *et al.*, 2013).

Although the SASP can be beneficial, if senescent cells are not effectively cleared then chronic inflammation associated with the SASP can promote adverse effects. Interestingly, a recent study found that the SASP could had the capacity to promote regeneration through the induction of cell plasticity and stemness. This phenomenon was observed both *in vitro* and *in vivo* in keratinocytes, however, chronic exposure to the SASP diminished the regenerative response (Ritschka *et al.*, 2017). Furthermore, a number of studies have revealed that if senescent cells are not cleared efficiently, then there are components of the SASP which can render fibroblasts and epithelial cells tumorigenic *in vitro* and *in vivo (Krtolica et al., 2001; Kang et al., 2011b).* Specifically in the liver of mice it has been shown that senescent hepatic stellate cells secrete a

SASP which drives hepatocellular carcinomas (Yoshimoto *et al.*, 2013). Interestingly, IL-8 which is highly secreted during senescence is also highly expressed in cancer cells and has been comprehensively studied and is known to promote aberrant cellular proliferation which leads to tumorigenesis, as well as the maintenance and metastasis of tumours (Waugh and Wilson, 2008).

1.5. The Physiological Significance of Cellular Senescence

Cellular senescence is an important biological process throughout the life course. At early stages, it is a key modulator of embryonic development, then as an organism progresses through life it is important in ensuring optimal wound healing and preventing the onset of tumours (Serrano *et al.*, 1997; Munoz-Espin *et al.*, 2013; Demaria *et al.*, 2014). However, it has now been firmly established that with age senescent cells accumulate and this burden contributes towards the development of ageing and age-related pathologies (Baker *et al.*, 2011; Xu *et al.*, 2015a; Baker *et al.*, 2016). From an evolutionary context, senescence is a good example of antagonistic pleiotropy, whereby it is beneficial in early stages of life but is detrimental in the later stages (Williams, 1957). In this section, the significance of senescent cells to the development of age-related diseases and the emergence of senolytics will be discussed.

1.5.1. Cellular Senescence and Ageing

It has been firmly established that with advancing age there is an accumulation of senescent cells within a range of tissues. One of the earliest observations *in vivo* was the increased number of SA-β-gal positive cells in human skin samples taken from elderly people when compared to their younger counterparts (Dimri *et al.*, 1995). Since then, it has been demonstrated that senescent cells accumulate in the tissues of a number of organisms, including; mice, primates, humans (Krishnamurthy *et al.*, 2004; Herbig *et al.*, 2006; Jeyapalan *et al.*, 2007; Wang *et al.*, 2009; Hewitt *et al.*, 2012; Waaijer *et al.*, 2012). However, until recently it was not known whether these cells were drivers of ageing.

To address this key question whether senescent cells are causal in the ageing process, mouse models were developed in which senescent cells could be selectively eliminated. Within the field, early work to assess the role of the tumour suppressor p16 as an effector of ageing was difficult as knockout transgenic animals have curtailed lifespans before the onset of age-related disorders due to the formation of tumours (Krimpenfort *et al.*, 2001). Therefore one of the initial studies implicating senescent cells in the ageing process employed a model of premature ageing,

the BubR1 progeroid mouse. It was observed that in p16 deficient BubR1 mice there was a reduction in the accumulation of senescent cells with age, furthermore, these animals displayed a reduction in a number of progeroid features in tissues lacking p16 accumulation, such as cataract development and the increase in subcutaneous adipose tissue. However, a number of progeroid features such as dermal thinning and the thickening of the arterial wall remained unchanged (Baker *et al.*, 2008). Following these findings, the same group set out to develop a model where p16 cells could be selectively killed. In order to do this they developed the INK-ATTAC (INK-linked apoptosis through targeted activation of caspase), this system expresses a FK506-binding protein fused to caspase 8. Following treatment with the drug AP20187, the fusion protein dimerises and induces apoptosis specifically in $p16^{INK4A}$ positive cells. This system was employed in the BubR1 background and following the selective elimination of senescent cells intermittently it was found that there was a reduction in some progeroid features of these mice such as cataract development, sarcopenia and accumulation of subcutaneous adipose tissue (Baker *et al.*, 2011).

Later on it was shown in wild-type mice that bi-weekly clearance of senescent cells from midlife onwards culminated in an extension in median lifespan (but not maximum lifespan) in two genetically distinct backgrounds. Furthermore, from a health span perspective, it was observed that cataract development, the accumulation of subcutaneous adipose tissue, glomerulosclerosis, cardiomyocyte hypertrophy and the development of cancer were also decreased following selective clearance of p16 positive cells (Baker *et al.*, 2016). Importantly these studies were the first to implicate senescence as potential drivers of the ageing process, not only that, they have provided a tool which can be used to address the role of senescent cells in various diseases. Alongside the INK-ATTAC mouse model, a similar model referred to as the p16-3MR mouse has been developed, whereby p16 positive cells can be selectively eliminated following administration of the drug ganciclovir (Demaria *et al.*, 2014). Together these two models have allowed the role of senescent cells in age-related diseases to be dissected (which will be discussed in detail in Section 1.5.3).

1.5.2. The Emergence of Senolytics

Following the INK-ATTAC model which established senescence as a causal player in the ageing process, naturally there have been a number of studies investigating pharmacological compounds which can selectively kill senescent cells (referred to as senolytics).

The first published senolytics were the combination therapy of the drugs dasatanib and quercetin (Zhu *et al.*, 2015b). These two compounds were identified as having senolytic therapies after it was discovered that the survival of senescent adipocytes was dependent on the ephrins EFNB1, EFNB3, PI3Kδ (phosphatidyl 3-kinase-δ), BCL-XL, p21 and the serpin plasminogen-activated inhibitor-2 (PAI2). Genetic silencing and pharmacological targeting of these factors resulted in the induction of apoptosis in senescent cells but not proliferating cells. It was found that dasatanib which is a pan-tyrosine kinase inhibitor and effectively blocks the ephrin receptors in conjunction with the flavonoid quercetin which can inhibit the serpins, together displayed senolytic activity comparable to that of the BCL-2 inhibitors. Furthermore, it was demonstrated *in vivo* that senescent cells were eliminated and subsequently resulted in an improvement in health span (reduced osteoporosis, improved exercise capacity and a delay in the development of age-related pathologies) in a progeroid mouse model (Zhu *et al.*, 2015b). Specifically addressing the implications of osteoporosis and age-associated bone loss in mice, it has been demonstrated that the combination of dasatanib and quercetin prevents the age-related loss and indeed reduces frailty. These effects were also observed using INK-ATTAC mice and were attributed to the pro-inflammatory environment associated with the presence of senescent cells, consistently, inhibition of the JAK/STAT pathway prevented the SASP and also improved bone formation (Farr *et al.*, 2017). Recently it was published that the onset of senescence can drive liver steatosis, the authors showed treatment with dasatanib and quercetin could reduce liver steatosis (Ogrodnik *et al.*, 2017). It has also been demonstrated that following the onset of obesity there is an accumulation of senescent cells which drive anxiety-related behaviour, it was shown that clearance of these senescent cells using dasatanib and quercetin could alleviate these behaviours (Ogrodnik *et al.*, 2019). Dasatanib and quercetin have also been shown to reduce fibrosis and hypertrophy in aged mice which was associated with a restoration of the regenerative capacity of the heart (Lewis-McDougall *et al.*, 2019). Senescent cells have also been implicated in the development of idiopathic pulmonary fibrosis, here, it was demonstrated that treatment with dasatanib and quercetin improves exercise capacity and lung compliance in a mouse model of pulmonary fibrosis (Schafer *et al.*, 2017). Following this, the first human clinical trial has been conducted to assess the safety of dasatanib and quercetin in idiopathic pulmonary fibrosis patients. In this study, the combination therapy was well tolerated and although there were no beneficial effects on pulmonary function there were improvements in physical function. Therefore warranting evaluation of dasatanib and quercetin in a larger cohort of patients for senescence associated diseases (Justice *et al.*, 2019).

As discussed earlier a common feature of senescent cells is their resistance to apoptotic stimuli. It has been demonstrated that in a number of cell types this resistance is facilitated by upregulation of anti-apoptotic BCL-2 family proteins; BCL-2, BCL-XL and BCL-W. These proteins prevent apoptosis from occurring by binding to and preventing the activation of pro-apoptotic BCL-2 family members. The senolytic compounds ABT737 and ABT263 (navitoclax) promote selective apoptosis in senescent cells by inhibiting the anti-apoptotic actions of BCL-2, BCL-XL and BCL-W. This allows the pro-apoptotic BCL-2 proteins which are usually rendered inactive in senescent cells to activate BAX and BAK (BCL-2 homologous antagonist/killer), together these proteins form pores in the outer mitochondrial membrane which allow cytochrome C to be released and subsequently trigger a caspase cascade culminating in apoptosis (Tse *et al.*, 2008; Song *et al.*, 2011; Chang *et al.*, 2016; Yosef *et al.*, 2016b). Navitoclax, ABT737 have both been demonstrated to selectively kill senescent cells both *in vitro* and *in vivo* (Chang *et al.*, 2016; Yosef *et al.*, 2016a; Zhu *et al.*, 2016). Additionally, it has been reported that fisetin (a flavone) and A1155463 and A1331852 can induce apoptosis in various senescent cells due to their action on BCL-XL (Zhu *et al.*, 2017). Specifically, it has been demonstrated that navitoclax can reduce senescent cells following sub-lethal irradiation. Furthermore, it has been demonstrated in normal aged mice that navitoclax-mediated clearance of senescent cells offset premature-ageing of the haemopoetic system and promoted rejuvenation of haemopoetic and muscle stem cells (Chang *et al.*, 2016; Zhu *et al.*, 2016). Navitoclax has also been demonstrated to be beneficial in atherosclerosis. Here, senescent cells accumulate and drive pathology by increasing the expression of atherogenic and inflammatory factors (Childs *et al.*, 2016). Using both navitoclax and the p16-3MR mouse model, the selective removal of senescent cells inhibits plaque growth and reduces the atherogenic environment (Childs *et al.*, 2016). In addition, it has been published that navitoclax decreases cardiac fibrosis and hypertrophy that occurs in aged mice (Anderson *et al.*, 2019). It has also been demonstrated that following a myocardial infarction navitoclax can improve functional outcomes and overall survival in mice (Walaszczyk *et al.*, 2019).

Another senolytic recently identified is UBX0101. UBX0101 inhibits the anti-apoptotic protein MDM2, thus preventing interaction and degradation of p53, and this leads to p53 overexpression and subsequently apoptosis. UBX0101 has been demonstrated to effectively clear senescent chondrocytes such as those found in arthritic joints (Jeon *et al.*, 2017). Furthermore, following clearance there was an increase in cartilage development, reduction in pain and an overall attenuation in the development of post-traumatic osteoarthritis.

Consistently, the same study reported the same beneficial effects following selective clearance of senescent cells in the p16-3MR mouse model (Jeon *et al.*, 2017). This molecule is also being progressed to phase 1 clinical trials in osteoarthritis patients.

Senescent cells can also undergo apoptosis when the interaction between p53 and FOXO4 (forkhead box protein 04) is disrupted. During senescence it has been identified that FOXO4 is upregulated and binds to p53, effectively preventing p53-mediated apoptosis. Thus, it was observed that treatment of senescent cells with the peptide D-retro inverso FOXO4 promoted p53 activation, release of cytochrome C and subsequent apoptosis. Furthermore in aged mice, the inhibition of FOXO4 has been demonstrated to improve a number of aspects of health span such as fitness, renal function and hair growth (Baar *et al.*, 2017).

A group of proteins referred to as heat shock proteins (HSP) which have roles in protein folding and degradation, as well as cell development and growth have been implicated as a senolytic target. HSP90 acts on AKT and p-AKT which are key proteins as part of the anti-apoptotic PI3K/AKT pathway that is upregulated in senescence. Furthermore, it has been discovered that inhibitors of HSP90 (tanespimycin, geldanamycin and alvespimycin) can induce apoptosis in an array of senescent cell types of both human and mouse origin. In vivo, intermittent treatment with HSP90 inhibitors reduced the number of p16 positive cells as well as various age-related symptoms such as kyphosis, grip strength and overall body condition (Fuhrmann-Stroissnigg *et al.*, 2017). Another molecule that has been identified as having senolytic activity is piperlongumine, although its mechanism is not fully understood, it is known to inhibit the phosphorylation of AKT (Makhov *et al.*, 2014). It has been demonstrated to have the capacity to eliminate senescent cells *in vitro* (Chang *et al.*, 2016).

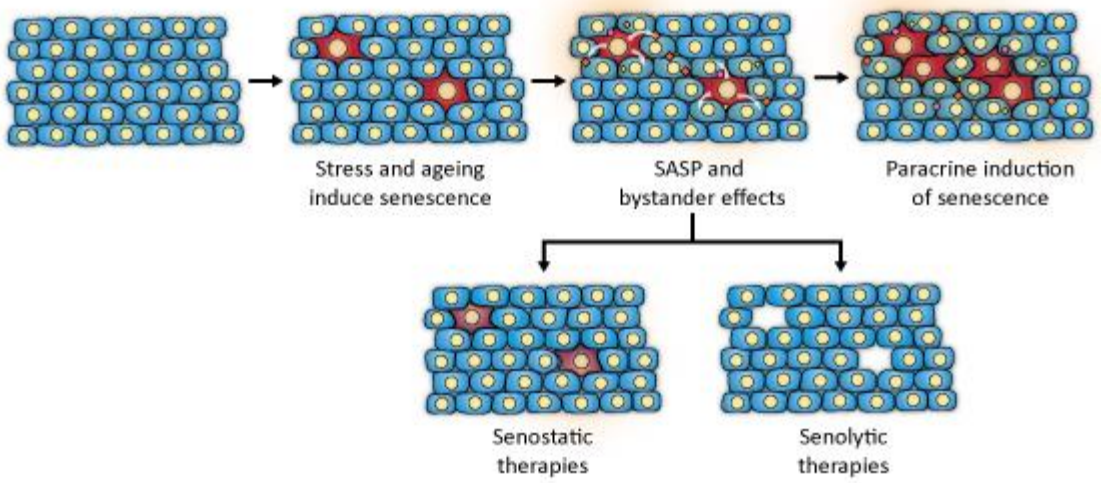

Figure 1.2 – Schematic demonstrating therapeutic strategies for alleviating the detrimental effects of senescent cells.

It has been firmly established that exposure to stressful stimuli promote the induction of senescence. Generally senescent cells are removed by the immune system, but with age these cells accumulate. The presence of these senescent cells can promote neighbouring cells to become senescent through a paracrine mechanism. This in turn contributes to a chronic inflammatory environment which is believed to exacerbate tissue dysfunction and promote the ageing process. Therefore two strategies have emerged to prevent the deleterious effects of senescence. The first strategy is senostatic therapies, these aim to suppress the SASP without removing the beneficial cell cycle arrest. The second is that of senolytics, which selectively eliminate senescent cells without impacting healthy proliferating cells. Figure adapted from (Chapman *et al.*, 2019)

1.5.3. Cellular Senescence and Age-Related Diseases

Senescent cells have been recognised as being present at the sites of disease for some time, however, it has been difficult to establish causality until recently. Collectively, the transgenic mouse models and the emergence of senolytics have provided excellent tools to dissect and understand the role of senescent cells in various age-related diseases. As such, a number of studies are currently underway and have been conducted to investigate these associations as summarised in **Table 1.1**.

As previously discussed, during the onset of the age-related diseases; osteoporosis, osteoarthritis and atherosclerosis, senescent cells have been observed to accumulate at the sites of disease. Furthermore, the removal of these senescent cells using either senolytics or the transgenic mouse models has clear beneficial effects in each of these diseases (Childs *et al.*, 2016; Roos *et al.*, 2016b; Farr *et al.*, 2017; Jeon *et al.*, 2017). Interestingly with age, there is

also a decrease in cardiac function, in the INK-ATTAC model it was observed that the clearance of senescent cells resulted in a decreased amount of cardiac hypertrophy as well as an increased resistance to cardiac stress (Baker *et al.*, 2016). Further work has revealed that during ageing, cardiomyocytes, a key cell type found in the heart develop a senescent-like phenotype that can promote fibrosis and hypertrophy through the SASP. Interestingly, clearance of senescent cells either genetically (INK-ATTAC) or pharmacologically (navitoclax) reduced both hypertrophy and fibrosis, and in fact, promoted cardiomyocyte regeneration (Anderson *et al.*, 2019). Similarly, it has recently been shown that senolytic treatment following acute myocardial infarction has beneficial effects by promoting tissue remodelling, improving cardiac function and improving overall survival (Walaszczyk *et al.*, 2019). Therefore, these studies highlight the detrimental effect that senescent cells exert on cardiac function with age.

Another tissue where function is impaired with advancing age is the lung. It loses elasticity and becomes more susceptible to pathogenic invasion. It has been previously highlighted that diseases of the lung such as chronic obstructive pulmonary disease and idiopathic pulmonary fibrosis display evidence of increased levels of senescent cells (Birch *et al.*, 2015; Schafer *et al.*, 2017). Interestingly, it has recently been demonstrated that the genetic clearance of $p19^{ARF}$ positive senescent cells improved the compliance and elasticity of lungs in aged mice, thereby partially restoring overall pulmonary function that deteriorates with age (Hashimoto *et al.*, 2016). Senescent cells have been demonstrated to be detrimental in idiopathic pulmonary fibrosis. Tissues from patients display exacerbated levels of senescent markers such as p21 and SA-β-gal (Yanai *et al.*, 2015; Schafer *et al.*, 2017). Furthermore, the negative effects of senescent cells were demonstrated when selective elimination of senescent cells using both transgenic mice and senolytics resulted in an improvement in overall pulmonary function, as well as a reduction in the SASP which has been demonstrated to be pro-fibrotic and thus aggravate the disease further (Schafer *et al.*, 2017; Munoz-Espin *et al.*, 2018).

Another organ where its overall function can become reduced with age is the kidney. It has been noted that in individuals with glomerulosclerosis and atrophy of the nephrons, there is an exacerbated number of p16 and p53 positive cells in these regions (Melk *et al.*, 2004). Clearance of senescent cells in the INK-ATTAC model resulted in an improvement of kidney function as well as a reduction in the hardening of the glomeruli of the kidney, i.e. a reduction in glomerulosclerosis (Baker *et al.*, 2016). With age, the liver also becomes more susceptible to developing non-alcoholic fatty liver disease. This is another disease where the presence of senescent cells is observed. It was recently reported that senescent hepatocytes drive fat

accumulation in the liver which in turn contributes to liver steatosis and non-alcoholic fatty liver disease. Consistently, the clearance of senescent cells using either the INK-ATTAC model or dasatanib and quercetin lead to an overall reduction in hepatic steatosis (Ogrodnik *et al.*, 2017). These studies have highlighted the contribution of senescent cells to the age-associated reduction in renal function and the development of non-alcoholic fatty liver disease.

An emerging area where senescent cells have been implicated is neurodegeneration, it has previously been highlighted that senescent markers are present in neurodegenerative diseases such as Alzheimer's disease (Bhat *et al.*, 2012; Musi *et al.*, 2018). It has recently been published that genetic and pharmacological clearance of senescent cells in a mouse model of Alzheimer's disease modulates accumulation of tau aggregates and in turn preserves cognitive function (Bussian *et al.*, 2018). Similarly, another group recently published that senolytic treatment reduces neuroinflammation and improves cognitive function in an Alzheimers disease model (Zhang *et al.*, 2019). Senescent cells have also been implicated in contributing to neuropsychiatric disorders. It was recently highlighted that obese mice harbour an increased burden of senescent cells. Specifically, high levels of senescent glial cells in proximity to the lateral ventricle (an important area for adult neurogenesis) were associated with an increase in anxiety-like behaviour(Ogrodnik *et al.*, 2019). Both genetic and pharmacological clearance of these senescent cells alleviated anxiety-like behaviour (Ogrodnik *et al.*, 2019).

A number of other diseases and pathologies have been associated with senescence such as sarcopenia, type II diabetes and cachexia (Baker *et al.*, 2011; Baker *et al.*, 2016; Chang *et al.*, 2016; Berry *et al.*, 2017; Xu *et al.*, 2018; Palmer *et al.*, 2019). However, it is important to consider that senescent cells have been demonstrated to be beneficial in some contexts. As previously mentioned, senescence is crucial for optimal wound healing and also is an important tumour suppressor mechanism to prevent the onset of cancer (Serrano *et al.*, 1997; Demaria *et al.*, 2014). Aside from these, senescent cells have also been demonstrated to be beneficial in diseases where they limit the progression of fibrosis. For example, during the development of liver cirrhosis senescent cells accumulate, the senescent cells are predominantly hepatic stellate cells, normally these cells proliferate and produce the fibrotic scar. However, the induction of senescence limits the formation of the fibrotic scar and these cells are subsequently cleared by natural killer cells which facilitates the resolution of the fibrosis (Krizhanovsky *et al.*, 2008). Similarly, the onset of senescence has been shown to reduce oral submucous fibrosis and cardiac fibrosis (Pitiyage *et al.*, 2011; Zhu *et al.*, 2013). There is also some evidence that senescence is beneficial in protecting against pulmonary hypertension. It has been observed

experimentally that mice deficient for p53 display aggravated pulmonary hypertension in response to hypoxia, consistently, activation of p53 can reverse pulmonary hypertension (Mizuno *et al.*, 2011; Mouraret *et al.*, 2013). Interestingly, the senescence programme can protect against the development of arthrosclerosis. Although at later stages of the disease clearance of senescent cells is beneficial, studies have observed that mice deficient for p21 or p53 are more susceptible to the development of artherosclerosis, thereby indicating that the senescence programme provides a protective function against the development of atherosclerotic plaques (Mercer *et al.*, 2005; Khanna, 2009; Childs *et al.*, 2016).

Finally, at this stage it seems that the clearance of senescent cells either genetically or using senolytics have generally been well tolerated *in vivo* with minimal side effects (Baker *et al.*, 2011; Justice *et al.*, 2019). However, it is important to note that previous clinical studies have implicated thrombocytopenia and neutropenia as a side effect of BCL-2 inhibitors (Kaefer *et al.*, 2014). Therefore work is currently underway to identify senolytics with minimal side effects, as such, a new class of drug has been reported as exhibiting senolytic activity; cardiac glycosides. As yet, these findings are unpublished, however, blockade of their target the Na/K-ATPase has been previously implicated as being able to mitigate cellular senescence (Sodhi *et al.*, 2018). However, at this stage the evidence from published studies clarifies that chronic treatment is not required to effectively clear senescent cells using existing senolytics, thereby intermittent administration has the capacity to minimise side effects (Zhu *et al.*, 2015b; Chang *et al.*, 2016; Yosef *et al.*, 2016b).

Disease	Genetic Clearance	Senolytic Therapy
Atherosclerosis	Childs et al., 2016	Roos et al., 2016 Childs et al., 2016
Alopecia	N/A	Yosef et al., 2016
Cachexia	Baker et al., 2016 Berry et al., 2017	Berry et al., 2017 Xu et al., 2018
Cataracts	Baker et al., 2011	N/A
Cardiac Ageing	Baker et al., 2016 Anderson et al., 2019	Zhu et al., 2015 Baker et al., 2016 Anderson et al., 2019
Diabetes	Palmer et al., 2019	Palmer et al., 2019
Fatty Liver Disease	Ogrodnik et al., 2017	Ogrodnik et al., 2017
Glomerulosclerosis	Baker et al., 2016	N/A
Idiopathic Pulmonary Fibrosis	Schafer et al., 2016	Yanai et al. 2015 Schafer et al. 2016 Muñoz-Espín et al., 2018
Lung Ageing	Hashimoto et al., 2019	N/A
Myocardial Infarction	N/A	Walaszczyk et al., 2019
Neurodegeneration	Bussian et al., 2018	Bussian et al., 2018 Musi et al., 2018 Zhang et al., 2019
Neuropsychiatric Disorders	Ogrodnik et al., 2019	Ogrodnik et al., 2019
Osteoarthritis	Jeon et al., 2017	Jeon et al., 2017
Osteoporosis	Farr et al., 2017	Farr et al., 2017
Sarcopenia	Baker et al., 2011	Chang et al., 2016 Xu et al., 2018

Table 1.1– Diseases that have been associated with cellular senescence.

It has been established using either genetic or pharmacological means of senescent cell clearance that senescent cells play a role in the development of a number of age-related diseases. This table summarises diseases where senescent cells have been implicated as having a causal role in the disease or where their presence has been associated with aggravating the disease.

1.6. The Role of Mitochondria in Cellular Senescence

Mitochondria are important organelles that regulate a myriad of cellular processes, for example they play a key role in the production of energy, orchestrating the apoptotic process as well as regulating various aspects of cellular metabolism (Nunnari and Suomalainen, 2012). Dysfunctional mitochondria are a prominent feature of cellular senescence, and both have been implicated as classical hallmarks of the ageing process (Lopez-Otin *et al.*, 2013). In this section we review the relationship between the two.

1.6.1. Mitochondrial Dynamics and ROS in Senescence

Mitochondria in senescent cells undergo several fundamental changes. For example, mitochondrial morphology is dramatically altered in senescent cells. A normal mitochondrial network constantly undergoes fission and fusion events to promote reorganisation, facilitate mitochondrial replication as well as segregate dysfunctional entities, this continuous process ensures that the metabolic needs of the cell are met (Detmer and Chan, 2007). Interestingly, the mitochondria networks of senescent cells and old cells are composed of a vastly increased number of mitochondria which exist in a hyper fused state (Jendrach *et al.*, 2005; Yoon *et al.*, 2006). This occurs in response to a dysregulation of fission and fusion machinery, whereby studies have revealed that senescent cells display a reduction in dynamin related protein 1 (DRP1) and mitochondrial fission protein 1 (FIS1) which are key mediators of the fission process, this culminates in an overall reduction of fission and fusion events in senescent cells (Mai *et al.*, 2010). Furthermore, *in vitro* it has been demonstrated that senescence can be induced when mitochondria are maintained in a fused state following the knock down of FIS1, if FIS1 is reintroduced then the senescence response is suppressed. In addition, if FIS1 is depleted in conjunction with the fusion regulator OPA1, then fragmented mitochondria results and no senescence response (Lee *et al.*, 2007). Consistently, in a model where DRP1 is downregulated due to depletion of a mitochondrial E3 ubiquitin ligase senescence, the fusion regulator MFN1 (mitofusin-1) accumulates and promotes an elongated mitochondrial network, in response, cells become senescent (Park *et al.*, 2010). Collectively, these data highlight that mitochondrial dynamics are a fundamental part of the senescence programme; however, it is not entirely clear how elongated mitochondria may drive the process.

It is believed that one way in which elongated mitochondria can initiate senescence is through the exacerbated production of ROS (Yoon *et al.*, 2006). In 1972, the "mitochondrial free radical theory of ageing" was proposed by Denham Harman, where he hypothesised that mitochondrial ROS could drive the ageing process as a consequence of the damage they inflict on DNA and

protein structures (Harman, 1972). The link between ROS and senescence was first observed when it was noted that cells cultured in low oxygen had reduced levels of oxidative damage and had an increased lifespan (Packer and Fuehr, 1977). The superoxide anion is the most damaging of the mitochondrial derived ROS and is produced as a consequence of electron leak along the electron transport chain. As cells reach the end of their replicative lifespan it has been observed that the production of ROS is exacerbated, this has been observed in a number of models of senescence such as replicative senescence, stress-induced and oncogene induced senescence (Saretzki *et al.*, 2003; Passos *et al.*, 2007; Moiseeva *et al.*, 2009; Passos *et al.*, 2010). Furthermore, it has been demonstrated by a number of groups that mitochondrial ROS is not just a feature of senescence it can in fact drive oxidative damage which can induce senescence in human fibroblasts through a ROS-mediated DDR (Chen *et al.*, 1995a; Passos *et al.*, 2007; Moiseeva *et al.*, 2009; Passos *et al.*, 2010). Oxidative stress which occurs in response to ROS has been demonstrated to accelerate telomere shortening and subsequently induce telomere-dependent senescence (von Zglinicki, 2002). It has since been established that telomeric regions are explicitly sensitive to the damage induced by ROS and damage occurring here induces senescence (Petersen *et al.*, 1998; Passos *et al.*, 2007; Hewitt *et al.*, 2012). Consistently, telomere dysfunction can be averted and replicative lifespan *in vitro* extended by mediators that reduce mitochondrial-derived ROS such as the antioxidant MitoQ, nicotinamide as well as mild mitochondrial uncoupling (Saretzki *et al.*, 2003; Kang *et al.*, 2006; Passos *et al.*, 2007). Similarly, *in vivo*, the inhibition of the antioxidant enzymes catalase and manganese super oxide dismutase (MnSOD) has been associated with an increase in telomeric damage. Furthermore, telomeric damage induced by overexpression of the pro-oxidant monoamine oxidase can be reduced following treatment with N-acetyl-cysteine (NAC) (Anderson *et al.*, 2019). There have been a vast number of studies demonstrating the increase in oxidative damage with age in various organisms (Oliver *et al.*, 1987; Hamilton *et al.*, 2001). However, there are a number of conflicting studies where manipulation of antioxidant defences and oxidant production do not support the hypothesised role of oxidative damage in ageing (Muller *et al.*, 2007). For example, the overexpression of catalase in mice does not lead to an extension in maximal life span (Chen *et al.*, 2004b).

Interestingly, ROS have been implicated in maintaining the senescence response as well as inducing it. Promoting overexpression of the main senescence effectors *in vitro* such as p16, p21, p53 and oncogenic Ras all promote an increase in ROS production (Lee *et al.*, 1999; Macip *et al.*, 2002). Following these observations, it was recently discovered that mitochondrial ROS

are involved in a positive feedback loop during the induction of senescence. Following the induction of senescence, ROS are produced where they induce short-lived DNA damage foci to instigate a DDR. ROS are continuously produced to maintain DNA damage which leads to a persistent DDR. This persistent DDR culminates in senescence, mechanistically, it has been demonstrated that this feedback loop is active until the growth arrest is firmly established, then it is no longer required (Passos *et al.*, 2010).

1.6.2. Mitochondrial Quality Control in Senescence

Dysfunctional mitochondria are traditionally cleared and recycled via a specialised form of autophagy termed mitophagy. This process enables the targeted degradation of mitochondria which have been tagged with polyubiquitin chains consisting of parkin and PINK1 (PTEN induced kinase 1). Recognition of these chains by the receptor proteins optineurin, NDP52 and TaxBP1 engages the autophagic machinery and these dysfunctional mitochondria are subsequently engulfed and recycled by autophagosomes (Zaffagnini and Martens, 2016). During the onset of senescence there is a clear accumulation of dysfunctional mitochondria, however, it is unclear whether mitophagy contributes to this process.

For mitochondria to be recycled they need to be isolated, however, as discussed earlier mitochondria in senescent cells have a reduction in the fission/fusion machinery and exist in a predominantly hyperfused state (Yoon *et al.*, 2006). Therefore it is unclear in senescence how effectively senescent cells can segregate dysfunctional mitochondria for mitophagy. Furthermore, PINK1 which is important for labelling mitochondria for degradation is downregulated in senescent cells. PINK1 also plays a role in promoting mitochondrial fission, therefore it may contribute to the hyperfused networks characteristic of senescence (Dalle Pezze *et al.*, 2014). Recent work has highlighted that senescent cells produce hydrogen peroxide via the mitochondrial enzyme monoamine oxidase-A, this production of ROS was associated with accumulation of p53 which inhibited parkin. This lead to mitochondrial dysfunction and an impairment of the mitophagy process with a subsequent induction of senescence via a classical DDR. Furthermore, they demonstrated that restoration of mitophagy either by mTOR inhibition or overexpression of parkin prevented the onset of both mitochondrial dysfunction and senescence (Manzella *et al.*, 2018). Similarly, during the induction of senescence it has been demonstrated that impaired mitophagy occurs following p53 accumulation which interacts with parkin preventing its translocation to damaged mitochondria. It was also demonstrated that restoring mitophagy decreased mitochondrial mass accumulation and delayed cellular senescence (Ahmad *et al.*, 2015). It has also been demonstrated that impairment of the

autophagy machinery by downregulation of key autophagic regulators such as ATG7, ATG12, and Lamp2 has been shown to induce premature senescence in primary human fibroblasts, furthermore, it was demonstrated that the onset of senescence could be delayed by antioxidants and inhibition of p53 (Kang *et al.*, 2011a). Interestingly, the transcription factor GATA4 which is normally degraded by autophagy is stabilised in senescence, this stabilisation activates NF-κB which instigates the SASP. The stabilisation of GATA4 is dependent on the DDR, but not on p53 or p16 (Kang *et al.*, 2015).

Although there is mounting evidence that supports the impairment of mitophagy and autophagy in senescence, there is also evidence that mitophagy and autophagy can promote the onset of senescence. For example, it is known that during autophagy there is formation of the TASCC (TOR-autophagy spatial coupling compartment), here mTOR and lysosomes accumulate during OIS. At the TASCC site there is a high number of amino acids which have been demonstrated to promote synthesis of the SASP factors IL-6 and IL-8 through mTOR (Narita *et al.*, 2011). Furthermore, in OIS it has been found that autophagy-related genes are upregulated, the authors also demonstrated that knockdown or inhibition of autophagic regulators delayed the senescence phenotype and SASP (Young *et al.*, 2009). Therefore at this stage, there is some conflicting evidence for the role of autophagy and mitophagy in senescence which requires further study to broaden our understanding of the relationship between the two.

1.6.3. Mitochondria are necessary for Development of the Senescence Phenotype

The relationship between mitochondria and senescence has been investigated for a number of years and has predominantly been associated with their role as ROS generators, however, previous studies have failed to concretely address whether mitochondria are required for the senescence process or the changes observed are merely a consequence of the senescence programme. Therefore our lab designed a proof of principle study to shed light on the role of mitochondria in senescent cells. A system was designed whereby fibroblasts overexpressing the ubiquitin ligase parkin found on mitochondria could be targeted to undergo mitophagy following the induction of mitochondrial depolarisation, this results in mitochondrial clearance (Tait *et al.*, 2013; Correia-Melo *et al.*, 2017). Viable fibroblasts could therefore be generated which are completely devoid of mitochondria and rely on glycolysis rather than mitochondrial-mediated ATP production. This system allowed mitochondria to be cleared prior to and post development of senescence to dissect the role of mitochondria. It was discovered that the clearance of mitochondria at the point of senescence induction resulted in a reduced cell size, SA-β-Gal and ROS, as well as a reduction in the cell cycle inhibitors p16 and p21 compared to

mitochondria competent fibroblasts. However, although proliferating slowly following the induction of senescence, these cells did undergo a complete cell cycle arrest. Perhaps most interestingly is that these mitochondrial depleted fibroblasts had a severely diminished SASP, the key factors IL-6, IL-8, GRO and MCP-1 were all significantly reduced (Correia-Melo *et al.*, 2016). Fundamentally, this study was the first of its kind to demonstrate that mitochondria are crucial for regulating the pro-oxidant and pro-inflammatory features of senescence.

Importantly this study also identified a novel pathway that is involved in the induction of senescence. It was demonstrated that the DDR activates ATM which directly phosphorylates Akt, this leads to phosphorylation and activation of mTORC1 (mammalian target of rapamycin complex 1). This in turn triggers mitochondrial biogenesis via PGC1-β (peroxisome proliferator-activated receptor-gamma coactivator 1β). It was demonstrated that inhibition of either mTORC1 or ATM *in vitro* could alleviate mitochondrial biogenesis observed during senescence and subsequently markers of senescence and the SASP. Furthermore, mTORC1 inhibition *in vivo* using rapamycin was associated with reduced mitochondrial content and markers of senescence (p21, SA-β-Gal and TAF) as well as reduced secretion of SASP factors (Correia-Melo *et al.*, 2017). Further work has revealed that the beneficial effects associated with alleviating the SASP via mTOR targeting with rapamycin can improve the health span of mice (Lesniewski *et al.*, 2017; Houssaini *et al.*, 2018; Correia-Melo *et al.*, 2019). In addition to this, a number of studies have demonstrated elongated lifespan following treatment with rapamycin, although this cannot be directly attributed to the SASP suppressive effects associated with targeting mTOR (Harrison *et al.*, 2009; Lesniewski *et al.*, 2017).

1.7. Mitochondrial Mechanisms Regulating the SASP

Following the observation that mitochondria underpin the pro-inflammatory features of senescence this raises the natural question as to what the possible molecular mechanisms are which provide the link between mitochondria and the SASP.

1.7.1. Mitochondrial Metabolites and Regulation of the SASP

An emerging link between senescence and mitochondria is the role of mitochondrial metabolites. The most comprehensively studied metabolite is perhaps nicotinamide adenine dinucleotide (NAD). The prominent function of NAD^+ is to act as a cofactor where it accepts and carries electrons in turn becoming reduced to NADH. This occurs along the electron transport chain as well as following oxidation of organic molecules during oxidative

phosphorylation (Genova and Lenaz, 2014). Generally the NAD^+/NADH is tightly regulated to maintain optimum mitochondrial function. Interestingly, it has been reported that senescent cells exhibit a lower ratio of NAD^+ to NADH. The increase in NADH has been attributed to decreased levels of the cytosolic enzyme malate dehydrogenase found in senescent cells, this enzyme functions to produce malate from oxaloacetate, in doing so it uses NADH (Lee *et al.*, 2012). Of further interest is a study which has implicated nicotinamide phosphoribosyltransferase (NAMPT) as being reduced in replicative senescent cells (Amano *et al.*, 2019). NAMPT functions to salvage NAD^+ from nicotinamide, as such its diminished activity is associated with exacerbating the low NAD^+/NADH ratio. This study also discovered that overexpression of NAMPT lead to a decrease in age-related increases in p53, which in turn resulted in an increase in cellular lifespan (van der Veer *et al.*, 2007). From an ageing perspective it has been noted that declining NAD^+ levels are observed in a number of older organisms (Braidy *et al.*, 2011; Gomes *et al.*, 2013). It was also recently identified that low NAD^+/NADH levels provoke a cell cycle arrest, but in addition also drive p53 activation through AMPK (5' adenosine monophosphate-activated protein kinase), this in turn was shown to initiate the IL-1 arm of the SASP (Wiley *et al.*, 2016). Recent work has identified NAMPT as being a regulator of the SASP independently of the cell cycle arrest (Nacarelli *et al.*, 2019). It was shown that NAD^+ metabolism is a key regulator of determining the level of SASP secretion. In contrast to the Wiley et al study, they found that NAD^+ suppresses AMPK, which decreases the p53-mediated inhibition of p38MAPK (P38 mitogen-activated protein kinases) which leads to an increase in NF-κB activity and subsequently an elevated SASP. It is proposed that this may explain why forms of senescence such as OIS which are associated with a higher NAD^+/NADH ratio have a more intense SASP than forms of senescence such as replicative and stress induced senescence which have a lower NAD^+/NADH ratio (Nacarelli *et al.*, 2019).

Emerging work has begun to demonstrate an intricate link between NAD^+ levels and downstream effectors of the senescence programme. NAD^+ may also impact on the senescence phenotype by its effect on the activity of mitochondrial enzymes, specifically the NAD^+ dependent malic enzymes 1 and 2. These enzymes process the tricarboxylic acid cycle metabolite malate into pyruvate, interestingly, cells depleted of malic enzyme 1 and 2 undergo premature senescence via a p53-dependent mechanism (Jiang *et al.*, 2013). NAD^+ has also been implicated as having a regulatory role in DNA damage repair. PARP, is a key element of the DDR which requires NAD^+ to effectively repair genomic damage. Consistently, it has been demonstrated that following irradiation PARP inhibition promotes an accelerated onset of

senescence due to unrepaired DNA damage (Efimova *et al.*, 2010). A further group of proteins associated with DNA damage repair is the sirtuins. The sirtuins are deacetylases that are dependent on NAD^+ in general, the sirtuins family are decreased in senescence and as such render cells more prone to oxidative stress and DNA damage, this is likely associated with the decreased levels of NAD^+ (Grabowska *et al.*, 2017; van de Ven *et al.*, 2017). From an *in vivo* perspective, the age-related decline in NAD^+ levels can be prevented by inhibiting NADase cluster of differentiation 38 (NADase CD38) which is responsible in part for degrading NAD^+, this has been associated with reduced levels of the senescence marker TAF in the muscles and liver of mice (Tarrago *et al.*, 2018). Similarly, supplementation of NAD^+ using the precursor nicotinamide mononucleotide was demonstrated to alleviate telomere dysfunction in mice in part due an increase in function of sirtuin 1 which is responsible for DNA repair (Amano *et al.*, 2019). Interestingly, CD38 is not highly expressed in senescent cells, however, exposure of non-senescent cells to the SASP promotes an increase in CD38 mRNA and protein levels which was associated with an increase in NADase CD38 activity. Therefore it has been suggested that the SASP may be responsible for disrupting NAD+ homeostasis during the ageing process (Chini *et al.*, 2019).

Another two mitochondrial peptides which have been implicated in the regulation of the SASP are humanin and MOTS-c. These two peptides have been found to be increased in senescent cells. Interestingly, it has been demonstrated that following the treatment of senescent cells with these two peptides, there is an engagement of mitochondrial energetics which results in an overall increase the SASP (Kim *et al.*, 2018). From a mechanistic perspective, it has been demonstrated that humanin is produced in response to stress and subsequently activates the JAK/STAT (janus kinase/signal transducers and activators of transcription) pathway. Previous work has implicated the JAK/STAT pathway as having a regulatory role in cytokine production, consistently, work *in vitro* has demonstrated that pharmacological inhibition of JAK/STAT can ameliorate the SASP and has beneficial effects such as reducing frailty in mice *in vivo* (Xu *et al.*, 2015b). The other peptide MOTS-c is a known activator of AMPK, which as discussed earlier can feed into mTOR/PGC1-β mediated mitochondrial biogenesis, as well as inducing a cell cycle arrest via p53 and p21 activation (Jiang *et al.*, 2013; Correia-Melo *et al.*, 2016; Kim *et al.*, 2018).

Interestingly, it has also been observed that AMPK can be engaged by increases in the AMP to ATP ratios (Mihaylova and Shaw, 2011). It is known that disruption to the electron transport chain can impact on the production of ATP, affecting this ratio. A number of studies have

reported that the AMP to ATP ratio is increased in senescent cells (Wang *et al.*, 2003; Zwerschke *et al.*, 2003). Furthermore, inhibition of ATP synthase to perturb the ratio also induces premature senescence in human fibroblasts (Stockl *et al.*, 2006). Defects in the electron transport chain have also been implicated in senescence, for example, inhibition of complex I using rotenone, complex II by 2-thenoyltrifluoroacetone and complex III by antimycin A induces senescence (Yoon *et al.*, 2003; Stockl *et al.*, 2006; Moiseeva *et al.*, 2009). In addition, it is known that for the electron transport chain to function effectively the mitochondrial membrane potential needs to be maintained, however, senescent cells display a depolarised membrane (Passos *et al.*, 2007). It has also been demonstrated that depolarisation of human fibroblasts by partial uncoupling using carbonylcyanide p-trifluoromethoxyphenylhydrazone leads to premature senescence and an increase in ROS (Stockl *et al.*, 2007). From an ageing perspective it has been demonstrated that genes associated with the electron transport chain become downregulated with age in a number of organisms such as flies, worms and monkeys (Kayo *et al.*, 2001; McCarroll *et al.*, 2004; Ferguson *et al.*, 2005). At this stage it is not entirely clear how defects in the electron transport chain can drive senescence and is the subject of ongoing research, however, one hypothesised idea is that defects promote an increase in the production of ROS which are a known driver of senescence.

Collectively, these studies are beginning to unveil the role of mitochondrial metabolites imbalances in provoking both senescence and the SASP. Therefore one strategy to offset the deleterious effects of senescence may be to restore the balance of these metabolites.

1.7.2. Mitochondrial DAMPs as Candidates for the SASP

An emerging and unexplored area in the context of senescence is that of damage associated molecular patterns (DAMPs). DAMPs can take the form of nuclear or cytosolic proteins which can engage the innate immune system to provoke a pro-inflammatory response. As previously discussed the molecular mechanism by which mitochondria trigger the SASP is not completely understood. One potential molecule which could trigger inflammation is mitochondrial DNA (mtDNA). Mitochondria have their own genome which is distinct from the nuclear genome, it is 16569bp and takes the form of a circular double helix located within the inner membrane. mtDNA is of prokaryotic origin and of striking similarity to that of bacterial DNA i.e. it is not methylated like nuclear DNA (Gustafsson *et al.*, 2016). As such, free mtDNA has been established as a potent DAMP which can provoke a strong inflammatory response via the innate immune system (West *et al.*, 2015). It has been demonstrated that in a variety of tissues mtDNA can provoke the secretion of various pro-inflammatory cytokines such as IL-1β, IL-6, IL-8 and

TNFα, all of which have been implicated in the SASP (Little *et al.*, 2014). From an ageing perspective mtDNA is particularly interesting as it has been observed that circulating mtDNA free from mitochondria increases with age in humans. This increase also correlates with the expression of a number of pro-inflammatory cytokines (Pinti *et al.*, 2014). Of further interest is that two studies investigating the relationship between mitochondria and the SASP have demonstrated that when Rho (0) fibroblasts which do not contain mtDNA are induced to become senescent they have a dramatically decreased secretion of SASP factors (Correia-Melo *et al.*, 2016; Wiley *et al.*, 2016). Mitochondrial DAMPs do not comprise solely of mtDNA, other DAMPs identified which can provoke a pro-inflammatory response include; transcription factor A (TFAM) which is bound to mtDNA, cytochrome C (a pro-apoptotic inner membrane protein), cardiolipin (an inner membrane lipid) and ATP (Wilkins *et al.*, 2017). Finally, it has also been recognised that in senescent cells DNases such as TREX1 and DNase 2 which are responsible for degrading cytoplasmic DNA are downregulated, as such it is possible that if mtDNA is escaping from mitochondria during senescence it would not be rapidly removed and therefore be available to promote a pro-inflammatory response (Takahashi *et al.*, 2018). Taken together these observations question whether mtDNA may be released by dysfunctional mitochondria during senescence and provoking the SASP through the innate immune system.

It is known that the toll-like receptors (TLR) have evolved to recognise unmethlyated DNA whereby a rapid immune response can be mounted following the detection of bacterial infection. It has recently been demonstrated that TLR9 specifically can identify mtDNA and generate an inflammatory response through p38 MAPK and NF-κB (Bao *et al.*, 2016). TLR9 is located on the endoplasmic reticulum prior to stimulation, its activation can also stimulate transcription of interferon (IFN) genes (Leifer *et al.*, 2004; Uematsu and Akira, 2007). This is particularly interesting as both NF-κB and type 1 IFN genes have been implicated in prompting the secretion of SASP factors in response to cytoplasmic nuclear DNA (Dou *et al.*, 2017; Gluck *et al.*, 2017; Yang *et al.*, 2017; De Cecco *et al.*, 2019). In addition, TLR2 has recently been implicated in controlling the senescence associated secretory phenotype in OIS through their recognition of acute-phase serum amyloids A1 and A2 which act as DAMPs, however, in this study there was no observable increase in gene expression of TLR9 (Hari *et al.*, 2018). Therefore, it is plausible that free mtDNA could be acting as a DAMP and triggering an inflammatory response through a TLR9 dependent mechanism.

Intracellular free mtDNA can also be recognised by the NLRP3 inflammasome (nucleotide binding domain and leucine-rich repeat pyrin domain containing 3) (Nakahira *et al.*, 2011;

Shimada *et al.*, 2012). The NLRP3 inflammasome responds to DAMPs and PAMPs (pathogen-associated molecular patterns), once activated it forms a complex with apoptosis-associated speck-like protein, this in turn recruits and promotes autocatalytic activation of caspase 1 into cleaved caspase 1. The role of cleaved caspase 1 is then to cleave pro-IL-1β to the mature form IL-1β, which promotes its secretion and that of IL-18 (Jo *et al.*, 2016). It has been demonstrated that macrophages which have been depleted of mtDNA have a vastly reduced secretion of IL-18 by the NLRP3 inflammasome (Shimada *et al.*, 2012). In the context of senescence, the NLRP3 inflammasome has been found to be active and contribute to the SASP in OIS and senescent vascular endothelial cells (Acosta *et al.*, 2013; Yin *et al.*, 2017; Wiggins *et al.*, 2019). The regulation of the NLRP3 inflammasome is not very clear, however there is evidence that AMPK plays an important role in its regulation (Cordero *et al.*, 2018). It has also been demonstrated that NLRP3 mediated low grade inflammation contributes to ageing as genetic clearance of NLRP3 relieves a number of age-related pathologies such as bone loss and loss of glycemic control (Youm *et al.*, 2013). Furthermore, anti-ageing drugs such as rapamycin, metformin and resveratrol which are known to inhibit the SASP *in vitro* have also been demonstrated to target and inhibit the NLRP3 inflammasome, therefore it is plausible that some of the SASP supressing effects may be due to action on the NLRP3 inflammasome (Li *et al.*, 2016; Ko *et al.*, 2017).

A third innate immune pathway which has been implicated in the recognition of mtDNA is the cGAS-STING (cyclic GMP-AMP synthase – stimulator of interferon genes) axis. cGAS is a cytosolic sensor which recognises double-stranded DNA and has recently been demonstrated to promote a response to mtDNA (West *et al.*, 2015). Under normal circumstances, cGAS exists in an auto-inhibited state, however, following the recognition of DNA, the active site of cGAS undergoes a conformational change and cyclic GMP-AMP (cGAMP) is synthesised as a secondary messenger. cGAMP binds to STING which is located at the endoplasmic reticulum, this activates STING and promotes its translocation to the golgi apparatus. STING then activates TBK1, which phosphorylates and leads to dimerization of IRF3 (interferon regulatory factor 3), IRF3 then translocates to the nucleus where it promotes transcription of INF-β genes. STING can also phosphorylate IKK (inhibitor of nuclear factor kappa-B kinase) which targets it for degradation, following IKK degradation, NF-κB is activated which also translocates to the nucleus and promotes transcription of IFN-β genes. This leads to induction of the inflammatory cytokines tumour necrosis factor (TNF), IL-1β and IL-6 (Chen *et al.*, 2016). The cGAS-STING axis has been widely implicated in senescence by a number of groups. It has

recently been demonstrated that during senescence Lamin B1, a protein which protects nuclear integrity is lost, in turn it has been observed that fragments of nuclear DNA bud off and form in the cytoplasmic region. These fragments of nuclear DNA have been termed cytosolic chromatin fragments (CCFs) and have been shown to promote the SASP following there recognition by cGAS and subsequent downstream activation of NF-κB (Ivanov *et al.*, 2013; Dou *et al.*, 2017; Gluck *et al.*, 2017; Yang *et al.*, 2017). These studies employed genetic ablation of cGAS and/or STING. It was found that the absence of cGAS in human fibroblasts impaired the SASP but did not avert the cell cycle arrest or DDR, however there was clear inactivation of NF-κB without cGAS. Furthermore, *in vivo* following irradiation in STING KO mice there was a depletion of SASP factors such as IL-1α and β, but no changes in markers of DNA damage such as γH2AX (Dou *et al.*, 2017). Interestingly in fibroblasts derived from mice, knockout of cGAS impaired both the SASP and the cell cycle arrest, furthermore, it was demonstrated that *in vivo* there was an overall reduction in senescent cells and the SASP in cGAS deficient mice following irradiation (Gluck *et al.*, 2017). To date, all studies addressing the role of cGAS and STING in senescence have used genetic silencing methods to suppress them. Naturally, this is the gold standard method for implicating the role of a protein in a process, however, there have been no pharmacological means of silencing these pathways. Recently, it has been identified for the first time that a subset of anti-malarial drugs such as quinacrine dihydrochloride (QC) and 9-amino-6-chloro-2-methoxyacridine (ACMA), chloroquine and primaquine disrupt the binding of DNA to cGAS and can prevent downstream activation of type 1 IFNs (An *et al.*, 2015). Furthermore, a small molecule inhibitor has been identified that inhibits the catalytic pocket of cGAS (but does not prevent binding to double stranded DNA), this inhibitor has been show to block type 1 interferon activity both *in vitro* and *in vivo* in an autoimmune disease model (Vincent *et al.*, 2017). There has been intense interest from the autoimmune field to discover inhibitors of the cGAS-STING axis, however, the role of these drugs has not been addressed in the context of senescence. Therefore it is of extreme interest to determine the role of these drugs as potential senostatic therapies (drugs which remove the deleterious SASP but not the tumour suppressive effects of the cell cycle arrest).

At this stage, there is evidence to suggest these innate immune pathways are active in senescence, but it is not determined whether mtDNA could be driving them.

1.8. Mitochondrial Outer Membrane Permeabilisation

A key question to address is; what are the mechanisms that could enable the release of mitochondrial DAMPs into the cytosol? Here we review an emerging phenomenon in the field of apoptosis where it has been identified that mitochondria can become permeabilised in the absence of triggering cell death. As there is significant overlap between apoptosis and senescence it is considered that this could be a potential molecular mechanism that could facilitate release of mitochondrial DAMPs into the cytosol.

1.8.1. Limited Mitochondrial Outer Membrane Permeabilisation

Apoptosis is a tightly regulated process which ensures that damaged and defective cells are eliminated quickly and effectively. The purpose being to prevent damaged cells dividing and potentially becoming tumourigenic (Taylor *et al.*, 2008). Apoptosis usually occurs in response to stressful intrinsic and extrinsic stimuli such as DNA damage and genotoxic stress. Following the induction of intrinsic damage, the pro apoptotic members of the BCL-2 family become activated. PUMA, BCL-2-associated agonist of cell death (BAD) and NOXA are pro-apoptotic members which supress the anti-apoptotic members BCL-XL and BCL-2 (Taylor *et al.*, 2008). As discussed earlier, these anti-apoptotic members are upregulated in senescent cells and hence render there resistance to apoptosis, these members are also the targets of senolytics such as navitoclax (Chang *et al.*, 2016). Once the anti-apoptotic members are inhibited, activation of BAX (BCL-2-associated x protein) and BAK (BCL-2 homologous antagonist killer) occurs. Bax and Bak are two nuclear-encoded proteins present in higher eukaryotes that function to permeabilise the mitochondrial outer membrane in a regulated manner to facilitate cell death via apoptosis. BAK is constitutively located at the outer membrane of the mitochondria where it is anchored via its hydrophobic C-terminal α9 helix, when inactive BAK exists as a monomer (Ferrer *et al.*, 2012). BAX exists in a more dynamic state, in non-apoptotic cells BAX localises to the mitochondria, however, it is constantly retro-translocated to the cytosol by BCL-XL to prevent formation of active oligomers (Schellenberg *et al.*, 2013). The activation of BAX and BAK can be triggered by intrinsic stimuli such as DNA damage or cytokine deprivation. Similarly, they can also be activated by external stimuli via the activation of the death receptor pathway which is initiated by TNF-α, Fas ligand and TNF-related apoptosis inducing ligand (Westphal *et al.*, 2011).

Following activation, both BAX and BAK undergo extensive conformational changes where there hydrophobic regions become buried within the outer membrane or surrounding protein interface, this process forms large oligomers which span the outer membrane to the cytosol.

Specifically for BAX, eversion of its α9 tail allows it to become integrated with the outer membrane, in doing so the 6A7 epitope is exposed which is a characteristic mark of its activation (Gavathiotis *et al.*, 2010). The formation of pores via BAX and BAK is an area of immense study and as yet is particularly unclear due to its complexity. It has been proposed that BAX forms a "daisy chain" like oligomer, whereas BAK forms a more doughnut shaped octameric pore (Reed, 2006; Pang *et al.*, 2012). At this stage, it is clear that BAX and BAK can form pores independently, however, it is unclear whether they co-interact during the formation of pores, although evidence does suggest there is an element of dependency for BAX during BAK pore formation (Mikhailov *et al.*, 2003). Of further interest in the context of senescence is that mitochondrial dynamics have been associated with oligomerisation of BAX. Specifically, the loss of DRP1 (a mediator of mitochondrial fission which is downregulated during senescence) has been associated with inhibiting apoptotic scission of mitochondria but does not prevent the translocation and accumulation of BAX clusters (Karbowski *et al.*, 2002; Montessuit *et al.*, 2010). Following pore formation, the mitochondrial membrane integrity is lost and the membrane becomes depolarised. Proteins that are normally conserved within the inner membrane can escape through the BAX and BAK pores. The process of pore formation and subsequent release of inner membrane proteins is referred to as mitochondrial outer membrane permeabilisation (MOMP). Specifically in the context of apoptosis, cytochrome C is released, once located in the cytosol it forms a complex with apoptotic protease-activating factor 1 and pro-caspase 9 which is referred to as the apoptosome. The apoptosome then activates caspase 9 which promotes cleavage of caspase 3 and 7. These two executioner caspases promote fragmentation of the nuclear DNA and promote blebbing of the cell membrane via activation of ROCK 1. Cells then shrink and are phagocytosed by macrophages, concluding the apoptosis process (Tait and Green, 2010).

Classically, MOMP has always been considered an all or nothing process, referring to that all previous work has demonstrated that the cell death process is either engaged or it is not. However, a recent study has revealed that in fact a small subset of mitochondria within a cell can become permeabilised without engaging the cell death machinery. Specifically, using super resolution microscopy it was observed that following mild stress there was an observable release of cytochrome C which was associated with sub-lethal activation and cleavage of caspase 3 and 7. However, it was demonstrated that limited mitochondrial outer membrane permeabilisation termed minority MOMP (miMOMP) does not meet the required threshold to induce cell death, however, the sub-lethal activation of caspase 3 and 7 results in DNA damage.

Specifically, the DNA damage induced by sub-lethal activation of caspase 3 and 7 occurs through the DNase CAD (caspase activated DNase). CAD is responsible for fragmenting DNA during apoptosis. During miMOMP, it was demonstrated both *in vitro* and *in vivo* that CAD induces double stranded DNA breaks and subsequently a DDR. Accordingly, it was demonstrated that CAD triggers cleavage of PARP1 and phosphorylation of JNK and H2AX in a caspase dependent manner (Ichim *et al.*, 2015).

Furthermore, this DNA damage and miMOMP were demonstrated to be tumourigenic *in vivo*. This permeabilisation and subsequent DNA damage was dependent on the formation of BAX and BAK pores (Ichim *et al.*, 2015). As DNA damage is a key feature of senescent cells and is essential in promoting the induction of senescence via the DDR, it is of significant interest to understand whether mitochondrial dysfunction that is characteristic of senescence is in part driven by this miMOMP process. Prior to the discovery of this miMOMP phenomenon, a separate group investigating the potential of BCL-2 inhibitors to induce apoptosis in cancer cells discovered that the same anti-apoptotic BCL-2 inhibitor (ABT737) was able to induce senescence in a cancer cell line. They discovered that this occurred in a p53 and p21 dependent manner due to DNA damage as a consequence of low grade caspase 3 activity which was insufficient to induce apoptosis (Song *et al.*, 2011). Therefore one may speculate that this observation was driven by miMOMP. Furthermore, could this miMOMP be a potential mechanism for releasing mitochondrial DAMPs and mediating the SASP?

Interestingly, this process of miMOMP can be induced by treatment using the BCL-2 inhibitor ABT737, which as mentioned earlier is a senolytic drug (Ichim *et al.*, 2015; Chang *et al.*, 2016). Therefore, it seems reasonable to question whether these inhibitors are in fact acting as a double edged sword. It has been established that they are effective in the abolition of senescent cells, however, it is yet to be addressed whether paradoxically these inhibitors may be inducing miMOMP in healthy proliferating cells leading to DNA damage and thus potentially promoting genomic instability and further senescence. This therefore raises a number of questions; firstly, will treatment with ABT737 be inducing damage in non-senescent cells? Secondly, is this process of miMOMP and subsequent DNA damage a form of mitochondrial dysfunction which could be a driver of senescence induction?

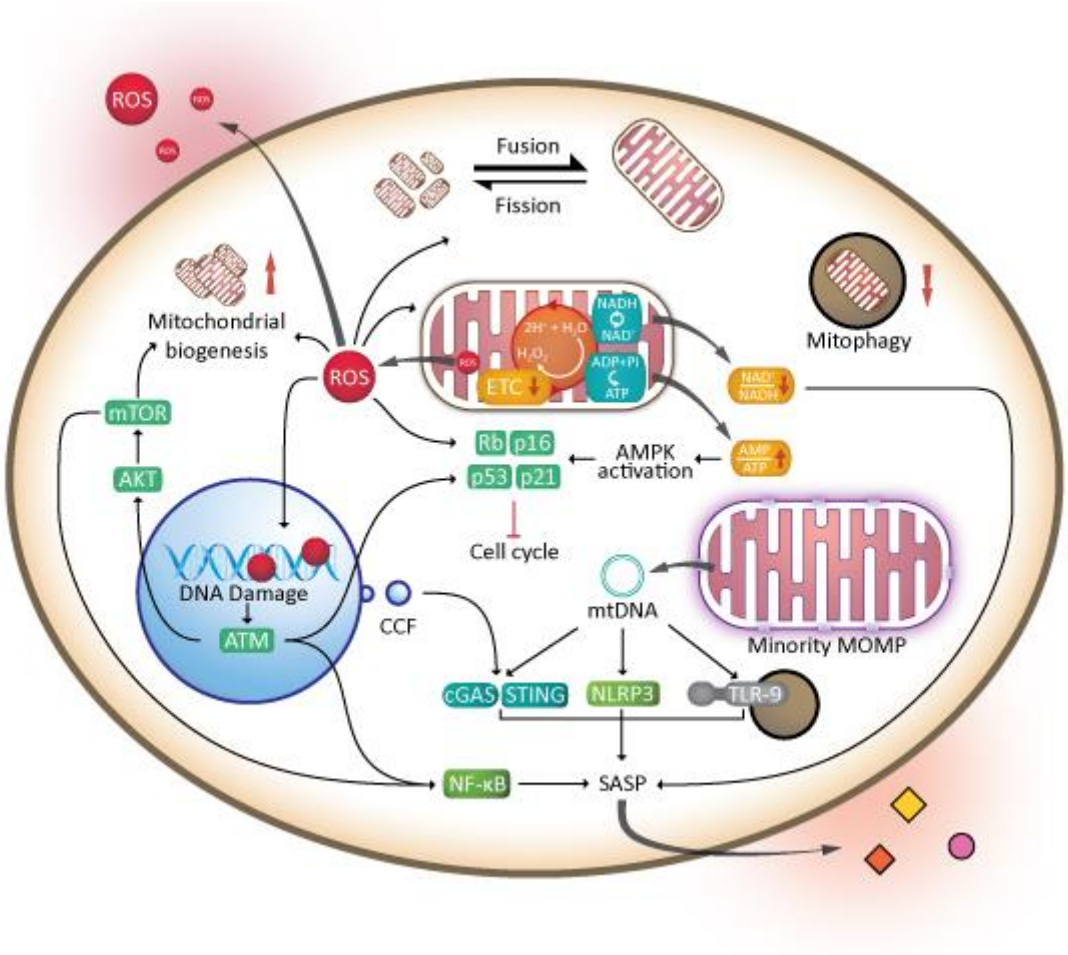

Figure 1.3– Overview of the role of mitochondria and cellular senescence.

During senescence there are dramatic changes to the morphology of the mitochondrial network, this is facilitated in part by increases in mitochondrial biogenesis, changes in the fission/fusion machinery as well as an impairment of mitophagy to clear dysfunctional mitochondria. Furthermore, there is disruption to the electron transport chain which has been associated with changes in metabolite levels such as that of AMP and NAD^+. Senescent cells are characterised by an exacerbation in the production of ROS, this has been demonstrated to drive senescence through the induction of DNA damage, as well as damage neighbouring cells. Finally, we hypothesise that the recently discovered phenomenon of miMOMP may be promoting release of mtDNA which could be promoting the SASP through one of the innate immune system pathways such as cGAS-STING, the NLRP3 inflammasome or TLR-9. Figure adapted from (Chapman et al., 2019).

1.8.2. Mechanisms facilitating mtDNA Release

Although a wide number of studies have identified cytosolic mtDNA and subsequent immune responses, it has not been known until recently how mtDNA can escape from the inner membrane of the mitochondria. Within the apoptotic field it was noted that cells undergoing caspase independent apoptosis produced a type 1 IFN response which was shown to occur as a consequence of mtDNA and subsequent cGAS activation (Rongvaux *et al.*, 2014; White *et al.*, 2014). These studies implicated that mtDNA release was dependent on BAX and BAK pores, however, recent work has highlighted the underlying mechanism. Using a combination of sophisticated live-cell imaging and super-resolution microscopy techniques it has been demonstrated that BAX and BAK form oligomers which result in enlarged pores, termed macropores. These macropores gradually widen up to 1µm which allow the inner membrane to herniate through. It is not exactly clear how mtDNA escapes but it is speculated that the inner membrane ruptures allowing the escape of mitochondria components including mtDNA to the cytosol (McArthur *et al.*, 2018; Riley *et al.*, 2018). Importantly, it was demonstrated that deletion of both BAX and BAK is required to prevent mtDNA release as single deletion of either BAX or BAK using CRISPR-CAS9 did not prevent its release. Therefore demonstrating that BAX or BAK can form macropores independent of each other (Riley *et al.*, 2018).

Of further interest is that these studies used the BCL-2 inhibitor ABT737 to provoke this process (McArthur *et al.*, 2018; Riley *et al.*, 2018). As discussed earlier, this drug is being considered as a senolytic (Zhu *et al.*, 2015b). Therefore it is of interest to understand whether a side effect of senolytic therapy using this family of drugs may in fact promote inflammation through mtDNA release. Not only that, considering there are wide spread changes in both mitochondrial function and morphology during senescence, it is plausible that a similar phenomenon of mtDNA release may be occurring to provoke the SASP through cGAS-STING.

1.8.3. The Relationship between Caspases and Senescence

Both apoptosis and senescence are intricate processes designed to avert damaged cells from replicating, as such there is significant mechanistic overlaps between the two. The caspases are a family of proteases which have been largely restricted to their role in apoptosis, however, emerging research has revealed that they participate in many other cellular processes such as T-cell maintenance, tissue differentiation and regeneration, as well as neural development. The role of caspases in senescence remains a vastly understudied area. Caspases can be broadly subdivided into two functions; those that facilitate apoptosis and those that regulate inflammation. In humans, caspases 2, 8, 9 and 10 have been implicated in initiating the

apoptotic process and caspase 3, 6 and 7 are recognised as executing the process. Caspase 1, 4, 5 and 12 on the other hand are known to regulate inflammation (Shalini *et al.*, 2015).

The role of caspases in apoptosis has been well defined. Their role is to dismantle and degrade the cell without damaging neighbouring cells or promoting inflammation by release of intracellular components. Apoptosis occurs in response to excessive stress intrinsically or extrinsically. Extrinsic activation occurs following activation of the death receptor, which leads to recruitment and dimerization of caspase 8 (Kang *et al.*, 2004). This dimerization promotes a caspase cascade which results in the cleavage and activation of the executor caspases 3, 6 and 7. Caspase 3 and 7 have similar substrate specificity whereas the contribution of caspase 6 is less clear. Caspase 3 is the best characterised and is known to activate the endonuclease CAD. CAD functions to cleave and fragment the nuclear DNA which leads its degradation (Sakahira *et al.*, 1998). In addition, caspase 3 acts on gelsolin which cleaves actin filaments. This process leads to reorganization and disintegration of the cell into apoptotic bodies which can then be targeted for non-inflammatory phagocytosis (Kothakota *et al.*, 1997; Fadok *et al.*, 2001). Caspase 8 also can promote cleavage of BID which can activate the intrinsic pathway to promote the caspase cascade. This is facilitated by the initiator caspase 9 which is regulated by the BCL-2 and BH-3 family of proteins. Release of cytochrome c binds and forms a complex termed the apoptosome with caspase 9 as described earlier, this leads to cleavage and activation of caspase 3 and subsequently apoptosis (Li *et al.*, 1997).

In the context of senescence, it has been recognised that both IL1α and IL-1β are primed by caspases. In OIS, caspase 1 levels are elevated, here, it functions as part of the NLRP3 inflammasome where it cleaves IL-1β to promote cytokine production. Furthermore, inhibition of caspase 1 reduced the SASP, as well as partially preventing the induction of p21-mediated cell cycle arrest (Acosta *et al.*, 2013). Interestingly, another subset of caspases have been identified in activating the IL-1α arm of senescence. IL-1α can provoke the SASP by a signalling cascade that activates NF-κB following activation of the IL-1 receptor. In humans this cleavage occurs via caspase 5 and in mice caspase 11, silencing of these lead to a reduction in the IL-1α arm of the SASP (IL-6, IL-8 and MCP-1). Furthermore, it was demonstrated that silencing of caspase 11 (the murine homologue of caspase 5 in humans) *in vivo* following senescence induction lead to a decrease in the infiltration of macrophages to the site of senescent cells, therefore indicating that caspase mediated activation of IL-1α is crucial in signalling to the immune system to clear senescent cells away (Wiggins *et al.*, 2019).

Interestingly, caspase 3 has also been implicated in driving senescence by inducing levels of DNA damage that are insufficient to induce apoptosis. This has been demonstrated in response to the BH3-mimetic ABT737 and the ROS peroxynitrite which is a nitric oxide radical (Matarrese *et al.*, 2005; Song *et al.*, 2011). Outside of senescence it has been demonstrated that caspase 3 can impact on proliferation. Specifically, B cells lacking caspase 3 show increased hyperproliferation both *in vitro* and *in vivo*. This proliferation can be rescued by dual knockout of caspase 3 and p21 (a substrate of caspase 3), suggesting that caspase 3 plays a role in regulating the expression of p21 (Woo *et al.*, 2003). Interestingly, a recent study has established that p21 plays a role in regulating the activation of caspase 3, as knockdown of p21 in senescent cells, leads to an enhancement of the DDR, ATM then triggers NF-κB/TNF-α signalling which leads to caspase 3 mediated cell death via JNK (Yosef *et al.*, 2017). Taken together it seems likely that activity of caspase 3 may well be reinforcing the DDR, and naturally its activity must be subject to tight regulation to prevent the balance being tipped and apoptosis occurring. Therefore, it is of particular interest to address whether miMOMP could be promoting this low grade caspase 3 activity in senescent cells.

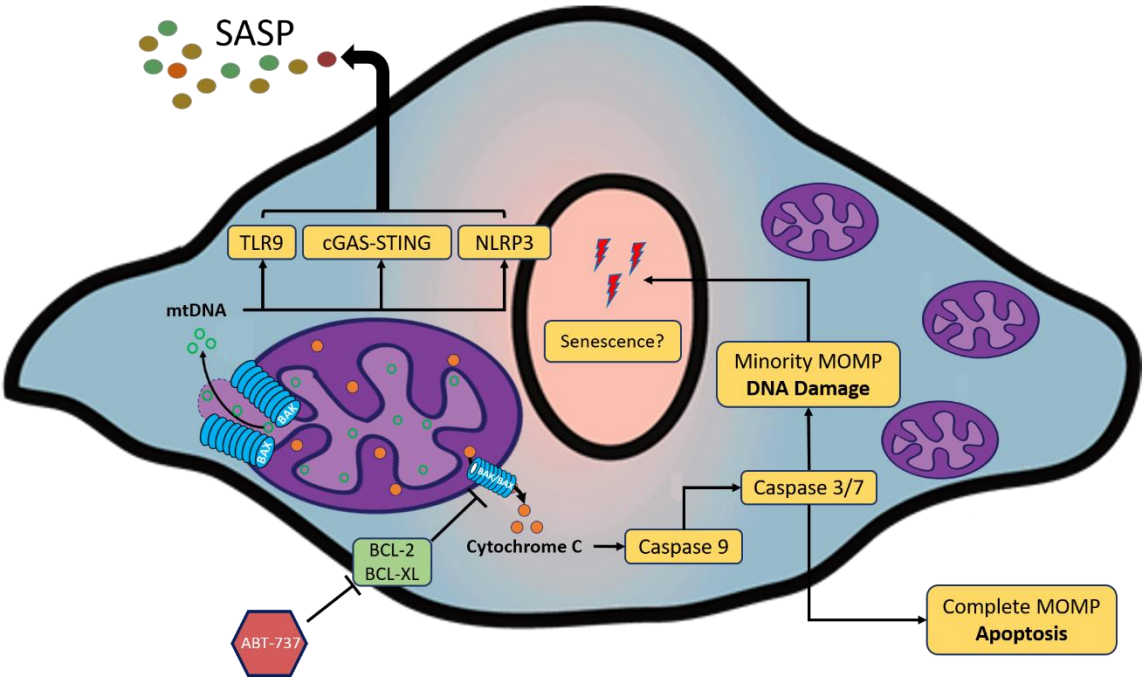

Figure 1.4– Hypothesised mechanism of mtDNA release and role of miMOMP as a driver of senescence.

First, it is hypothesised that during senescence mtDNA may be escaping from dysfunctional mitochondria, it is plausible that this is being facilitated by the formation of BAX and BAK macropores where the inner mitochondrial membrane herniates and allows its release. Once in the cytosol it could promote the SASP through one of the innate immune pathways such as TLR9, cGAS-STING or NLRP3. Second, it has been demonstrated that a small number of mitochondria can be permeabilised in the absence of cell death, termed minority MOMP. It is of interest to understand whether this process is a feature of senescence, as it can promote a DDR through sub-lethal caspase 3 activity. In addition, it is feasible that miMOMP may facilitate mtDNA release. The process of miMOMP can be provoked pharmacologically using the BH3 mimetic ABT-737 which inhibits the anti-apoptotic BCL-2 and BCL-XL proteins which normally prevent mitochondria from permeabilising via BAX and BAK pores. Therefore the capacity for miMOMP to induce senescence can be assessed using ABT-737.

1.9. Research Aims

At this stage, mitochondria have been implicated as having an essential role in driving the pro-inflammatory features of senescence, although the underlying mechanisms responsible remain unknown. Furthermore, using genetic manipulation it has been demonstrated that the cGAS-STING axis is involved in the regulation of the SASP, however, the effects of pharmacological inhibitors on this pathway have not been explored. Therefore, the overall aim of this study is to dissect the intricate relationship between mitochondria and cellular senescence.

Specifically, the aims of this study were:

1. Investigate the involvement of mtDNA in senescence and as a potential candidate to act as a DAMP for the induction of the SASP.

2. Explore the role of sub-lethal stress as a driver of mitochondrial permeabilisation. Does this process play a role in driving senescence or the SASP?

3. Determine whether pharmacological inhibitors of the cGAS/STING pathway have potential as a therapeutic strategy for suppressing the SASP.

2. Materials and Methods

2.1. Cell Culture

Cell culture work has been performed using human embryonic lung MRC5 fibroblasts acquired from ECACC, Salisbury, UK that were stored in aliquots of 1 million cells at -180°C. These cells have been cultured at 37°C, 5% CO_2, 20% O_2 in Dulbecco's Modified Eagle's Medium D5796 – High Glucose. 500ml media is supplemented with 10% FBS (foetal bovine serum), 6ml of penicillin-streptomycin (100µg/ml) and 6ml of 2mM L-glutamine.

HEK293T cells were used for lentiviral transduction and were maintained in DMEM as detailed above with further supplementation using 1% non-essential amino acids, G418 antibiotic (10µl/ml) and sodium pyruvate (5ml of 100mM stock solution).

Parental and rho (0) osteosarcoma 143B cells were a gift from the Mitochondrial Research Group at Newcastle University. These cells were maintained in DMEM as detailed above with further supplementation using 5% non-essential amino acids and 25µg/ml of Uridine.

U20S cells were a gift from Dr Stephen Tait at the Beatson Institute, Glasgow. These were maintained in DMEM media as listed above.

2.2. Induction of Senescence

For stress-induced senescence, MRC5 fibroblasts were subjected to 20Gy of X-ray irradiation using an X-Rad 225 irradiator (Precision X-Ray, N-Branford, CT USA). Stress-induced senescent cells were analysed 10 days post X-ray irradiation (whereby the day of irradiation is classed as day 0). The induction of senescence *in vitro* was confirmed at day 10 by characterising cells for the presence of SA-β-Gal, the induction of p16 and p21, as well as the absence of proliferative markers such as Ki67 and EdUincorporation. In addition, cells were assessed for morphological changes such as an increase in cell size, nuclear size and a more flattened appearance. Details of how these experiments were conducted is described later in this section.

In order to attain a model of replicative senescence, cells were maintained in culture until they stopped dividing and developed the senescence phenotype. Replicatively senescent cells were confirmed by culturing until a growth plateaux was achieved, cells were then maintained for a further 4 weeks to confirm that there was less than 0.5 population doublings. The senescence phenotype was then confirmed using the parameters described above.

2.3. Maintenance, Storage and Revival of Cells

Cells were counted using a 0.2mm Fuchs-Rosenthal haemocytometer with 20µl of cell suspension. Cells were manually counted on a DMIL Leica Microscope. An average of four counts of 8 adjacent squares gives the number of cells x 10^4/ml, subsequently the population doubling was calculated using the following calculation:

PD = Initial PD + (log(Total number of cells/Number of cells seeded)/log(2))

For long-term storage of cells, cells were trypsinised, counted, centrifuged at 800g and then suspended in of 95% FBS/5% DMSO and aliquoted at a density of $1x10^6$ into a cryogenic vial. These were then placed in a Nalgene Cryo freezing container for 24 hours at -80°C prior to storage in liquid nitrogen.

In order to return cells stored in liquid nitrogen to culture, the cryo-vials were placed at 37°C. Once defrosted these cells were seeded into a 75 cm^2 flask, once attached the media was replaced with fresh media to remove any residual DMSO.

2.4. Drugs and Inhibitors

For each drug/inhibitor used a stock solution was prepared, this was then aliquoted and stored at the appropriate temperature to avoid repeat freezing and thawing. Drugs and inhibitors were diluted in media prior to being added to cells.

The following drugs and inhibitors were used:

Drug/Inhibitor	Supplier and Catalogue Number
ABT737	Abcam (ab141336)
ACMA	ThermoFisher Scientific (A1324)
BAX Channel Blocker	Adooq Biosciences (A15335)
BAM7	Sigma (SML0641)
BIPv5	Sigma (SML0641)
Bongkrekic Acid	Abcam (ab142111)
Caspase 1 Inhibitor (Ac-YVAD-cmk)	Sigma (SML0429)
Caspase 2 Inhibitor (Ac-VDVAD-CHO_	Sigma (SCP0076)
Caspase 3 Inhibitor (Ac-LDESD-CHO)	Sigma (SCP0079)
Caspase 4 Inhibitor (Ac-LEVD-CHO)	Sigma (SCP0087)
Cyclosporin A	Sigma (SML1575)
2',3'-Dideoxycytidine (ddC)	Abcam (ab142240)
Olesoxime (TRO 19622)	Sigma (T3077)
RU.521	Glixx Laboratories (GLXC-10900)
Quinacrine Dihydrochloride	Sigma (Q3251)
QVD	Abcam (ab141421)

Table 2.1 - List of drugs and inhibitors used in experiments as well as suppliers and catalogue numbers.

2.5. Generating stably expressing BAK/BAX and STING deficient cell lines

Plasmid expansion and purification:

Plasmid elution

Plasmids (BAX, BAK, STING (three separate constructs #1, #2 and #3) and Empty Vector) were received precipitated on filter paper. The plasmid DNA was eluted by cutting out a small section of filter paper using sterile scissors, and placing it into a 1.5ml micro-centrifuge tube

with 20µl of nuclease-free H_2O. The filter paper was then mixed with the H_2O using a sterile pipette tip, and left at room temperature for 2 minutes.

Bacterial transformation

2µl of eluted plasmid DNA was added to 10µl of NEB Stable Competent E. *coli* cells in an Eppendorf tube, and mixed by gently vortexing. Tubes were then placed on ice for 30 minutes, and the cells were subsequently heat-shocked at 42°C for 30 seconds, and placed on ice for a further 5 minutes. Then, 500µl of SOC outgrowth medium (Invitrogen, Cat. Number 15544-034) was added to the cells and DNA, which was then placed on an orbital shaker at 190 RPM at 37°C for 60 minutes. Whilst incubating, agar selection plates with the appropriate antibiotic drug were placed at room temperature. Following the incubation period, cells were mixed thoroughly and 300µl of the cell suspension was streaked onto the agar selection plates. Cells were incubated for 24 hours at 37°C.

Alternatively, if previously transformed NEB Stable Competent E. coli cells have been stored in glycerol at -80°C, then 300µl of cell stocks can be incubated in SOC medium and then cultured on to pre-warmed agar selection plates, and incubated for 24 hours at 37°C.

Plasmid expansion

A single NEB Stable Competent E. coli colony was picked using a sterile pipette tip, which was then placed in 5ml lysogeny broth (LB) medium (Table 2.1) and incubated with horizontal shaking at 30°C for 6 hours. The cell suspension was then transferred to a vented conical flask containing 100ml LB with antibiotics (50ng/ml Ampicillin), and incubated on an orbital shaker at 180RPM at 30°C for 24 hours.

Bacterial glycerol stocks

In order to make bacterial glycerol stocks, 2ml of cell suspension from the previous step was transferred to a 15ml centrifuge tube and centrifuged at 5000g for 10 minutes at room temperature. The supernatant was then aspirated and the cell pellet was re-suspended in 1ml of a solution containing 30% glycerol: 70% LB (v/v), and was then placed in a cryovial for long-term storage at -80°C.

Plasmid isolation

Following expansion, plasmids were purified from NEB Stable Competent E. coli cells using the PureYield^{TM} Plasmid Midiprep System (Promega). Briefly, 100ml of LB and NEB Stable

Competent E. coli cell suspension was transferred into two 50ml centrifuge tubes, and centrifuged at 5000g for 10 minutes at room temperature. The pellets were then re-suspended in 3ml of Cell Suspension Solution and combined together, followed by the addition of 3ml of Cell Lysis Solution, and then mixed by inverting 5 times. Following a 3 minute incubation, 5ml of Neutralisation Solution was added and mixed by inverting 10 times, and the lysates were centrifuged at 15,000g for 15 minutes. A PureYield™ Clearing Column (blue) was placed on top of a PureYield™ Binding Column (white) and assembled onto a vacuum pump. The liquid was poured into the column stack and a vacuum was applied until the solution was drawn through. 5ml of Endotoxin Removal Wash was added to the binding column, and again the solution was pulled through by applying a vacuum. 20ml of Column Wash was added, and a vacuum was applied to pull all the solution through. A vacuum was then applied to the dry binding column for 60 seconds, and was then removed and placed onto a paper towel to remove any excess ethanol.

The DNA was eluted by placing the binding column into a clean 50ml centrifuge tube, followed by the addition of 600µl of nuclease-free H_2O and incubating for 1 minute. Next, the binding column was centrifuged at 2,000g for 5 minutes in a swinging bucket rotor centrifuge, and the filtrate was collected into a clean 1.5ml Eppendorf tube.

Assessing nucleic acid purity and quantification

DNA quality and quantification was performed using Nanodrop® 1000 spectrophotometer (Thermo Scientific). For purity, a 260/280 ratio of around 1.8 was considered satisfactory.

Plasmid solutions were stored at -20°C for future use.

Plasmid expansion

Individual colonies were selected and grown overnight at 37°C in 5ml LB medium (Table 2.1) with Ampicillin (50ng/ml).

Plasmid isolation

Following expansion, plasmids were purified from B100 E. coli cells using the PureYield™ Plasmid Midiprep System (Promega), as described above.

Plasmid analysis

Following plasmid purification, the plasmid DNA was digested with the *XhoI* and *XbaI* restriction enzymes to confirm that the Gibson assemble yielded the correct plasmids.

2.6. Transfection and transduction protocols

Retroviral plasmid transfection and viral production were carried out following class II safety procedures.

NEB Stable Competent E. Coli cells transformed with the packaging plasmid, d8.9, or the envelope protein, VSVG, were grown and expanded as previously described under "Plasmid expansion". DNA was purified as described under "Plasmid isolation" using the PureYield™ Plasmid Midiprep System (Promega).

$5x10^6$ HEK293FT cells were seeded in a 10cm dish and incubated for 24 hours in DMEM (supplemented with 1:100 non-essential amino acids and 1:100 sodium pyruvate (10mM stock; Sigma Aldrich, S8636). Cells were approximately 80% confluent at the point of transfection using Lipofectamine™ 3000 reagent (Invitrogen, L3000015) Transfection was done in accordance with the manufacturers' protocol. 6hrs post transfection, medium was removed from HEK293FT cells, and 10ml of fresh medium without antibiotics was added (use medium designated for target cells). Culture medium containing viral particles was harvested 48 hours later, then filtered through a 0.45µm pore PVDF filter and mixed with polybrene (10µg/ml final concentration). The medium was then added to MRC5 Fibroblasts which were approximately 70% confluent. MRC5 fibroblasts were in 6 well plates, therefore different virus titres were added to each well (0, 0.5, 1, 2, 4 and the remaining viral media). After 24 hours, the virus containing media was removed and fresh culture medium was added. Cells were then left for 1-3 days to allow them to recover from exposure to the viral media. Once recovered, cells were maintained under selection by treating MRC5 Fibroblasts with 50ng/ml Puromycin (for BAX, BAK and Empty Vector) or Blasticidin 50ng/ml (STING #1, #2 and #3) for 5 days. Following selection, only transduced cells should remain to repopulate the wells. It is estimated that approximately 10-30% of MRC5s are successfully transduced prior to selection using this protocol. Transduced cells were confirmed by western blot.

2.7. Transient Transfections

MRC5 cells were seeded on coverslips at a density of 50,000 per well of a 12 well plate and left overnight to achieve a confluency of approximately 70-90% at the point of transfection. In accordance with the Lipofectamine™ 3000 Reagent protocol, the DNA-lipid mix was prepared using Opti-MEM™ Medium (120µl per well of a 12 well plate) the Lipofectamine™ 3000 reagent (1.875µl per well of a 12 well plate), P3000 reagent (2.5µl per well of a 12 well plate) and 1250ng DNA per well of a 12 well plate. Once prepared the mix was incubated for 15

minutes and then 125µl was added to cells for 36 hours. For a 0 day time point, cells were fixed at this point. For those used for studying senescence, they were irradiated at this point and fixed at the relevant time point. The following plasmids were used for transient transfections; cGAS-GFP, TFAM-GFP and STING-mCHERRY. Transfected cells can be identified under the microscope by the fluorescent tags. This same protocol was used for transfecting mtDNA into MRC5 fibroblasts.

2.8. Enzyme Linked Immunosorbent Assay

Prior to Enzyme Linked Immunosorbent Assay (ELISA) analysis, cells were maintained in serum free media for 24 hours. This media is then collected. A sandwich ELISA (R&D Systems; DY206/DY208) was used to measure the concentration of SASP factors IL-6, IL-8 and IP-10. A capture antibody at a concentration of 240µg/ml in PBS was used to coat the wells of a 96-well plate, and left to incubate overnight on an orbital shaker. The next day, the wells were washed twice using 150µl of 0.05% PBS-Tween20 wash buffer. Once washed, plates were blocked for 90 minutes using 150µl of reagents diluents; 1% BSA in PBS for IL-6 and 0.1% BSA in PBS for IL-8. Following blocking, two washes were performed using the wash buffer. 25µl of standards and samples were loaded per well, incubated for 90 minutes. Two washes performed. 25µl of detection antibody was diluted 1:100 in the reagent diluents, 25µl added to each well and incubated for 90 minutes. Two washes performed. 12.5µl of Streptavidin-HRP diluted 1:200 in reagent diluents. 25µl of added to each well and incubated for 20 minutes. Two washes performed. A substrate reagent was prepared from Colour Reagent A and B, 1:1 H_2O_2 and tetramethylbenzidine. 50µl added to each well. Plates incubated until colour develops, approximately 10-20 minutes. Once developed, 25µl of $2NH_2SO_4$ added to each well to stop the reaction. An absorbance reader was used to determine the optical density at a wavelength of 450nm.

2.9. Cytokine Array

Conditioned media was collected 10 days post 20Gy X-ray irradiation following 24 hours of serum-deprivation. 30µL of media was then aliquoted into 500µl centrifuge tubes for analysis by cytokine array. The array was performed by Eve Technologies and the samples were analysed by a Human Cytokine 42-Plex.

2.10. Western Blotting

<u>Protein Extraction from Cells</u>

Prior to collection, cells were rinsed in ice cold PBS, cells were then lysed using ice cold RIPA buffer (25µl per well in a 6 well plate). Cells were then scraped from the well and transferred to a 1.5ml Eppendorf tube. Tubes are vortexed quickly and transferred immediately to -80°C storage.

Protein Quantification

Lysates collected were placed on ice to defrost. Once defrosted they were centrifuged at 16100g, 4°C for 10 minutes. Following this the protein concentration was determined using a colorimetric Bio-Rad DC protein assay kit was used in accordance with the manufacturer's instructions (Bio-Rad; Reagent A, B and C, Catalogue numbers 500-0113/4/5 respectively). Once developed, the absorbance of the 96 well plate was measured using a Fluostar Omega microplate reader (BMG labtech). Using the absorbance value generated, the protein concentration was determined and samples were made up to the same concentration using RIPA buffer. The same volume of Mercaptoethanol (Sigma; Cat. Number M6250) was then added to each sample. Samples were denatured at 100°C for 5 minutes, then placed on ice to cool prior to storage at -80°C.

Electrophoresis

An acrylamide running gels was prepared and placed into a cassette (Invitrogen; Cat. Number NC2015 or NC2010) as per the table. The gel prepared was dependent upon the size of the proteins of interest. Once the running gel had set a 5% stacking gel was made up and placed into the cassette. Depending on the number of samples to be analysed a loading comb was placed into the cassette to produce loading wells.

Once the stacking gel had set, the cassette was placed into an Invitrogen XCell Sure Lock™ Mini-Cell Electrophoresis System and covered with Tris-Glycine running buffer. The comb was then removed, a protein standard (Bio-Rad, Cat Number; 161-0374) was loaded followed by the samples of interest. Once loaded, the samples were ran at 120V and 35mA for 90minutes.

Acylamide Gel Composition	5%	10%	12%	15%
MQ H^2O (mL)	6.8	5.1	4	3.3
30% Acylamide (mL) (Severn Biotechnology; 20-2100-10)	1.7	2.6	3.3	4
1.5M Tris pH8.8 (Sigma; T6066)	2.5	2.5	2.5	2.5
10% SDS (Sigma; L4390)	100	100	100	100
10% Ammonium Persulphate (Sigma; 215589)	100	100	100	100
TEMED (Sigma; T9281)	8	4	4	4

Table 2.2 Composition of acrylamide gels prepared for western blotting

Transfer of Proteins on to a Nitrocellulose Membrane

Once the gel had finished running a Trans-Blot SD Semi-Dry Transfer Cell (BioRad) was used to transfer the proteins from the gel to a nitrocellulose membrane (Millipore; IPVH00010). The gel was placed on the membrane, between two transfer pads soaked in transfer buffer. Transfer was performed at 20V for 1 hour. Successful transfer of proteins was determined by a brief staining with Ponceaux solution.

Blotting of Membranes with Primary Antibodies

Following transfer, the membrane was rinsed three times with PBS. It was then blocked for 1 hour at room temperature using 5% milk in 0.05% PBS-Tween. Once blocked, the membrane was incubated in primary antibody overnight at 4°C. The next day, the membrane was rinsed three times for 5 minutes in PBS followed by incubation with the secondary antibody for 1 hour at room temperature for one hour. The membrane was then rinsed with PBS three times for 5 minutes, 0.05% PBS-Tween for 5 minutes followed by a further three 5 minute washes with PBS.

Detection of Protein Bands using Chemiluminescence

Once rinsed sufficiently, the membrane was coated in Clarity Western ECL substrate (Bio-Rad; Cat Number 170-5060) and placed inside a FujiFilm Intelligent Dark Box II. The images were then developed and acquired using the software Image Reader Las-1000. Analysis was

performed using ImageJ, the background was subtracted and intensity of the band was measured, this was then normalised to the relevant loading control.

Western Blotting Solutions

RIPA Buffer

- 150mM NaCl,
- 1% NP40
- 0.5% NaDoC,
- 0.1% SDS
- 50mM Tris pH 7.4
- Phosphatase and protease inhibitor cocktail (Thermo Scientific; 78442)

Ponceaux Staining Solution

- 0.5% Ponceaux
- 5% Acetic Acid
- 94.5% H_2O

Western Blot Running Buffer

- 250µM Tris
- 1.92mM Glycine
- 0.1% SDS

Western Blot Transfer Buffer

- 250µM Tris
- 1.92mM Glycine

Primary Antibodies for Western Blotting				
Protein	**Species**	**Host**	**Dilution**	**Reference**
γH2AX (Ser139)	Human Mouse Rabbit	Rabbit Polyclonal	1:1000	5438 – Cell Signalling
53BP1 (E7N5D)	Human Mouse	Rabbit Monoclonal	1:1000	88539 – Cell Signalling
α-Tubulin	Human Mouse	Mouse Monoclonal	1:2000	T9026 - Sigma Aldrich
β-Tubulin	Human Mouse Rabbit	Rabbit Polyclonal	1:10000	2146S - Cell Signalling
β-Actin	Human Mouse Rabbit	Mouse Monoclonal	1:10000	Ab8226 - Abcam
BAK (D4E4)	Human Mouse Rabbit	Rabbit Monoclonal	1:1000	12105 - Cell Signalling
BAX (D2E11)	Human	Rabbit Monoclonal	1:1000	5023 - Cell Signalling
BAX (6A7)	Human Rabbit	Mouse Monoclonal	1:1000	Sc-23959 - Santa Cruz
BCL2	Human	Rabbit Monoclonal	1:1000	23F6 - Cell Signalling
Caspase 1 (D7F10)	Human	Rabbit Monoclonal	1:1000	3866 - Cell Signalling
Caspase 2 (C2)	Human	Mouse Monoclonal	1:1000	2224 – Cell Signalling
Cleaved IL-1β (Asp116) (D3A3Z)	Human	Rabbit Monoclonal	1:1000	83186 – Cell Signalling

Cleaved Caspase 3 (D175 hAIE)	Rabbit	Rabbit Monoclonal	1:500	9664S - Cell Signalling
Cytochrome C (D18C7)	Mouse Human	Rabbit Monoclonal	1:1000	11940S – Cell Signalling
IRF3 (D6I4C)	Human Mouse	Rabbit Monoclonal	1:1000	11904 – Cell Signalling
Lamin B1	Human	Rabbit Polyclonal	1:1000	Ab16048 - Abcam
NF-κB p65 (D14E12)	Human Mouse Rabbit	Rabbit Monoclonal	1:1000	8242S – Cell Signalling
NLRP3 (D4D8T)	Human Mouse	Rabbit Monoclonal	1:1000	15101 – Cell Signalling
p16INK4a/Anti-CDKN2A (DCS50.1)	Human	Mouse	Mouse Monoclonal	Ab16123 - Abcam
p21 Waf1 Cip1 (12D1)	Rabbit	Rabbit Monoclonal	1:1000	2947S - Cell Signalling
PGC-1β	Human	Rabbit Monoclonal	1:1000	Ab176328 - Abcam
Phospho-IRF3 (Ser386)	Human	Rabbit Monoclonal	1:1000	37829S - Cell Signalling
Phospho-NF-κB p65 (Ser536) (93H1)	Human Mouse Rabbit	Rabbit MonoClonal	1:1000	3033S – Cell Signalling
STING (D2P2F)	Human	Rabbit Monoclonal	1:1000	13647S - Cell Signalling
TFAM (D5C8)	Rabbit	Rabbit Monoclonal	1:200	8076S - Cell Signalling
TLR9 (D9M9H)	Human	Rabbit Monoclonal	1:1000	13674S - Cell Signalling

UQCR2	Human	Rabbit Polyclonal	1:1000	Ab103616 - Abcam
VDAC1	Human Mouse	Mouse Monoclonal	1:1000	Ab14734 - Abcam
Secondary Antibodies for Western Blotting				
Goat Anti-Rabbit HRP Conjugated	Rabbit	Goat	1:5000	A0545 - Sigma Aldrich
Goat Anti-Mouse HRP Conjugated	Mouse	Goat	1:5000	A2554 - Sigma Aldrich

Table 2.3 - Summary of primary and secondary antibodies used for Western Blotting

2.11. Mitochondrial Membrane Potential Assay using the JC-10 Kit

To measure mitochondrial membrane potential, cells are first trypsinised, suspended in media and then spun down at 800RPM for 2minutes to pellet the cells. Once pelleted, the supernatant is removed and cells are re-suspended in serum free media at a density of 1000,000 cells per 1ml. 100µl of the cell suspension is then seeded in duplicate into a clear bottom, black walled 96 well plate to give 100,000 cells per well. 50µl of the JC-10 dye loading solution (Abcam JC-10 Mitochondrial Membrane Potential Assay Kit, ab112134) is then added to each well. Cells are then incubated for 1 hour at 37°C and 5% CO_2. Following incubation, 50µl of Assay Buffer B was added to each well. Immediately following this the fluorescent intensity of each well (excitation/emission - 490/525nm and 540/590nm) was read using a Fluostar Omega microplate reader (BMG labtech). Prior to each well of the plate being read, the machine was set up to give the plate a gentle 2 second shake. Following reading, the ratio of fluorescence intensity at 520nm/590nm was performed to give an indication of the mitochondrial membrane potential. This ratio is then expressed as a percentage of the control.

2.12. Electron Microscopy

Cells were grown on transwell inserts (Sigma, Cat Number CLS3413) in 24 well plates and fixed using 2% glutaraldehyde (Sigma, Cat Number G5882) in 0.1M Phosphate Buffer (Sigma). Cells were maintained in this solution until processing.

At the point of processing, cells were washed for 2 hours in Phosphate Buffer. Following washing, cells were further fixed using 1% Osmium Tetroxide (Sigma, Cat Number 05500) in 0.1M Phosphate Buffer for 1 hour. Following incubation, cells were washed for a further hour in 0.1M Phosphate Buffer. Cells were subsequently dehydrated using 70, 90 and 100% ethanol for 15 minutes each (twice at 100%). Cells were then incubated for 10 minutes in Propylene Oxide (Sigma, Cat Number 471968). The cells were then embedded for an hour in 50% epoxy resin in propylene oxide. Cells were stored overnight on a shaker in fresh epoxy resin (Agar Scientific, Cat Number R1031). The following day, fresh epoxy resin was added and cells were maintained for a further 8 hours. Cells were then placed in BEEM embedding capsules (Ted Pella, Cat Number 130-SPC) with fresh epoxy resin and incubated for 48 hours at 60°C. Sections were then cut and stained with uranyl acetate and lead citrate. Samples were then analysed using a transmission electron microscope.

2.13. Immuno Electron Microscopy

Cells were grown on transwell inserts and fixed in 2% PFA in PBS for 5 minutes. Cells were then rinsed three times in PBS for 5 minutes each. Permeabilisation and blocking was performed for 1 hour using 0.1% Saponin, 1% BSA and 3% NGS in PBS. Following incubation, samples were rinsed three times in PBS for 5 minutes each. Samples were incubated with the antibody of interest overnight at 4°C (See Table X for antibody details). The following day the inserts were rinsed three times in PBS for 5 minutes each. Samples were incubated with the gold labelled secondary antibody for 3 hours at room temperature. Once incubated, samples were rinsed three times for 5 minutes each in PBS. Samples were then fixed in 2% Glutaraldehyde in 0.1M Phosphate Buffer prior to processing for Electron Microscopy as detailed in Section 2.12.

2.14. Mitochondrial Isolation

Cells were grown in 10cm dishes, at the point of collection, cells were quickly rinsed in ice cold PBS. 5ml of ice-cold PBS was then added and cells were scraped from the well and collected in a Falcon tube. Once collected, they were centrifuged at 800g for 5 minutes at 4°C. Cells were then re-suspended in Mitochondrial Isolation Solution and transferred to a glass homogeniser. Cells were broken open using 60 strokes within the homogeniser. The solution was then centrifuged for 5 minutes at 800g, 4°C, to remove cell nucleus and membranes. The supernatant was transferred to a new tube and centrifugation was repeated to ensure all of the membranes have been removed. A small aliquot of the supernatant was taken for a whole cell extract, the remaining supernatant was centrifuged at 16100g for 10 minutes at 4°C. The supernatant was

collected as this is the cytosolic fraction. The pellet is the mitochondrial fraction. 1ml of Mitochondrial Isolation Solution is added and centrifuged at 16100g for 10 minutes at 4°C to wash the pellet. This step is repeated. The pellet is then re-suspended in 100µl of solution. Protein quantification is performed as detailed in Section 2.10. All fractions stored at -80°C.

Mitochondrial Isolation Solution

- 20mM HEPES-KOH pH7
- 220mM Mannitol (MW=182.17g/mol): 4g/100ml
- 70mM Sucrose (MW342.3g/mol): 2.39g/100ml
- 1mM EDTA (2ml of 0.05M stock in 100ml)
- 0.5 mM PMSF (add on the day of use)
- 2mM DTT (add on the day of use)

2.15. Mitochondrial DNA Extraction

Following mitochondrial isolation a Qiagen DNeasy Blood and Tissue extraction kit was used to extract mitochondrial DNA. The isolated mitochondria were centrifuged at 16100g for 10 minutes to pellet the mitochondria. The pellet was reuspended in 200µl of PBS and 20µl of proteinase K was added, followed by 200µl of Buffer AL. Mitochondria thoroughly vortexed and incubated at 56°C for 10 minutes. 200µl of 100% ethanol was then added and thoroughly vortexed. The mixture was then transferred into the designated DNeasy Mini spin column and centrifuged at 6000g for 1 minute. The flow through collected in the collection tube was discarded. The spin column was placed into a new collection tube and 500µl of buffer AW1 was added and centrifuged at 6000g for 1 minute. Again, the flow through and collection tube was discarded. The spin column was placed into a new collection tube and 500µl of buffer AW2 was centrifuged for 3 minutes at 20000g. Flow through and collection tube discarded. The spin column was placed into a fresh collection tube and 200µl of buffer AE was added and incubated for 1 minute. The sample was then centrifuged for 1 minute at 6000g to elute the DNA. This final step was repeated to enhance the DNA yield.

2.16. DNA Gel Electrophoresis

To determine that the extracted mtDNA was exclusively DNA of mitochondrial origin a DNA gel was ran. First, an 0.8% agarose gel was prepared (0.8g of agarose with 100ml of TAE). 5µl of 1x SafeView Nucleic Acid Stain was added to the solution. The solution was then microwaved for approximately 1 minute until sufficiently dissolved. The gel was then cast and loading comb inserted. Once set satisfactorily, the gel was placed into the electrophoresis tank

and TAE buffer was added until the gel was completely submerged. The comb was then removed. First, a GeneRulerTM 10kb plus DNA Ladder was added, and then 20µl of isolated mtDNA was added to the subsequent sample wells. Once loaded, the gel was ran for 1 hour, 90V, 66mA and 6W. Once the gel had ran satisfactorily, it was analysed and imaged under a UV lamp.

TAE Buffer (50X)

- 242g Tris base
- 57.1ml glacial acetic acid
- 100ml of 500mM EDTA (pH 8.0)
- 1L distilled H_2O

2.17. MitoSOX Staining for ROS Measurement using Flow Cytometry

MitoSOX is a red dye that targets mitochondria and is specifically oxidised by superoxide ions, it therefore can be used to detect mitochondrial ROS. Cells grown in 6 well plates were rinsed with PBS and subsequently trypsinised, media was added and cells transferred to a falcon tube. Cells were centrifuged for 3 minutes at 1600RPM. Media was then aspirated. Cells were then re-suspended in 500µl of MitoSOX (MitoSOX diluted 1:1000 in serum free media, Invitrogen, M36008) and incubated for 10 minutes at 37°C. Following incubation, the media was aspirated and cells were re-suspended in 2ml of serum free media. Unstained control cells were not incubated with MitoSOX, they were just trypsinised and re-suspended in serum free media. MitoSOX fluorescence intensity was determined by flow cytometry (Partec) using the red fluorescence channel (FL3 channel). Each measurement was performed in triplicate.

2.18. Measurement of Cellular Bioenergetics using Seahorse XF24 Analyser

Analysis of ATP production via oxidative phosphorylation and glycolysis was assessed using a Seahorse XF24 analyser. Prior to analysis, cells were placed in unbuffered basic media for one hour (supplemented with 5mM glucose, 2mM l-glutamate and 3% FBS). Cellular bioenergetics were measured by oxygen consumption rate (OCR) and extracellular media acidification rate (ECAR). In order to determine the source of ATP a number of inhibitors are required to dissect cellular bioenergetics and assess mitochondrial function. An inhibitor of ATP synthase oligomycin (1µM) was used to inhibit ATP generation, in order to assess maximal ATP production the mitochondrial chain uncoupler carbonyl cyanide p-trifluoromethoxy-phenylhydrazone was used. In addition, complex 1 inhibitor rotenone

(0.5µM) and complex 3 inhibitor antimycin (2.5µM) were used together to energy production via the respiratory chain. The OCR indicates total ATP production. In order to calculate the amount derived from mitochondria the OCR with oligomycin is subtracted from the basal OCR, this is then multiplied by the phosphorus/oxygen ratio of 2.3 (Brand, 2005). In order to determine ATP derived from glycolysis, the ECAR is used. This is because during glycolysis there is a 1:1 ratio of ATP production with lactate production. ECAR occurs due to lactate and bicarbonate production. Therefore, when ECAR is calibrated to the proton production rate, the rate of glycolysis can be determined (Wu *et al.*, 2007; Birket *et al.*, 2011).

2.19. Huygens Software for miMOMP

Images for miMOMP analysis were acquired from cells labelled with Cytochrome C and TOM20 antibodies by 3D imaging using z-stacks on the Leica SP8 Confocal microscope. Approximately 30 z-stacks were acquired for each coverslip imaged. All images were acquired using the same parameters on the microscope. Following imaging, micrographs were processed for deconvolution using the Huygens Deconvoltion Software. Once optimised, identical parameters were used to deconvolve each image to remove any background or noise from the image. Deconvolution was used to improve the quality of the images and provide the optimum quality for analysing the colocalisation of two channels. Once all images were deconvolved the level of colocalisation was assessed using the colocalisation tool within the Huygens Deconvolution Software. This was performed by individually "cutting" each cell out in 3D from the z-stack. Once isolated, the software performed a statistical colocalisation analysis using the Pearson Correlation Coefficient, Spearman's Coefficient and the overlap between channels. These were then recorded in an excel spreadsheet.

2.20. Immunofluorescent Staining of Cells

Cells for staining by immunofluorescence were grown on sterile coverslips in 12-well plates. Fixation was performed using 4% paraformaldehyde in PBS for 10 minutes (for staining of mitochondrial proteins, 0.2% glutaraldehyde was added to the fixation solution). Once fixed cells were stored in PBS at -80°C. For staining, coverslips were rinsed twice for 5 minutes in PBS, permeabilisation was then performed using 0.5% Triton-X in PBS for 15 minutes at room temperature. A further two 5 minute PBS washes were carried out. Blocking was then performed for one hour at room temperature using 5% NGS in PBS. Once blocked, cells were incubated overnight at 4°C with the primary antibody diluted in 5%NGS/PBS as detailed in Table 2.4. Following overnight incubation, cells were rinsed briefly ten times using PBS. They were then incubated for 2 hours at room temperature in the secondary antibody as detailed in

Table 2.4. They were then quickly rinsed ten times in PBS and mounted using ProLong Gold with DAPI.

Primary Antibodies for Immunofluorescence				
Protein	**Species**	**Host**	**Dilution**	**Reference**
AIF	Human Mouse	Rabbit Polyclonal	1:500	Ab1998 – Abcam
BAK (D4E4)	Human Mouse Rabbit	Rabbit Monoclonal	1:200	12105 - Cell Signalling
BAX (D2E11)	Human	Rabbit Monoclonal	1:200	5023 - Cell Signalling
BAX (6A7)	Human	Mouse Monoclonal	1:200	Sc-23959 - Santa Cruz
Cytochrome C (D18C7)	Mouse Human	Rabbit Monoclonal	1:200	11940S – Cell Signalling
Cytochrome C (Clone - 6H2.B4)	Human	Mouse Monoclonal	1:200	612301 - Biolegend
Anti-DNA (Clone AC-30-10)	Human	Mouse Monoclonal	1:100	CBL186 Merck-Millipore
Ki67	Human Mouse	Rabbit Polyclonal	1:1000	ab15580 - Abcam
p16 (E6H4)	Human	Mouse Monoclonal	1:5	705-4713 - Roche
P21 Waf1 Cip1 (12D1)	Human	Rabbit Monoclonal	1:1000	2947S - Cell Signalling
Phosphorylated Histone H2AX (S139) JBW301	Human Mouse	Mouse Monoclonal	1:1000	05 -636 - Temecula California Biosciences
Phosphorylated Histone H2AX (S139) (20E3)	Human Mouse	Rabbit Monoclonal	1:2000	9718S - Cell Signalling

STING (D2P2F)	Human Mouse	Rabbit Monoclonal	1:200	13647S - Cell Signalling
TFAM (D5C8)	Human Mouse	Rabbit Monoclonal	1:200	8076S - Cell Signalling
TOM20	Mouse Human	Mouse Monoclonal	1:200	612278 – BD Biosciences
TOM20	Human Mouse	Rabbit Monoclonal	1:200	HPA011562 - Santa Cruz
Secondary Antibodies for Immunofluorescence				
Wavelength	**Reactivity**	**Host**	**Dilution**	**Reference**
647	Rabbit	Goat	1:500	40839 - Sigma Aldrich
647	Rabbit	Goat	1:1000	1700082 - Life Technologies
594	Rabbit	Goat	1:1000	1745478 - Life Technologies
594	Mouse	Goat	1:1000	1310420 – Life Technologies
555	Mouse	Goat	1:1000	A-21422 - Invitrogen
488	Mouse	Goat	1:1000	1664729 - Life Technologies
488	Rabbit	Goat	1:1000	1275894 – Life Technologies
Anti Mouse 10nm Gold Conjugate	Mouse	Goat	1:50	EM.GMHL10 - BBI Solutions
Anti Rabbit 10nm Gold Conjugate	Rabbit	Goat	1:50	EM.GAR10 - BBI Solutions

Table 2.4 - Primary and secondary antibodies used for Immunofluorescent Staining

2.21. Senescence-associated β-Galactosidase Staining of Cells

Cells were grown on sterile coverslips in 12-well plates and fixed using 2% paraformaldehyde and 0.2% glutaraldehyde in PBS for 5 minutes. Once fixed, cells were rinsed three times in PBS for 5 minutes. Cells were than incubated in 1ml of SA-β-Gal staining solution at 37°C for approximately 24 hours. Once stained, cells were rinsed three times in PBS for 5 minutes and coverslips were mounted on to slides using ProLong Gold with DAPI. Imaging was performed on a Leica DM550 microscope using the LasX software. Approximately 10 random images were taken and quantified using the LasX software.

SA-β-Gal Staining Solution

- 1.5ml 1M sodium chloride
- 20µl 1M magnesium chloride
- 800µl 0.5M citric acid
- 1.2ml 0.1M sodium phosphate
- 5ml distilled water

Staining solution pH adjusted to 6.0 using NaOH, volume then made up to 10ml using distilled water.

- 8.8ml staining solution detailed above
- 200µl X-Gal at 20mg/ml in dimethylformamide
- 1ml potassium ferro-cyanide

2.22. Imaging using Stimulated Emission Depletion Microscopy

Imaging using Stimulated Emission Depletion Microscopy (STED) has been performed using a Lecia SP8 Confocal gSTED 3D Super Resolution microscope based in the BioImaging Unit at Newcastle University.

For ImmunoFISH staining for STED analysis of telomeres, the same protocol was employed as detailed above with a few minor changes for optimised compatibility with STED. Notably, 5µl of Cy3 Telomere probe is used in the hybridisation mix and following the final PBS rinse an addition 5 minute PBS rinse is performed. Once complete, the samples are incubated in ToPro3 (1:8000 in PBS) to stain the nucleus. A further three 5 minute rinses in PBS are performed. Samples are then mounted using ProLong Diamond without DAPI.

2.23. Gene Expression Analysis on BAX^{fl}/BAK-/- Livers

Experiments performed using liver tissue from BAX^{fl}/BAK-/- and BAK -/- mice were performed by Dr Stephen Tait, Dr Joel Riley and Dr Catherine Cloix from the Beatson Institute for Cancer Research at Glasgow, UK.

In order to delete BAX specifically in the liver, 8 week old BAX^{fl}/BAK-/- mice were injected with an Adeno-associated virus (AAV). Specifically, AAV mediated recombination was performed using a Virus carrying the Cre recombinase under the control of a hepatocyte-specific thyroid-binding globulin (TBG) promoter. Briefly, viral particles (2×10^{11} genetic copies/mouse) of AAV8.TBG.PI.Cre.rBG (Addgene, Catalog number: 107787-AAV8) diluted in 100 µl PBS were injected via tail vein in 8 week old mice. Following the injection of the virus, the mice were left for 7 days, they were then subsequently irradiated with 4Gy. Livers were collected from BAX^{fl}/BAK-/- and BAK -/- mice 7 days post-irradiation/sham irradiation for gene expression analysis. Within each of the 4 experimental groups, there were 5 mice (3 males and 2 females).

RNA extraction, cDNA synthesis and Real Time Polymerase Chain Reaction (RT-PCR) were performed at the Beatson Institute for Cancer Research. The following target genes were assessed: CXCL1, IFNα, IL-1α, IL-1β, IL-6, Inhibin A, MMP3, OAS1, p16 and p21. 18S was used as the reference gene and mRNA expression of target genes was normalised to 18S using the ΔΔC(t) method.

The AAV.TBG.PI.Cre.rBG was a gift from James M. Wilson (Addgene viral prep #107787-AAV8; http://n2t.net/addgene:107787)

2.24. Statistical Analysis

GraphPad Prism 6.0 was used for statistical analysis, results are considered as statistically significant when $p\leq0.05$. For normally distributed data, the differences between two groups was tested for statistical significance using an independent samples two-tailed t-test. For data which was normally distributed and there was more than one group a one-way ANOVA was used, a Tukey's comparison post-hoc test was also performed. Where data was not normally distributed a Mann-Whitney U-test was used for determining statistical significance

3. Chapter 3: Mitochondrial pores BAX and BAK release mtDNA during senescence and regulate the SASP

Previous work in the senescence field has largely depicted the role of mitochondria as ROS producers which function to maintain the DDR and subsequently stabilise the cell cycle arrest (Passos *et al.*, 2010). However, the role of mitochondria in senescence is multi-faceted, it has been established that mitochondria undergo a number of distinct changes in terms of dynamics and function (Jendrach *et al.*, 2005; Yoon *et al.*, 2006). Furthermore, it has recently been revealed that the characteristic pro-inflammatory response of senescent cells is in fact dependent on mitochondria (Correia-Melo *et al.*, 2016). Naturally, this raises the question of how mitochondria are driving the SASP from a mechanistic perspective.

mtDNA release into the cytosol has been shown to be a major factor driving pro-inflammatory phenotypes, mostly through its binding to cGAS and activation of STING pathway (West *et al.*, 2015; Bao *et al.*, 2016). Interestingly, the cGAS STING pathway has also been shown to be a major regulator of the SASP, however, the role of mtDNA in this process has not been investigated (Dou *et al.*, 2017; Gluck *et al.*, 2017; Yang *et al.*, 2017).

In this chapter, I hypothesised that mitochondrial dysfunction characteristic of senescent cells is associated with an increased cytosolic release of mtDNA and that this process may explain the SASP. Additionally, I investigated the mechanisms by which mtDNA can be released to the cytosol during senescence. Finally, I investigated the impact of blocking mtDNA release on the senescent phenotype.

Therefore, the first aim of this study was to characterise whether mitochondrial DNA was present outside of the mitochondria in senescent cells. Secondly, following the observation that mtDNA was present in the cytosol, work was undertaken to understand the mechanism which was facilitating its release. Finally, it was assessed what the impact of blocking mtDNA release has on the senescent phenotype.

3.1. Mitochondria are dysfunctional during senescence

The initial aim of this study was to characterise mitochondria in senescence. Previous work has described mitochondria in senescent cells as having a hyperfused morphology which consists of elongated, interconnected mitochondrial networks (Yoon *et al.*, 2006). Similarly, it has been reported that mitochondrial mass increases following the onset of senescence (Passos *et al.*, 2007). Following the establishment of stress-induced senescence in MRC5 fibroblasts

mitochondrial networks were visualised using immunofluorescent labelling of the mitochondrial outer membrane protein TOM20 (outer membrane translocase domain 20) (Figure 3.1A). The size of the network was determined by manually drawing around the mitochondrial staining. It was found that the size of the mitochondrial network was significantly increased compared to proliferating cells ($p<0.0001$) (Figure 3.1B). Previous studies have highlighted that the increased mitochondrial networks observed during senescence occur in response to a DDR mediated activation of MTORC1 and the mitochondrial biogenesis mediator PGC-1β, in addition, this promotes increased production of ROS (Correia-Melo *et al.*, 2016). First, I assessed VDAC which is a highly conserved mitochondrial outer membrane protein which serves as a reliable marker of overall mitochondrial content (Lemasters and Holmuhamedov, 2006). I found that senescent cells had a 1.5 fold increase in VDAC compared to proliferating cells ($p=0.0474$, Figures 3.1C and D). Consistently, I found that PGC-1β protein levels were significantly increased in senescent cells compared to proliferating cells ($p=0.0258$) (Figures 3.1C and E). In addition, measurements of MitoSOX fluorescence using flow cytometry revealed that superoxide anion production was increased approximately 15-fold in senescent cells compared to their proliferating counterparts ($p=0.0063$) (Figure 3.1F). Finally, I assessed mitochondrial membrane potential using the fluorescent dye JC-10, which indicated that both stress-induced and replicatively senescent cells display decreased mitochondrial membrane potential compared to proliferating cells ($p<0.0001$ and $p=0.0038$, Figure 3.1G).

Collectively, these results highlight that mitochondria in senescent cells differ fundamentally in terms of morphology and functionality.

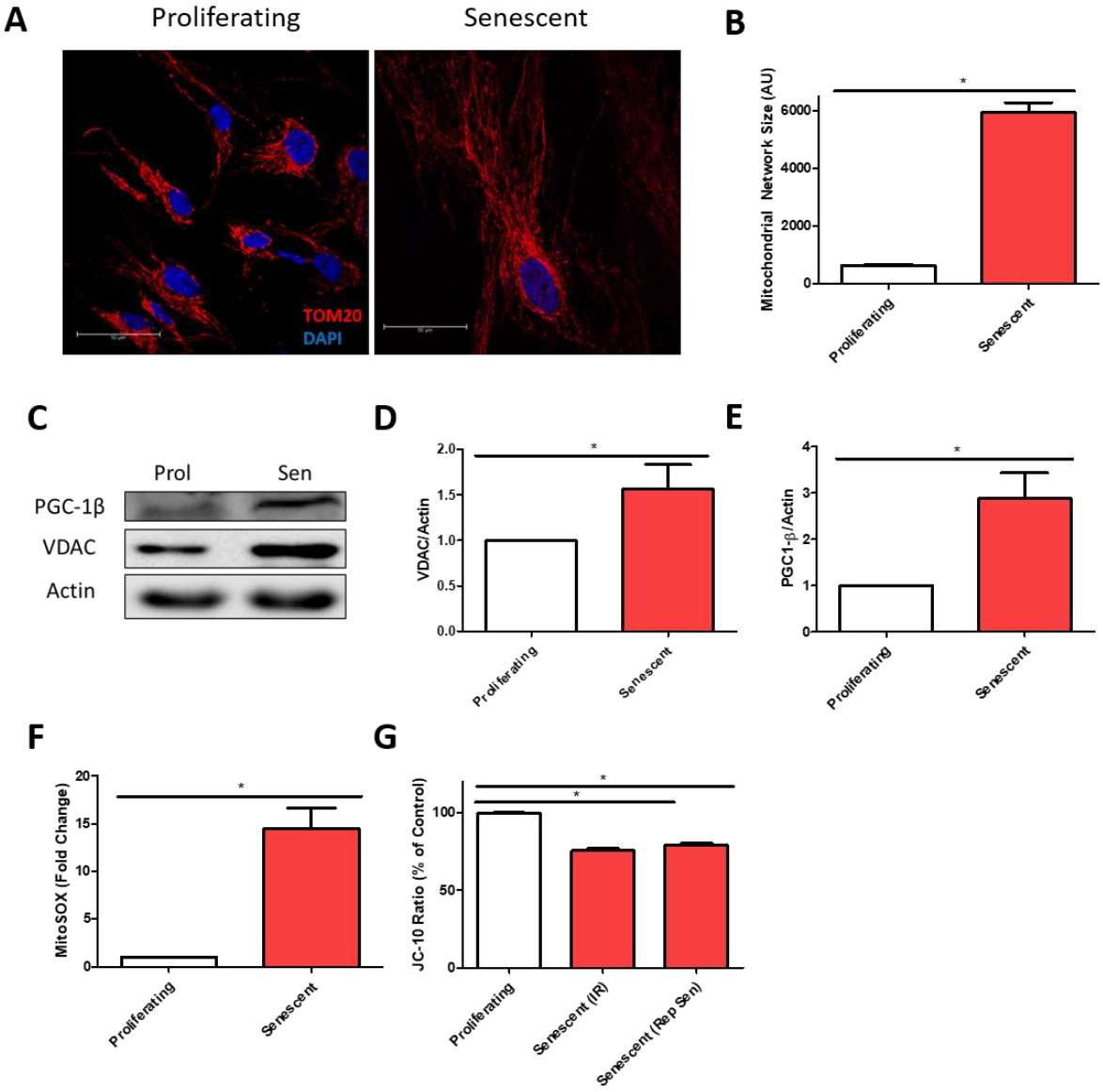

Figure 3.1 - Characterisation of mitochondria in senescent cells.

MRC5 fibroblasts were induced to become senescent either by 20Gy irradiation (10 days post-IR) or through replicative exhaustion. **(A)** Representative images of mitochondrial networks from proliferating and senescent cells labelled using TOM20 and the nuclear stain DAPI, cells were imaged on a 63x objective by confocal microscopy. **(B)** Bar graph illustrating the size of mitochondrial networks as measured by manually drawing around the TOM20 staining in proliferating (white bars) and senescent (red bars), n=4 independent experiments. **(C)** Representative western blot of PGC-1β, VDAC (voltage dependent anion channel) and actin. **(D and E)** Bars graph demonstrating quantification of VDAC **(D)** and PGC1-β **(F)** normalised to actin in proliferating (white bars) and senescent (red bars), n=3-6 independent experiments. **(F)** Bar graph showing the fold change of MitoSOX in proliferating (white bar) and senescent cells (red bar) as measured by flow cytometry, n=4 independent experiments. **(G)** Bar graph depicting measurement of mitochondrial membrane potential using the JC-10 dye in proliferating (white bar) and senescent (red bars) cells, n=5-8 independent experiments. Bar graph data is shown as mean + SEM, the box and whisker plot demonstrates second and third

quartiles with the median (box) and lower and upper quartiles depicted by horizontal lines either side of the box. Statistical significance was determined using a two-tailed unpaired t test. For **(G)** a one-way ANOVA was used.

3.2. mtDNA is present in the cytosol of senescent cells

Previous studies investigating the location of cytosolic mtDNA have utilised confocal microscopy with antibodies against mitochondria and double stranded DNA (West *et al.*, 2015). Therefore, in order to investigate the sub-cellular localisation of mtDNA in proliferating and senescent cells, super-resolution and confocal microscopy were employed to visualise the mitochondrial networks by immunofluorescence using an antibody for TOM20 and an anti-DNA antibody. In proliferating cells, the majority of DNA detected in the cytosol co-localised with the mitochondrial network. However, in both replicative and stress-induced senescent cells the mean number of nucleoids outside of the mitochondrial network and the percentage of cells displaying free mtDNA was significantly increased compared to proliferating cells (Figures 3.2A, B and C). In addition to fluorescence microscopy I confirmed our data using Immuno-Electron microscopy. I examined cytosolic DNA in proliferating and senescent mouse adult fibroblasts by labelling DNA using a gold-conjugated secondary antibody which can be visualised using transmission electron microscopy. In senescent cells, labelling of DNA outside of the mitochondria is visible (Figure 3.2D). Furthermore, the cytosolic fraction was separated from whole cell lysates acquired from proliferating, stress-induced and replicatively senescent cells and the presence of mtDNA was assessed using PCR. My results show that mtDNA was enriched approximately 7-fold in cytosolic fractions from senescent cells compared to proliferating cells (Figure 3.2E). Finally, by Western Blot I probed mitochondrial and cytosolic extracts taken from proliferating and senescent cells for the protein TFAM, a transcription factor responsible for packaging mtDNA nucleoids. It was found that there was a 3-fold increase in the level of TFAM observable in the cytosolic fraction of senescent cells compared to proliferating cells ($p=0.0265$, Figures 3.2F and G).

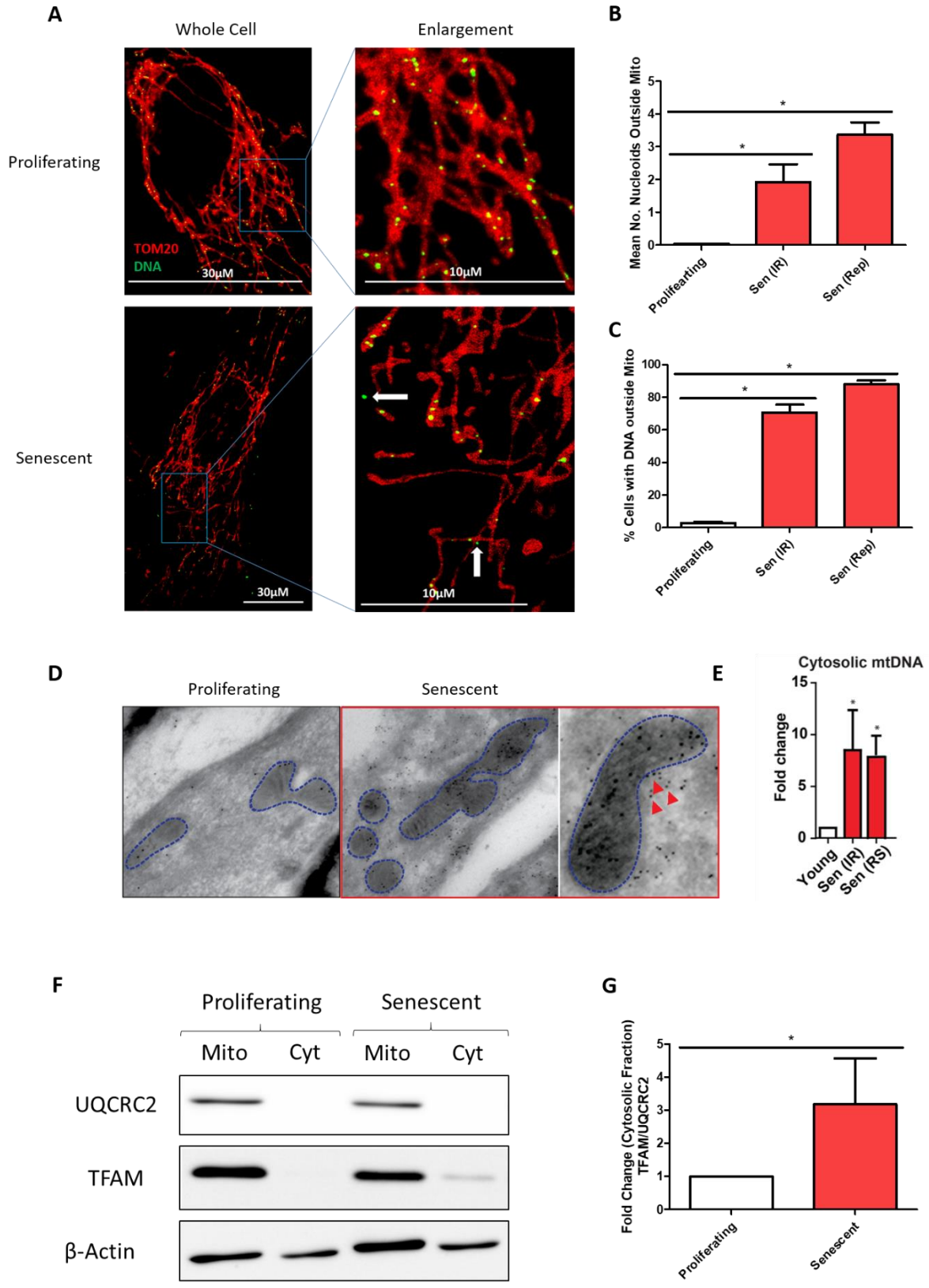

Figure 3.2– mtDNA is present in the cytosol of senescent cells.

(A) Representative images of proliferating and senescent cells labelled for DNA (green) and mitochondria (red) taken using super-resolution microscopy, white arrows in the enlarged images highlight mtDNA nucleoids located outside of the mitochondrial network. **(B)** Bar graph depicting quantification of the mean number of DNA nucleoids outside of the mitochondrial network in proliferating (white bar) and senescent (red bars) cells, n=4 independent experiments. **(C)** Bar graph depicting the percentage of cells displaying DNA outside of the mitochondrial network in proliferating (white bar) and senescent (red bars) cells, n=4 independent experiments **(D)** Representative immune-electron microscopy images of proliferating and senescent cells labelled using an anti-DNA antibody with a gold-conjugated secondary antibody. Red arrows highlight labelled DNA outside of the mitochondrial network. **(E)** Bar graph depicts the fold-change of mtDNA specific DNA present in cytosolic fractions from proliferating and senescent cells as measured by PCR. **(F)** Representative Western Blot image where protein levels of UQCRC2, TFAM and β-Actin were measured in mitochondrial extracts and cytosolic fractions acquired from proliferating and senescent cells. **(G)** Bar graph depicts the quantification of TFAM in the cytosolic fraction of proliferating and senescent cells normalised to the mitochondrial protein UQCRC2 and expressed as fold-change. Bar graph data is shown as mean, error bars represent the standard error of the mean, statistical significance was determined using either a one-way ANOVA or a two-tailed unpaired t test. *(The representative immuno-electron microscopy image and PCR data was performed by Hanna Salmonowicz).*

When the presence of cytosolic DNA was assessed using immunofluorescence in Figure 3.2A and by immuno-electron microscopy in Figure 3.2D, the DNA was labelled using an anti-DNA antibody. Although this method of labelling mtDNA nucleoids is widely used in the mitochondrial field it is important to note that it binds all forms of double-stranded DNA, therefore it would also bind nuclear DNA if it was present in the cytoplasm (West *et al.*, 2015; McArthur *et al.*, 2018; Riley *et al.*, 2018). To determine if DNA found in the cytosol was of mitochondrial origin we determined if it co-localised with TFAM by super-resolution microscopy (Figure 3.3A). Analysis of proliferating cells reveals that majority of mtDNA nucleoids are present within the mitochondrial networks where TFAM staining is also present. In senescent cells I observed that there is an increased number of cytosolic DNA nucleoids visible outside of the mitochondrial network (2.9 vs 0.2 in proliferating cells, p,0.001) (Figure 3.2B). It was discovered that in senescent cells 53% of cytosolic DNA nucleoids were also co-localised with positive staining for TFAM, whereas in proliferating cells only 5% of cytosolic DNA colocalised with TFAM ($p<0.001$, Figures 3.3B and C). These data suggests that a large % of cytosolic DNA in senescent cells is of mitochondrial origin.

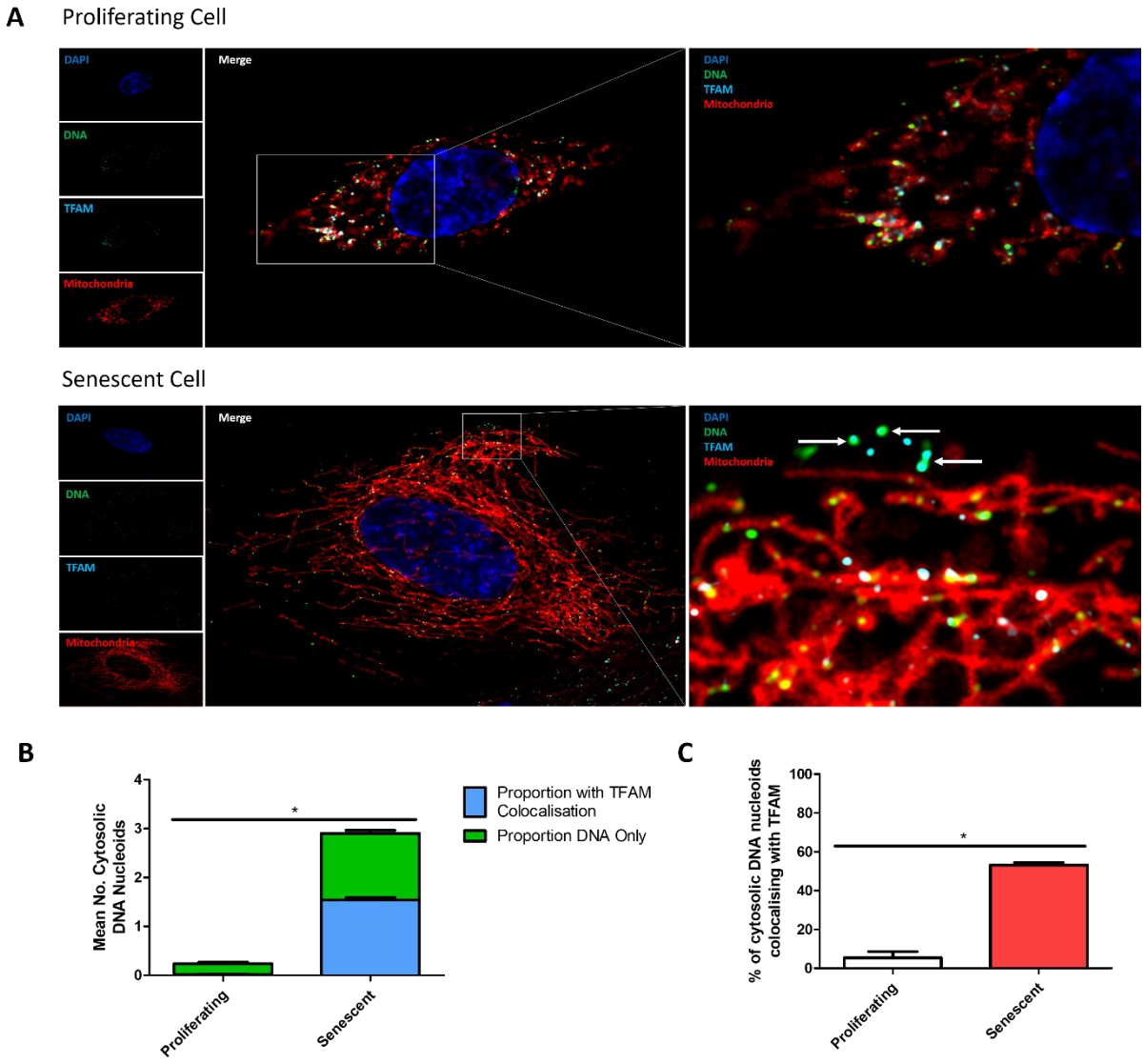

Figure 3.3 – Cytosolic DNA in Senescent Cells colocalises with TFAM.

(A) Representative immunofluorescence image of DAPI (blue), DNA (green), TFAM (cyan) and mitochondria (red labelled using BAC-MAM 2.0-RFP) in a proliferating and a stress-induced senescent cell acquired on a 63x objective using super resolution airyscan microscopy. White arrows indicate colocalisation of cytosolic DNA and TFAM. **(B)** Bar graph depicting quantification of the mean number of nucleoids in the cytosol in proliferating and senescent cells, the blue represents the proportion of cytosolic nucleoids which colocalise with TFAM, and the green represents the proportion which is positive for DNA staining only. **(C)** Bar graph represents the percentage of cytosolic DNA which colocalises with TFAM in proliferating and senescent cells. Bar graph data is shown as mean, error bars represent the standard error of the mean, statistical significance was determined using a two-tailed unpaired t test., n=4 independent experiments.

Collectively, my data demonstrates that mtDNA/TFAM complexes relocalise beyond the mitochondrial outer membrane. It has been reported that in certain instances cytosolic mtDNA can be attached to fragments of the inner mitochondrial membrane (Riley *et al.*, 2018). Thus far the inner membrane integrity has not been explored in this study. For example, it is possible that during senescence the outer membrane could be damaged or broken down whereby mtDNA complexes in the cytosol could still be localised with the inner membrane. As such, I wanted to understand whether mtDNA was crossing the inner and outer membrane of the mitochondria, or whether it was still localised with the inner membrane. To investigate this a triple immunofluorescence staining was used to label the mtDNA nucleoids, the inner membrane protein AIF (apoptosis inducing factor) and the outer membrane by labelling TOM20. Analysis revealed that compared to proliferating cells, senescent cells had an increased mean number of mtDNA nucleoids in the cytosol which were not associated with AIF or TOM20 ($p=0.0021$) (Figures 3.4A and B). Furthermore, senescent cells also displayed an increased percentage of cells displaying free mtDNA which did not colocalise with AIF or TOM20 ($p<0.0001$) (Figures 3.4A and C).

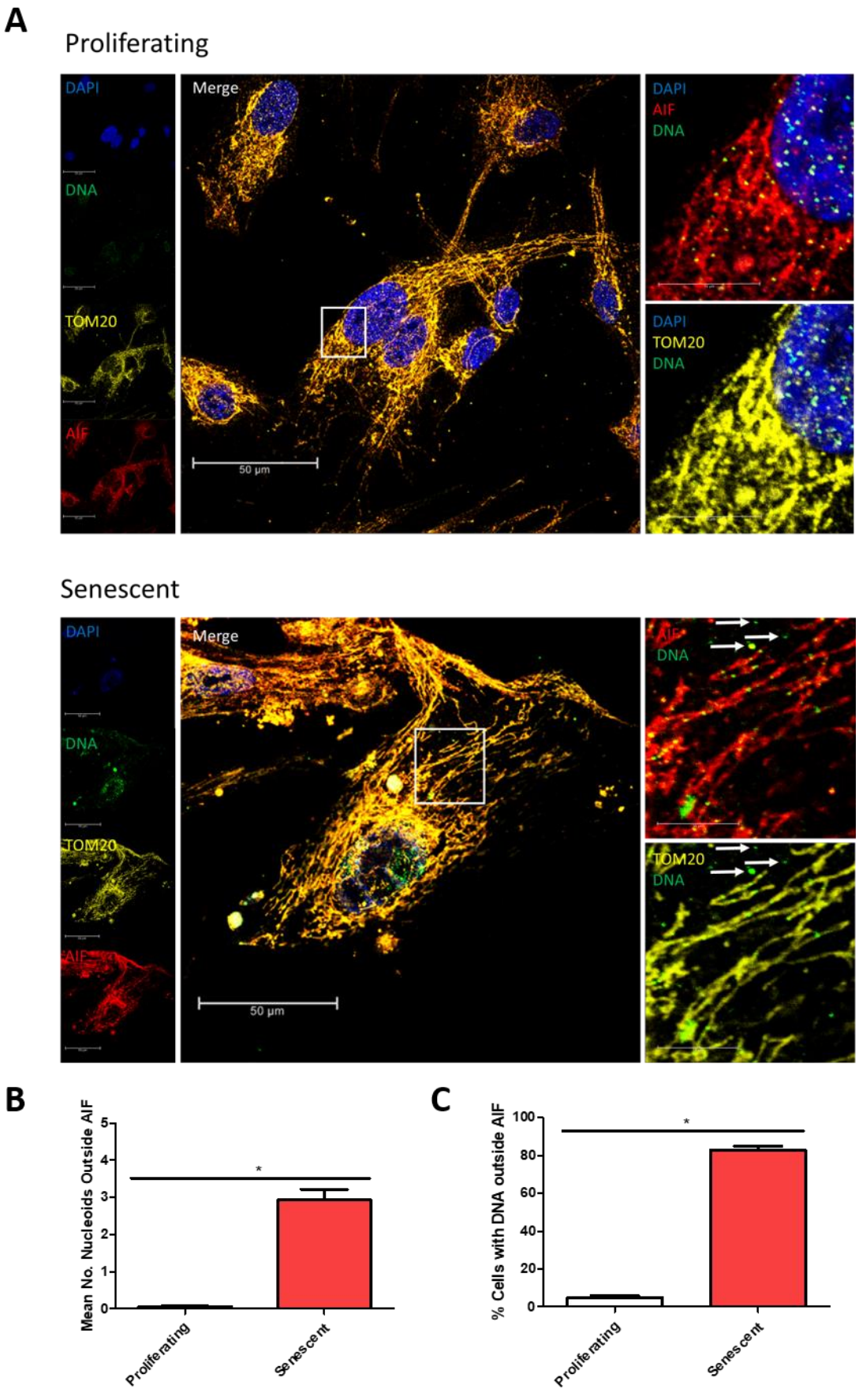
A
Proliferating
DAPI
DNA
TOM20
AIF
Merge
50 µm
DAPI
AIF
DNA
DAPI
TOM20
DNA
Senescent
DAPI
DNA
TOM20
AIF
Merge
50 µm
AIF
DNA
TOM20
DNA
B
Mean No. Nucleoids Outside AIF
0
1
2
3
4
5
*
Proliferating
Senescent
C
% Cells with DNA outside AIF
0
20
40
60
80
100
*
Proliferating
Senescent

Figure 3.4 – Cytosolic mtDNA does not colocalise with mitochondrial inner membrane protein AIF.

(A) Representative immunofluorescence images of DAPI (blue) DNA (green), TOM20 (yellow) and AIF (red) acquired by confocal microscopy using a 63x objective in both proliferating and senescent cells. **(B)** Bar graph depicting quantification of the mean number of DNA nucleoids outside of the mitochondrial network (i.e. did not colocalise with TOM20 or AIF) in proliferating (white bar) and senescent (red bar) cells, n=4 independent experiments. **(C)** Bar graph depicting the percentage of cells displaying DNA outside of the mitochondrial network (i.e. did not colocalise with TOM20 or AIF) in proliferating (white bar) and senescent (red bar) cells, n=4 independent experiments. Bar graph data is shown as mean, error bars represent the standard error of the mean, statistical significance was determined using a two-tailed unpaired t test.

3.3. mtDNA provokes an inflammatory response in fibroblasts

It has been reported by a number of groups that free mtDNA is recognised as a DAMP by the immune system and can promote the secretion of inflammatory factors. This can occur either through TLR9, the NLRP3 inflammasome or the cGAS-STING axis (Shimada *et al.*, 2012; West *et al.*, 2015; Bao *et al.*, 2016). Therefore, I questioned whether mtDNA provokes an inflammatory response in MRC5 fibroblasts where I previously observed mtDNA to be visible in the cytosol upon induction of senescence. To address this question, mitochondria were isolated and the mtDNA was then extracted and purified. This extracted DNA was then ran on a DNA gel to confirm that it corresponded to the 16,569bp size of circular mtDNA (Figure 3.5A). The extracted mtDNA was then transfected into proliferating MRC5 cells, following transfection, DNA was visible in the cytosol of the cells (Figures 3.5B and C). Post mtDNA transfection, the secretion of the cytokine IL-6 and the chemokine IL-8 was measured. IL-6 and IL-8 are key factors secreted as part of the SASP and in response to mtDNA (Campisi and d'Adda di Fagagna, 2007; Little *et al.*, 2014). It was found that transfection of whole mtDNA led to an increased secretion of both IL-6 and IL-8 ($p<0.0001$ for IL-6 and IL-8), furthermore, mtDNA which had been sonicated to apply shear stress and subsequently form fragments also led to an increase in both IL-6 and IL-8 ($p<0.0001$ for IL-6 and IL-8) (Figures 3.5D and E).

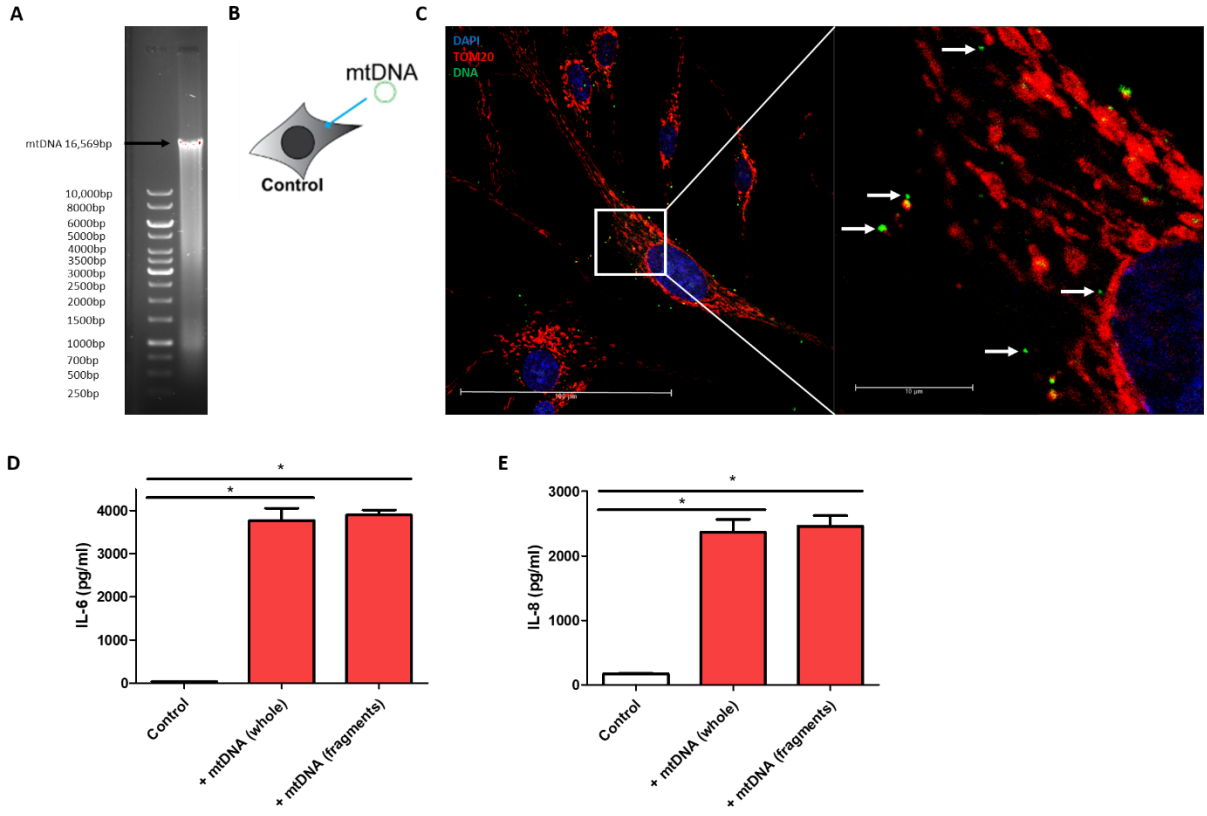

Figure 3.5 - Transfection of mtDNA into the cytosol provokes the secretion of IL-6 and IL-8.

(A) Mitochondria from MRC5 cells were isolated by centrifugation to remove any nuclear DNA and mtDNA was subsequently extracted. The extracted mtDNA was ran on a 0.5% agarose gel to confirm that it conformed to the 16,569bp size of whole circular mtDNA. **(B)** Schematic overview of experimental introduction of mtDNA into MRC5 human fibroblasts. **(C)** Proliferating MRC5 cells were transfected with mtDNA for 48 hours, following transfection, cells were labelled with DAPI (blue), DNA (green) and TOM20 (red) to confirm that mtDNA was visible in the cytosol of the transfected cells. Representative image taken on a 63x objective by confocal microscopy. **(D and E)** Bar graph depicts the levels of IL-6 **(D)** and IL-8 **(E)** secreted into the media 48 hours post transfection as measured by ELISA, n=6 independent experiments. Bar graph data is shown as mean, error bars represent the standard error of the mean, statistical significance was determined using a one-way ANOVA.

In order to further investigate the impact of mtDNA in the induction of the SASP I used cells which were completely devoid of mtDNA (Rho (0) cells) and induced them to become senescent, then I measured the secretion of the key SASP cytokines IL-6 and IL-8 and compared them to their mtDNA proficient counterparts (Figures 3.6A and B).

Following the induction of senescence, I observed a significant increase in the secretion of IL-6 and IL-8 in the mtDNA proficient parental cells compared to the proliferating parental cells ($p<0.0001$ for both IL-6 and IL-8). However, Rho (0) cells displayed a significantly ameliorated secretion of IL-6 and IL-8 compared to their mtDNA proficient counterparts. (Figures 3.6A and B).

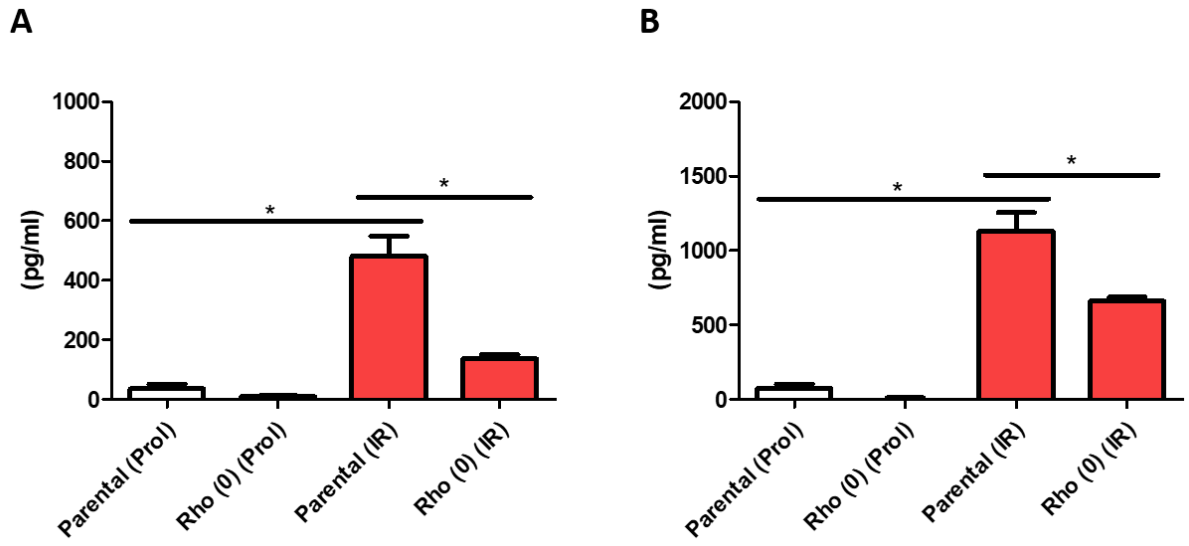

Figure 3.6 – Rho (0) cells display reduced secretion of the SASP factors IL-6 and IL-8.

The concentration (pg/ml) of secreted IL-6 and IL-8 was measured via ELISA in parental (mtDNA proficient) and Rho (0) (mtDNA deficient) osteosarcoma 143B cells were either maintained in a proliferating state or induced to become senescent via irradiation (10Gy irradiation 5 days post). **(A and B)** Bar graph depicts the levels of IL-6 **(A)** and IL-8 **(B)** secreted into the media in proliferating and senescent parental and Rho (0) cells as measured by ELISA, n=6 independent experiments. Bar graph data is shown as mean, error bars represent the standard error of the mean, statistical significance was determined using a one-way ANOVA.

3.4. Characterisation of BAX and BAK in senescent cells

Following my earlier observations that mtDNA was present in the cytosol of senescent cells and that mtDNA can provoke a pro-inflammatory response similar to that of the SASP I investigated the mechanism by which mtDNA can escape to the cytosol. It has recently been published that the presence of cytosolic mtDNA occurs due to the formation of BAX and BAK macropores, which allows the inner membrane to herniate and mtDNA release (McArthur *et al.*, 2018; Riley *et al.*, 2018). Therefore I wanted to characterise the pore forming proteins BAX and BAK in senescent cells.

Firstly, the total protein levels of BAX and BAK were assessed in whole cell extracts (Figure 3.7A). It was found that the total level of BAX was not statistically different in senescent cells compared to proliferating cells when normalised to the mitochondrial protein VDAC or β-Actin (p=0.7608 and 0.8898 respectively, Figures 3.7B and C). However, BAK expression was increased in senescent cells both when normalised to both mitochondrial and total protein levels (p=0.0456 and 0.0201 respectively, Figures 3.7 D and E)

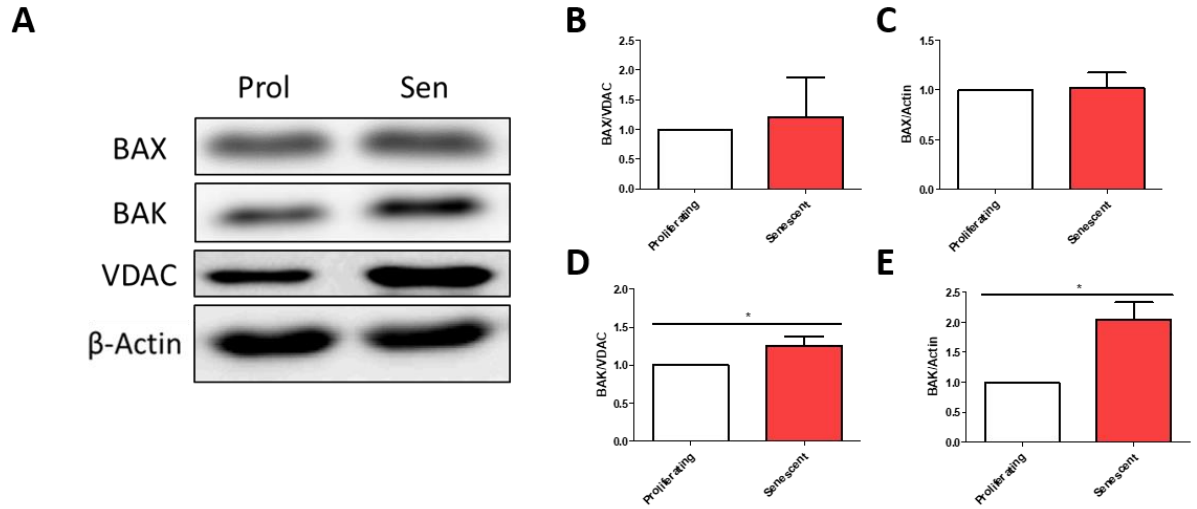

Figure 3.7 – Total levels of BAK but not BAX are increased in senescent cells.

The total protein levels of BAX and BAK were analysed in proliferating and stress-induced senescent cells (10 days post irradiation) **(A)** Representative western blot of the total levels of BAX, BAK, VDAC and β-Actin. Bar graphs demonstrating quantification of BAX normalised to VDAC **(B)** and β-actin **(C)** in proliferating (white bars) and senescent (red bars). Quantification of BAK normalised to VDAC and β-Actin is shown in bar graphs (**D)** and (**E)**. Bar graph data is shown as mean + SEM and represents 6 independent experiments, statistical significance was determined using a two-tailed unpaired t test.

Next, I wanted to characterise further the cellular location of both BAX and BAK. It has been reported that BAK is maintained in the mitochondria where it is anchored in an inactive state (Ferrer *et al.*, 2012). BAX on the other hand is continuously retro-translocated from the mitochondria to the cytosol in non-apoptotic cells, however, when it accumulates on the outer membrane of the mitochondria this has been observed to enhance the sensitivity to apoptotic stimuli (Schellenberg *et al.*, 2013). As such I wanted to understand whether there was any changes in the cellular location of BAX and BAK in proliferating and senescent cells. Therefore, I separated proliferating and senescent cells into mitochondrial and cytosolic fractions which were subsequently probed for BAX and BAK.

I found that BAK was localised to the mitochondrial fraction of senescent cells (95% of BAK) and proliferating cells (85%) to a similar extent (, Figures 3.8A and B). A similar level was observed in replicatively senescent cells (85%), this however needs to be confirmed independently to establish whether it is statistically significant

When the percentage of mitochondrially localised BAX was assessed it was found that there was a significant decrease in senescent cells (30% of BAX) compared to proliferating cells (70%) ($p<0.0001$, Figures 3.8A and C), a similar trend was observed in replicatively senescent cells (20%) although statistical significance was not tested due to the inadequate sample size.

It is known that the dynamic nature of BAX shuttling from the mitochondria to the cytosol is facilitated by the pro-survival proteins BCL-2 and BCL-XL, specifically, BCL-2 can prevent shuttling of BAX to the mitochondria (Edlich *et al.*, 2011; Schellenberg *et al.*, 2013). The total protein level of BCL-2 was measured in proliferating and senescent cells to understand whether it may be contributing to the increased amount of cytosolic BAX observed in senescent cells. Consistently, I found that BCL-2 was increased approximately 1.5 fold in senescent cells compared to proliferating cells when normalised to mitochondrial and total protein levels ($p=0.0283$ and 0.0049 respectively, Figures 3.8D, E and F).

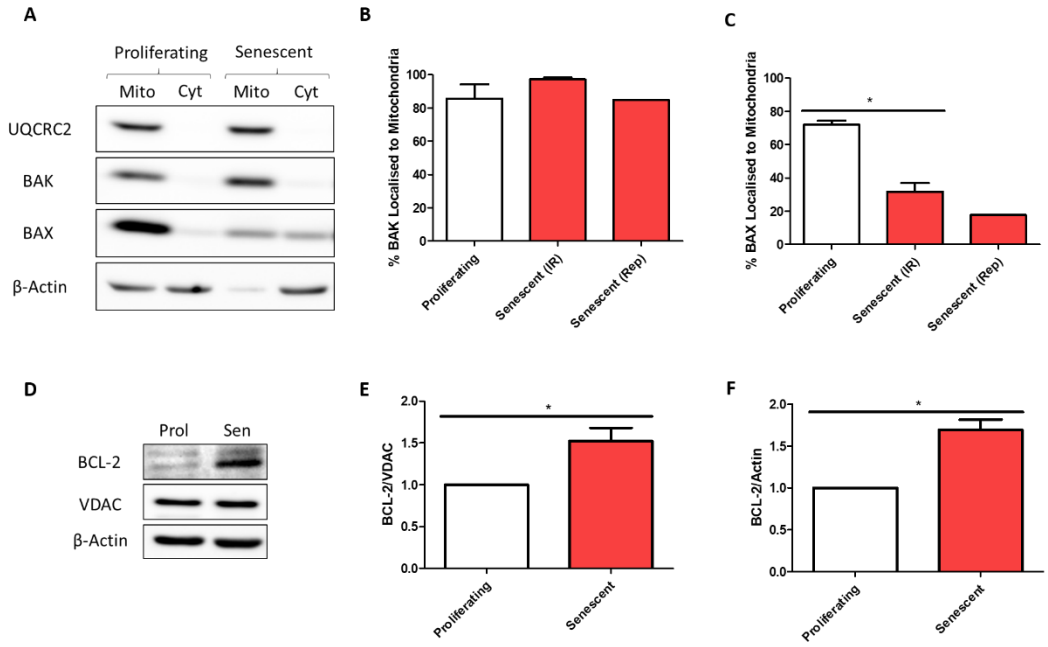

Figure 3.8 - Characterisation of the sub-cellular location of BAX and BAK.

Proliferating and senescent cells (stress-induced by irradiation and replicatively exhausted cells) were separated into mitochondrial and cytosolic fractions prior to characterisation via Western Blotting. **(A)** Representative Western Blot image of UQCRC2, BAX, BAK and β-Actin. **(B)** Bar graph representing the percentage of BAK localised to mitochondria in proliferating (white bar) and senescent (red bars) cells. **(C)** Bar graph depicting quantification of the percentage of BAX localised to mitochondria in proliferating (white bars) and senescent (red bars) cells. **(D)** Representative Western Blot image of the total levels of BCL-2, VDAC and β-Actin. Bar graphs demonstrating quantification of BCL-2 normalised to VDAC **(E)** and β-actin **(F)** in proliferating (white bars) and senescent (red bars). Bar graph data is shown as mean + SEM and represents 6 independent experiments for **(B and C, note replicative senescent quantification n=1)**, and 3 independent experiments for **(E and F)**, statistical significance was determined using a two-tailed unpaired t test.

The characterisation of BAX and BAK in the previous figures highlights that following the development of senescence the total levels of BAK are increased, whereas the total levels of BAX are not changed. However the assessment of overall protein levels does not provide information on whether BAX or BAK are existing in an inactive or an active state. It is particularly difficult to determine whether these proteins are active, however, it has been demonstrated that when BAX is in an active state it undergoes a conformational change which exposes the 6A7 epitope (Gavathiotis *et al.*, 2010). Therefore an antibody against the BAX 6A7 epitope was used to characterise proliferating and senescent cells via Western Blotting and Immunofluorescence. First, the total levels of BAX (6A7) were assessed. It was found that there

was no difference between proliferating and senescent cell when normalised to either the mitochondrial protein VDAC or overall protein level ($p=0.1574$ and 0.4958, Figures 3.9A, B and C). Next the levels of BAX (6A7) were assessed in mitochondrial and cytoplasmic fractions derived from proliferating and senescent cells. It was found that in the mitochondrial fraction, the level of BAX (6A7) was decreased in senescent cells compared to proliferating cells ($p<0.0001$, Figures 3.9D and E). Furthermore, it was found that the ratio of mitochondrial to cytoplasmic BAX (6A7) was decreased in senescent cells compared to proliferating cells, indicating that there is more cytoplasmic BAX (6A7) in senescent cells ($p=0.0110$, Figures 3.9D and F). Finally, proliferating and senescent cells were labelled with the 6A7 antibody as shown in the representative images in Figure 3.9G and the mean fluorescence intensity of the staining was measured. Conversely, it was found that the mean fluorescence intensity was significantly increased in senescent cells compared to proliferating cells indicating that BAX (6A7) is more abundant in senescent cells ($p=0.0286$, Figures 3.9G and H).

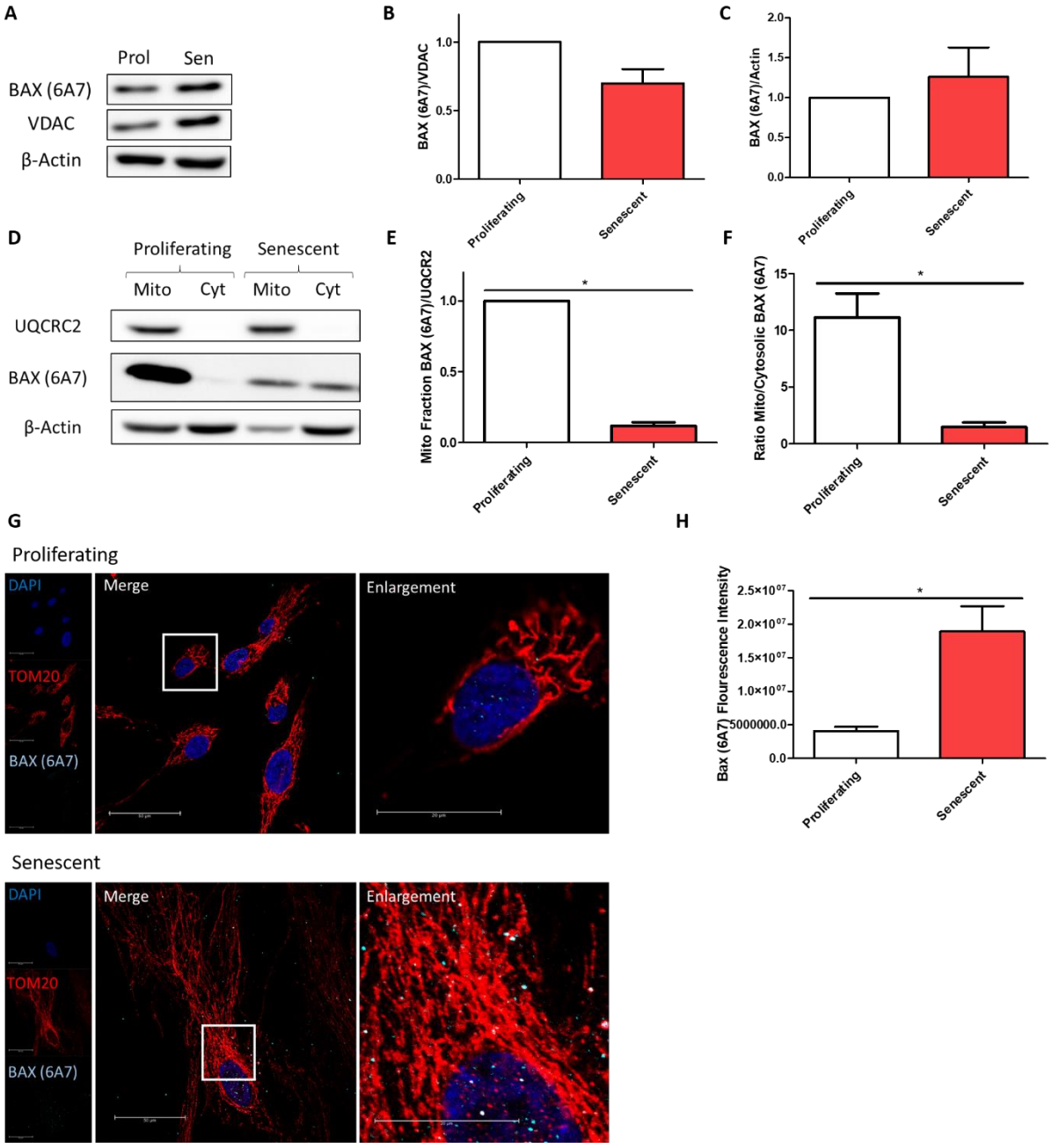

Figure 3.9 – Characterisation of BAX (6A7) in proliferating and senescent cells.

The total protein levels of BAX and BAK were analysed in proliferating and stress-induced senescent cells (10 days post irradiation). **(A)** Representative western blot of the total levels of BAX (6A7), VDAC and β-Actin. Bar graphs demonstrating quantification of BAX (6A7) normalised to VDAC **(B)** and β-actin **(C)** in proliferating (white bars) and senescent (red bars), n=6 independent experiments. **(D)** Representative Western Blot image of UQCRC2, BAX (6A7) and β-Actin. **(E)** Bar graph demonstrating the fold change of BAX (6A7) normalised to the mitochondrial protein UQCRC2 in the mitochondrial fraction of proliferating (white bar) and senescent (red bars) cells. **(F)** Bar graph depicting quantification of the ratio of mitochondrial/cytosolic BAX (6A7) in proliferating (white bars) and senescent (red bars) cells, n=3 independent experiments. **(G)** Representative image of proliferating and senescent cells

labelled with DAPI (blue), TOM20 (red) and BAX (6A7) (cyan) imaged by confocal microscopy using a 63x objective. **(H)** Bar graph represents quantification of the mean fluorescence intensity of BAX (6A7) as measured by the mean integrated density in proliferating (white bar) and senescent cells (red bar), n=4 independent experiments. Bar graph data is shown as mean + SEM, statistical significance was determined using a two-tailed unpaired t test.

3.5. The presence of cytosolic mtDNA is dependent on BAX and BAK pores

It has recently been reported that the escape of mtDNA from within the mitochondrial matrix occurs due to the formation of BAX and BAK macropores (McArthur *et al.*, 2018; Riley *et al.*, 2018). Therefore I wanted to address whether the formation of BAX and BAK pores can facilitate the release of mtDNA observed during senescence. In order to do this, I utilised the CRISPR-Cas9 gene editing tool to generate cells that were deficient for both BAX and BAK alongside an empty vector control cell line (Figure 3.10B). Then, to test whether BAX and BAK pores impact on the release of mtDNA, I induced both the empty vector control and BAX/BAK deficient cells to become senescent alongside proliferating controls. As expected, the senescent empty vector control cells displayed mtDNA nucleoids in the cytoplasmic region (Figure 3.10A), however, in BAX/BAK deficient cells the mean number of cytoplasmic mtDNA was significantly reduced ($p<0.0001$, Figure 3.10C), similarly, the percentage of BAX/BAK deficient cells displaying cytoplasmic mtDNA was significantly reduced compared to senescent empty vector control cells ($p<0.0001$) (Figure 3.10D).

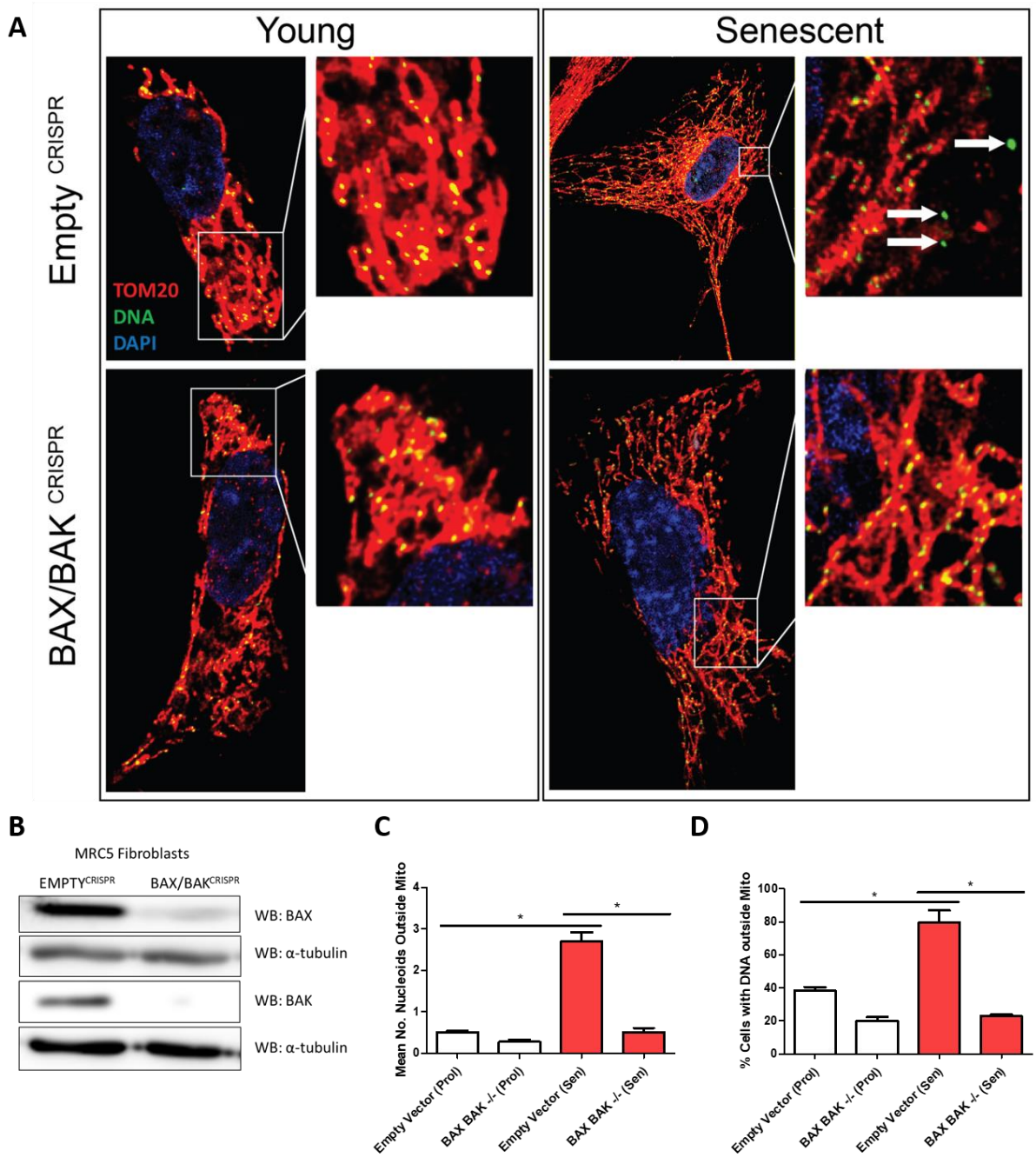

Figure 3.10 – Release of mtDNA during senescence is dependent on BAX and BAK pores.

(A) Representative images of empty vector and BAX/BAK deficient MRC5 fibroblasts labelled with DAPI (blue), DNA (green) and TOM20 (red), shown are proliferating and stress-induced senescent cells which have been imaged by confocal microscopy on a 63x objective. (B) Representative western blot showing protein levels of BAX and BAK in empty vector^{CRISPR} and BAX/BAK^{CRISPR} cells. **(C)** Bar graph depicting the mean number of nucleoids in proliferating (white bars) and senescent (red bars) empty vector and BAX/BAK deficient cells. n=4 independent experiments. **(D)** Bar graph depicting the percentage of cells displaying mtDNA nucleoids outside of the mitochondrial network in proliferating (white bars) and senescent (red bars) empty vector and BAX/BAK deficient cells. n=4 independent experiments. Bar graph

data is shown as mean, error bars represent the standard error of the mean, statistical significance was determined using a one-way ANOVA.

3.6. The SASP is dependent on mtDNA release by BAX and BAK pores

Following the observation that cells deficient for BAX and BAK no longer display cytosolic mtDNA I wanted to assess what the wider implications of this were on the senescence phenotype. As the transfection of mtDNA into MRC5 fibroblasts provoked a pronounced inflammatory response (Figure 3.5), it was of particular interest to understand whether BAX/BAK cells which no longer display mtDNA had any observable changes in there pro-inflammatory secretome. It has been previously been published that following the induction of stress-induced senescence it typically takes between 7 and 10 days for the senescence phenotype and SASP to be established (Coppe *et al.*, 2008; Passos *et al.*, 2010). Therefore, once the senescent phenotype had established 10 days post exposure to X-ray irradiation, the levels of IL-6 and IL-8 being secreted by senescent empty vector and BAX/BAK deficient cells were measured by ELISA (Figures 3.11A and B). It was observed that senescent empty vector control cells had a marked increase in the secretion of IL-6, and IL-8 compared to their proliferating counterparts ($p<0.0001$ for both cytokines). BAX/BAK deficient senescent cells on the other hand were not significantly increased compared to BAX/BAK deficient proliferating cells for any of the cytokines. Interestingly, the secretion of IL-6 and IL-8 was dramatically attenuated in senescent BAX/BAK deficient cells compared to senescent empty vector cells ($p<0.0001$ in both instances, Figures 3.11A and B). Following these observations, I wanted to assess the secretome profile more widely and comprehensively. In order to do this media was taken from proliferating and senescent empty vector and BAX/BAK deficient cells at 10 days post senescence induction and then analysed by cytokine array (Figure 3.11C). Consistently, IL-6 and IL-8 were both upregulated in empty vector senescent cells compared to their proliferating counterparts. Notably, IP-10, FGF-2 (fibroblast growth factor 2), GM-CSF (granulocyte-macrophage colony-stimulating factor), Gro-α, MCP-3 (monocyte chemoattractant protein 3), IL-15 and VEGF-A (vascular endothelial growth factor A) were all also upregulated. Comparing between the senescent empty vector and BAX/BAK deficient cells, each of these noted cytokines were downregulated. Although reduced compared to senescent empty vector cells, in senescent BAX/BAK deficient cells the cytokines Gro-α, G-CSF (granulocyte-colony stimulating factor) and IL-6 were still upregulated to a small extent compared to this proliferating counterparts (Figure 3.11C).

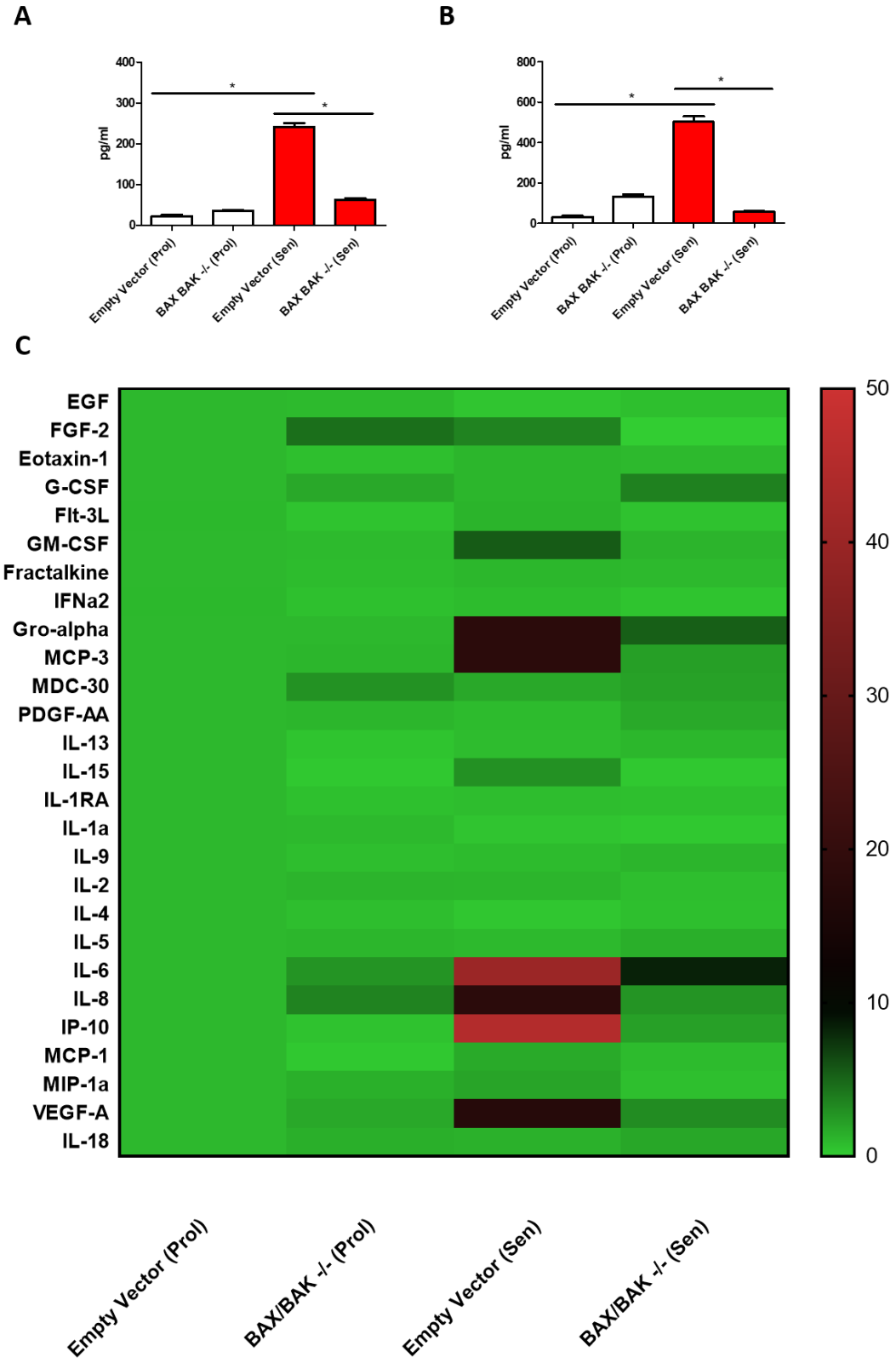

Figure 3.11 – The SASP is dependent on BAX and BAK pores.

Empty vector and BAX/BAK deficient cells were induced to undergo stress-induced senescence using irradiation, 20Gy. Serum-free media was collected 10 days post irradiation following 24 hours of serum starvation. Samples were then analysed either by ELISA or cytokine array. **(A and B)** Bar graphs depict the levels of IL-6 and IL-8 (pg/ml) secreted into the media as measured by ELISA for proliferating (white bars) and senescent (red bars) empty vector and BAX/BAK deficient cells, n=6 independent experiments normalised to the number of cells per sample. **(C)** Tabular summary of secreted cytokine array represented as fold change compared to the proliferating empty vector control samples, where green equals no fold change and red equates to up to a 50-fold change in accordance with the scale on the right hand side, n=6 independent experiments. Bar graph data is shown as mean, error bars represent the standard error of the mean, statistical significance was determined using a one-way ANOVA.

3.7. BAX and BAK do not regulate the cell cycle arrest

After it was observed that senescent cells deficient for BAX and BAK no longer displayed the pro-inflammatory senescence signature, it was of further interest to characterise whether there was an impact on the cell cycle arrest. Therefore, I assessed the expression of two key cyclin-dependent kinase inhibitors which have been associated with enforcing the cell cycle arrest, p16 and p21 (Campisi and d'Adda di Fagagna, 2007). As cellular senescence is characterised by a stable cell cycle arrest, the proliferation marker Ki67 was also analysed. Furthermore, SA-β-Gal is considered a classical marker of senescent cells and was therefore also measured (Dimri *et al.*, 1995). First, SA-β-Gal was assessed by histochemical staining for beta-galactosidase activity at pH 6.0 (Figure 3.12A). Following the induction of senescence it was found that empty vector senescent cells compared to proliferating cells displayed a vast increase in the percentage of cells positive for SA-β-Gal ($p<0.0001$), similarly, BAX/BAK deficient cells displayed a large increase in the percentage of cells positive for SA-β-Gal compared to their proliferating controls ($p<0.0001$). Furthermore, there was no statistical difference in the number of positive cells between senescent empty vector and BAX/BAK deficient cells (Figures 3.12A and B). To assess levels of p16 and p21, immunofluorescence was utilised. It has been demonstrated that activation of both p16 and p21 results in translocation of these proteins to the nuclear region (Stein *et al.*, 1999; Rodriguez-Vilarrupla *et al.*, 2002). Therefore, the percentage of proliferating and senescent empty vector and BAX/BAK deficient cells with positive staining for each of these markers was assessed (Figure 3.12C). For p16, it was demonstrated that the percentage of positive cells was significantly increased in empty vector senescent cells compared to proliferating empty vector cells ($p<0.0001$). Similarly, BAX/BAK deficient cells had significantly increased p16 levels compared to proliferating BAX/BAK deficient cells ($p<0.0001$). There was no statistically significant difference between p16 positive senescent empty vector and BAX/BAK deficient cells (Figures 3.12C and D). Nuclear p21 was detected by using an antibody against the $p21^{cip1/WAF1}$ antigen (Figure 3.12C). It was demonstrated that the percentage of positive cells was significantly enhanced in empty vector senescent cells compared to proliferating empty vector cells ($p<0.0001$). Furthermore, BAX/BAK deficient cells had significantly increased p21 levels when compared to their proliferating counterparts ($p<0.0001$). Comparison of empty vector and BAX/BAK deficient cells revealed no statistically significant difference (Figures 3.12C and E). Finally, in order to assess whether cells were undergoing replication the proliferation marker Ki67 was assessed by immunofluorescence (Figure 3.12F). As such, the proliferating empty vector and BAX/BAK

deficient cells displayed approximately 35% of cells stained positively for this marker. In the senescent groups, both the empty vector and BAX/BAK deficient cells displayed very few Ki67 positive cells indicating that these cells were no longer dividing, there was no significant difference between the two. Both senescent groups displayed significantly reduced levels of Ki67 compared to their proliferating controls ($p<0.0001$ for both empty vector and BAX/BAK deficient cells) (Figure 3.12F and G).

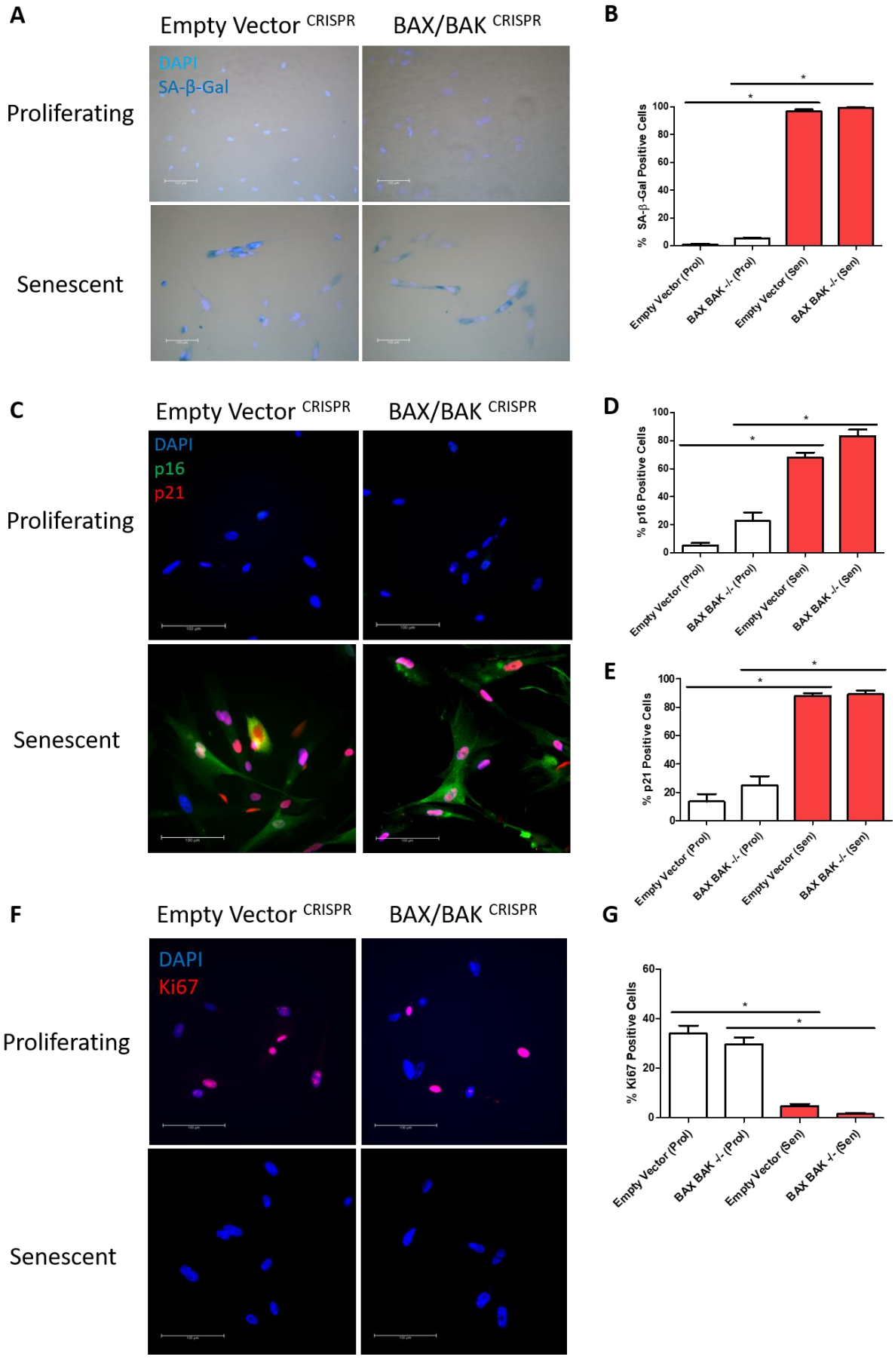
A
Empty Vector CRISPR
BAX/BAK CRISPR
Proliferating
Senescent
DAPI
SA-β-Gal
B
% SA-β-Gal Positive Cells
Empty Vector (Prol)
BAX BAK -/- (Prol)
Empty Vector (Sen)
BAX BAK -/- (Sen)
C
Empty Vector CRISPR
BAX/BAK CRISPR
Proliferating
Senescent
DAPI
p16
p21
D
% p16 Positive Cells
E
% p21 Positive Cells
F
Empty Vector CRISPR
BAX/BAK CRISPR
Proliferating
Senescent
DAPI
Ki67
G
% Ki67 Positive Cells

Figure 3.12 – BAX and BAK do not affect the expression of cyclin dependent kinase inhibitors p16, p21 and SA-β-Gal activity.

Empty vector and BAX/BAK deficient cells were induced to become senescent by X-ray irradiation, 20Gy. Markers of senescence were subsequently analysed 10 days post irradiation when the senescent phenotype has developed. **(A)** SA-β-Gal activity was detected by histochemical staining for beta-galactosidase activity at pH 6.0. Representative images of SA-β-Gal staining (histochemical light blue) and DAPI (immunofluorescence dark blue nuclear stain), acquired using a 20x objective on a wide-field microscope. **(B)** Bar graph depicts the percentage of cells positive for SA-β-Gal staining in proliferating (white bars) and senescent (red bars) empty vector and BAX/BAK deficient cells, n=4 independent experiments. **(C)** Representative images following staining of cells for DAPI (blue), p16 (green) and p21 (red) acquired using a 40x objective on a wide-field microscope. Cells were considered positive for p16 or p21 when they displayed nuclear staining. **(D)** Bar graph depicts the percentage of cells positive for p16 staining in proliferating (white bars) and senescent (red bars) empty vector and BAX/BAK deficient cells, n=7 independent experiments. **(E)** Bar graph depicts the percentage of cells positive for p21 staining in proliferating (white bars) and senescent (red bars) empty vector and BAX/BAK deficient cells, n=7 independent experiments. **(F)** Representative images following staining of cells for DAPI (blue) and Ki67 (red), acquired using a 40x objective on a wide-field microscope. Cells were considered positive for Ki67 when they displayed nuclear staining. **(G)** Bar graph depicts the percentage of cells positive for Ki67 staining in proliferating (white bars) and senescent (red bars) empty vector and BAX/BAK deficient cells, n=4 independent experiments. Bar graph data is shown as mean, error bars represent the standard error of the mean, statistical significance was determined using a one-way ANOVA.

3.8. BAX and BAK do not mediate DNA damage or ROS production.

Previous work has implicated that the cell cycle arrest occurs in response to a DDR. Furthermore, it has been demonstrated that ROS provide a positive feedback loop by driving DNA damage which reinforces the cell cycle arrest (Alcorta *et al.*, 1996; Passos *et al.*, 2010; Correia-Melo *et al.*, 2016). Phosphorylation of histone H2AX, referred to as γH2AX, occurs in response to DNA damage as a signal to mediate DNA damage repair, therefore, it provides a reliable marker of DNA damage. As there was BAX/BAK deficient cells displayed no change in p16 and p21 which induce and maintain the cell cycle arrest, it was therefore of interest to assess whether DNA damage was affected (Figure 3.13A). Analysis of γH2AX 10 days post-induction of senescence revealed that senescent empty vector cells had a significant 2-fold increase in the mean number of γH2AX foci compared to proliferating empty vector cells ($p<0.0001$), similarly, BAX/BAK deficient senescent cells displayed a 2-fold increase in the mean number of γH2AX foci ($p<0.0001$). There was no significant difference in the number of foci between senescent empty vector and BAX/BAK deficient cells (Figure 3.13B). As it is known that mitochondrial derived ROS are responsible for inducing short-term foci which maintain the DDR, I wanted to assess whether cells lacking BAX/BAK had any changes in ROS generation. Therefore, ROS was measured using MitoSOX. It was found that ROS was vastly increased in senescent empty vector cells compared to their proliferating controls ($p<0.0001$), the same increase was observed in BAX/BAK deficient senescent cells and their proliferating controls ($p<0.0001$). However, no significant difference was observed between BAX/BAK deficient senescent cells and senescent empty vector cells (Figure 3.13C).

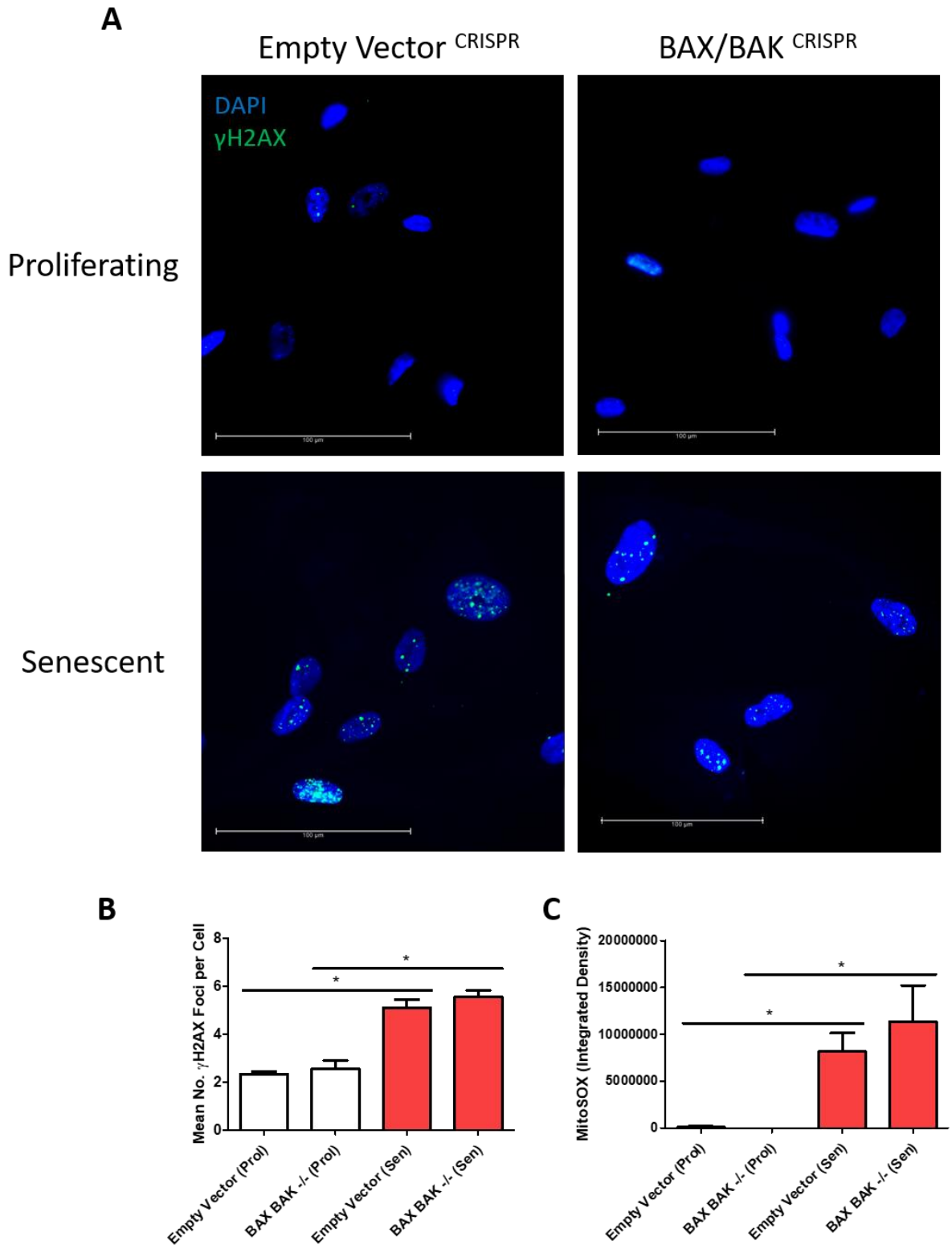

Figure 3.13 – BAX and BAK do not mediate DNA damage or ROS production.

Empty vector and BAX/BAK deficient cells were induced to become senescent by X-ray irradiation, 20Gy. Markers of senescence were subsequently analysed 10 days post irradiation when the senescent phenotype has developed. **(A)** Representative images of proliferating and

senescent empty vector and BAX/BAK deficient cells labelled for γH2AX (green) and DAPI (blue). Imaged using a 40x objective using a wide-field microscope, individual γH2AX foci were counted in each nucleus. **(B)** Bar graph depicting the mean number of γH2AX foci per cell in proliferating (white bars) and senescent (red bars) empty vector and BAX/BAK deficient cells, n=4 independent experiments. **(C)** Bar graph depicting MitoSOX integrated intensity measured following imaging using a 63x objective on a confocal microscope in proliferating (white bars) and senescent (red bars) empty vector and BAX/BAK deficient cells, n=4 independent experiments. Bar graph data is shown as mean, error bars represent the standard error of the mean, statistical significance was determined using a one-way ANOVA.

3.9. BAX/BAK deficient cells do not undergo metabolic reprogramming

Following the observation that BAX/BAK deficient cells display a diminished SASP, I wanted to assess whether this could be associated with metabolic changes. It has been reported that cells deficient for BAX are less able to produce ATP via oxidative phosphorylation and shift to energy production via glycolysis (Boohaker *et al.*, 2011). Moreover, in the study where it was demonstrated that senescent cells which were depleted of mitochondria lacked a SASP, these cells were also entirely dependent on glycolysis for their energy requirements (Correia-Melo *et al.*, 2016). Therefore, it is plausible that the SASP reducing effects may be due to metabolic reprogramming to glycolysis following genetic deletion of BAX and BAK. As such, I wanted to investigate how BAX/BAK deficient cells produce there ATP.

First, using the Seahorse XF analyser which measures overall ATP production it was discovered that both senescent Empty Vector and BAX/BAK deficient cells had a significantly increased overall ATP production compared to their proliferating counterparts (Figure 3.14A). When the overall ATP production was normalised to represent the percentage that was acquired from glycolysis and oxidative phosphorylation it was found that there was no difference in the source of ATP between proliferating and senescent Empty Vector and BAX/BAK deficient cells (Figure 3.14B).

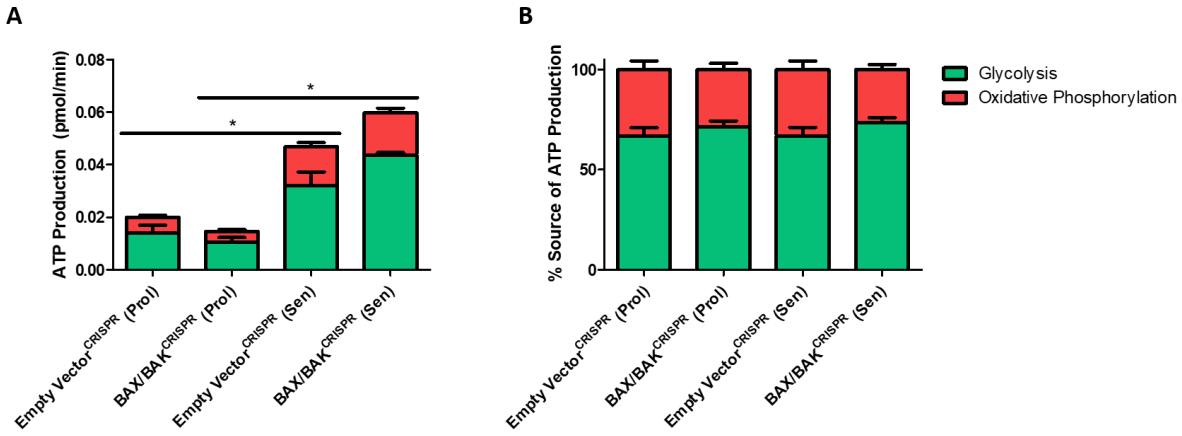

Figure 3.14 - BAX/BAK deficient cells do not undergo metabolic reprogramming

Proliferating and senescent Empty Vector and BAX/BAK deficient MRC5 human fibroblasts were assessed for ATP production using the Seahorse XF24 analyser. **(A)** The bar graph represents overall ATP production for proliferating and senescent Empty Vector and BAX/BAK deficient MRC5 human fibroblasts. Green represents the amount of energy derived from glycolysis and red by oxidative phosphorylation. **(B)** The bar graph represents the energy

production by glycolysis or oxidative phosphorylation normalised to total ATP production and expressed as a percentage. Green represents the percentage of energy derived from glycolysis and red by oxidative phosphorylation. In both cases n=5 independent experiments. Bar graph data is shown as mean, error bars represent the standard error of the mean, statistical significance was determined using a one-way ANOVA.

3.10. The MPTP pore does not contribute to mtDNA release

Whilst characterising the function of mitochondria in senescent cells I observed that they exist in a depolarised state (Figure 3.1G). Mitochondria are maintained in this state of depolarisation by the mitochondrial permeability transition pore (MPTP). The MPTP allows the influx/efflux of molecules up to 1500 Da from the mitochondrial matrix, its opening is associated with mitochondrial depolarisation and has been demonstrated to result in an impairment of energetic function, promote Ca^{2+} release. Collectively, these changes are associated with matrix swelling which leads to release of pro-apoptotic proteins such as cytochrome C (Halestrap, 2009; Rasola and Bernardi, 2011). Therefore I investigated whether the MPTP contributes to the release of mtDNA during senescence. It has been demonstrated that Cyclosporin A can block the MPTP by its binding to the mitochondrial cyclophilin D (Halestrap *et al.*, 1997). To address the role of the MPTP, I treated senescent cells with Cyclosporin A and then measured mtDNA release and the SASP factors; IL-6, IL-8 and IP10. In proliferating cells, treatment with Cyclosporin A had no effect on the mean number of free mtDNA nucleoids or the percentage of cells with mitochondrial-free DNA. Following the induction of senescence, as expected, there was an increase in the mean number of nucleoids present outside of the mitochondria, as well as an increase in the percentage of cells exhibiting mitochondrial-free DNA compared to proliferating cells ($p<0.0001$). However, treatment with Cyclosporin A did not affect the percentage of cells with cytoplasmic DNA, however, there was a small but non-significant decrease in the mean number of nucleoids outside of the mitochondria compared to control senescent cells (Figures 3.15A, B and C). Furthermore, treatment of senescent cells with Cyclosporin A provoked an enhancement in the levels of IL-6, IL-8 and IP10. This was significant for all of the measured cytokines ($p<0.0001$). Cyclosporin A had no effect on the secretion of these cytokines in proliferating cells. (Figures 3.15D, E and F).

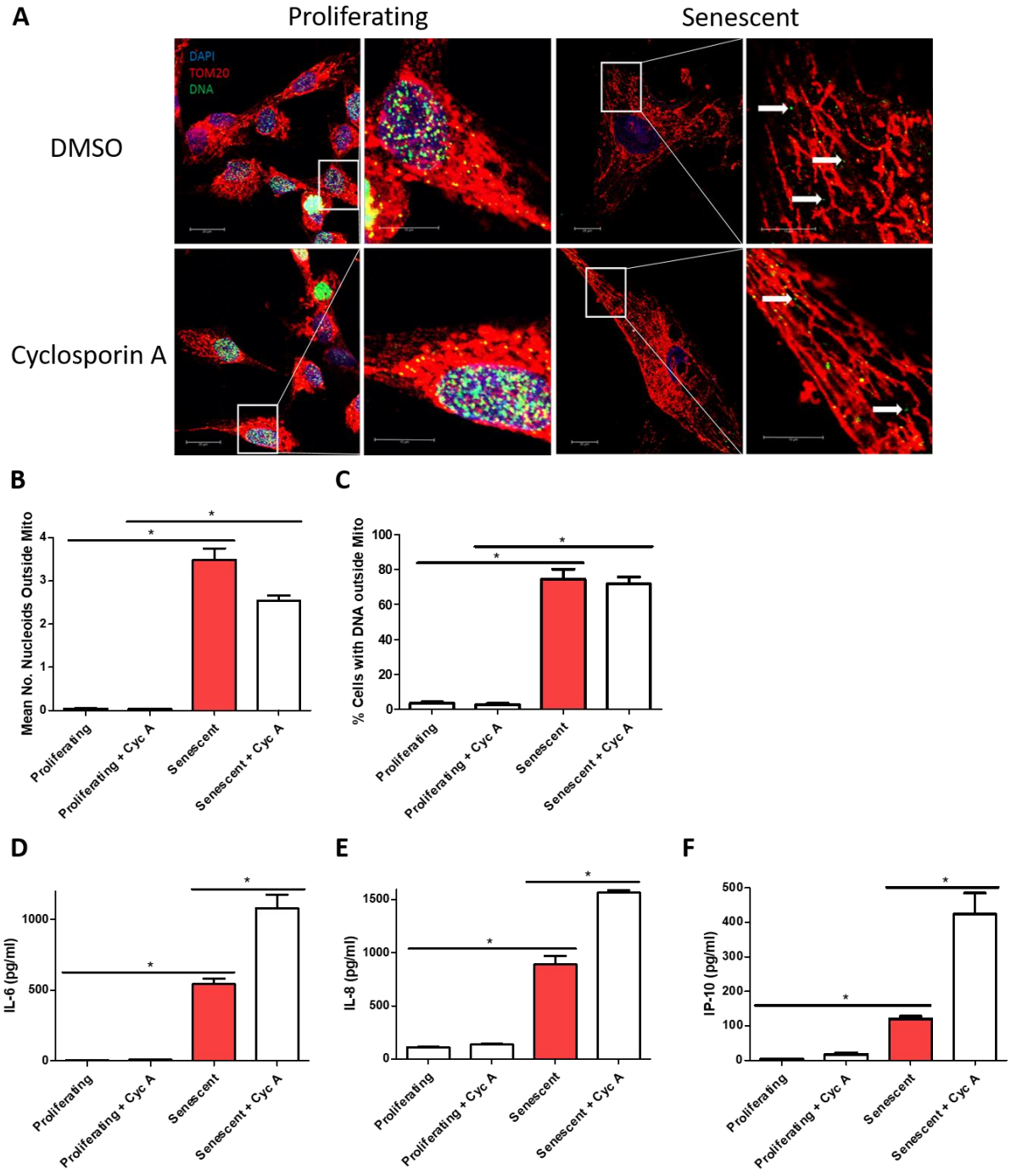

Figure 3.15 – The MPTP pore does not contribute to mtDNA release.

MRC5 fibroblasts were induced to undergo stress-induced senescence (20Gy irradiation). Following the induction of senescence, cells were maintained with Cyclosporin A. Leakage of mtDNA and secretion of SASP factors was assessed 10 days later **(A)** Representative images of proliferating and senescent cells labelled with DAPI (blue), TOM20 (red) and DNA (green) which have been treated with either Cyclosporin A (1µM) or DMSO only as a control. Images acquired using a 63x objective by confocal microscopy. **(B)** Bar graph depicts quantification of the mean number of mtDNA nucleoids outside of the mitochondrial network in proliferating and senescent cells treated with Cyclosporin A (1µM) or DMSO only as a control, n=4

independent experiments. **(C)** Bar graph depicts the percentage of cells exhibiting mtDNA nucleoids outside of the mitochondrial network in proliferating and senescent cells treated with Cyclosporin A (1µM) or DMSO only as a control, n=4 independent experiments. **(D, E and F)** Bar graphs depict the levels of IL-6, IL-8 and IP10 (pg/ml) secreted into the media as measured by ELISA for proliferating and senescent cells treated with Cyclosporin A (1µM) or DMSO only as a control, n=4 independent experiments. Bar graph data is shown as mean, error bars represent the standard error of the mean, statistical significance was determined using a one-way ANOVA.

Although not fully understood at this stage, it is recognised that the MPTP pore is composed of a number of subunits, such as cyclophilin D, the adenine nucleotide translocase (ANT) and the voltage dependent anion channel (VDAC) (Briston *et al.*, 2017). Following the observation that inhibition of the cyclophilin D by Cyclosporin A had no effect on mtDNA release and did not suppress the SASP, it was therefore of interest to assess whether the drugs Olesoxime (which inhibits VDAC) and Bongkrekic acid (which inhibits ANT) have any effect on the SASP (Bordet *et al.*, 2010; Anwar *et al.*, 2017). To address the effect of these inhibitors on the SASP, senescent cells were treated with either Olesoxime or Bongkrekic acid, then IL-6 or IL-8 were measured. Treatment of senescent cells with Olesoxime (1µM) promoted a small but non-significant increase in the secretion of both IL-6 and IL-8 (Figures 3.16A and B). Furthermore, blockage of ANT using Bongkrekic acid (0.1 - 25µM) had no effect on the secretion of IL-8 in senescent cells (Figure 3.16C).

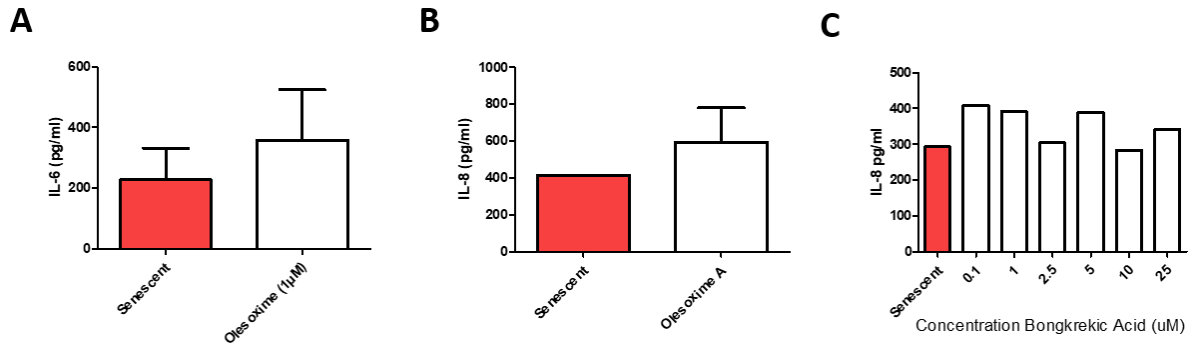

Figure 3.16 – Pharmacological inhibition of VDAC or ANT does not suppress the SASP

MRC5 fibroblasts were induced to undergo stress-induced senescence (20Gy irradiation). Following the induction of senescence, cells were maintained with either Olesoxime or Bongkrekic acid. Secretion of SASP factors was assessed 10 days later. **(A and B)** Bar graphs depict the levels of IL-6 and IL-8 (pg/ml) secreted into the media as measured by ELISA for senescent (red bars) and senescent cells treated with Olesoxime (1µM) (white bars), n=3 technical replicates. **(C)** Bar graph depicts the levels of IL-8 (pg/ml) secreted into the media as measured by ELISA for senescent (red bars) and senescent cells treated with Bongkrekic acid

(0.1 - 25μM) (white bars), n=1. Bar graph data is shown as mean, error bars represent the standard error of the mean, for A and B statistical significance was determined using a two-tailed unpaired t-test.

3.11. Pharmacological inhibition of BAX prevents mtDNA release and the SASP

Next, I wanted to assess whether I could suppress mtDNA release and subsequently, the SASP, using pharmacological inhibitors of BAX and BAK. The formation of pores can be prevented using the pharmacological agent BAX-inhibiting peptide v5 (BIP v5) which suppresses translocation of BAX to the mitochondria by inhibiting the Ku70 binding domain found on the BAX protein (Sawada *et al.*, 2003). As such to test whether pharmacological blockage of BAX and BAK pores could prevent mtDNA release, cells were treated with BIP v5 following the induction of senescence. As previously observed, the induction of senescence provokes an increase in the mean number of cytosolic mitochondrial nucleoids, interestingly, the inhibition of pore formation using BIP v5 significantly decreases the release of mtDNA to a level comparable with that of proliferating cells ($p<0.001$) (Figures 3.17A and B). Similarly, the percentage of cells displaying cytosolic mtDNA is significantly reduced in senescent cells treated with BIP v5 compared to those which have not ($p<0.001$) (Figures 3.17A and C). In proliferating cells, BIP v5 has no effect on the mean number of mtDNA nucleoids outside of the mitochondrial network or the percentage of cells displaying mitochondrial free DNA (Figures 3.17A, B and C). Following the finding that BIP v5 could prevent mtDNA release, I next wanted to understand whether this could potentially suppress the SASP.

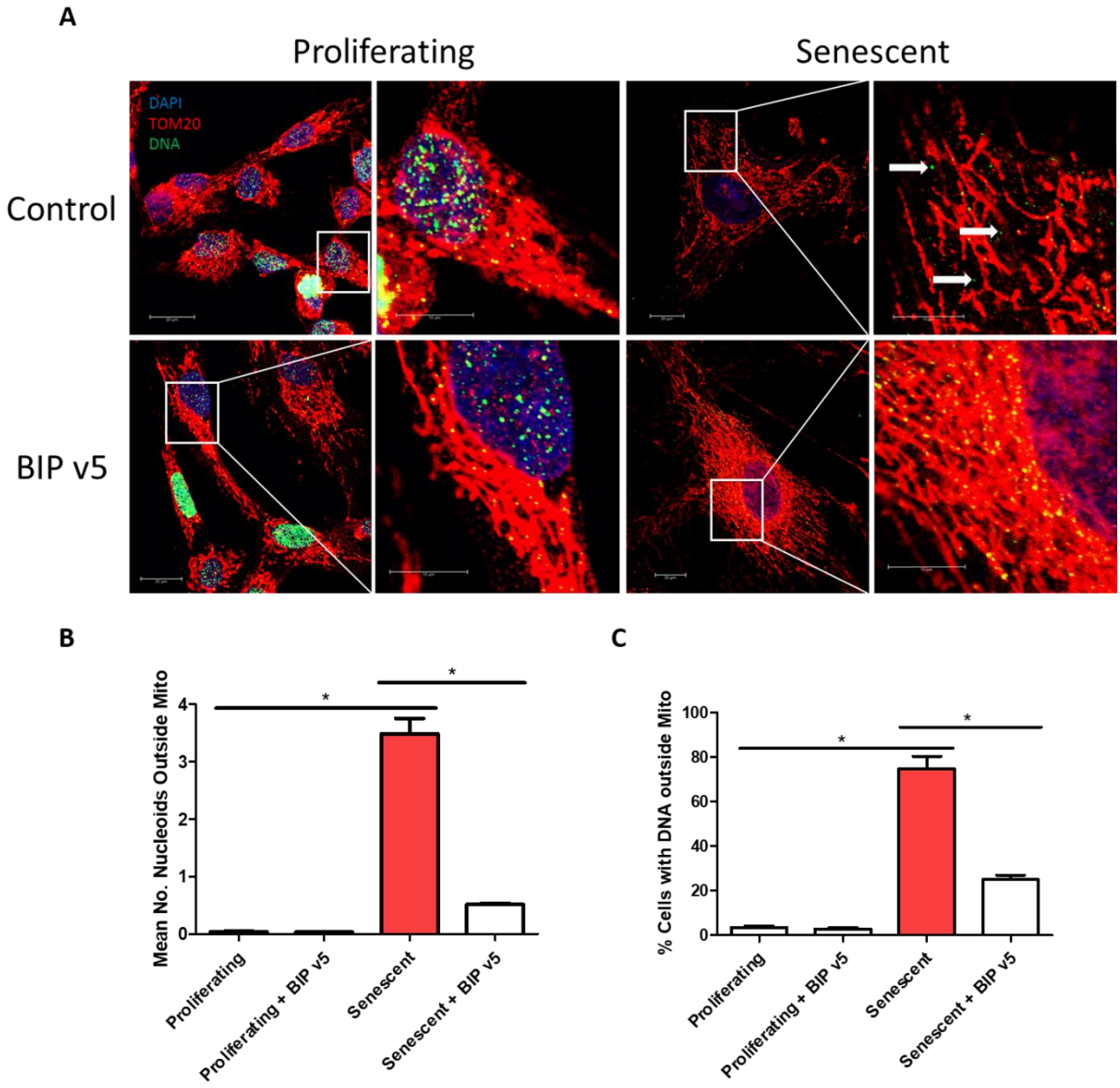

Figure 3.17 – Pharmacological inhibition of BAX prevents mtDNA release.

MRC5 fibroblasts were induced to undergo stress-induced senescence (20Gy irradiation). Following the induction of senescence, cells were maintained with BIP v5. Leakage of mtDNA was assessed 10 days later. **(A)** Representative images of proliferating and senescent cells labelled with DAPI (blue), TOM20 (red) and DNA (green) which have been treated with either BIP v5 (100µM dissolved in water) or untreated as a control. Images acquired using a 63x objective by confocal microscopy. **(B)** Bar graph depicts quantification of the mean number of mtDNA nucleoids outside of the mitochondrial network in proliferating and senescent cells treated with BIP v5 (100µM dissolved in water) or untreated as a control, n=4 independent experiments. **(C)** Bar graph depicts the percentage of cells exhibiting mtDNA nucleoids outside of the mitochondrial network in proliferating and senescent cells treated with BIP v5 (100µM dissolved in water) or untreated as a control, n=4 independent experiments. Bar graph data is shown as mean, error bars represent the standard error of the mean, statistical significance was determined using a one-way ANOVA.

In order to assess whether pharmacological inhibition of BAX and BAK pores could prevent the SASP, MRC5 fibroblasts were induced to become senescent and subsequently maintained with BIP v5. The senescent cells displayed a large increase in the secretion of the SASP factors IL-6, IL-8 and IP10 ($p<0.0001$ in each case). Treatment of senescent cells with low doses of BIP v5 (1-10μM) does not have any significant effect on the secretion of IL-6, IL-8 or IP10. However, treatment of senescent cells with high doses of BIP v5 (50 and 100μM) significantly decreases the secretion of IL-6, IL-8 and IP10 in untreated senescent cells. Furthermore, treatment of proliferating cells with BIP v5 had no effect on cytokine secretion at any of the tested concentrations (Figures 3.18A, B and C).

Another drug which blocks pores is the BAX channel blocker (BCB), however the mechanism of action of this drug is slightly different. This does not prevent BAX undergoing its conformational change during activation, but blocks pores that have formed. BCB has been demonstrated to prevent apoptosis and the release of inner membrane proteins such as cytochrome C following pore blockage (Bombrun *et al.*, 2003). As such, MRC5 fibroblasts were induced to become senescent and then maintained in the presence of the BCB. The induction of senescence lead to a significant increase in each of the measured cytokines (IL-6, IL-8 and IP10). Treatment of senescent cells with BCB lead to a significant decrease in IL-6 and IP10 at each of the tested concentrations, 0.1, 1 and 2.5μM. Interestingly, for IL-8, only the 2.5μM concentration was effective at suppressing the SASP, where an approximate 40% decrease was observed. Treatment with BCB had no effect on any of the cytokines in proliferating cells (Figures 3.18D, E and F).

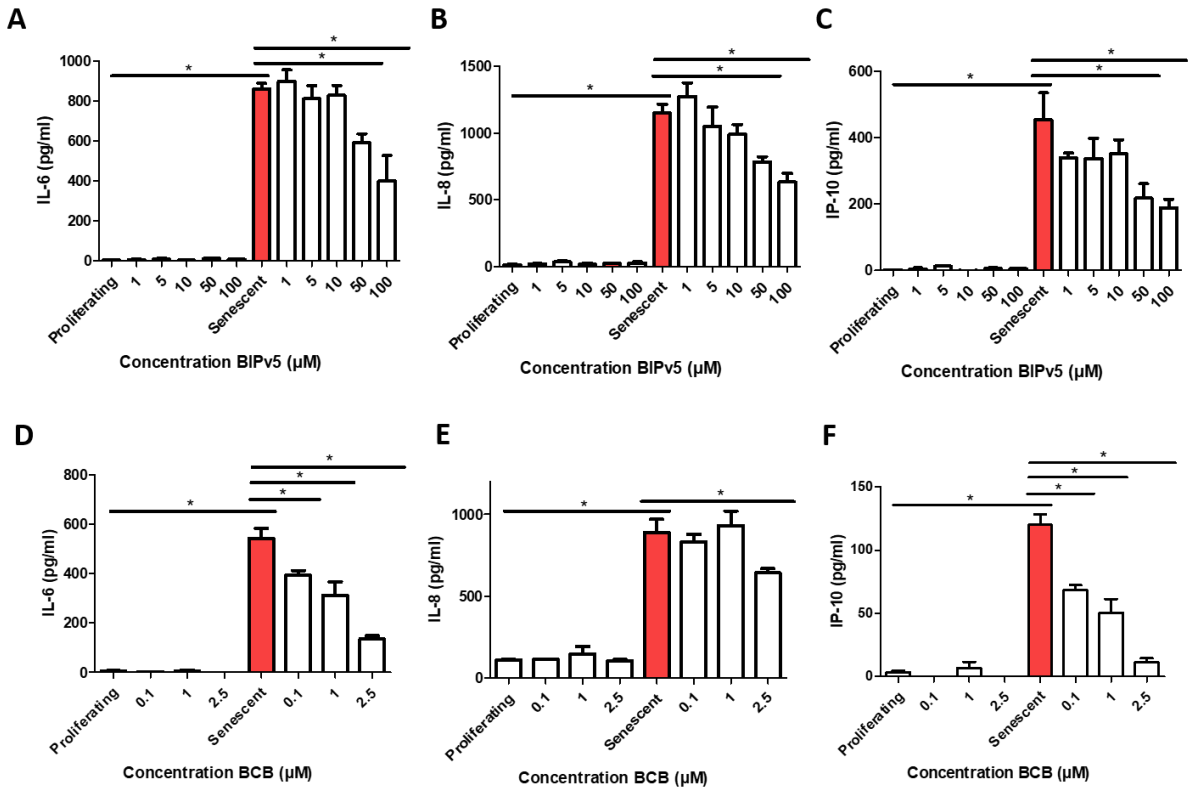

Figure 3.18 - Pharmacological inhibition of BAX suppresses the SASP.

MRC5 fibroblasts were induced to undergo stress-induced senescence (20Gy irradiation). Following the induction of senescence, cells were maintained with either BIP v5 or BCB at a range of concentrations. Secretion of SASP factors was assessed 10 days later. **(A, B and C)** Bar graphs depict the levels of IL-6, IL-8 and IP10 (pg/ml) secreted into the media as measured by ELISA for proliferating and senescent cells treated with BIP v5 (1-100μM) or untreated as a control, n=4 independent experiments. **(D, E and F)** Bar graphs depict the levels of IL-6, IL-8 and IP10 (pg/ml) secreted into the media as measured by ELISA for proliferating and senescent cells treated with BCB (01-2.5μM) or treated with DMSO only as a control, n=4 independent experiments. Bar graph data is shown as mean, error bars represent the standard error of the mean, statistical significance was determined using a one-way ANOVA.

Following my observations *in vitro* that genetic removal and pharmacological inhibition of BAX and BAK alleviate the SASP I wanted to test whether these findings can be translated *in vivo*. It has been recently demonstrated that liver tissue obtained from irradiated mice display upregulation of the SASP genes IL-1α, IL-1β, IFN-α, IL-6, CXCL1 and MMP3 (Dou *et al.*, 2017). Furthermore, another study demonstrated that a number of interferon related genes are upregulated in adipose tissue 3 months following irradiation; IFN1α, OAS1 and inhibin A (De Cecco *et al.*, 2019). To dissect the role of BAX and BAK in the SASP, mice with BAX and BAK deleted (BAX^{fl}/BAK-/-) specifically from the liver were irradiated and the SASP genes

listed above were assessed alongside p16 and p21 7 days later, BAK-/- mice were used as a control.

In the BAK-/- control mice following irradiation there was a trend for an increase in the following inflammatory genes; CXCL1 (15.5 fold), IFNα (1.6 fold), IL-1α (2.4 fold), IL-1β (2.2 fold), IL-6 (1.5 fold), Inhibin A (1.7 fold), MMP3 (2.2 fold), OAS1 (2.4 fold). Following irradiation in the BAX^{fl}/BAK-/- mice there was no increase in any of the inflammatory genes. The following genes were significantly decreased in irradiated BAX^{fl}/BAK-/- mice compared to irradiated BAK-/- mice; IL-1α ($p<0.05$), IL-1β ($p<0.001$) and OAS1 ($p<0.05$). There was a tendency although not significant for the other inflammatory genes to be decreased in BAX^{fl}/BAK-/- irradiated mice compared to BAK-/- irradiated mice; CXCL1, IFNα, IL-6, Inhibin A and MMP3 (Figures 3.19A-H).

Next, the cell cycle kinase inhibitors p16 and p21 were assessed. Following irradiation in BAK-/- mice, there was a non-significant increase in both p16 (1.5 fold) and p21 (2.0 fold). For the BAX^{fl}/BAK-/- mice there was no observable increase in p16 or p21 expression following irradiation. Irradiated BAX^{fl}/BAK-/- mice had lower expression of p16 ($p<0.05$) and p21 compared to irradiated BAK-/- mice (Figures 3.19I and J).

The heat map in Figure 3.19K summarises the fold change for each of the 10 genes assessed in Figures 3.19A-J.

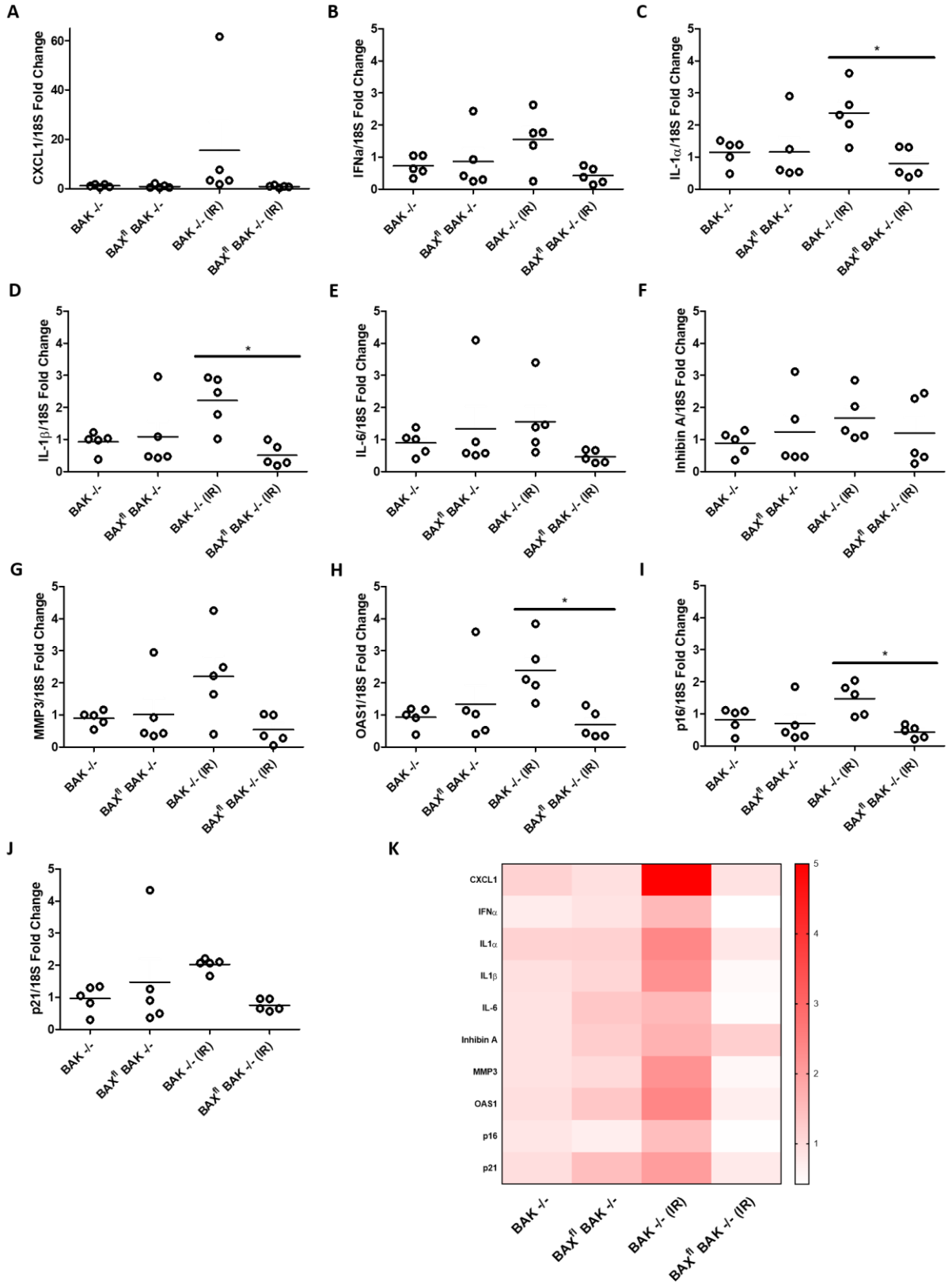

Figure 3.19 – BAX and BAK deletion reduces the SASP *in vivo*.

Mice harbouring BAK-/- and BAX^{fl}/BAK-/- deleted livers were either irradiated (4Gy) or sham irradiated. Livers were collected and analysed 7 days post-irradiation for inflammation and senescence associated genes by RT-PCR. Fold change in CXCL1**(A)**, IFNα **(B)**, IL-1α **(C)**, IL-1β **(D)**, IL-6 **(E)**, Inhibin A **(F)**, MMP3 **(G)**, OAS1 **(H)**, p16 **(I)** and p21 **(J)** mRNA levels from wild type and BAX BAK -/- mice as determined by RT-PCR. Data are normalised to the 18s house keeping gene for each sample, and then normalised to the median wild type non-irradiated mice to determine fold-change in gene expression (n=5 per group). **(K)** Heat map summarising the fold change of target genes analysed in **A-J**. *The animal work was performed by Stephen Tait and Joel Riley from the Beatson Institute for Cancer Research.* Dot plots shown as mean with each dot representing an individual animal, statistical significance was determined using a one-way ANOVA.

3.12. Discussion

Our lab recently established for the first time an essential role of mitochondria in senescence. It was shown that during the development of senescence the DDR drives mitochondrial biogenesis through MTORC1, moreover, the removal of mitochondria from human fibroblasts led to senescent cells which were devoid of the pro-inflammatory features of senescence. Similarly, a reduction of mitochondrial content *in vivo* by either MTORC1 inhibition or silencing of PGC1-β ameliorated aspects of the senescence phenotype (Correia-Melo *et al.*, 2016). Therefore the first aim of this study was to decipher a potential mechanism by which mitochondria contribute to the SASP. Collectively, our data has pinpointed the role of mtDNA as an immunostimulatory molecule which is found in the cytoplasmic region of senescent cells. This leakage is attributed to pro-apoptotic BAX and BAK pores which occur during senescence.

Research over a number of years has established that the state of mitochondria are fundamentally altered in senescent cells with regards to dynamics, metabolic function and the production of ROS (Passos *et al.*, 2007; Wiley *et al.*, 2016; Correia-Melo *et al.*, 2017; Chapman *et al.*, 2019). First, I wanted to validate that following the induction of senescence in MRC5 human fibroblasts there was detectable changes in line with the existing literature. The initial characterisation of the mitochondrial network size revealed that its size was exacerbated in senescent cells compared to proliferating cells. Although, it is not entirely understood why senescent cells accumulate more mitochondria it has been established in the literature that this increase in network size has been associated with the expression of mTOR dependent activation of PGC1-β (Correia-Melo *et al.*, 2016). Consistently, I found PGC1β to be increased in senescent cells. Moreover, the protein VDAC which is a highly conserved mitochondrial outer membrane protein was also increased in senescent cells indicating that overall mitochondrial content is increased in senescent cells. Interestingly, both with age and the onset of senescence there is evidence that mitochondria have a reduced mitochondrial membrane potential, indeed our data in both stress-induced and replicative senescence corroborate these published findings (Nicholls, 2004; Passos *et al.*, 2007).

Furthermore, one of the ways in which mitochondria have been demonstrated to drive the senescence phenotype is through the production of ROS. ROS instigates cellular damage which in turn promotes the activation of p53 and p21 which has been shown to stabilise the growth arrest (Passos *et al.*, 2010; Luo *et al.*, 2011). Furthermore, the excessive production of endogenous ROS has been associated with a number of models of senescence: replicative, OIS

and stress-induced senescence (Saretzki *et al.*, 2003; Moiseeva *et al.*, 2006; Ramsey and Sharpless, 2006; Passos *et al.*, 2007; Passos *et al.*, 2010). Consistently, I found that stress-induced senescent cells displayed a clear increase in the production of mitochondrial superoxide as measured by the mitochondrial ROS specific dye MitoSOX.

Together, these data corroborate published findings that mitochondria are dysfunctional during senescence. A recent proof of principle study demonstrated mitochondria are essential for the SASP. It was shown that the complete removal of mitochondria prior to the induction of senescence lead to the development of a senescence phenotype which was completely lacking the pro-inflammatory element of senescence (Correia-Melo *et al.*, 2016). Furthermore, the inhibition of mTOR which drives mitochondrial biogenesis in senescence through PGC1-β has been demonstrated to attenuate the SASP (Herranz *et al.*, 2015; Correia-Melo *et al.*, 2016). Similarly, knockout of PGC1-β both *in vitro* and *in vivo* has been shown to ameliorate aspects of senescence (Correia-Melo *et al.*, 2016). However, the mechanism linking mitochondria and the SASP is not understood.

A study investigating the links between mitochondrial function and regulation of the SASP observed that senescent Rho (0) IMR90 cells (which have a diminished ability to undergo oxidative phosphorylation) no longer displayed an increase in IL-6 mRNA levels or its secretion when compared to their proficient counterparts (Correia-Melo *et al.*, 2016; Wiley *et al.*, 2016). However, Rho (0) cells are also completely devoid of mtDNA, therefore I speculated that mtDNA could in fact be responsible for the pro-inflammatory response observed during senescence. From an ageing perspective mtDNA is particularly interesting as it has been observed that circulating mtDNA which is free from mitochondria increases with age in humans. This increase also correlates with the expression of a number of pro-inflammatory cytokines (Pinti *et al.*, 2014). In addition, increased levels of circulating mtDNA have been observed in a number of diseases where senescent cells have been implicated, for example; idiopathic pulmonary fibrosis, type-2 diabetes, acute myocardial infarctions and Alzheimer's disease amongst others (Ryu *et al.*, 2017; Schafer *et al.*, 2017; Wu *et al.*, 2017; Anderson *et al.*, 2019; Palmer *et al.*, 2019; Silzer *et al.*, 2019; Walaszczyk *et al.*, 2019; Zhang *et al.*, 2019). It has also been observed that mtDNA copy number is increased in senescent cells (Passos *et al.*, 2007; Correia-Melo *et al.*, 2016; Hubackova *et al.*, 2019). Furthermore, there is evidence that mtDNA can activate a number of inflammatory pathways through its action as a DAMP, primarily the NLRP3 inflammasome, cGAS-STING axis and TLRs (Nakahira *et al.*, 2011;

West *et al.*, 2015; Bao *et al.*, 2016). These pathways have also been previously implicated in senescence and regulation of the SASP (Dou *et al.*, 2017; Gluck *et al.*, 2017; Yin *et al.*, 2017; Hari *et al.*, 2018).

Therefore I wanted to begin by assessing whether there was mitochondria-free mtDNA present in senescent cells. Using confocal, electron and super-resolution microscopy it was revealed that there was DNA visible in the cytosol of cytosol. Although these methods are widely used in the field to determine the sub-cellular location of mtDNA, the anti-DNA antibody labels both nuclear and mitochondrial double stranded DNA. Therefore, to ensure what I were observing was specifically of mitochondrial origin I used a triple-immunofluorescent assay to label mitochondria, DNA and TFAM. Using this assay it was observed that the DNA staining outside of the mitochondrial network also colocalised with TFAM, this was further supported by analysis of TFAM protein levels and mRNA levels in cytosolic fractions acquired from proliferating and senescent cells. Furthermore, the quantification of the number of mtDNA nucleoids in the cytosol via microscopy does not allow us to dissect whether this may in fact be occurring due to the overall increase in mitochondrial mass and content that is associated with senescence (Correia-Melo *et al.*, 2016). Whereas Western Blot and PCR allowed us to normalise the cytosolic fraction of mtDNA relative to overall mitochondrial content in proliferating and senescent cells. Collectively, these data indicate that mtDNA is escaping from the mitochondria to the cytosol where it is available for detection via DNA sensors which can mediate an inflammatory response. However, it would be expected that cytosolic mtDNA (or nuclear DNA) would be rapidly degraded by DNases to prevent an inflammatory response. It was recently published that senescent cells exhibit downregulation of the cytoplasmic DNases TREX1 and DNase2, which could explain why mtDNA persists in senescent cells (Takahashi *et al.*, 2018). This therefore is likely the explanation as to why mtDNA is detectable in the cytosolic fraction of senescent cells.

Next, mtDNA was isolated and transfected into human fibroblasts to confirm that mtDNA had the capacity to induce an inflammatory response in human fibroblasts. I found a clear increase in both IL-6 and IL-8 which are key constituents of the SASP. This fits with data demonstrating that mtDNA promotes an inflammatory response and production of IL-6 and IL-8 via cGAS mediated upregulation of IFN-1 genes (Little *et al.*, 2014; West *et al.*, 2015; Chen *et al.*, 2016; Yang *et al.*, 2017). Furthermore, it has been shown that when the release of mtDNA is induced pharmacologically using BH3 mimetics, the upregulation of IFN-B1 genes does not occur in

cells which do not express STING (Riley *et al.*, 2018). I also observed that Rho (0) cells lacking mtDNA displayed an impaired secretion of both IL-6 and IL-8 when compared to their mtDNA proficient counterparts, this supports published observations that Rho (0) cells display an impaired SASP (Correia-Melo *et al.*, 2016; Wiley *et al.*, 2016). However, it is important to note that this experiment was conducted in human osteosarcoma 143B cells which are not routinely used for the study of senescence due to being an immortalised cancer cell line. As such, it would be preferable to generate Rho (0) cells in primary fibroblasts using either ethidium bromide (inhibits mtDNA synthesis) or 2',3'-dideoxycytidine (blocks mtDNA replication) to deplete mtDNA. The two aforementioned studies demonstrated that these cells exhibited a diminished SASP as a consequence of these cells being unable to undertake oxidative phosphorylation, however they did not investigate the potential for mtDNA to be contributing to the SASP (Correia-Melo *et al.*, 2016; Wiley *et al.*, 2016).

As part of the study, I wanted to investigate how mtDNA escapes to the cytosol. I hypothesised that non-specific mitochondrial rupture could contribute to mtDNA release. I also hypothesised that either the MPTP or BAX and BAK pores could facilitate its release. I found that the release of mtDNA during senescence is dependent on the ability for fibroblasts to form BAX and BAK pores as when I removed these proteins using the CRISPR CAS9 system the amount of mtDNA present in the cytosol was reduced. Conversely, inhibition of the MPTP using Cyclosporin A did not prevent mtDNA release. In agreement with our data two published studies have demonstrated that BAX and BAK form macropores which can facilitate this release in the context of apoptosis. Furthermore, they also found that cells which were deficient for cyclophilin D (a key component of the MPTP and target of Cyclosporin A) still released mtDNA (McArthur *et al.*, 2018; Riley *et al.*, 2018). In our study I did not assess the individual contribution of BAX and BAK to the release of mtDNA, however, the study by Riley et al indicates that individual knockout of BAX or BAK did not block mtDNA release, only when they were both removed was mtDNA release prevented (Riley *et al.*, 2018). In the context of senescence it would be interesting to understand the individual contribution of BAX and BAK to mtDNA release, therefore, this is currently being investigated.

With regards to senescence, it is widely acknowledged that senescent cells are resistant to a number of apoptotic stimuli (Wang, 1995; Chaturvedi *et al.*, 1999; Chen *et al.*, 2000; Yeo *et al.*, 2000). This is in part due to the overexpression of pro-survival BCL-2 family proteins which are a senolytic target (Wang, 1995; Chen *et al.*, 2000; Sanders *et al.*, 2013; Chang *et al.*, 2016).

Conventionally, pro-survival BCL-2 proteins maintain the pro-apoptotic proteins BAX and BAK in an inactive state by occupying their active sites (Tait and Green, 2010). Indeed, I observed upregulation of the anti-apoptotic protein BCL-2. As such it would be expected that BAX and BAK would exist in an inactive state and therefore it is a paradox that they are enabling the release of mtDNA. Characterisation of BAK and BAX. Revealed that total levels of BAK but not BAX were increased in senescence cells relative to overall mitochondrial content. When I assessed the cellular location of BAK I found as expected that it was solely located in the mitochondrial fraction as published work indicates that it remains anchored within the mitochondrial outer membrane both in both its active and inactive form (Ferrer *et al.*, 2012). Although I observed increased levels of BAK in senescent cells, this only gives us information on the total amount of protein and does not allow us to determine whether it is in an active state or not.

Interestingly, the distribution of BAX was different between proliferating and senescent cells. In proliferating cells BAX was found to exist almost entirely in the mitochondrial fraction, whereas in senescent cells BAX was evenly dispersed between the mitochondrial and cytosolic fraction. This finding was puzzling as these cells were in a healthy proliferating state and there was no evidence of apoptosis. The dynamic nature of BAX is still an area of intense research and not well understood. There is evidence that where BAX accumulates predominantly on the mitochondria it is generally in an inactive state (6A7 negative), however, whilst localised at the mitochondria it is primed ready for activation. This accumulation has been associated with low levels of pro-survival proteins, it was shown that the accumulation of mitochondrial BAX was reversed when pro-survival protein levels were increased (Schellenberg *et al.*, 2013). This matches our observations of proliferating cells where the expression of BCL-2 was low and the proportion of mitochondrial BAX was vastly increased compared to cytosolic BAX. Where survival signals are higher, i.e. increased expression of BCL-2 as observed in senescent cells BAX is generally shuttled from the mitochondria to the cytosol. This process of retro-translocation occurs continuously and matches our findings in senescent cells. Interestingly, a cells ability to alter the distribution of BAX has been associated with being able to alter the sensitivity to apoptosis and is referred to as apoptotic priming (Certo *et al.*, 2006; Schellenberg *et al.*, 2013). Cells where BAX is predominantly located on the mitochondria are more sensitive to apoptotic stimuli and readily undergo MOMP (Schellenberg *et al.*, 2013). These findings suggest that senescent cells are more resistant to apoptotic stimuli than proliferating cells which

agrees with existing findings regarding senescent cells (Wang, 1995; Chaturvedi *et al.*, 1999; Chen *et al.*, 2000; Yeo *et al.*, 2000; Chang *et al.*, 2016).

Furthermore, there is evidence that there are two distinct populations of mitochondrial BAX within cells; one population which is stably bound to mitochondria and maintained by BCL-XL and a second population which is in a dynamic state between the cytosol and mitochondria (Llambi *et al.*, 2011; Schellenberg *et al.*, 2013). Furthermore, only a few hundred molecules of BAX per mitochondria are required to form a functional pore (Dussmann *et al.*, 2010). Therefore it is possible that although senescent cells display a reduced proportion of mitochondrial BAX, these may in fact be active and contributing to mtDNA release. Corroborating with this notion, it has been identified that a sub-population of mitochondria can become permeabilised via BAX and BAK in the absence of cell death (Ichim *et al.*, 2015).

To address the idea that senescent cells may harbour an increased proportion of active mitochondrial BAX compared to proliferating cells I assessed the active BAX epitope 6A7 which is exposed following its conformational change during its activation (Gavathiotis *et al.*, 2010). First, the total protein levels of BAX (6A7) were assessed via Western Blot in whole cell, mitochondrial and cytosolic extracts. Interestingly, the findings matched exactly those found for BAX when it was assessed earlier in the study. This was particularly unusual as it would not be expected that proliferating cells would display the 6A7 epitope which is indicative of BAX activation and initiation of the apoptotic process. Therefore it seems plausible to suggest that during sample preparation the protein denaturation step may lead to exposure of this epitope. As such, BAX (6A7) was also analysed via confocal microscopy using immunofluorescence. Here, it was found that the intensity of the staining was increased in senescent cells indicating that BAX (6A7) is more prevalent in senescent cells than proliferating cells. This conflicts with the Western Blot data, therefore it is difficult to draw direct conclusions on the state of BAX in senescent cells. However, taken together with the observations that both genetic removal and pharmacological inhibition of BAX and BAK prevent the release of mtDNA it seems clear that at least a small proportion of BAX and BAK must be constitutively active to enable the release of mtDNA. Further confidence could be gained in this finding by assessing the size of BAX (6A7) pores labelled by immunofluorescence. It is known that an individual mtDNA nucleoids is approximately 100nm in size, therefore using super-resolution microscopy to determine the number of BAX (6A7) pores over 100nm in proliferating and senescent cells may shed light on the presence of BAX

and BAK macropores which could facilitate its release. Furthermore, it is unknown at what stage following the induction of senescence that mtDNA is released. Live-cell imaging experiments in cells expressing fluorescent proteins on the mitochondria, TFAM and BAX (6A7) would provide a useful insight to determine the point at which mtDNA is released during senescence.

Interestingly, both the genetic knockout and pharmacological inhibition of BAX and BAK lead to a reduction in the presence of cytosolic mtDNA, furthermore this was associated with a reduced secretion of SASP factors. I assessed the SASP by ELISA and cytokine array in BAX and BAK deficient cells, I found that a number of the key SASP constituents (IL-6, IL-8, IP-10, MCP-3, Gro-α and VEGF-A) were downregulated when cells were unable to form BAX and BAK pores. These findings suggest that mtDNA is associated with regulation of the SASP.

I also explored the role of other mitochondrial pores in the regulation of the SASP. The MPTP is crucial for maintaining mitochondrial homeostasis allowing the release of calcium and ROS following transient opening. When it is permanently open it facilitates the apoptotic process (Panel *et al.*, 2018). Interestingly, the sensitivity of this pore to opening has been shown to increase with age (Hepple, 2016). I and others have found that mitochondria are depolarised during senescence indicating that this pore is open to an extent, furthermore, it has been shown that calcium accumulates in the mitochondria of senescent cells as a consequence of alterations in the opening of the MPTP (Nicholls, 2004; Passos *et al.*, 2007; Wiel *et al.*, 2014). In the literature, studies investigating the pro-inflammatory effects of mtDNA have demonstrated that mtDNA fragments can escape via the MPTP and the associated inflammation can be prevented by blocking the MPTP using Cyclosporin A (Patrushev *et al.*, 2004; Nakahira *et al.*, 2011). Together, these observations warrant investigating the role of the MPTP in contributing to mtDNA release during senescence.

I found that inhibition of the MPTP using Cyclosporin A did not prevent the release of the mtDNA and subsequently I did not observe a decrease in the SASP. In fact, Cyclosporin A lead to an increase in the secretion of IL-6, IL-8 and IP-10 during senescence. This seems conflicting as Cyclosporin A is used routinely in the clinic as an immunosuppressive agent for the recipients of organ transplants (Faulds *et al.*, 1993). However, it is recognised that sustained exposure to Cyclosporin A promotes nephrotoxicity. Furthermore, it has been demonstrated in renal tubular epithelial cells that Cyclosporin A promotes exacerbated production of H_2O_2. This

induced DNA damage which led to an upregulation of the p53-p21 axis and consequently induction of stress-induced senescence (Jennings *et al.*, 2007). Therefore, it is plausible that in our scenario Cyclosporin A is elevating the SASP by exacerbating the DDR through increased production of ROS. This leads to the activation of ATM and ATR as part of the DDR, it is known that during senescence they are responsible for the stabilisation of the transcription factor GATA binding protein 4 (GATA4). GATA4 is an upstream regulator of NF-κB, a master regulator of the SASP (Chien *et al.*, 2011; Kang *et al.*, 2015). Alternatively, blockage of the MPTP could be leading to intracellular calcium accumulation. This could in turn promote activation of the protease calpain, which leads to proteolytic cleavage of IL-1α and the subsequent upregulation of cytokines associated with the SASP such as IL-6 and IL-8 (McCarthy *et al.*, 2013; Wiel *et al.*, 2014).

Although not entirely clear, it is known that the MPTP is made up of a number of subunits, specifically; cyclophilin D, ANT and VDAC. (Briston *et al.*, 2017). Following the inhibition of cyclophilin D by Cyclosporin A, I further tested the inhibition of the MPTP by targeting ANT using Bongkrekic acid and VDAC using Olesoxime. Similarly, I found that neither inhibition of ANT or VDAC promoted a reduction in secretion of the SASP. Although I found that inhibition of cyclophilin D did not prevent mtDNA release, I did not test whether inhibition of ANT and VDAC impacted on the release of mtDNA.

Together, these data implicate that the MPTP is not responsible for mtDNA release during senescence, furthermore, blockade of the MPTP using pharmacological inhibitors does not lead to a reduction in the secretion of pro-inflammatory factors. Earlier I observed that senescent cells display cytosolic mtDNA, in addition, the transfection of mtDNA into fibroblasts promoted a profound pro-inflammatory response, as measured by the secretion of IL-6 and IL-8. Supporting these findings I established that when mtDNA release was prevented either by genetic knockout or pharmacological inhibition of BAX and BAK, there was a substantial decrease in secretion of the SASP. Collectively, these observations provide strong evidence that mtDNA is mediating the link between mitochondria and regulation of the SASP in senescence. The mechanistic basis concerning how mtDNA promotes this inflammatory response is explored and discussed later in this study.

It is important to consider that mtDNA is not the sole candidate that can act as a mitochondrial DAMP. In fact, it is recognised that cytochrome C, N-formyl peptide, succinate, cardiolipin and

ATP are all of mitochondrial origin and can induce a pro-inflammatory response if they escape from the confines of the mitochondria to the cytosol (Grazioli and Pugin, 2018). I investigate and discuss the role of cytochrome C later in this study. N-formyl peptide and succinate have not been extensively investigated in the context of senescence. Previously, cardiolipin (a glycerophospholipid located in the inner mitochondrial membrane) has been shown to accumulate in senescent cells, in addition to this, it has been shown that exposure of fibroblasts to cardiolipin leads to the induction of senescence (Arivazhagan *et al.*, 2004; Wan *et al.*, 2014). In this study the authors demonstrated that cardiolipin accumulates during senescence, however they did not investigate its sub-cellular location and measured only total protein. It is likely that their observation of cardiolipin accumulating in senescent cells occurs as a consequence of the increase in mitochondrial mass that is observed during senescence (Arivazhagan *et al.*, 2004). Indeed, another study demonstrated that mitochondrial mass increases during senescence using nonyl acridine orange staining, it is known that nonyl acridine orange binds to cardiolipin, this therefore supports the idea that cardiolipin accumulates in senescence as a consequence of increased mitochondrial content (Passos *et al.*, 2010). With regards to ATP, there is evidence that ATP levels are reduced during senescence as cells display a high AMP:ATP ratio, consistently, inhibition of ATP synthase or depletion of ATP induces senescence via a p53-AMPK mediated mechanism (Wang *et al.*, 2003; Zwerschke *et al.*, 2003; Stockl *et al.*, 2006; Jiang *et al.*, 2013). It has recently been shown that the mitochondrial peptides MOTS-c (mitochondrial open reading frame of the 12S rRNA-c, which acts on AMPK) and humanin (activates the JAK/STAT pathway) are elevated in senescent cells, furthermore, exposure of senescent cells to these peptides enhances mitochondrial energetics and leads to an increase in the SASP (Kim *et al.*, 2018). These observations warrant the investigation of further understanding of other mitochondrial DAMPS which could influence the SASP.

I found that genetic removal of BAX and BAK could alleviate the SASP, but this did not prevent the cell cycle arrest from occurring following the induction of stress-induced senescence. I found that SA-β-Gal, p16, p21 and Ki67 were unchanged compared to senescent Empty Vector control cells. This suggests that the release of mtDNA via BAX and BAK pores regulate the SASP but not progression of the cell cycle. This complements the recent study which demonstrates that mitochondrial depletion removes the pro-inflammatory features of senescence (both at the protein and mRNA level) but does not prevent the growth arrest (Correia-Melo *et al.*, 2016). The SASP (specifically IL-8) has been implicated in stabilising and

reinforcing the senescence phenotype via its autocrine effects (Acosta *et al.*, 2008; Passos *et al.*, 2010). It was therefore postulated that BAX and BAK deficient cells which display a dramatically ameliorated SASP may not completely undergo the cell cycle arrest. However, the growth arrest that occurs in senescence is also associated with the DDR. It has been demonstrated that mitochondria can drive the DDR by producing ROS which induce short-lived foci and maintain it until a stable growth arrest occurs through p21 and p53 (Passos *et al.*, 2010; Luo *et al.*, 2011). In BAX and BAK deficient cells I found that the production of mitochondrial derived ROS (MitoSOX) and induction of DNA damage (measured by γH2AX) were unaffected compared to senescent Empty Vector control cells. These findings suggest that the DDR is still being maintained by a mitochondrial ROS mediated feedback loop and as such the stable growth arrest is unaffected, therefore potentially explaining the growth arrest still occurring despite the SASP being reduced.

Following our *in vitro* observations, I wanted to experimentally dissect the role of BAX and BAK in regulation of the SASP *in vivo*. It has been previously reported that following the induction of senescence using sub-lethal irradiation there is an upregulation of the SASP related genes; IL-1α, IL-1β, IFN-α, IL-6, CXCL1, MMP3, IFN1α, OAS1 and inhibin A (Dou *et al.*, 2017; De Cecco *et al.*, 2019). Therefore, we assessed whether mice harbouring BAX and BAK deleted livers displayed an altered SASP in liver tissue following irradiation compared to BAK-/- mice. Following irradiation, we observed an enrichment for each of the target genes compared to non-irradiated BAK-/- mice, however, none of these were significant. Of further interest, following irradiation we did not observe an increase for any of the target genes in mice with BAX^{fl}/BAK-/- deleted livers. For the genes IL-1α, IL-1β, OAS1 and p16 there was a significant decrease in irradiated BAX^{fl}/BAK-/- mice compared to irradiated BAK-/- mice. Within this experiment the n numbers were relatively small with only 5 mice per group. Collectively, there is evidence for a clear trend of SASP genes being upregulated in BAK-/- but not BAX^{fl}/BAK-/- mice following irradiation, this corroborates our *in vitro* data where removal of BAX and BAK impairs the SASP. To confidently clarify this relationship an increase in the n numbers per group are required to increase the statistical power. Also, it is interesting that neither p16 nor p21 were upregulated in BAX^{fl}/BAK-/- mice following irradiation as *in vitro* I demonstrated that BAX/BAK deficient cells still underwent the cell cycle arrest and had observable upregulation of both p16 and p21. This highlights the need for further investigation using a larger sample size and the analysis of other genes associated with regulation of the cell cycle.

A further limitation to the *in vivo* data is the use of a BAK-/- mouse as the control rather than a wild-type control. This study has not dissected the relative role of BAX and BAK individually *in vitro*. However, published data suggests that the deletion of both BAX and BAK together is required to prevent mtDNA release as individual knockout of BAX or BAK still leads to mtDNA release (McArthur *et al.*, 2018; Riley *et al.*, 2018). This agrees with the *in vivo* data which has shown that BAK-/- mice have an increase in SASP-related genes following sub-lethal irradiation but BAX^{fl}/BAK-/- mice do not. However, in contrast to this it has been shown in this study that the BAX inhibitors BCB and BIPv5 can diminish the SASP *in vitro*. This therefore questions whether BAX may be more important than BAK in facilitating mtDNA release. Alternatively, it may be that these inhibitors are not specific to BAX and may also inhibit BAK. This therefore needs to be tested comprehensively. In addition, further work is required to elucidate the exact contribution of BAX and BAK individually to mtDNA release.

Together these observations highlight the potential of targeting mitochondrial BAX and BAK as a senostatic therapy. Senostatic therapies are beneficial as they maintain the beneficial tumour suppressive role of senescent cells and potentially do not disrupt tissue architecture by preserving senescent cells. The SASP has also been associated with the induction of senescence in neighbouring cells; this process is referred to as paracrine senescence (Nelson *et al.*, 2012; Acosta *et al.*, 2013). It is postulated that the induction of paracrine senescence could be a potential mechanism which explains the accumulation of senescent cells and inflammation with age. With that in mind, there is significant clinical interest in finding strategies to remove the chronic inflammation that is associated with the presence of senescent cells that occur with age and for the first time this study demonstrates that pharmacological targeting of BAX and BAK can alleviate the SASP (Birch and Passos, 2017). However, it is important to consider that the SASP also plays a role in signalling to the immune system for senescent cell clearance (Kang *et al.*, 2011b; Munoz-Espin *et al.*, 2013; Brighton *et al.*, 2017; Egashira *et al.*, 2017). If this signal is supressed by senostatic therapies then this may further contribute to the accumulation of senescent cells. To address this caveat, there is evidence that immune system function declines with age, furthermore, it has recently been reported that the accumulation of senescent cells occurs due to a compromised immune capacity associated with advancing age (Montecino-Rodriguez *et al.*, 2013; Ovadya *et al.*, 2018).

The role of BAX and BAK has not been previously investigated in senescence and regulation of the SASP. The observation that both of the pharmacological inhibitors BIPv5 and BCB

promote an alleviation of the SASP without impacting upon the cell cycle arrests is of clear clinical interest. At this stage it remains to be seen whether these findings will translate and have beneficial effects within aged organism. However, there is some evidence within the field that BAX and BAK inhibitors may be clinically useful. It has been established that senescent cells are present in idiopathic pulmonary fibrosis disease and correlate with disease severity. Furthermore, the removal of senescent cells either genetically (INK-ATTAC mouse) or pharmacologically (dasatanib and quercetin) improves pulmonary function and physical health in a bleomycin-injury idiopathic pulmonary fibrosis model (Schafer *et al.*, 2017). Not only do senescent cells alleviate aspects of idiopathic pulmonary fibrosis but there is also evidence that extracellular mtDNA is increased in both plasma and bronchoalveolar lavage acquired from patients with idiopathic pulmonary fibrosis. Additionally, the authors demonstrated that the concentration of mtDNA correlated with disease mortality (Ryu *et al.*, 2017). Interestingly, in pulmonary fibrosis BAX has been implicated with driving inflammation through TGF-β and matrix metalloproteinases (Kang *et al.*, 2007). TGF-β has been implicated as an inducer of senescence and the secretion of matrix metalloproteinases are upregulated as part of the SASP (Coppe *et al.*, 2010; Senturk *et al.*, 2010; Wu *et al.*, 2014). It was demonstrated that BAX knockout mice and mice treated with the BIPv5 inhibitor display attenuation of bleomycin-induced lung injury as measured by degree of injury and overall survival (Kang *et al.*, 2007; Suzuki *et al.*, 2017). Considering that both the removal of senescent cells and the inhibition of BAX have beneficial effects, it seems plausible to hypothesise that in this scenario senescent cells are aggravating pulmonary fibrosis as a consequence of BAX and BAK mediated release of mtDNA driving inflammation.

Despite these potential benefits, caution would certainly be required as BAX and BAK are crucial for engagement of the apoptosis process. Naturally, if apoptosis is inhibited then the chances of tumorigenic transformation occurring are exacerbated.

4. Chapter 4: Limited mitochondrial permeabilisation contributes to mtDNA release and the DDR via sub-lethal caspase activity

Recent work has unveiled a previously unknown phenomenon referred to as limited mitochondrial permeabilisation or miMOMP. Specifically, miMOMP is a process whereby a small sub-set of mitochondria experience outer membrane permeabilisation which facilitates the release of cytochrome C via BAX and BAK pores. This release is insufficient to induce cell death, however it promotes DNA damage through sub-lethal activation of caspases 3 and 7 (Ichim *et al.*, 2015).

Senescent cells have been shown to have dysfunctional mitochondria (Passos et al. 2007, 2010) and a persistent DDR (Rodier 2009; Passos et al. 2010; Hewitt et al. 2012). Additionally, mitochondria have been proposed to contribute to the DDR mostly via the generation of ROS (Passos et al. 2010). However, the relationship between the DDR and miMOMP during senescence is not understood.

Furthermore, I have observed that mitochondria release mtDNA to the cytosol, a process which is dependent on the presence of BAX and BAK pores (see chapter 3). Therefore it is of significant interest to investigate whether these phenotypes may in fact be occurring as a consequence of miMOMP.

Firstly, I investigated whether mitochondria in senescent cells displayed miMOMP. Secondly, I aimed to investigate whether miMOMP could be a driver of senescence and the mechanisms involved. Finally, as miMOMP promotes the sub-lethal activation of caspases I dissected the role of caspases in the induction of the senescence phenotype.

4.1. Senescent cells display reduced colocalisation of Cytochrome C and TOM20

In order to investigate mitochondrial outer membrane permeabilisation in senescent cells immunostained fixed cells with antibodies against cytochrome C (a small protein loosely associated with the mitochondrial inner membrane) and TOM20 (an outer mitochondrial membrane protein). Then, I performed confocal 3D imaging of the cells, followed by rendering and processing of the images to statistically measure the extent of cytochrome C and TOM20 colocalisation. A reduced colocalisation was indicative of mitochondrial permeabilisation.

Using this methodology, I first determined the co-localisation between cytochrome C and TOM20 in proliferating, stress-induced senescent cells and replicatively senescent cells. I noted that while in proliferating cells most TOM20 co-localized with cytochrome C, in senescent cells I observed some discrete areas which were positive for TOM20 but negative for cytochrome c. Representative images of rendered 3D images are shown in Figure 4.1A where mitochondria are represented in red and cytochrome C in green, where the two colocalise the overlap is displayed in orange.

In order to quantitatively evaluate the level of co-localisation between TOM20 and cytochrome C I performed the Pearson Correlation Coefficient statistical test. I found that both stress-induced senescent cells and replicatively senescent cells displayed a reduced level of co-localisation between TOM20 and cytochrome C compared to proliferating cells ($p<0.0001$ for both, Figures 4.1A and B). I found that stress-induced senescent cells displayed a 37% decrease in co-localisation and replicatively senescent cells displayed a 15% reduction in co-localisation compared to proliferating cells ($p<0.0001$ and <0.05 respectively, Figures 4.1A and C). Interestingly, cytochrome C was visible in the cytosol of senescent cells (see Figure 4.1A). To further explore if cytochrome C is present in the cytosol of senescent cells, I conducted fractionation of the cytosol and mitochondria followed by Western blotting to detect cytochrome C. Western Blotting revealed that compared to proliferating cells there was a 4-fold increase in the levels of cytosolic cytochrome C in stress-induced senescent cells ($p=0.0238$, Figures 4.1D and E), and a 3-fold increase in replicatively senescent cells ($p=0.0441$, Figure 4.1E).

Finally, it has been published that miMOMP promotes genomic DNA damage through sub-lethal caspase activity (Ichim *et al.*, 2015). In order to assess this, I used Western Blotting to characterise the levels of cleaved caspase 3 by measuring the presence of its cleaved counterparts detectable at 17 and 19kDa (Figure 4.1F). In senescent cells there was a significant enrichment in the presence of both bands compared to proliferating cells ($p=0.0104$ and 0.0240 for 17 and 19kDa respectively, Figures 4.1G and H).

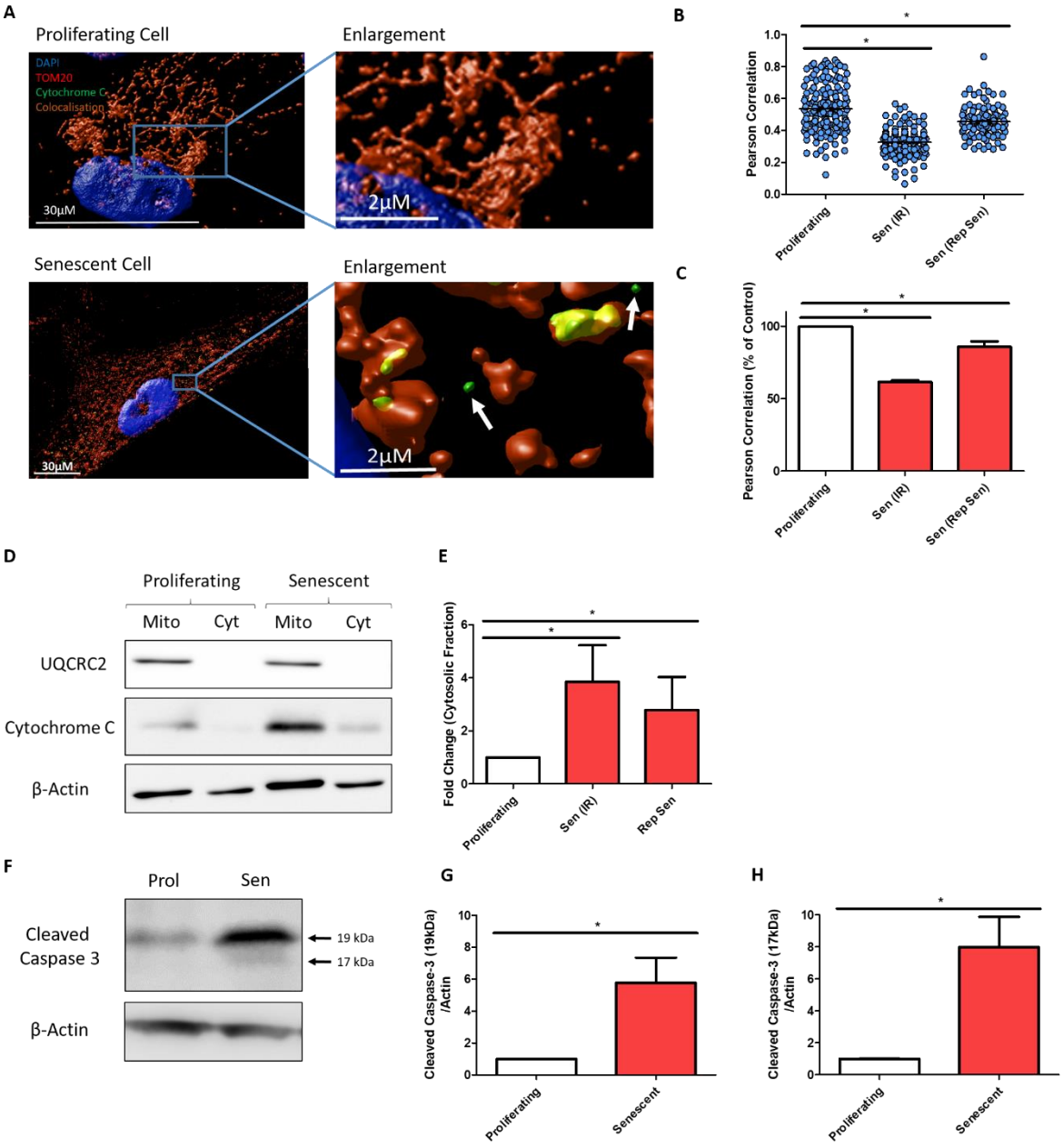

Figure 4.1 – Senescent cells display reduced colocalisation of cytochrome C and TOM20.

Proliferating, stress-induced senescent (analysed 10 day's post 20Gy x-ray irradiation) and replicatively senescent MRC5 cells were analysed for colocalisation of cytochrome C and Tom20 using confocal microscopy and the presence of cytosolic cytochrome C by Western Blotting. **(A)** Representative images of a proliferating and replicatively senescent cells labelled using DAPI (blue), TOM20 (red) and cytochrome C (green). Colocalisation of TOM20 and cytochrome C is displayed in orange. Images acquired in z-stacks by confocal microscopy using a 63x objective, following acquisition, the images were rendered using Huygens Deconvolution Software and colocalisation was measured using the Pearson Correlation Coefficient. White arrows in the enlarged image highlight cytosolic cytochrome C **(B)** Dot plot represents the statistical analysis of colocalisation of cytochrome C and TOM20 using the Pearson Correlation Coefficient where 1.0 is perfect colocalisation between the two channels. Each dot represents an individual cell. **(C)** Bar graph represents the Pearson Correlation Coefficient for proliferating

(white bar) and senescent cells (red bars) expressed as a percentage of the control. n=3 independent experiments. **(D)** Representative Western Blot image of UQCRC2, Cytochrome C and β-Actin in mitochondrial and cytosolic extracts taken from proliferating and stress-induced senescent cells. **(E)** Bar graph represents quantification of cytosolic cytochrome C expressed as fold-change compared to the control for proliferating (white bar) and senescent cells (red bars). For stress induced senescent cells n=6 and for replicatively induced senescent cells n=3 independent experiments. **(F)** Representative Western Blot image of Cleaved Caspase 3 and β-Actin in proliferating and stress-induced senescent cells. **(G and H)** Bar graph shows the fold change in protein levels of cleaved caspase 3 19kDa **(G)** and 17kDa **(H)** in proliferating (white bars) and senescent cells (red bars), n=4 independent experiments. Bar graphs represent mean +SEM, statistical analysis performed using a One-way ANOVA for **(B, C and E)**. For **(G and H)**, an unpaired two tailed t-test was used.

4.2. Pharmacological induction of miMOMP promotes a senescence-like response

miMOMP can be promoted by low doses of the BH3 mimetic ABT737 (Ichim et al., 2015). ABT737 inhibits the pro-survival proteins BCL-2 and BCL-XL which are normally bound to BAX and BAK proteins which prevents them from forming pores. Furthermore, it was demonstrated that treatment with ABT737 induced miMOMP, which was associated with cytochrome C release and subsequent caspase-mediated DNA damage. Specifically, caspase 3, 7 and 9 were found to be active at sub-lethal levels during miMOMP, which was associated with activation of CAD (caspase-activated DNase) which is responsible for DNA fragmentation during the apoptotic process (Ichim *et al.*, 2015). The mechanism of action of ABT737 is highlighted in Figure 4.2A.

First, it was important to verify that ABT737 was inducing miMOMP. To test this, I measured co-localization between cytochrome C and TOM20. It was found that treatment with ABT737 (2.5μM) for 48 hours promoted a significantly reduced level of co-localisation between cytochrome C and TOM20 in individual cells as measured using the Pearson Correlation Coefficient ($p<0.0001$, Figure 4.2B). Furthermore, when colocalisation was expressed as a percentage of control it was observed that there was a 12% decrease in the level of colocalisation ($p=0.0128$, Figure 4.2C).

Following the confirmation that ABT737 was inducing permeabilisation of mitochondria in the absence of cell death, I investigated whether this was associated with caspase 3 activity and subsequent DNA damage. The Western Blot image in Figure 4.2D indicates that control cells display no cleavage of caspase 3, however when treated with ABT737 for 48 hours there is visible cleavage of caspase 3. As such, I questioned whether this caspase 3 activity was associated with the induction of DNA damage. To dissect this relationship, cells were treated with ABT737 alone, and another cohort were treated with ABT737 in the presence of the broad spectrum caspase inhibitor QVD to determine whether caspase activity was contributing to the DDR.

Following treatment with ABT737 there was a significant increase in the mean number of γH2AX foci ($p<0.001$) which was suppressed by QVD ($p<0.001$, Figure 4.2E). It is well established that in the context of senescence that mitochondrial ROS can promote a DDR (Passos *et al.*, 2010). Furthermore, caspase dependent disruption of mitochondrial function through cleavage of the respiratory complex I protein, NDUFS1, has been shown to generate ROS following MOMP (Ricci *et al.*, 2004). Therefore, it is possible that miMOMP may

contribute to mitochondrial ROS and the DDR. In order to test the involvement of ROS in miMOMP induced DDR, I measured mitochondrial-derived ROS using the ROS-indicator dye MitoSOX by flow cytometry. I found that both treatment with ABT737 or ABT7373+ QVD had no effect on MitoSOX fluorescence levels, supporting the concept that ROS is not involved in the process (Figure 4.2F).

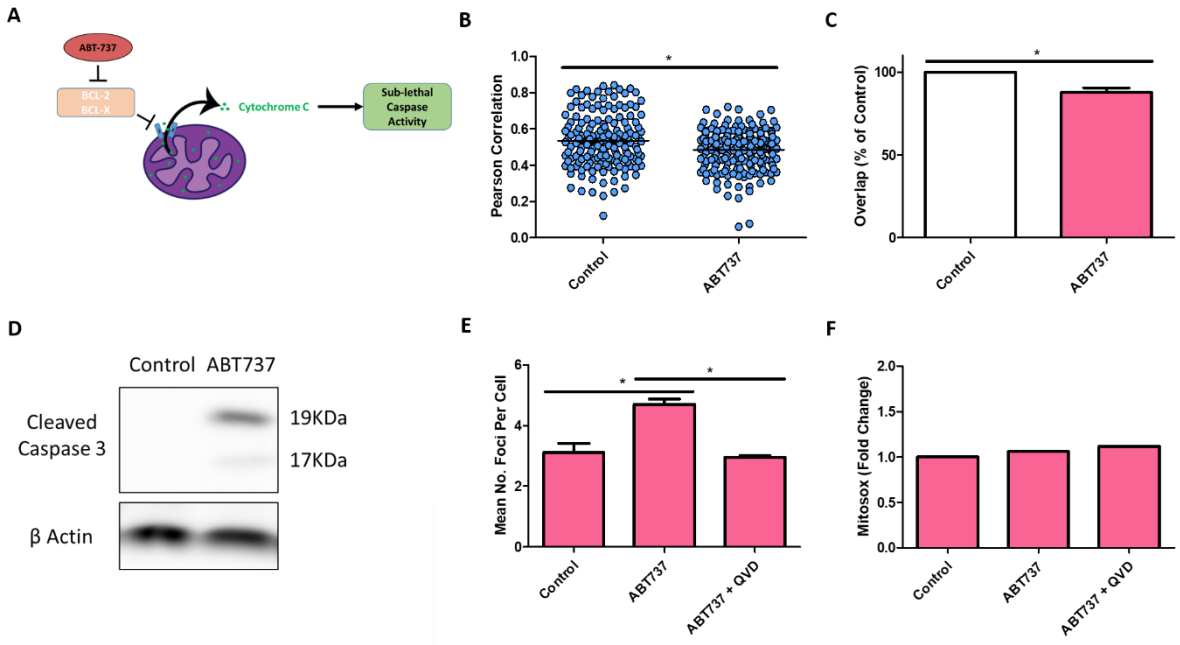

Figure 4.2 – ABT737 induces miMOMP.

Proliferating MRC5 cells were treated with either DMSO (control), ABT737 (2.5µM) or ABT737 (2.5 µM) + QVD (1µM) for 48 hours. **(A)** Schematic outlining the mechanism of action by which ABT737 induces miMOMP. **(B)** Dot plot represents the statistical analysis of colocalisation of cytochrome C and TOM20 using the Pearson Correlation Coefficient where 1.0 is perfect colocalisation between the two channels. Each dot represents an individual cell. **(C)** Bar graph represents the Pearson Correlation Coefficient for proliferating (white bar) and ABT737 treated cells (pink bars) expressed as a percentage of the control. n=3 independent experiments. **(D)** Representative Western Blot image of Cleaved Caspase 3 and β-Actin in control proliferating cells and ABT737 treated cells. **(E)** Bar graph represents the quantification of the mean number of γH2AX foci in control, ABT737 and ABT737 + QVD treated cells. **(F)** Bar graph represents the fold change in MitoSOX fluorescence as measured by flow cytometry in control, ABT737 and ABT737 + QVD treated cells, n=3 independent experiments. Bar graphs represent mean +SEM, statistical analysis performed using an unpaired two tailed t-test for **(B and C)**, a One-way ANOVA was used for **(E and F)**.

Following the observation that ABT737 can induce miMOMP and a subsequent DNA damage response I aimed to test whether prolonged treatment with ABT737 would result in a senescent arrest. It has previously been published that ABT737 can induce senescence in apoptosis-resistant cancer cell lines (Song *et al.*, 2011). Conversely, it has also been demonstrated that ABT737 is a senolytic agent and can in fact promote apoptosis in senescent cells which overexpress pro-survival BCL-2 proteins (Yosef *et al.*, 2016b). Following the continued exposure of MRC5 human fibroblasts to ABT737 for 9 days I observed that that there was a detectable increase in the number of SA-β-Gal positive cells (approximately 10%) compared to the control group (3% positive) ($p<0.0001$, Figures 4.3A, B). As it is known that ABT737 induces miMOMP and subsequent caspase-mediated DNA damage it was of interest to assess whether the increase in SA-β-Gal was dependent on caspase-mediated DNA damage. Interestingly, I found that cells co-treated with ABT737 and QVD for 9 days displayed a reduction in the number of SA-β-Gal positive cells compared to those treated with ABT737 alone ($p<0.001$, Figures 4.3A, B). Cells were continually cultured in the presence of ABT737 for 23 days and it was found that there was an increase to approximately 10% of cells positive for SA-β-Gal ($p<0.0001$), however there was no further increase compared to the 9 day time point. Similarly, co-treatment with ABT737 and QVD prevented the increase in the number of SA-β-Gal induced by ABT737 alone ($p<0.05$, Figure 4.3B).

As it was hypothesised that ABT737 drives its effects through caspase-mediated DNA damage I wanted to verify that levels of DNA damage were increased at each time point by ABT737. Following 9 days of culture with ABT737 I observed a significant increase in the mean number of γ-H2AX foci (1.8 to 3.2 per cell on average, $p<0.05$) which was reversed following co-treatment with QVD ($p<0.05$, Figure 4.3C). At 23 days, again there was a detectable increase following treatment with ABT737 compared to the controls ($p<0001$) which was dependent on caspase activity as it was prevented following co-treatment with QVD ($p<0.001$, Figure 4C). At 23 days the baseline level of γH2AX foci was slightly higher in the control group compared to the 9 day controls (3.2 compared to 1.9), however this was non-significant. Similarly, treatment with ABT737 was slightly higher following 23 days of treatment compared to 9 days (4.4 compared to 3.2), however this was non-significant (Figure 4.3C).

Next I wanted to assess whether sustained exposure to ABT737 would provoke a SASP. Therefore IL-6 and IL-8 were measured following treatment for 9 and 23 days. At the 9 day time point ABT737 there was no increase in the secretion of IL-6, there was a small increase in IL-8 although this was no significant. At the 23 day time point there was a highly significant

increase in the secretion of both IL-6 and IL-8 ($p<0.0001$ in both cases), the increase in both IL-6 and IL-8 was dependent on caspase activity as co-treatment with QVD lead to a significantly decreased secretion of IL-6 and IL-8 ($p<0.0001$ in both cases, Figures 4.3D and E).

As senescence is associated with an up-regulation of cell cycle inhibitors, expression of the key senescence mediators p16 and p21 were assessed following treatment with ABT737 alone and in conjunction with QVD. At 9 days, there was a small increase in the percentage of p16 positive cells following treatment with ABT737 (16% to 21% of cells p16 positive), however this was not significant. Similarly co-treatment with QVD had no effect on the percentage of cells positive for p16 (Figure 4.3F). Next p21 was assessed, it was found that there was a significant increase in the percentage of p21 positive cells following ABT737 treatment ($p<0.05$, 31% to 40%), which was prevented following co-treatment with QVD ($p<0.05$, 40% to 32%, Figure 4.3G).

Our data shows that induction of miMOMP can induce various senescent markers such as a DDR, increased expression of p21, SA-b-GAL and secretion of SASP components IL-6 and IL-8 in a caspase-dependent manner. However, the effects of ABT-737 on markers of the senescence arrest are considerably milder than its effects on the secretion of SASP components which are comparable to the ones found in stress-induced and replicatively senescent cells.

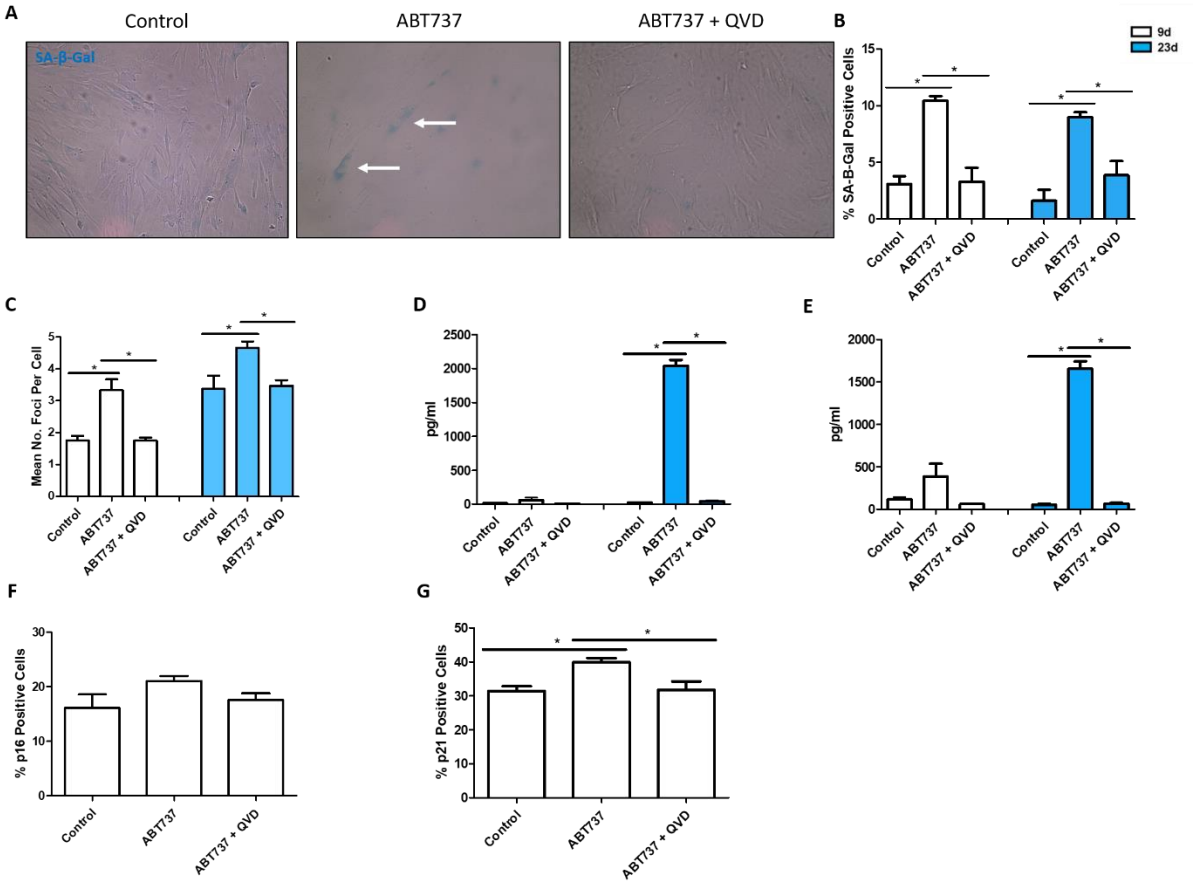

Figure 4.3 – Sustained exposure to ABT737 induces a pro-inflammatory response and a low level of induction of the growth arrest pathways.

MRC5 fibroblasts were maintained with either DMSO (control group), ABT737 (2.5µM dissolved in DMSO) or ABT737 + QVD (2.5µM and 1µM dissolved in DMSO) for 9 days or 23 days and then analysed for markers of senescence. **(A)** Representative images of SA-β-Gal for the control group, ABT737 alone and ABT737 + QVD after 9 days of treatment. White arrows denote positive SA-β-Gal staining. **(B)** Bar graph shows quantification of the percentage of SA-β-Gal positive cells following treatment with either DMSO, ABT737 or ABT737 + QVD for 9 days (white bars) and 23 days (blue bars), n=4 independent experiments. **(C)** Bar graph shows quantification of the mean number of γH2AX foci per cell following treatment with either DMSO, ABT737 or ABT737 + QVD for 9 days (white bars) and 23 days (blue bars), n=4 independent experiments. **(D and E)** Bar graphs show the secretion of IL-6 **(D)** and IL-8 **(E)** following treatment with either DMSO, ABT737 or ABT737 + QVD for 9 days (white bars) and 23 days (blue bars), n=3 independent experiments. (**F and G**) Bar graphs show the quantification of the percentage of p16 **(F)** and p21 **(G)** positive cells following treatment with either DMSO, ABT737 or ABT737 + QVD for 9 days, n=5 independent experiments. Bar graphs represent mean +SEM, statistical analysis performed using a One-way ANOVA.

4.3. miMOMP promotes mtDNA release

Earlier it was observed that treatment of cells with ABT737 could promote a senescent-like phenotype which was associated with the secretion of IL-6 and IL-8. Whilst investigating caspase-independent apoptosis it has been reported that treatment of cells with high doses of ABT737 promotes mtDNA release and associated inflammation (McArthur *et al.*, 2018; Riley *et al.*, 2018). It was therefore questioned whether low doses of ABT737 which promote miMOMP could be associated with contributing to the release of mtDNA. To investigate this cells were maintained with ABT737 and assessed at the following time points for mtDNA release; 0, 2, 9 and 23 days.

At 0 days the mean number of nucleoids visible outside of the mitochondrial network was low (0.04 per cell), this was non-significantly increased to 0.15 following 2 days of 2.5μM ABT737 exposure, after 9 days there was 0.42 nucleoids visible per cell ($p<0.0001$ compared to the 0 day time point), and after 23 days of treatment there was 0.60 nucleoids per cell ($p<0.0001$ compared to the 0 day time point, Figures 4.4A and B).

When assessed as the percentage of cells displaying cytosolic DNA, there were 2.8% of cells displaying nucleoids outside of the mitochondrial network at the 0 day time point. This was non-significantly increased to 12.1% of cells following 2 days of 2.5μM ABT737 exposure, after 9 days there was 28.5% of cells displaying cytosolic nucleoids ($p<0.0001$ compared to the 0 day time point), and after 23 days of treatment there was 45.5% of cells with cytosolic nucleoids ($p<0.0001$ compared to the 0 day time point, Figures 4.4A and C).

As it has been reported that high doses of ABT737 can promote mtDNA release via herniation of the inner membrane through BAX and BAK macropores, I assessed the effect of 20μM ABT737 on mtDNA release. Using immuno-gold labelling of DNA in conjunction with electron microscopy I observed that in untreated cells (0 hours) mtDNA was conserved within the inner mitochondrial membrane. Following ABT737 treatment, there were mitochondria which displayed evidence of mitochondrial blebbing, extrusion of the inner mitochondrial membrane and cytosolic mtDNA labelling (Figure 4.4D).

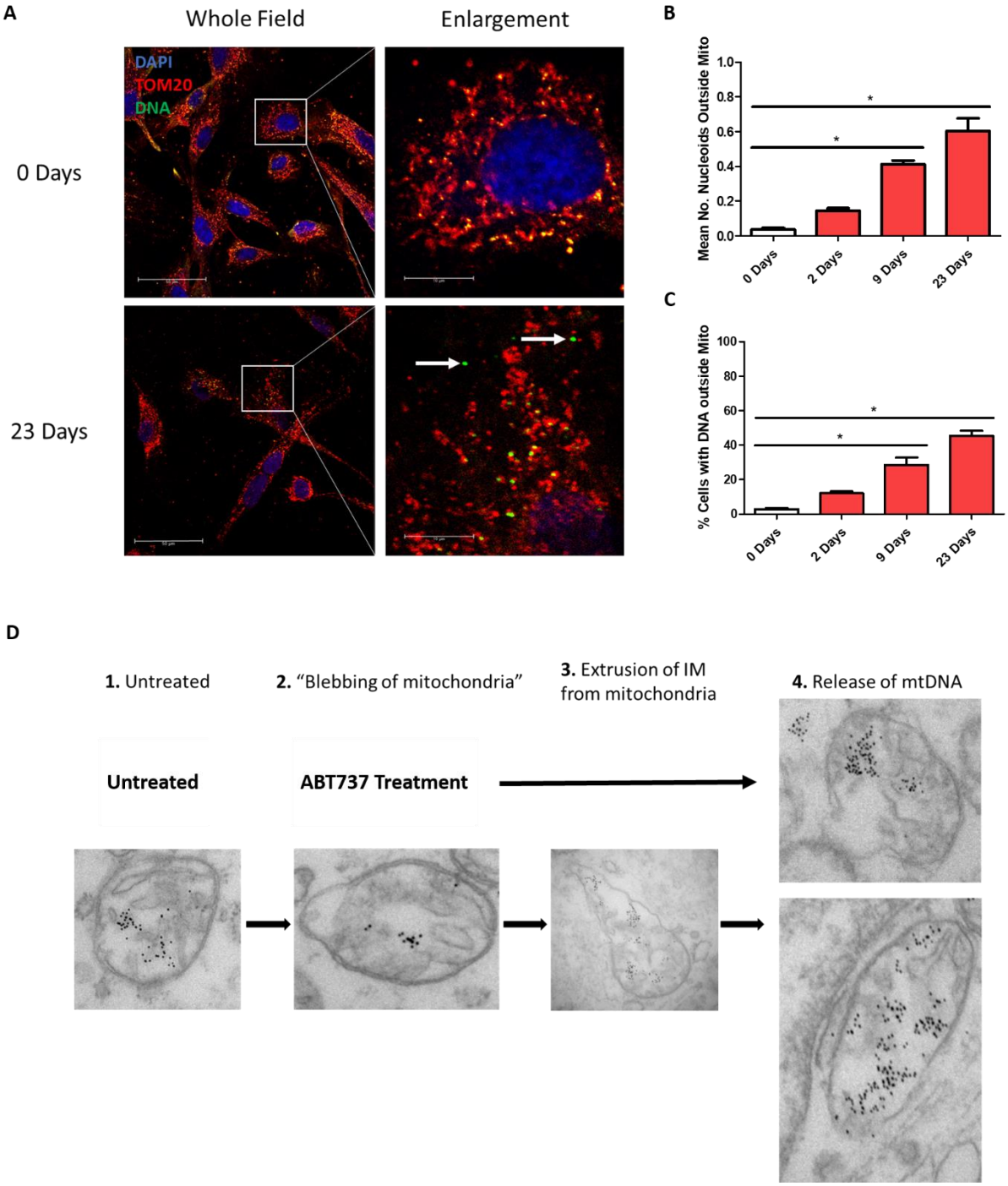

Figure 4.4 – miMOMP promotes mtDNA release.

Proliferating MRC5 human fibroblasts were maintained with either ABT737 (2.5µM) for 0 days, 2 days, 9 days and 23 days and then assessed for leakage of mtDNA. **(A)** Representative images of ABT737 treated cells at 0 days and 23 days labelled for DAPI (blue), DNA (green) and TOM20 (red) taken using confocal microscopy on a 63x objective, white arrows in the enlarged images highlight mtDNA nucleoids located outside of the mitochondrial network. **(B)** Bar graph depicting quantification of the mean number of DNA nucleoids outside of the mitochondrial network in U20S cells treated with ABT737 for 0, 2, 9 and 23 days, n=3-4 independent experiments. **(C)** Bar graph depicting the percentage of cells displaying DNA outside of the mitochondrial network in in cells treated with ABT737 for 0, 2, 9 and 23 days,

n=3-4 independent experiments. **(D)** Representative electron microscopy images of untreated and 20μM ABT737 treated (90mins) U20S cells labelled for DNA using a 10μm gold-conjugated secondary antibody. Bar graphs represent mean +SEM, statistical analysis performed using a One-way ANOVA.

4.4. miMOMP is dependent on BAX and BAK

It has been reported by *Ichim et al* that damage associated with miMOMP is dependent on the presence of BAX and BAK pores to facilitate cytochrome c release (Ichim *et al.*, 2015). As such, it was of interest to determine whether BAX and BAK deficient cells displayed a reduced colocalisation of cytochrome C and TOM20 following the development of senescence. Therefore the assay developed in Figure 4.1 was employed to assess miMOMP in proliferating and stress-induced senescent cells following CRISPR/CAS9 mediated deletion of BAX and BAK as shown in Figure 4.5A.

The level of colocalisation for individual cells was measured using the Pearson Correlation Coefficient statistical test, there was no statistical difference between proliferating Empty Vector and BAX/BAK deficient cells (0.81 vs 0.85). It was found that stress-induced senescent Empty Vector cells displayed a reduced level of colocalisation compared to proliferating Empty Vector cells (0.67 vs 0.81 respectively, $p<0.001$ in both cases). Senescent BAX/BAK deficient cells did not display a reduced level of colocalisation compared to proliferating BAX/BAK deficient cells (0.85 vs 0.81, Figures 4.5A and B). Similarly, when expressed as a percentage of the control, it was found that Empty Vector senescent cells were significantly reduced compared to their proliferating counterparts (87% vs 100%, $p<0.001$), whereas, senescent BAX/BAK deficient cells did not display a reduced level of co-localisation (95%, Figure 4.5C).

Earlier it was observed that treatment of MRC5 fibroblasts with ABT737 (2.5µM) for 9 and 23 days promoted the secretion of IL-6 and IL-8. Therefore, I wanted to assess whether BAX/BAK deficient cells would secrete IL-6 and IL-8 in response to ABT737 treatment (Figure 4.5D and E). Treatment of Empty Vector cells led to a significant increase in both IL-6 and IL-8 ($p<0.001$ in both cases). Treatment of BAX/BAK deficient cells led to a significant increase in both IL-6 and IL-8 ($p<0.01$ in both cases). Empty Vector cells treated with ABT737 had an increased secretion of IL-6 compared to BAX and BAK deficient cells treated with ABT737 (160 vs 95 pg/ml, $p<0.01$, Figure 4.5D). Similarly, Empty Vector cells treated with ABT737 had an increased secretion of IL-8 compared to BAX and BAK deficient cells treated with ABT737 (486 vs 329 pg/ml, $p<0.05$, Figure 4.5E).

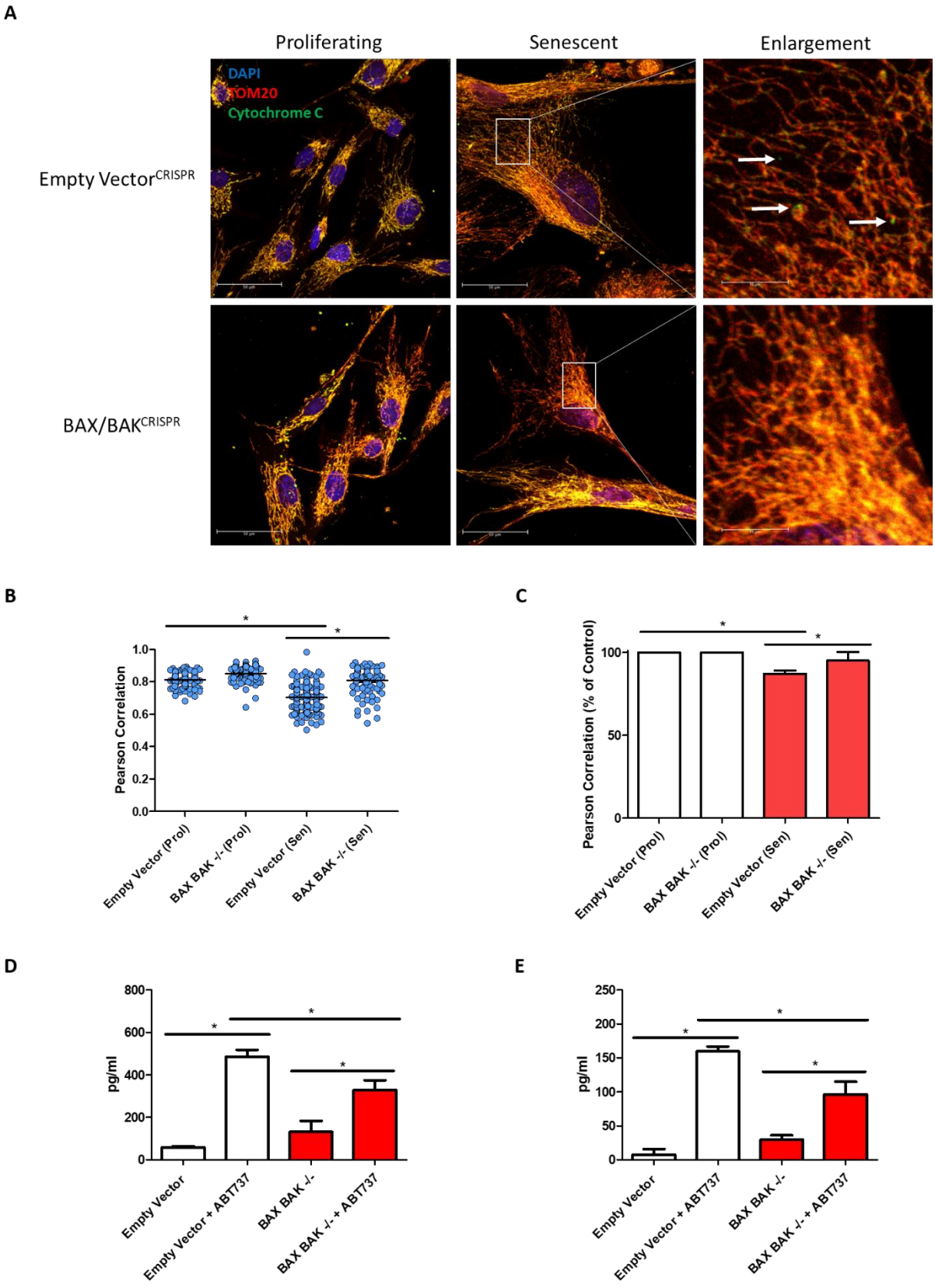

Figure 4.5 – miMOMP is dependent on BAX and BAK.

Proliferating and stress-induced senescent cells (Empty Vector and BAX/BAK deficient cells) were analysed for colocalisation of cytochrome C and Tom20 using confocal microscopy. **(A)**

Representative images of a proliferating and stress-induced senescent cells labelled using DAPI (blue), TOM20 (red) and cytochrome C (green). Images acquired in z-stacks by confocal microscopy using a 63x objective, following acquisition, the images were rendered using Huygens Deconvolution Software and colocalisation was measured using the Pearson Correlation Coefficient. White arrows in the enlarged image highlight cytosolic cytochrome C **(B)** Dot plot represents the statistical analysis of colocalisation of cytochrome C and TOM20 using the Pearson Correlation Coefficient where 1.0 is perfect colocalisation between the two channels. Each dot represents an individual cell from 3 independent experiments. **(C and D)** Bar graphs show the secretion of IL-6 **(C)** and IL-8 **(D)** following treatment with either DMSO or ABT737 for 9 days, n=3 independent experiments. Bar graphs represent mean +SEM, statistical analysis performed using a One-way ANOVA.

4.5. Caspases have a role in regulating the SASP and DDR

It was observed that ABT737 can induce a senescence-like phenotype which could in part be ameliorated by caspase inhibitors. This observation therefore led me to question whether caspases have a role in regulating different aspects of the senescent phenotype. Published work on the role of caspases in senescence has mostly focused on the role of caspase 1 activating the NLRP3 inflammasome as part of the SASP in OIS (Acosta *et al.*, 2013). Recent work has also highlighted the requirement of caspase 5 for activation of the IL-1α arm of the SASP following inflammasome activation, furthermore, caspase 11 was demonstrated to be a requirement for SASP-driven immune surveillance of senescent cells *in vivo* (Wiggins *et al.*, 2019).

As such I used the broad scale caspase inhibitor QVD in human senescent fibroblasts induced by both X-ray irradiation and replicative exhaustion. Consistently with previous observation, I found that following the development of the senescence phenotype in both models there was a robust increase in the secretion of IL-6 and IL-8 compared to the proliferating controls (<0.0001 in each case, Figures 4.6A and B). Following the induction of stress-induced senescence, cells were maintained with QVD to inhibit caspase activity whilst the senescence phenotype developed (10 days). I observed that both IL-6 and IL-8 were decreased following treatment with QVD compared to the untreated stress-induced senescent cells ($p<0.05$ for IL-6 and <0.001 for IL-8, Figures 4.6A and B). Replicatively senescent cells were maintained with the caspase inhibitor for 10 days following replicative exhaustion. It was found that when treated with QVD there was a significant decrease in the secretion of both IL-6 and IL-8 ($p<0.001$ for IL-6 and <0.0001 for IL-8, Figures 4.6A and B).

Earlier it was observed that ABT737 provokes sub-lethal caspase activity which drives a DDR. Senescent cells are characterized by a persistent DDR which is thought to contribute to the stabilization of the senescent phenotype (Rodier *et al.*, 2009; Passos *et al.*, 2010). However, the role of caspases in this process is not known. To test this I inhibited caspase activity in both stress-induced senescent cells and replicative cells using QVD and then assessed γH2AX. I found that both models of senescence displayed an enhanced mean number of γH2AX foci compared to the proliferating control cells ($p<0.001$ for stress induced senescence and $p<0.0001$ for replicative senescence) which was significantly decreased by treatment with QVD ($p<0.05$ for stress induced and $p<0.0001$ for replicatively senescence cells, Figure 4.6C).

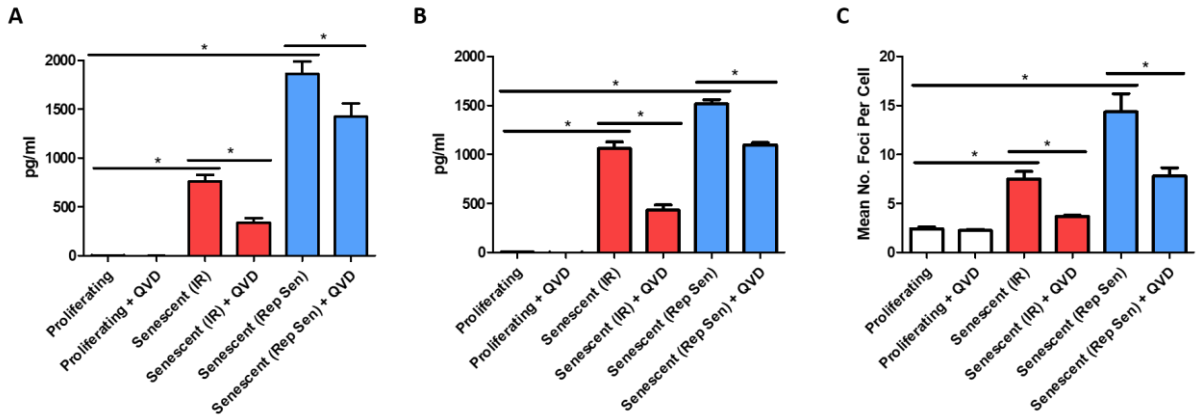

Figure 4.6 – Caspases mediate the SASP and DDR during senescence.

Proliferating and senescent cells (stress-induced and replicatively exhausted cells) were treated with the caspase inhibitor QVD (1µM) for 10 days or a DMSO control and then assessed for secretion of IL-6, IL-8 and the formation of DNA damage foci via γH2AX. **(A and B)** The bar graphs show the secretion of IL-6 **(A)** and IL-8 **(B)** in proliferating, stress-induced (red bars) and replicatively senescent cells (blue bars) treated with either QVD or the DMSO control. **(C)** The bar graph shows the mean number of γH2AX foci per cell in proliferating, stress-induced (red bars) and replicatively senescent cells (blue bars) treated with either QVD or the DMSO control. Bar graphs represent mean +SEM for 5 independent experiments, statistical analysis performed using a One-way ANOVA.

4.6. Caspase inhibition does not rescue the cell-cycle arrest characteristic of senescent cells

In order to comprehensively characterise the role of caspases in the senescence phenotype I analysed markers associated with senescence and the cell cycle arrest. First, I assessed whether caspase inhibition had an impact on the number of cells which displayed SA-β-Gal positive staining. Compared to proliferating cells, both stress-induced and replicatively senescence cells displayed an increased percentage of cells positive for SA-β-Gal ($p<0.0001$ in both cases). However, when stress-induced and replicatively senescent cells were treated with QVD there was no effect on the number of cells that displayed SA-β-Gal positive staining (Figure 4.7A).

As senescence is associated with a termination of the cell cycle, Ki67, a marker of proliferation, was analysed. I found that treatment with QVD did not impact on the frequency of KI67 positive cells in senescent cells.

Proliferating cells were approximately 60% positive for Ki67, following the induction of senescence, this was significantly reduced to 15% in stress-induced senescence cells ($p<0.0001$) and 3% in replicatively senescent cells ($p<0.0001$). When senescent cells which had been treated with the caspase inhibitor QVD were analysed there was no restoration of the decrease in Ki67 positivity for either stress-induced or replicatively senescent cells. (Figure 4.7B).

Next, the cyclin-dependent kinase inhibitors p16 and p21 were assessed. In proliferating cells, its expression was low with 15% of cells on average being positive for p16 and 23% for p21, following the induction of senescence, 56% and 94% of stress-induced senescent cells were positive for p16 and p21 respectively ($p<0.0001$ in both cases), replicatively senescent cells were 60% and 95% positive for p16 and p21 respectively ($p<0.0001$ in both cases). Treatment with QVD had no effect on the number of p16 or p21 positive cells in any of the groups; proliferating, stress-induced senescence and replicatively senescent cells (Figures 4.7C and D).

Finally, I assessed for the presence of Lamin B1. Lamin B1 is a protein responsible for maintaining nuclear integrity and has been reported to be decreased following the onset of senescence (Freund *et al.*, 2012). Therefore I wanted to assess whether caspase inhibition could prevent this loss. Using Western Blotting it was found that the protein Lamin B1 was present in proliferating cells and proliferating cells treated with QVD. It was not present in both stress-induced senescence and replicative senescence. Treatment of senescent cells with QVD did not prevent the decrease in Lamin B1 (Figure 4.7E).

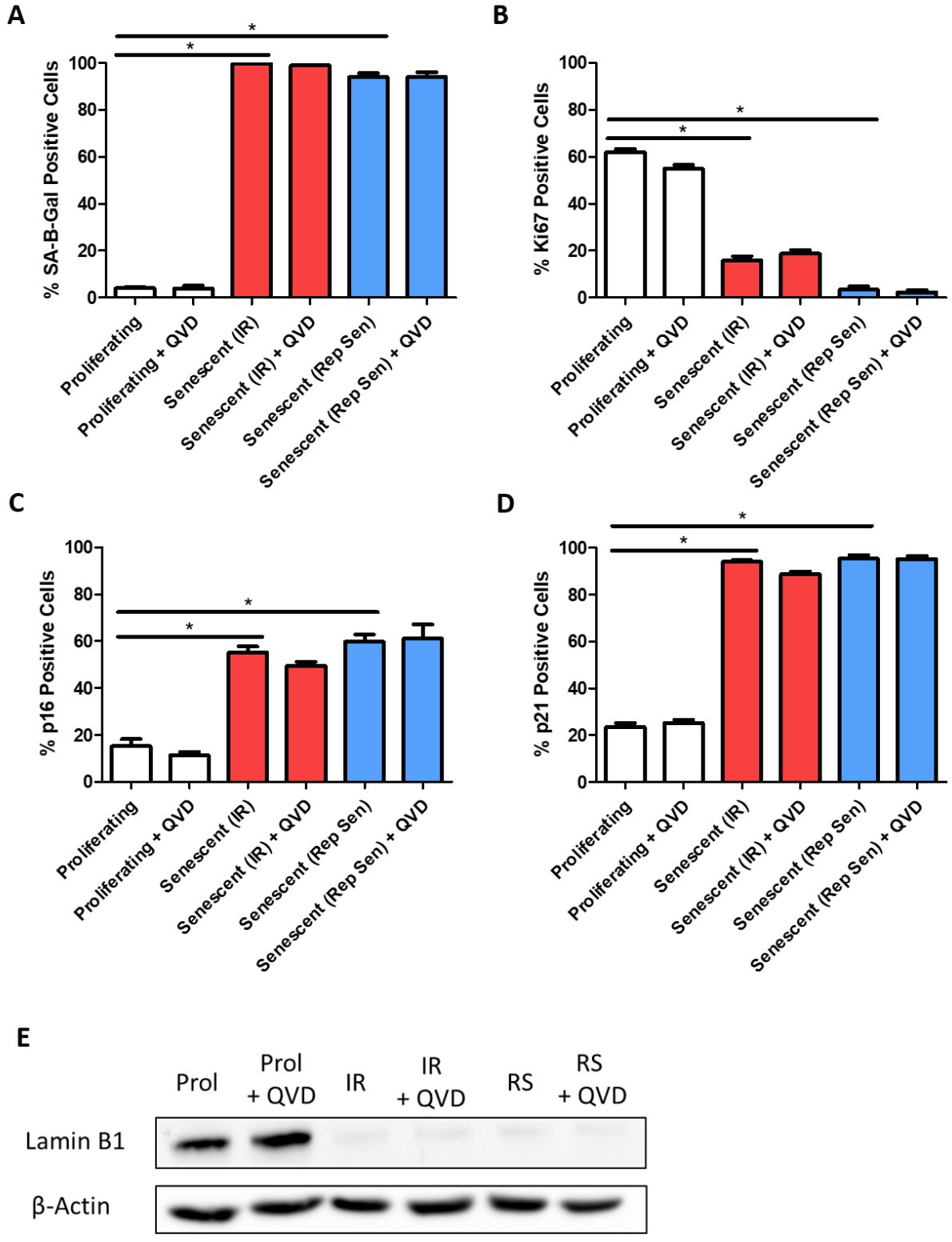

Figure 4.7 – Caspases do not have a role in regulation of the cell cycle arrest features of senescence or SA-β-Gal activity.

Proliferating and senescent cells (stress-induced and replicatively exhausted cells) were treated with the caspase inhibitor QVD (1μM) for 10 days or a DMSO control and then assessed for markers of senescence. **(A)** The bar graph shows the percentage of cells positive for SA-β-Gal

in proliferating, stress-induced (red bars) and replicatively senescent cells (blue bars) treated with either QVD or the DMSO control. **(B)** The bar graph shows the percentage of cells positive for Ki67 in proliferating, stress-induced (red bars) and replicatively senescent cells (blue bars) treated with either QVD or the DMSO control. **(C)** The bar graph shows the percentage of cells positive for p16 in proliferating, stress-induced (red bars) and replicatively senescent cells (blue bars) treated with either QVD or the DMSO control. **(D)** The bar graph shows the percentage of cells positive for p21 in proliferating, stress-induced (red bars) and replicatively senescent cells (blue bars) treated with either QVD or the DMSO control. **(E)** Representative Western Blot image of total protein levels of Lamin B1 and β-Actin in proliferating, stress-induced and replicatively senescent cells treated with either QVD or the DMSO control. Bar graphs represent mean +SEM for 5 independent experiments, statistical analysis performed using a One-way ANOVA.

4.7. Caspase 3 contributes to DNA damage and has a small role in the SASP during senescence

Earlier it was demonstrated that there was evidence of caspase 3 cleavage in senescent cells, furthermore, both the SASP and DDR that occurs during senescence are reduced by QVD treatment which is a known irreversible broad spectrum inhibitor of caspases. It has been reported that QVD has potent efficacy against caspases 1, 3, 8 and 9, as well as a lower level of activity against caspase 2, 5, 6, 7, 10 and 12 (Kuzelova *et al.*, 2011). The caspases 1 and 4 have been associated with the inflammasome and processing of IL-1β which can modulate inflammation (Martinon and Tschopp, 2004). Caspase 5 has also been reported to regulate the IL-1α arm of the SASP during senescence (Wiggins *et al.*, 2019). Caspase 3 is classically an executor caspase which is activated by caspase 8 and 9, once activated it fulfils the apoptosis process by inducing cleavage of DNA and degradation of cytoskeletal proteins (Elmore, 2007). In addition it has been reported that caspase 3 can promote sub-lethal DNA damage in the absence of cell death (Ichim *et al.*, 2015). Caspase 2 has been associated with promoting formation of BAX and BAK pores during the apoptotic process (Gao *et al.*, 2005). As such I decided to test the effect of inhibiting Caspases 1-4 individually on the SASP. Proliferating and stress-induced senescence cells were maintained in caspase inhibited conditions for 10 days prior to cytokine measurement. Initiation of senescence provoked a pronounced secretion of IL-6, IL-8 and IP-10 ($p<0.0001$ in each case). In senescent cells, individual inhibition of caspases 1, 2, 3 and 4 had no effect on the secretion of IL-6 (Figure 4.8A). With regards to IL-8, inhibition of caspases 1, 2 and 4 did not significantly alter the secretion of this cytokine, although caspase 1 and 2 did provoke a small decrease. Inhibition of caspase 3 on the other hand promoted a significant decrease of IL-8 ($p<0.001$, Figure 4.8B). Inhibition of caspases 1, 2, 3 and 4 provoked a small decrease in the secretion of IP-10 compared to senescent cells alone, however, none of these were significant.

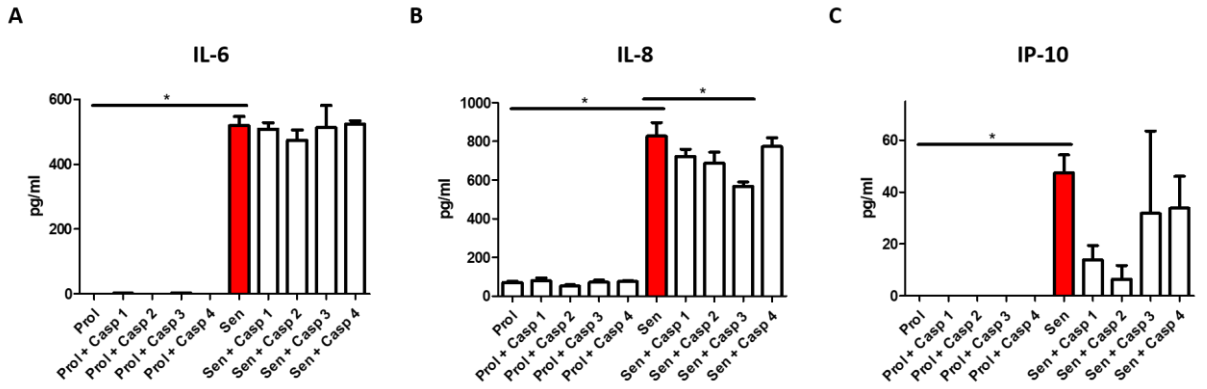

Figure 4.8 – Inhibition of Caspase 3 decreases the SASP component IL-8.

Proliferating and stress-induced senescent cells (20Gy irradiation) were maintained under control conditions (DMSO) or with one of the following caspase inhibitors; caspase 1, 2, 3 and 4 at 10µM for 10 days. **(A, B and C)** Bar graphs show the secretion of IL-6 **(A)**, IL-8 **(B)** and IP-10 **(C)** following treatment with either DMSO or the caspase 1, 2 3 and 4 inhibitors, n=4 independent experiments. Bar graphs represent mean +SEM, statistical analysis performed using a One-way ANOVA.

As part of investigating which caspases were contributing to the SASP and DDR, I assessed the activity of caspases 1 and 2 in senescent cells. To do this I assessed whether there was evidence for cleavage of these caspases which indicates that it is functionally active. First, I assessed Caspase 1. Interestingly, total protein levels of caspase 1 measured by pro-caspase 1 revealed that there was a significant 3-fold increase in the levels found in senescent cells ($p=0.0216$) (Figures 4.9 A and B). Indeed, there was also a 3-fold increase in the levels of cleaved-caspase 1 in senescent cells when compared to proliferating cells ($p=0.0012$, Figure 4.9C). When the level of cleaved-caspase 1 was normalised to the total amount of caspase 1 there was not a significant difference (Figure 4.9D). Next, I measured caspase 2 which was significantly decreased in senescent cells when compared to proliferating cells ($p<0.0001$, Figures 4.9E and F), in addition, there was no detectable difference in the levels of cleaved caspase 2 (Figures 4.9G).

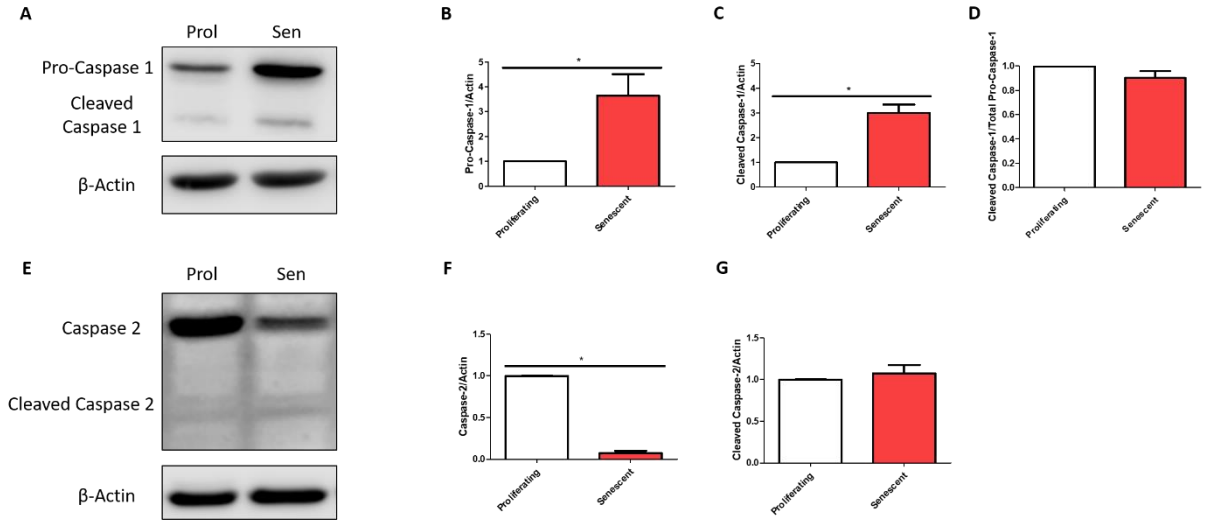

Figure 4.9 – Caspase1 cleavage is increased in senescent cells.

Proliferating and stress-induced senescent cells (20Gy irradiation) were assessed for activity of caspase 1, 2 and 3. **(A)** Representative image of total protein levels of pro-caspase 1, cleaved caspase 1 and β-Actin. **(B)** Bar graph shows the fold change in protein levels of pro-caspase 1 normalised to β-Actin in proliferating (white bars) and senescent cells (red bars). **(C)** Bar graph shows the fold change in protein levels of cleaved caspase 1 in proliferating (white bars) and senescent cells (red bars) normalised to the total level of β-Actin. **(D)** Bar graph shows the fold change in protein levels of cleaved caspase 1 in proliferating (white bars) and senescent cells (red bars) normalised to the total level of Caspase-1. **(E)** Representative image of total protein levels of total caspase 1, cleaved caspase 2 and β-Actin. **(F)** Bar graph shows the fold change in protein levels of caspase 2 in proliferating (white bars) and senescent cells (red bars). **(G)** Bar graph shows the fold change in protein levels of cleaved caspase 2 in proliferating (white bars) and senescent cells (red bars). Bar graphs represent mean +SEM, n=3-4 independent experiments, statistical analysis performed using a two tailed unpaired t-test.

In this study, I found that there was evidence of increased caspase-1 cleavage and caspase-3 activity in senescent cells. The treatment of senescent cells with a known inhibitor of caspase 1 did not have an effect on the SASP, caspase 3 inhibition on the other hand was associated with a reduced secretion of IL-8. Therefore, I wanted to characterise further whether it contributes to the DDR in senescence. Therefore proliferating and senescent cells were cultured alone and in the presence of the caspase 3 inhibitor. Then the senescence marker Lamin B1 and constituents of the DDR γH2AX and 53BP1 were assessed by Western Blot. It was found that senescent cells lost the expression of Lamin B1 ($p<0.0001$) compared to proliferating cells. Treatment with the caspase 3 inhibitor had no effect on its expression in the proliferating cells, in addition, its inhibition did not prevent the loss of Lamin B1 in senescent cells (Figures 4.10A and B). Next, 53BP1 levels were measured. 53BP1 is part of the DNA damage repair signalling

network, particularly in response to DSBs. It was found that senescent cells had a significantly increased total level of 53BP1 compared to proliferating cells (p=0.0391). Senescent cells treated with the caspase 3 inhibitor displayed a 50% reduction in the fold change of 53BP1 compared to untreated senescent cells, although this was not significant (p=0.1835). The caspase 3 inhibitor had no effect on the levels of 53BP1 in proliferating cells (Figures 4.10A and C). Finally, γH2AX was assessed. Senescent cells displayed a 2.5 fold increase in total levels of γH2AX compared to proliferating cells (p=0.0765). This increase was not observed in senescent cells treated with the caspase 3 inhibitor (1.2 fold higher than proliferating cells), these treated cells had a 50% decreased level of γH2AX compared to untreated senescent cells (p=0.2142). The caspase 3 inhibitor had no effect on the proliferating cells (Figures 4.10A and D).

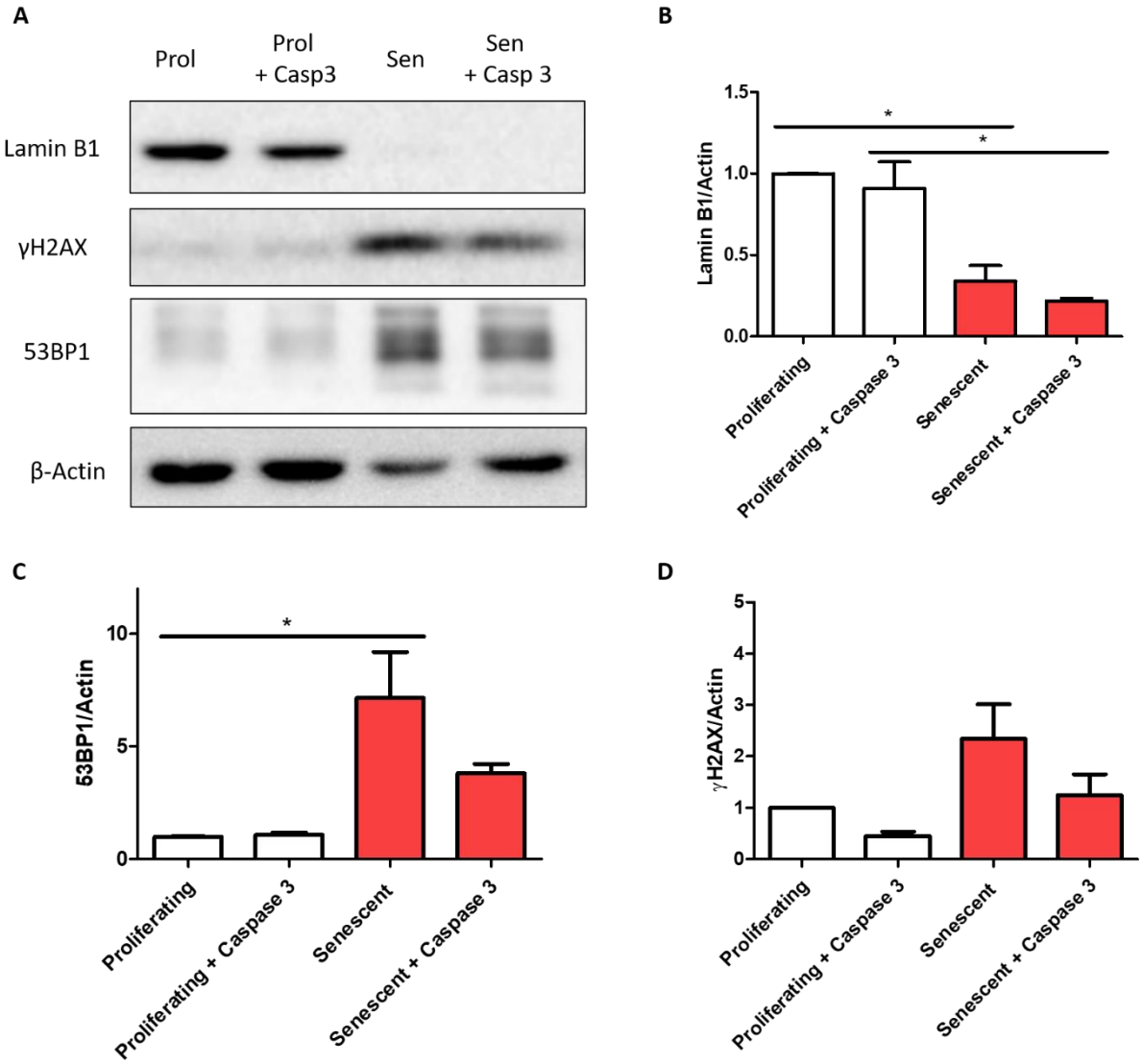

Figure 4.10 – Caspase 3 inhibition leads to a small reduction in the DDR.

Proliferating and stress-induced senescent cells (10 days post 20Gy irradiation) treated with the caspase 3 inhibitor (10μM) or a DMSO control were analysed for Lamin B1, γH2AX and 53BP1 by Western Blotting. **(A)** Representative Western Blot image of total protein levels of Lamin B1, γH2AX, 53BP1 and β-Actin. **(B)** Bar graph shows the fold change in protein levels of Lamin B1 in proliferating (white bars) and senescent cells (red bars). **(C)** Bar graph shows the fold change in protein levels of 53BP1 in proliferating (white bars) and senescent cells (red bars). **(D)** Bar graph shows the fold change in protein levels of γH2AX in proliferating (white bars) and senescent cells (red bars). Bar graphs represent mean +SEM, n=3 independent experiments, statistical analysis performed using a One-way ANOVA.

4.8. Discussion

Following our observation that senescent cells harbour cytosolic mtDNA as a consequence of BAX and BAK pores I wanted to further investigate the underlying process which could facilitate this. Recent work has unveiled a phenomenon called limited mitochondrial outer membrane permeabilisation (Ichim *et al.*, 2015). I set out to investigate this in the context of senescence. Collectively, we demonstrate that senescent cells display evidence of miMOMP. Moreover, the pharmacological induction of miMOMP promotes mtDNA release and a senescence phenotype. Finally, I provide evidence that miMOMP leads to cytochrome C release and subsequent sub-lethal caspase 3 activity which can instigate DNA damage in senescent cells.

Classically the process of mitochondrial outer membrane permeabilisation was considered an all or nothing process; either mitochondria were completely permeabilised and apoptosis was engaged or not at all (Tait and Green, 2010). As I observed that mtDNA leakage during senescence is dependent on BAX and BAK pores, I wanted to understand how mitochondrial permeabilisation could facilitate this. In the cancer field, it was recently discovered that cells can have a subset of mitochondria permeabilised which are releasing inner mitochondrial proteins such as cytochrome C in the absence of cell death (Ichim *et al.*, 2015). As mitochondria are widely associated with being dysfunctional during senescence I speculated that this process could be contributing to mtDNA release during senescence (Passos *et al.*, 2007; Passos *et al.*, 2010; Correia-Melo *et al.*, 2016; Wiley *et al.*, 2016; Chapman *et al.*, 2019). As such our first step was to characterise senescent cells for miMOMP. It has been reported that cytochrome C is detectable by confocal microscopy in the cytosol of cells undergoing miMOMP (Ichim *et al.*, 2015). By Western Blotting I discovered that cytochrome C was detectable in the cytosolic fraction of stress-induced and replicatively senescent cells but not proliferating cells. As cytochrome C is distributed completely through the mitochondrial network rather than individual nucleoids like mtDNA it is difficult to quantify the extent to which cytochrome C is present in the cytosol. In the *Ichim et al., 2015* paper cells were used which expressed a fluorescent tag on their mitochondria (mCherry) and a fluorescent tag in the cytoplasm (cytoGFP), when the mitochondria become permeabilised the cytosolic tag can pass into the mitochondria where it dimerises with the mitochondrial mCherry tag and provides a fluorescent signal to indicate mitochondrial permeabilisation. In this study I utilised confocal microscopy to acquire 3D images of cells labelled with TOM20 and cytochrome C. Following acquisition the Huygens Deconvolution Software was used to process these images and statistically analyse

them to determine how well the two channels co-localised. Using a Pearson's Correlation Coefficient test both stress-induced and replicatively senescent cells had a reduced level of colocalisation compared to proliferating cells. In normal proliferating cells, cytochrome C and TOM20 colocalise completely. In senescent cells there was cytochrome C staining visible which did not colocalise with TOM20. Indeed, I also observed areas of TOM20 which no longer colocalised with cytochrome C. These data indicate that in senescent cells there is an overall reduction of colocalisation between cytochrome C and TOM20 suggesting that these cells are undergoing miMOMP. However, there are some limitations to our analysis. First, as part of the processing to improve the reliability of the statistical analysis it is necessary to remove the background signal from images by deconvolution. Background signal needs to be removed as this is different between channels and will interfere with the colocalisation measurement between the two channels as it will be registered as signal by the software. All images are acquired and deconvolution is performed using identical parameters to avoid introducing any bias. However, the background does vary very slightly between individual coverslips and areas of coverslips. As such there is naturally a slight element of variation between images. This can be seen in the proliferating cells where it would be expected that there would be perfect colocalisation between cytochrome C and TOM20, however, looking at the dot plot for individual proliferating cells there is a degree of cell to cell variability in the level of colocalisation. Therefore, the data has been expressed both on an individual cell basis using the raw colocalisation value and in the bar graph as a percentage of the control cells where perfect colocalisation would be expected.

Following the development of our assay for measuring colocalisation of cytochrome C and TOM20 as a measure of miMOMP I wanted to validate that it could detect miMOMP in conditions known to induce miMOMP. In the literature it has been reported that mild stress using BH3 mimetic drugs such as ABT737 can induce miMOMP (Ichim *et al.*, 2015). Therefore I treated fibroblasts with ABT737 and then assessed our cells for miMOMP using our assay. Indeed, I found that cells treated with ABT737 displayed a reduced level of cytochrome C and TOM20 colocalisation compared to control fibroblasts. In the literature, ABT737 treatment was associated with approximately 5% of cells displaying miMOMP with approximately 3% of mitochondria being permeabilised (as measured by volume permeabilised) (Ichim *et al.*, 2015). For our data, I have not stratified it into an assessment of whether an individual cell displays permeabilisation or not. However, when expressed as a percentage of the control I observed a 12% decrease in the level of colocalisation, this therefore suggests that 12% of mitochondria

display miMOMP. With that in mind, it is possible that our assay is not quite as stringent as the one used by *Ichim et al*, although the experiments were performed in different cell lines (U20S cancer cells and MRC5 human fibroblasts) which may explain the slight differences seen (Ichim *et al.*, 2015). Alternatively, as the *Ichim et al* method measures the dimerization signal rather than the overall colocalisation between the two channels it may be that our method introduces more variability due to the removal of background during image processing.

The downstream effects of miMOMP induced by ABT737 include the release of cytochrome C and subsequent sub-lethal caspase 3 activity which drives DNA damage (Ichim *et al.*, 2015). Consistent with this notion, I observed cleavage of caspase 3 in cells treated with ABT737. Moreover, I found that treatment with ABT737 lead to an increase in DNA damage (measured by γH2AX). I found that this DNA damage was dependent on caspase activity as the co-treatment of cells with ABT737 and the caspase inhibitor QVD lead to a decrease in the level of DNA damage compared to ABT737 alone. Corroborating the finding that this DNA damage is driven by caspases I also found that ABT737 did not have an effect on the production of mitochondrial ROS. Collectively, these findings demonstrate that I can induce miMOMP using ABT737 and our assay is reliable enough to detect miMOMP.

In the context of senescence, I also observed downstream effects of cytochrome C release. In senescent cells I observed by Western Blot that there is increased caspase 3 activity compared to proliferating cells. In line with this finding, I found that in both stress-induced and replicatively senescent cells the inhibition of caspase activity using QVD led to a reduction in the number of γH2AX foci. These data in conjunction with the reduced colocalisation of cytochrome C and TOM20 in senescent cells provides good evidence that senescent cells have permeabilised mitochondria which are driving DNA damage through caspase 3 activity. The link between mitochondria and caspases has not been explored in senescence, therefore these observations raised two pivotal questions; first, can miMOMP be a driver of senescence? Second, to what extent do caspases regulate the senescence phenotype?

Our work has discovered that mitochondria in senescent cells display evidence of permeabilisation. However, at this stage it is difficult to determine whether miMOMP is a driver of senescence or a feature that occurs in response to the dysfunctional nature of mitochondria found in senescent cells. To address whether miMOMP can drive senescence I cultured cells continually in the presence of ABT737 (at 2.5μM which I demonstrated to induce miMOMP) and then assessed markers that are characteristic of senescence. After 9 days of continuous

culture, compared to control cells ABT737 led to an increase in SA-β-Gal, γH2AX and p21, there was also a tendency for increases in p16 and the secretion of IL-6 and IL-8. After 23 days of culture, the number of SA-β-Gal positive cells remained the same but there was a further increase in γH2AX and the secretion of IL-6 and IL-8. However, at this time point p16 and p21 have not been measured. The levels of p16 and p21 were relatively low at the 9 day time point, it may be that a longer period of exposure such as 23 days is required to observe upregulation of the growth arrest pathways. Therefore future work should seek to address this caveat. Together, these results highlight that sustained culture with ABT737 is promoting markers of senescence. As ABT737 induces caspase-mediated DNA damage I speculated that this could be responsible for driving the induction of senescence. As such, I also co-cultured cells with both ABT737 and QVD. Interestingly, at both the 9 and 23 day time point markers of senescence such as SA-β-Gal, γH2AX and the secretion of IL-6 and IL-8 were diminished in cells co-treated with QVD. These data support the idea that ABT737 is inducing miMOMP, which in turn is driving DNA damage through sub-lethal caspase activity. This damage is instigating the DDR which leads to an upregulation of p21 and increased expression of SA-β-Gal. As the senescence phenotype develops the secretion of IL-6 and IL-8 increases. This mechanisms supports a previous study where it was observed that ABT737 could induce senescence (p21, SA-β-Gal, IL-6 and IL-8 increased) in an apoptosis-resistant breast cancer cell line through caspase mediated DNA damage (Song *et al.*, 2011). Interestingly, they demonstrated that the DNA damage was generated by an increase in ROS production which was responsible for caspase 3 activation, however, in our study there was no observed increased production of ROS following treatment with ABT737. It is possible that cell line differences account for differences in ROS production, it is also plausible that as ABT737 can promote mitochondrial permeabilisation this could be associated with stress which results in an increased production of ROS. However, *Ichim et al* demonstrated that AB737 promotes activation of caspase 3 as a consequence of cytochrome C release by miMOMP (Ichim *et al.*, 2015). This fits with our observations as we observed both miMOMP and no increase in ROS production.

Interestingly, in the study by *Song et al*, they observed (depending on the cell line used) between 60 and 75% of cells being positive for SA-β-Gal following treatment with ABT737 whereas in our study we only observed approximately 10% of cells being positive for SA-β-Gal at both time points (Song *et al.*, 2011). It has recently been established that ABT737 belongs to a class of BH3 mimetic drugs which can induce apoptosis in senescent cells (Chang *et al.*, 2016; Yosef

et al., 2016b). ABT737 has been demonstrated to be effective at killing senescent human fibroblasts (IMR90s), MEFs and senescent cells *in vivo* due to their dependence on the upregulation of pro-survival proteins BCL-2 and BCL-XL (Yosef *et al.*, 2016b). Therefore it is likely that cells which become senescent following ABT737 driven miMOMP will undergo apoptosis due to exposure to ABT737. Furthermore, the study by *Song et al* was performed in cancer cell lines which were found to be resistant to apoptosis. It has been shown that the senolytic ABT-263 which is structurally similar to ABT737 is not effective in all cell types (Zhu *et al.*, 2016; Zhu *et al.*, 2017). Therefore it is plausible that when senescent these cancer cells may be less reliant on BCL-2 and BCL-XL mediated survival and therefore not undergo apoptosis when exposed to ABT737. This is likely the explanation as to why our study has observed a low number of SA-β-Gal and p21 positive cells compared to *Song et al* (Song *et al.*, 2011).

The observation that miMOMP can promote DNA damage and an increase in markers of senescence is particularly interesting as ABT737 and its related family members are currently being proposed as promising senolytic drugs. Naturally, this therefore raises the question of what the effects of ABT737 will be on healthy cells and tissue. Our data indicates that it can induce substantial amounts of DNA damage which can drive a senescence-like phenotype. Furthermore, there is evidence in the literature that ABT737 can be pro-tumourigenic (Ichim *et al.*, 2015). These data suggest that using ABT737 as a senolytic agent may in fact be a double edged sword as it can remove the detrimental senescent cells, but it may provoke senescence in healthy cells. Pharmacological clearance of senescent cells generally seems to be performed using intermittent dosing rather than continual treatment (Chang *et al.*, 2016; Ovadya *et al.*, 2018; Walaszczyk *et al.*, 2019). This is therefore likely to mitigate the effects on healthy tissue. However, our data indicates that 48 hours of exposure was sufficient to induce DNA damage. In addition, the literature demonstrates that within three hours of ABT737 treatment there is detectable DNA damage measured by γH2AX in vitro. Moreover, the authors also demonstrated increased γH2AX following 1 day of ABT737 treatment *in vivo* which was not associated with an increase in TUNEL staining (a measure of DNA fragmentation that occurs during apoptosis) (Ichim *et al.*, 2015). These data indicate that caution should be employed when administering BH3 mimetics as senolytics to ensure that the benefit of senescent cell clearance outweighs the detriment of DNA damage. As such, this supports the idea of senescent cell clearance intermittently during the later stages of life rather than throughout the life course of an organism.

It has been reported by *Ichim et al* that damage associated with miMOMP is dependent on the presence of BAX and BAK pores to facilitate cytochrome c release (Ichim *et al.*, 2015). Consistent with this observation, I found that in the context of senescence, cells deficient for BAX and BAK did not display reduced colocalisation of cytochrome C and TOM20 to the same extent as senescent Empty Vector cells. This indicates that miMOMP in senescence is dependent on BAX and BAK. Future experiments should seek to understand whether treatment of cells with BIPv5 or BCB also prevent miMOMP from occurring. Moreover, it was demonstrated earlier in this study that the SASP is dependent on BAX and BAK as a consequence of mtDNA release. It has been published that the release of mtDNA can occur in response to mitochondrial permeabilisation following treatment of fibroblasts with ABT737, similarly this has been shown to be dependent on BAX and BAK (McArthur *et al.*, 2018; Riley *et al.*, 2018). Therefore, we reasoned that the pro-inflammatory response that occurs in response to treatment with ABT737 could be promoting the release of mtDNA by miMOMP. Therefore I assessed whether miMOMP induced by ABT737 was associated with mtDNA release.

It has been reported that high doses of ABT737 promote mtDNA release during apoptosis (McArthur *et al.*, 2018; Riley *et al.*, 2018). However, it has not been assessed whether low doses which induce miMOMP lead to mtDNA release. As I observed that senescent cells display evidence of miMOMP and cytosolic mtDNA which were both dependent on BAX and BAK being present, I speculated that miMOMP could be responsible for facilitating mtDNA release. Indeed, I found that the pharmacological induction of miMOMP using ABT737 led to an increase in the level of cytosolic mtDNA. The increase was small after 48 hours, but was significantly increased at 9 days and further increased by 23 days of sustained exposure. These findings indicate that miMOMP can promote mtDNA release. Interestingly, both the percentage of cells and the mean number of cytosolic nucleoids per cell were lower in ABT737 treated cells at each time point compared to the number of nucleoids observed in senescent cells which were characterised in the previous chapter. In line with this observation, it was also observed that both stress-induced and replicatively senescent cells had a reduced level of cytochrome C/TOM20 colocalisation compared to the level of colocalisation observed in cells treated with ABT737. These data suggest that senescent cells have an increased proportion of permeabilised mitochondria compared to ABT737 treated cells which may explain the increased level of cytosolic DNA in senescent cells. Alternatively, this observation could be explained by activity of cytosolic DNases responsible for degrading cytosolic DNA. As senescent cells have downregulated activity of the cytoplasmic DNases TREX1 and DNase2 it could be plausible

that DNA released by ABT737 induced miMOMP is rapidly removed from the cell, hence the lower observed level of cytosolic mtDNA (Takahashi *et al.*, 2018). As both senescent markers and the level of cytosolic mtDNA increase at 9 days and 23 days, it is therefore possible that as the senescent phenotype develops following ABT737 mediated miMOMP there is reduced activity of DNases which could explain the accumulation of cytosolic mtDNA at the later time points.

Surprisingly, treatment of BAX and BAK deficient cells with ABT737 still resulted in an increased secretion of IL-6 and IL-8. Although the level of secretion was not as high as control Empty Vector cells it would be expected that if mtDNA release in response to ABT737 was solely responsible for the pro-inflammatory response then this would not be detectable in BAX and BAK deficient cells. Interestingly, work by *Riley et al* demonstrated that in response to ABT737 mediated mtDNA release there is a 100-fold increase in Ifnb1 in control cells, in BAX/BAK deficient cells there is a 20-fold increase compared to the control cells (Riley *et al.*, 2018). As they also observed an increased pro-inflammatory response following exposure of BAX and BAK deficient cells to ABT737 this suggests that the effects of ABT737 are not completely attributed to mtDNA release. Therefore future work should seek to explore alternative mechanisms that ABT737 may be promoting part of its inflammatory response through.

Interestingly, the secretion of IL-6 and IL-8 which occurs in response to ABT737 treatment can be prevented by caspase inhibition. I speculated that as miMOMP can promote mtDNA release co-treatment of ABT737 with QVD would not have an effect on the secretion of IL-6 and IL-8 as mtDNA would presumably still be being released regardless of caspase activity. Indeed, it has been demonstrated that doses of ABT737 which are sufficient to induce apoptosis still lead to an inflammatory response under caspase inhibited conditions through NF-κB (Giampazolias *et al.*, 2017). Moreover, it has been demonstrated that caspases are responsible for silencing the inflammatory response to mtDNA which is released during apoptosis, they demonstrated that during apoptosis under caspase inhibited conditions an inflammatory response was observed (White *et al.*, 2014). Contrastingly, in this study I observed that caspase inhibition completely prevented the inflammatory response to ABT737. Interestingly, in senescent cells caspase inhibition reduced IL-6 and IL-8 secretion by approximately 25-30% rather than completely as observed in response to ABT737. These observations indicates that in the context of ABT737 exposure the inflammatory response is potentially associated with caspase-mediated DNA damage rather than solely attributed to mtDNA release. As such, it is plausible that cytosolic

DNA which is released in response to ABT737 may be rapidly degraded before an inflammatory response is mounted. Alternatively, caspases may contribute mechanistically to the release of mtDNA. There is evidence that caspases 3, 6, 7 and 8 can promote cytochrome c release (Bossy-Wetzel and Green, 1999; Garrido *et al.*, 2006). It is known that cytochrome C release occurs via BAX and BAK pores, therefore, hypothetically these caspases could enable mtDNA release which would not occur in cells co-treated with both ABT737 and QVD (Tait and Green, 2010). It would therefore be of interest in the future to experimentally test this by assessing mtDNA leakage in cells which have been co-treated with ABT737 and QVD. At this stage the data demonstrates a caspase-mediated reduction in SA-β-Gal, γH2AX and p21 therefore lending weight to the idea that the reduction in IL-6 and IL-8 secretion is attributed to a reduced number of cells becoming senescent due to reduced DNA damage induction through sub-lethal caspase activity. This highlights the requirement for further work to dissect the relationship between mtDNA, caspases and the secretion of IL-6 and IL-8.

As it has been established that senescent cells display evidence of miMOMP and the effects of pharmacologically inducing miMOMP can be mitigated by caspase inhibition, we questioned whether inhibition of caspases could be beneficial in the context of senescence. To address this I used the broad spectrum caspase inhibitor QVD for 10 days during the development of stress-induced senescence and following the development of replicative senescence and then characterised markers of the SASP and the cell cycle arrest. I found that DNA damage was reduced in both models of senescence when the caspases were inhibited, in addition, I also found that the SASP was reduced by approximately 50% in stress-induced senescent cells and 30% in replicatively senescent cells. These two findings highlight that caspases have a multi-faceted role during senescence, first, they are in part responsible for inducing DNA damage in senescent cells, and secondly, they have a role in SASP regulation which will be discussed in detail later. However, it seems that the role of caspases in senescence are restricted to the SASP and DNA damage as there were no observable effects on other markers of senescence/cell cycle arrest such p16, p21, Ki67, SA-β-Gal or the loss of Lamin B1 in both models of senescence. At this stage it is important to consider that although QVD and the individual caspase inhibitors are known to inhibit the relevant caspases, I have not verified mechanistically that caspase activity has been inhibited. Therefore, future work should seek to confirm that their activity has been blocked in MRC5 human fibroblasts.

Following these observations I wanted to investigate further the role of caspases instigating DNA damage. Previous studies have largely linked the induction of DNA damage during

senescence with the production of ROS (Saretzki *et al.*, 2003; Ramsey and Sharpless, 2006; Passos *et al.*, 2007). However, as it was established that damage associated with miMOMP was linked with caspase 3 activity, I assessed the cleavage of caspase 3 in senescent cells (Ichim *et al.*, 2015). Western blotting revealed that compared to their proliferating counterparts there was an increased level of cleaved caspase 3 in senescent cells indicating its activation. Both γH2AX and 53BP1 are reliable markers of DNA damage which have been demonstrated to be upregulated as part of the DDR (d'Adda di Fagagna, 2008). Western blotting revealed that the selective inhibition of caspase 3 in stress-induced senescent cells led to a non-significant reduction of both γH2AX and 53BP1. Although it is possible that the number of samples in this experiment was not sufficient to determine statistical significance, an important point of consideration in this experiment is that western blotting may not be sufficiently sensitive to determine physiologically relevant differences in small numbers of γH2AX foci. Therefore, these data should be treated as preliminary until the individual number of γH2AX foci have been characterised using confocal microscopy.

In senescent cells it was found that neither broad-scale inhibition of caspases using QVD nor the selective inhibition of caspase 3 reduced DNA damage levels back to the levels found in proliferating cells. This indicates that caspase 3 is not solely responsible for the DNA damage in senescence. This fits with the literature which has pinpointed a key role of ROS in maintaining DNA damage during the development of senescence to ensure the robust upregulation of p21 (Passos *et al.*, 2010; Nelson *et al.*, 2018). A recent study demonstrated that p21 was important for preventing apoptosis in stress-induced senescent cells by restraining the activity of caspase 3 in senescent cells as the silencing of p21 led to apoptosis in senescent cells by JNK-caspase 3 activity. Interestingly, in their study p21 proficient stress-induced senescent cells still display an increase in the protein levels of cleaved caspase 3 compared to growing cells (although substantially lower than the p21 silenced cells which were undergoing apoptosis) (Yosef *et al.*, 2017). Although their study was not investigating sub-lethal caspase 3 activity, their observation matches ours of sub-lethal caspase activity in senescent cells. As caspase inhibition only partly ameliorated DNA damage levels with no effect on the cell cycle arrest, it is likely that ROS is still being produced which is important for maintaining the DDR positive feedback loop during the development of senescence. It would be interesting to test whether the DDR can be further reduced by inhibiting both caspase 3 and ROS using an antioxidant and subsequently assess whether this has prevents the cell cycle arrest.

Another interesting aspect of our observation is that the broad scale inhibition of caspase activity in replicative senescent cells also reduced the level of DNA damage. As caspase inhibition was performed in cells where the senescent phenotype was already established it suggests that caspase activity is not restricted to the development of senescence but also occurs once the cell cycle is averted and the senescent phenotype is fully developed. As such, it seems likely that the effects of caspase 3 on DNA damage occur in response to mitochondrial dysfunction which is promoting miMOMP. A way to dissect the link between caspase 3 activity and miMOMP would be to measure caspase 3 activity in BAX/BAK deficient cells which do not undergo miMOMP during senescence. It would be expected that BAX/BAK deficient cells would have a reduced level of DNA damage and caspase 3 activity as cytochrome C is not being released. Indeed, it has been published that treatment of BAX/BAK deficient cells with ABT737 does not lead to an increase in γH2AX as miMOMP cannot occur (Ichim *et al.*, 2015). However, in the previous chapter I found that senescent BAX/BAK deficient cells do not have a reduced level of DNA damage. It may be speculated that their metabolic function may be altered as a consequence of BAX and BAK being genetically removed which could influence the amount of DNA damage. Although non-significant, it was observed that there was a small increase in ROS production in senescent BAX/BAK deficient cells. Therefore it is plausible that this increased production of ROS could explain why BAX/BAK deficient cells do not have a decreased amount of DNA damage despite not having evidence of miMOMP. In line with this, I found that treatment with ABT737 does not promote ROS production which explains why *Ichim et al* observed a complete reduction in γH2AX following the treatment of BAX/BAK deficient cells with ABT737 (Ichim *et al.*, 2015).

To further dissect the relationship between mitochondria and caspase regulation, it would be of significant interest to test for sub-lethal caspase 3 activity in senescent fibroblasts which have no mitochondria such as those generated by *Correia-Melo et al* (Correia-Melo *et al.*, 2016; Correia-Melo *et al.*, 2017).

The observation that broad scale caspase inhibition could partially decrease the SASP is a relationship that has not been previously explored. Therefore it was of interest to understand specifically which caspases had a regulatory role in the production of the SASP. As such, caspases 1-4 were individually inhibited. It has previously been published that in OIS, caspase 1 levels are elevated, here, it functions as part of the NLRP3 inflammasome where it cleaves IL-1β to promote cytokine production. Furthermore, inhibition of caspase 1 reduced the SASP, as well as partially preventing the induction of p21-mediated cell cycle arrest (Acosta *et al.*,

2013). However, the findings of this study suggest that caspase 1 does not have a SASP regulatory role in stress-induced senescence as its inhibition did not have an effect on the secretion of IL-6 or IL-8. Although, in stress-induced senescence I found evidence of caspase 1 cleavage, this cleavage was not associated with activation of the inflammasome (characterised thoroughly in the subsequent chapter). Furthermore, when the level of cleavage was normalised to the total amount of caspase 1 there was no difference between proliferating and senescent cells. This therefore suggests that there is only an increased level of cleaved caspase 1 because senescent cells harbour an increased total protein level of caspase 1. As such, it would be interesting in future studies to understand specifically why there is an increased amount of caspase 1in senescent cells and whether the observed increase in caspase 1 cleavage has a functional output in stress-induced senescence.

Outside of the context of senescence, caspase 4 has also been associated with the inflammasome and processing of IL-1β which can modulate inflammation (Martinon and Tschopp, 2004). It was found that its inhibition did not have an effect on the secretion of IL-6 and IL-8. As both caspase 1 and 4 have a regulatory role in the inflammasome these data suggest that these caspases are not responsible for SASP regulation, similarly they also suggest that the inflammasome does not facilitate the SASP in stress-induced senescence.

Caspase 2 has been associated with promoting formation of BAX and BAK pores during the apoptotic process by promoting cleavage of BID to tBID (Gao *et al.*, 2005). It was therefore postulated that perhaps caspase 2 could be promoting BAX and BAK pore formation which is leading to mtDNA release and subsequently the SASP. However, it was found that the total protein level of caspase 2 was significantly downregulated in senescent cells. Moreover, the inhibition of caspase 2 during senescence was not associated with an effect on the secretion of IL-6 and IL-8. Together, these data highlight that caspase 2 is not active during senescence and indeed it is not contributing to the SASP.

Caspase 3 is classically an executor caspase responsible for implementing the apoptosis process by inducing cleavage of DNA and degradation of cytoskeletal proteins (Elmore, 2007). As previously discussed it was found to be active and contributing towards DNA damage in senescence. Interestingly, the specific inhibition of caspase 3 led to a decrease in the secretion of IL-8. This suggests that caspase 3 can regulate the SASP. In the literature there is some evidence that caspase 3 is responsible for the cleavage of IL-16 indicating that it does have a role in the regulation of inflammation (Zhang *et al.*, 1998; Sciaky *et al.*, 2000). However, IL-

16 is not observed as part of the SASP and caspase 3 has not been implicated in the regulation of other pro-inflammatory cytokines. This suggests that the effect of caspase 3 inhibition on IL-8 is likely attributed to its effect on the DDR. Indeed, there is evidence in the literature that a reduction in the DDR can lead to a reduction in the SASP. For example, the DDR factors ATM and ATR stabilise GATA4 which regulates NF-κB, a key modulator of the SASP (Chien *et al.*, 2011; Kang *et al.*, 2015).

Broad scale inhibition of the caspases led to a reduction in the SASP of approximately 50 and 30% in stress-induced and replicative senescence respectively. The specific inhibition of caspase 3 led to an approximate 25% reduction in IL-8 but had no effect on IL-6. It is not entirely clear why IL-8 was reduced but not IL-6. As suggested earlier, it seems that the most likely cause is due to the associated reduction in the DDR. However, there are alternative possibilities to consider. First, it may be that the SASP is regulated by a mechanism which involves the interaction between multiple caspases. Therefore, it would be interesting to explore this experimentally to either inhibit or genetically knockout various caspases in conjunction with caspase 3 to determine whether the effects are exacerbated.

Secondly, as I only inhibited caspases 1-4 individually it is possible that other caspases are responsible for the effects observed by broad caspase inhibition. Other than the caspases discussed above it has been reported that QVD can also act against caspases 8 and 9, with a lower efficacy against 5, 6, 7, 10 and 12 (Kuzelova *et al.*, 2011). In the context of senescence, caspase 5 has recently been demonstrated as being essential for the IL-1α arm of the SASP (IL-6, IL-8 and MCP-1). Consistently, they demonstrated that caspase 5 (caspase 11 in mice) is responsible for cleavage of IL-1α, consistently, silencing of caspase 5 led to a robust reduction in the SASP (Wiggins *et al.*, 2019). Therefore, this warrants investigating whether inhibition of caspase 5 alone could replicate the effects of broad scale caspase inhibition. Taken together, it indicates that caspase 3 has an effect on the SASP (likely associated with the DDR), however, it seems probable that alternative caspases such as caspase 5 are also important in regulating the SASP.

5. Chapter 5: Pharmacological inhibition of the cGAS-STING axis ameliorates the SASP

It has been reported that the integrity of the nucleus in senescent cells becomes impaired and fragments of DNA termed CCFs (cytoplasmic chromatin fragments) bud off to the cytosol (Ivanov *et al.*, 2013). Once located in the cytosol, they have a key role in inducing the SASP through the cGAS-STING pathway. Specifically, CCFs are identified by the DNA sensor cGAS, which leads to activation of STING. This in turn promotes phosphorylation of TBK1 and subsequently IRF3 which leads to transcription of type 1 IFN genes. Similarly, STING can activate IKK which in turn acts on NF-κB, a known regulator of the SASP. A number of groups have reported that activation of cGAS occurs during senescence as a consequence of CCFs, which lead to induction of the SASP (Dou *et al.*, 2017; Gluck *et al.*, 2017; Yang *et al.*, 2017).

As part of this study we wanted to address whether cytosolic mtDNA observed during senescence could also be participating in the SASP via activation of the cGAS-STING pathway. Studies to date have employed the use of genetic tools to indicate the role of the cGAS-STING axis in senescence. First and foremost this is the gold standard of indicating the role of a protein in a process, however, until recently there has been no pharmacological means of inhibiting cGAS. Therefore, one of aim of this study was to characterise the potential of pharmacological cGAS inhibitors as a strategy for targeting the SASP.

5.1. Cytosolic mtDNA activates the cGAS-STING axis in senescence

In Chapter 3 I have shown that mtDNA is more abundant in the cytosol of senescent cells. Furthermore, I have shown that genetic or pharmacological inhibition of BAX and BAK can suppress mtDNA release and the SASP. Following this finding, I aimed to investigate the pathways by which mtDNA contributes to the SASP.

The first pathway that was assessed as a potential candidate for promoting mtDNA-mediated inflammation was the cGAS-STING axis. It has previously been published that cGAS-STING is implicated in regulation of the SASP, as well as detection of mtDNA (West *et al.*, 2015; Dou *et al.*, 2017; Gluck *et al.*, 2017; Yang *et al.*, 2017). To understand whether cGAS was responsible for detecting mtDNA I generated MRC5 fibroblasts expressing a GFP fluorescent tag on the cGAS protein, therefore allowing us to assess its location within the cell. First, the

mean number of cGAS signals detectable within a cell were measured. It was observed that there was a significant enhancement in the number of cGAS-GFP signals in senescent cells compared to proliferating ($p=0.0317$) cells (Figures 5.1A and B). However, it is well acknowledged that cGAS can detect nuclear fragments of DNA as well as mtDNA in senescent cells (Dou *et al.*, 2017; Gluck *et al.*, 2017). Therefore to understand the contribution of mtDNA, I specifically measured the number of cGAS signals which colocalised with TFAM (located outside mitochondrial networks). It was discovered that the percentage of cells which displayed cGAS colocalising with TFAM was vastly increased in senescent cells compared to proliferating cells ($p=0.0079$) (Figures 5.1A and C). In addition, specifically addressing the percentage of cells which displayed cGAS colocalising with cytosolic TFAM was significantly increased in senescent cells compared to proliferating cells ($p=0.0097$) (Figures 5.1A and D).

Following the observation that cGAS was colocalising with TFAM in senescent cells, I wanted to assess whether blockage of mtDNA release had any effect on the activation of this pathway. In response to cytosolic DNA, the activation of the cGAS-STING axis leads to the translocation of NF-κB and the phosphorylation of IRF3 (Tanaka and Chen, 2012; Liu *et al.*, 2015). Together, NF-κB and IRF3 promote the transcription of type 1 IFNs and other cytokines (Li and Chen, 2018).

First, I assessed proliferating and stress-induced senescent cells by Western Blot (Figure 5.1E). Senescent cells displayed an increased expression of the CDKIs p16 and p21 compared to their proliferating counterparts. It was found that the total amount of STING was significantly increased by 2.5 fold in senescent cells compared to proliferating cells ($p=0.0004$, Figure 5.1F). It was also found that phosphorylated NF-κB was significantly increased by 1.4 fold in senescent cells when compared to proliferating cells ($p=0.0013$, Figure 5.1G).

Next, I assessed the protein levels of phosphorylated IRF3 in proliferating, senescent and senescent cells which had been treated with the BAX inhibitor BCB to block mtDNA release. It was found that in senescent cells there was an increase in the phosphorylation of IRF3 compared to proliferating cells, following the inhibition of mtDNA release using BCB the level of phosphorylation was reduced (Figure 5.1H).

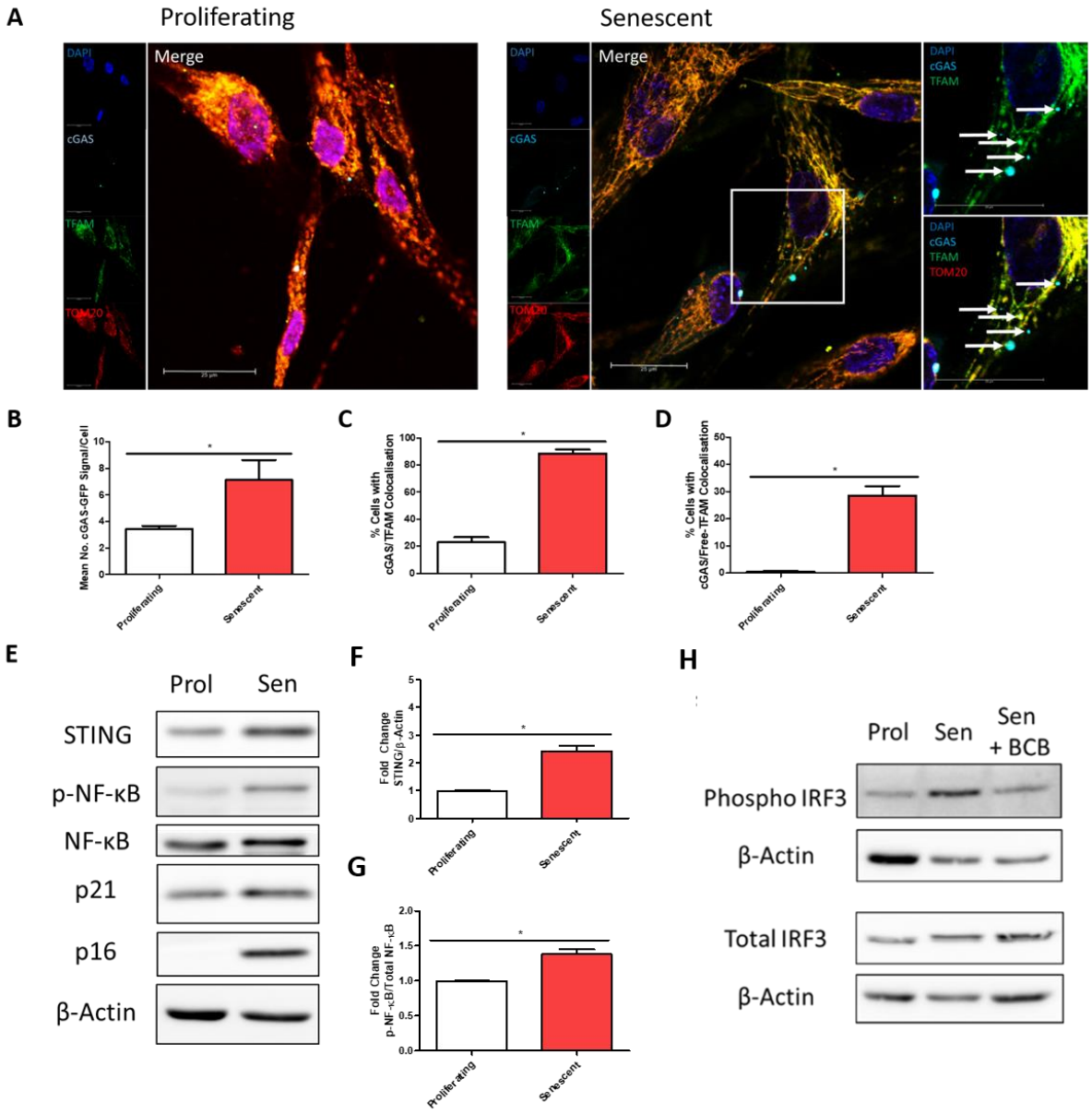

Figure 5.1 – cGAS colocalises with cytosolic mtDNA.

MRC5 fibroblasts were generated which expressed cGAS with a GFP tag. Following transfection, cell were induced to become senescent via irradiation, 20Gy. Following irradiation, cells were analysed 6 days later. **(A)** Representative images of proliferating and senescent cells labelled with DAPI (blue), cGAS-GFP (cyan), TFAM (green) and TOM20 (red). Images acquired using a 63x objective by confocal microscopy. White arrows in the enlarged image indicate cGAS colocalisation with TFAM. **(B)** Bar graph depicts the mean number of cGAS-GFP signals counted in proliferating and senescent cells, n=5 independent experiments. **(C)** Bar graph depicts the percentage of cells which display cGAS-GFP signals colocalising with TFAM in proliferating and senescent cells, n=5 independent experiments. **(D)** Bar graph depicts the percentage of cells which display cGAS-GFP signals colocalising with free-TFAM (which does not colocalise with TOM20) in proliferating and senescent cells, n=5 independent experiments. **(E)** Representative western blot of STING, phospho-NF-κB (p65), total NF-κB (p65), p21, p16 and β-Actin in proliferating, and senescent cells. n=4 independent experiments. **(F and G)** Bar graphs represent the fold change of STING **(F)** normalised to β-Actin and

phospho-NF-κB **(G)** normalised to total NF-κB which had been normalised to β-Actin in proliferating and senescent cells, n=4 independent experiments.. **(H)** Representative western blot of phosho-IRF3 and the total IRF3 in proliferating, senescent and senescent cells treated with BCB (2.5μM), n=2 independent experiments. Bar graph data is shown as mean, error bars represent the standard error of the mean, statistical significance was determined using a two-tailed unpaired t-test.

Collectively, we observed that the cytosolic DNA sensor cGAS was colocalising with cytosolic TFAM, in addition we have also shown indirect evidence that this pathway is activated in senescence via the measurement of phosphorylated IRF3. This phosphorylation was not observed when mtDNA release was blocked using a drug which blocks BAX channels. Following on from these observations I wanted to further understand the contribution of the cGAS-STING axis to inflammation in response to mtDNA. To test this, using the CRISPR CAS9 system I generated cells which were deficient for STING using three STING constructs (Figure 5.2A).

Following the generation of $STING^{CRISPR}$ MRC5 cell lines, mtDNA was transfected into the cells and known SASP components IL6 and IL-8 were measured (Schematic in Figure 5.2B). Following transfection, there was a clear increase in the Empty Vector control cell line for both IL-6 and IL-8 ($p<0.0001$ for both cytokines, Figures 5.2C and D). For each of the three STING KO cell lines there was a significant decrease in the secretion of IL-6 and IL-8 following the introduction of mtDNA compared to the Empty Vector cells transfected with mtDNA ($p<0.0001$ for both cytokines, Figures 5.2C and D).

The suppression of the SASP induced by mtDNA was not complete- suggesting that other pathways apart from STING may be involved.

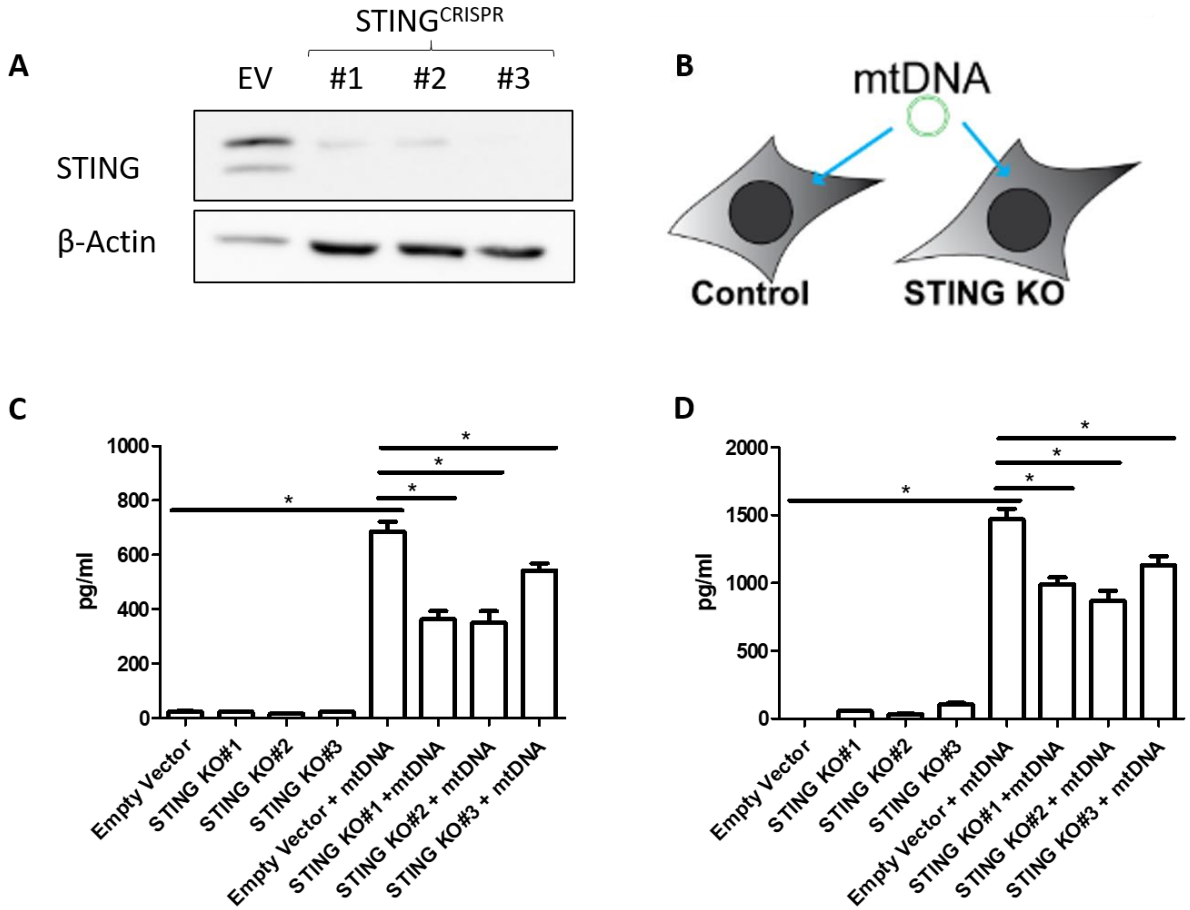

Figure 5.2 - Genetic knockout of STING ameliorates the inflammatory response to mtDNA.

(A) Representative Western Blot image of total protein levels of STING and β-Actin for Empty Vector control cells and the three STING deficient cell lines created (#1, #2 and #3). (B) Schematic representation of experimental introduction of mtDNA into Empty Vector and STING KO cells. **(C and D)** Bar graph depicts the levels of IL-6 **(C)** and IL-8 **(D)** secreted into the media 24 hours post transfection as measured by ELISA following 24 hours of transfection with mtDNA in proliferating Empty Vector and the three STING deficient cell lines, n=6 independent experiments. Bar graph data is shown as mean, error bars represent the standard error of the mean, statistical significance was determined using a one-way ANOVA.

The presence of CCFs during senescence has been reported in both mouse embryonic fibroblasts and human fibroblasts in a number of models of senescence such as oxidative stress induced, OIS and replicatively exhausted cells (Ivanov *et al.*, 2013; Dou *et al.*, 2017; Gluck *et al.*, 2017). Mechanistically, it has been reported that nuclear fragments occur due to the loss of the nuclear envelope protein Lamin B1. Downregulation of Lamin B1 leads to the loss of nuclear envelope integrity which promotes the budding off of nuclear fragments of DNA (Ivanov *et al.*, 2013; Gluck *et al.*, 2017). Therefore, the first aim was to assess whether CCFs were detectable in MRC5 human fibroblasts.

First, the presence of Lamin B1 was assessed by Western Blot. In senescent cells there was a clear reduction in the overall protein level of Lamin B1 compared to proliferating cells as previously shown in the literature ($p<0.0001$, Figures 5.3A and B) (Ivanov *et al.*, 2013; Dou *et al.*, 2017). Next we wanted to assess the presence of CCFs in proliferating and senescent cells, in addition, we wanted to verify that these fragments were identified by cGAS. To address this, cells were generated which expressed cGAS-GFP and then they were subsequently labelled with DAPI and an anti- DNA antibody to allow for CCF identification. Quantification of the mean number of CCFs per cell revealed that senescent cells had more detectable CCFs than proliferating cells, on average, 0.4 CCFs were detectable compared to 0.05 in proliferating cells ($p=0.0079$, Figures 5.3A and D). Similarly, it was observed that the percentage of cells positive for harbouring CCFs was higher in senescent cells compared to proliferating cells, on average 13% of senescent cells displayed CCFs compared to only 4% of proliferating cells ($p<0.0001$, Figures 5.3A and E). Following these observations we wanted to verify if these observable CCFs co-localize with cGAS. Therefore we evaluated colocalisation between cGAS-GFP. We found that 100% of detectable CCFs in both proliferating and senescent cells were positive for cGAS colocalisation consistent with previously published results (Figures 5.3A and F) (Ivanov *et al.*, 2013; Dou *et al.*, 2017).

Published work has found that approximately 40% of IMR90scells are positive for CCFs when induced to become senescent by OIS or genotoxic stress, in some cell types such as BJ cells the CCFs are detectable in approximately 60% of cells, whereas MEFs have a lower frequency of CCFs; approximately 30% of cells are positive (Ivanov *et al.*, 2013; Dou *et al.*, 2017; Gluck *et al.*, 2017). I found that only 13% of stress-induced MRC5 fibroblasts were positive for CCFs, but approximately 70% were positive for cytosolic mtDNA. As such, in our case I wanted to understand whether CCFs in our model which have largely been regarded as being only of nuclear origin could in fact be misidentified and in some cases be of mtDNA origin (Ivanov *et*

al., 2013; Dou *et al.*, 2017; Gluck *et al.*, 2017). The dye DAPI which is commonly used to label nuclear DNA labels all double-stranded DNA, therefore it is plausible that some DAPI-positive CCFs could be mtDNA rather than nuclear DNA. Therefore cGAS-GFP expressing cells which were labelled with TOM20, TFAM and DAPI earlier in this study (Figure 5.1A) were assessed. Of these CCFs which colocalised with cGAS we found in proliferating cells that 12% were positive for TFAM and DAPI, with the remaining 88% colocalising with DAPI only. In senescent cells 50% of CCFs were positive for both TFAM and DAPI ($p<0.01$ compared to proliferating cells), with the remaining 50% being positive for DAPI only, (Figure 5.3G).

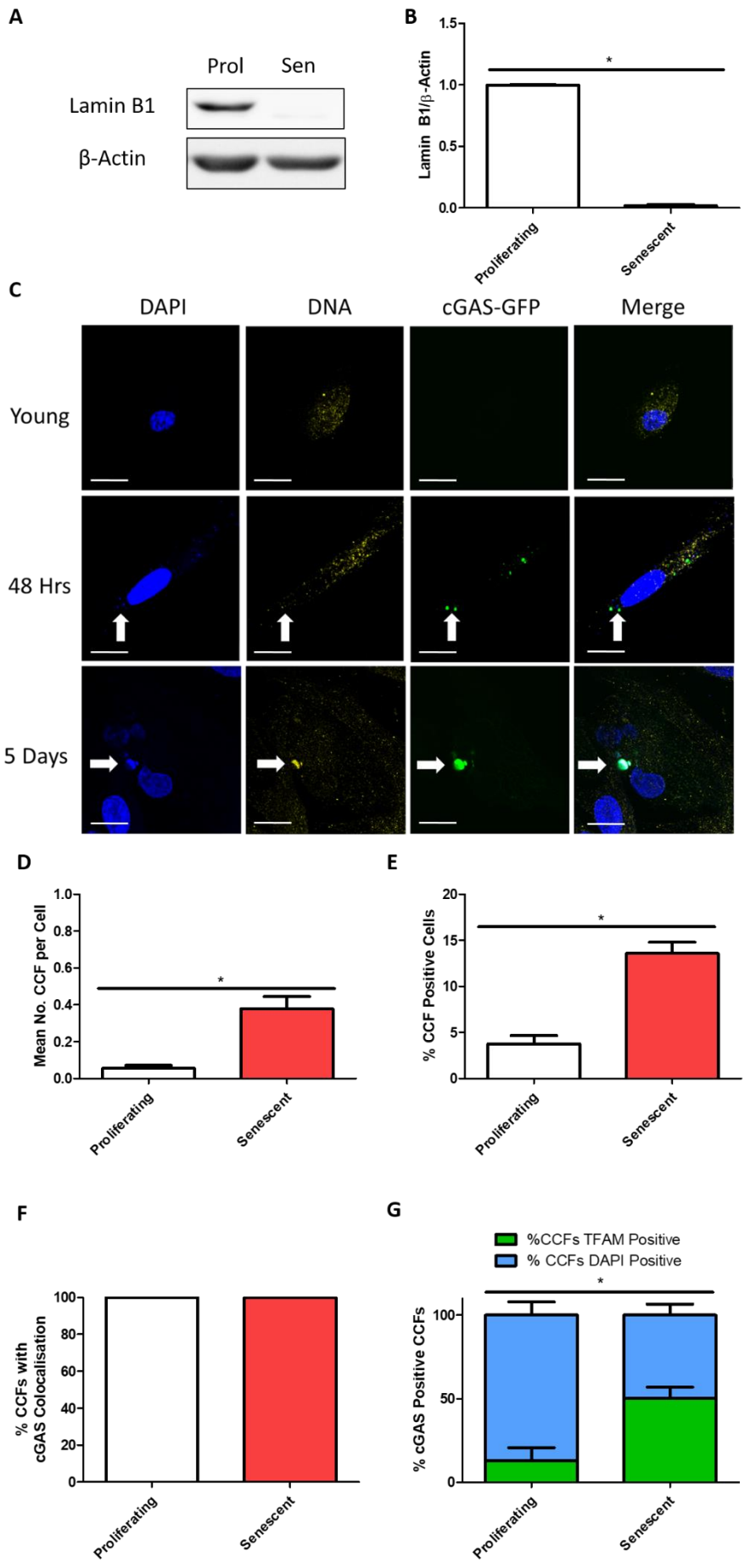
A
Prol
Sen
Lamin B1
β-Actin
B
Lamin B1/β-Actin
1.5
1.0
0.5
0.0
*
Proliferating
Senescent
C
DAPI
DNA
cGAS-GFP
Merge
Young
48 Hrs
5 Days
D
Mean No. CCF per Cell
1.0
0.8
0.6
0.4
0.2
0.0
*
Proliferating
Senescent
E
% CCF Positive Cells
20
15
10
5
0
*
Proliferating
Senescent
F
% CCFs with cGAS Colocalisation
100
80
60
40
20
0
Proliferating
Senescent
G
%CCFs TFAM Positive
% CCFs DAPI Positive
% cGAS Positive CCFs
100
50
0
*
Proliferating
Senescent

Figure 5.3 – Senescent cells lack Lamin B1 and have CCFs which are recognised by cGAS.

(A) Representative Western Blot image of total protein levels of Lamin B1 and β-Actin. **(B)** Bar graph represents the fold change of Lamin B1 in proliferating and stress-induced senescent cells (10 days post 20Gy irradiation) normalised to β-Actin, n=4 independent experiments. **(C)** Representative images of proliferating cells and stress-induced senescent cells (48 hours and 5 days post induction of senescence by irradiation 20Gy) expressing cGAS-GFP and labelled with DAPI and DNA acquired by fluorescent microscopy using a 63x objective. White arrows denote cGAS positive CCFs (characterised by being a separate entity from the nucleus and being positive for both DAPI and DNA). Scale bars are 20μm. **(D)** Bar graph represents the quantification of the number of mean number of CCFs per cell in proliferating and stress-induced senescent cells (5 days post induction), n=5 independent experiments. **(E)** Bar graph represents the quantification of the percentage of cell which display CCFs in proliferating and stress-induced senescent cells (5 days post induction), n=5 independent experiments. **(F)** Bar graph represents the quantification of the percentage of CCFs which colocalise with cGAS in proliferating and stress-induced senescent cells (5 days post induction), n=5 independent experiments. **(G)** Bar graph represents the percentage of cGAS positive CCFs which display colocalisation with TFAM and DAPI (green) or DAPI alone (blue) in proliferating and stress-induced senescent cells (5 days post induction), n=5 independent experiments. Bar graph data is shown as mean, error bars represent the standard error of the mean, statistical significance was determined using a two-tailed unpaired t test.

Following the observation that CCFs are detectable in senescent MRC5 human fibroblasts and display co-localisation with cGAS, we wanted to understand their relative contribution to the SASP compared to mtDNA. Therefore we assessed the number of CCFs detectable in BAX/BAK deficient cells, which we demonstrated earlier in this study to display a reduced amount of cytosolic mtDNA in conjunction with an attenuated SASP.

Analysis of the mean number of CCFs per cell revealed that there was no difference in the mean number of CCFs in proliferating Empty Vector cells and proliferating BAX/BAK deficient cells. Furthermore, senescent Empty Vector cells had a significantly increased number of CCFs (0.05 to 0.38 mean CCFs per cell, $p<0.0001$). Senescent BAX and BAK cells also displayed an increase of 0.07 to 0.22 CCFs on average per cell, however this increase was non-significant. The difference between senescent Empty Vector and BAX/BAK deficient cells was also non-significant (Figure 5.4A).

In addition to characterising the mean number of CCFs, the percentage of cells harbouring CCFs was also analysed. Similarly, I found that there was no difference in the percentage of cells containing CCFs in the proliferating Empty Vector and BAX/BAK deficient cells. Senescent Empty Vector cells displayed a significant increase from 3.7% of cells to 13.5% of cells ($p<0.001$). Senescent BAX/BAK deficient cells also showed an increase from 4.4% to

12.2% of cells ($p<0.05$). Analysis of the percentage of CCF positive cells revealed that there was no significant difference between senescent Empty Vector and BAX/BAK deficient cells (Figure 5.4B).

At this stage, whilst our data supports that cGAS can bind to TFAM- alternative methods will need to be applied to confirm these results. For instance, ChIP-seq to determine which type of DNA is bound to cGAS, similarly immunoprecipitation between TFAM and cGAS would be crucial.

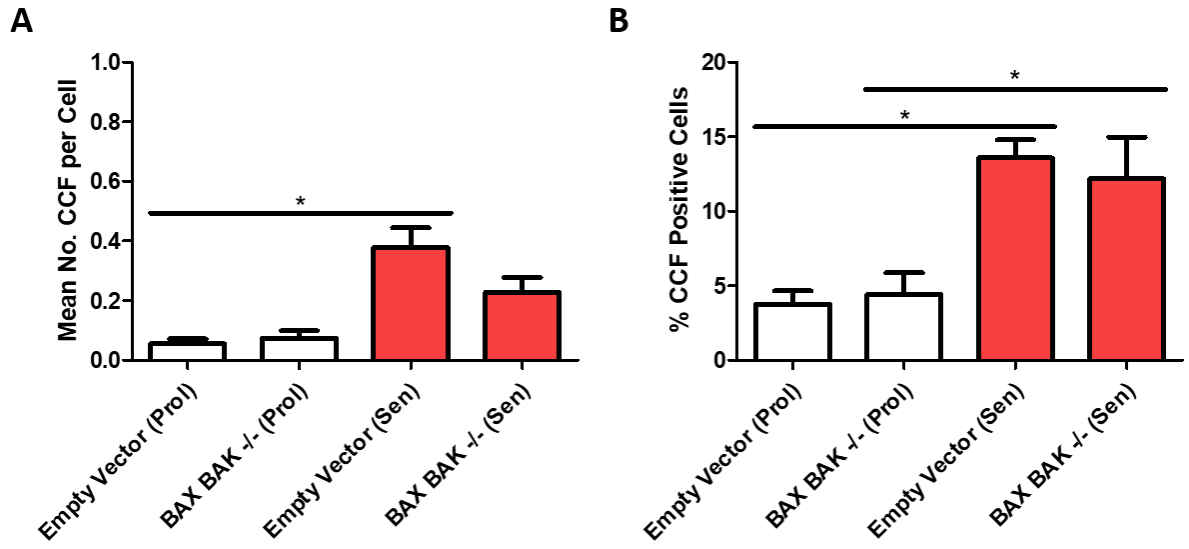

Figure 5.4 – BAX/BAK deficient cells harbour as many CCFs as Empty Vector cells.

Proliferating and stress-induced senescent (10 days post 20Gy irradiation) Empty Vector and BAX/BAK deficient cells were assessed for the presence of CCFs. **(A)** Bar graph represents the quantification of the number of mean number of CCFs per cell in proliferating and stress-induced senescent cells (5 days post induction). **(B)** Bar graph represents the quantification of the percentage of cell which display CCFs in proliferating and stress-induced senescent cells (5 days post induction). n=5 independent experiments. Bar graph data is shown as mean, error bars represent the standard error of the mean, statistical significance was determined using a one-way ANOVA.

5.2. Genetic ablation of STING alleviates the SASP

It has been reported in the literature that following the detection of CCFs cGAS drives the SASP, this is mediated through cGAMP production which activates STING, which proceeds to form a complex with TBK1 which promotes phosphorylation and activation of the transcription factors IRF3 and NF-κB (Chen *et al.*, 2016). This leads to production of type 1 IFNs and inflammatory cytokines associated with the SASP. It has been demonstrated that in both MEFs and human fibroblasts that the genetic removal of cGAS alleviates the SASP (Dou *et al.*, 2017; Gluck *et al.*, 2017). As such, I wanted to verify whether the genetic knockout of STING which would impair the cGAS-STING signalling pathway would also prevent the SASP. Therefore STING deficient MRC5 fibroblasts generated earlier in the study were used.

In proliferating cells which harbour an Empty Vector or have had STING genetically ablated there was no difference in the secretion of IL-6 and IL-8. Following the development of senescence in the empty vector control cell line there was a clear significant increase in the production of both IL-6 and IL-8 ($p<0.0001$ for both cytokines). In each of the three STING deficient cell lines following the development of senescence there was no increase in the production of IL-6 or IL-8 compared to their proliferating counterparts. Furthermore, for each of the senescent STING deficient cell lines the secretion of IL-6 and IL-8 was significantly decreased compared to the senescent empty vector control cells ($p<0.0001$ in each case) (Figures 5.5A and B).

Next, the cell cycle regulators p16 and p21 were assessed in proliferating and senescent Empty Vector and STING deficient cells by western blot (Figure 5.5C). Senescent Empty Vector cells displayed an increased expression of p16 and p21 compared to their proliferating counterparts ($p<0.01$ in both cases, Figures 5.5D and E). Similarly, STING deficient cells displayed an increased expression of p16 compared to their proliferating counterparts ($p<0.01$), although p21 was not increased (Figure 5.5D and E).

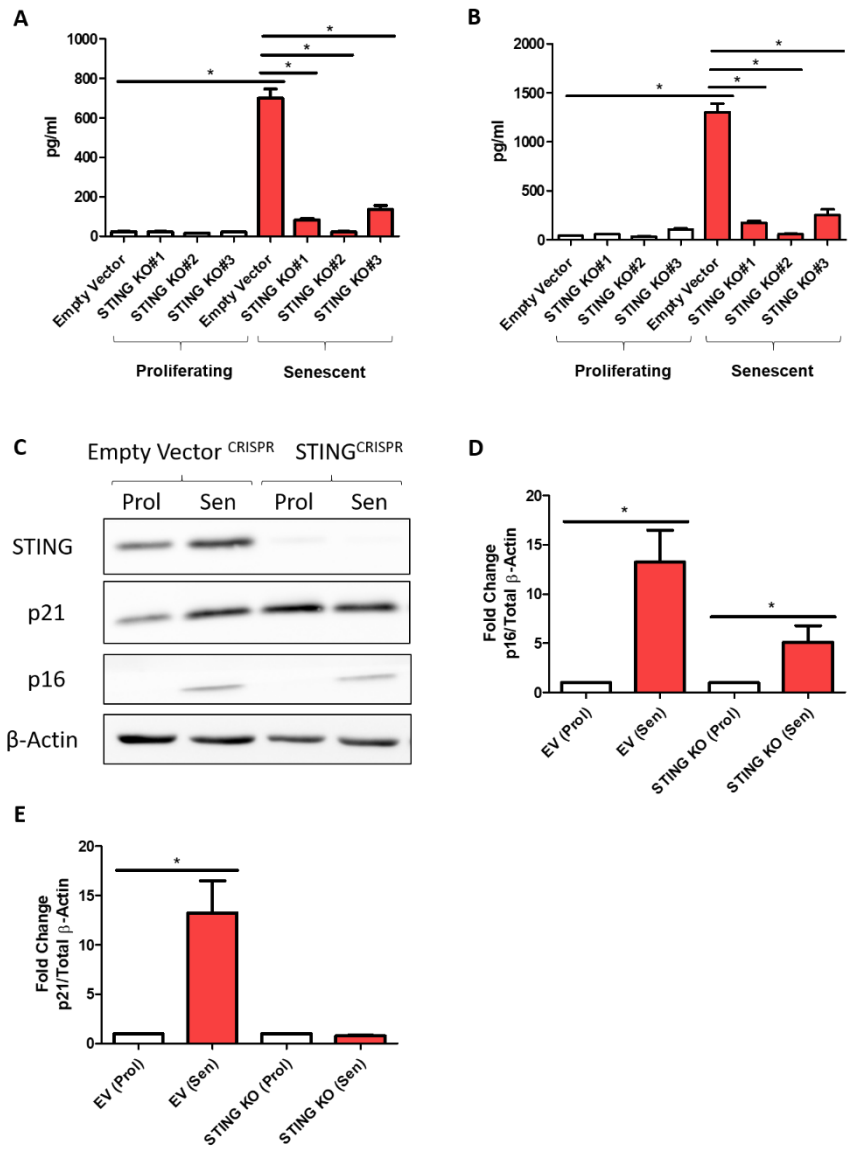

Figure 5.5 – Genetic removal of STING diminishes the SASP.

The SASP was assessed by ELISA in empty vector (control) and STING deficient cells (#1, #2 and #3) in proliferating and stress-induced cells (10 days post 20Gy irradiation). **(A and B)** Bar graph depicts the levels of IL-6 **(A)** and IL-8 **(B)** secreted into the media by proliferating and senescent Empty Vector and the three STING deficient cell lines, n=6 independent experiments. **(C)** Representative Western Blot image of total protein levels of STING, p21, p16 and β-Actin for Empty Vector control cells and STING deficient cells. **(D and E)** Bar graphs represent quantification of total p16 **(D)** and p21 **(E)** protein levels in proliferating and senescent empty vector (control) and STING deficient cells n=4 independent experiments. Bar graph data is shown as mean, error bars represent the standard error of the mean, statistical significance was determined using a one-way ANOVA.

Earlier in Chapter 3 I observed that the BAX inhibitor BCB could decrease the SASP, similarly, I found that genetic removal of STING diminishes the SASP, as such I wanted to assess whether the effects of BCB in Empty Vector cells were similar to the genetic depletion of STING, secondly, I wanted to see whether treatment of STING deficient cells with BCB would have any further impact on the secretion of IL-6 and IL-8.

Following the development of stress-induced senescence both IL-6 and IL-8 were increased in senescent Empty Vector cells ($p<0.0001$ for both cytokines), no increase was observed in STING deficient cells. As observed earlier, treatment with BCB prompted a significant decrease of both IL-6 and IL-8 in Empty Vector senescent cells ($p<0.0001$ for both cytokines). In STING deficient cells, no further decrease was observed following treatment with BCB. For the secretion of IL-6 and IL-8 there was no statistically significant difference between senescent Empty Vector + BCB and senescent STING KO (Figures 5.6A and B).

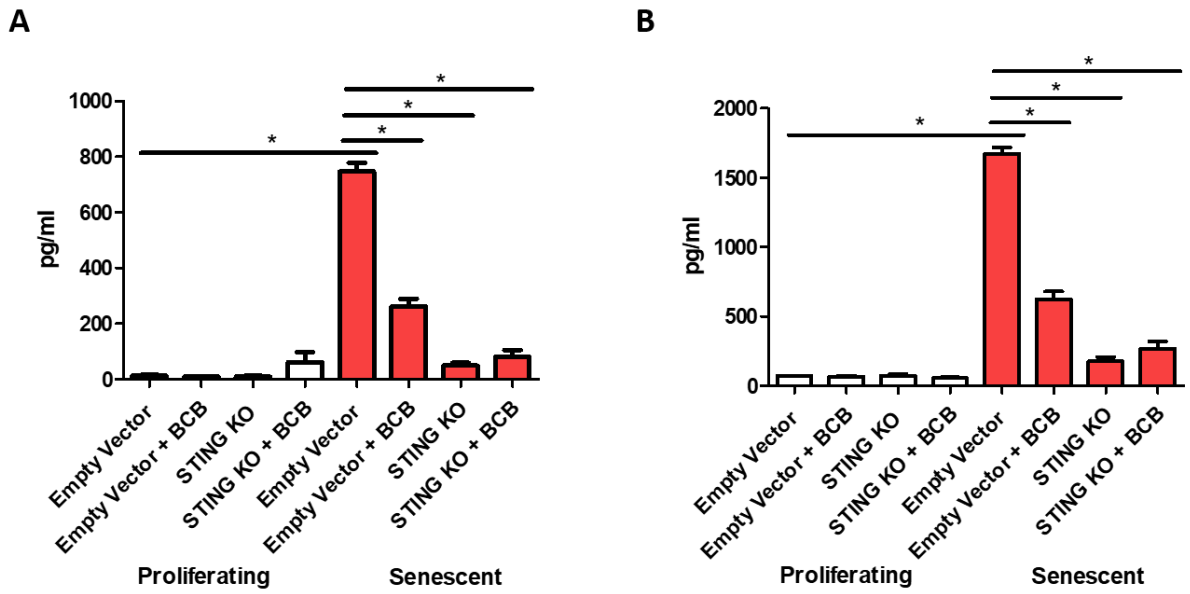

Figure 5.6 – Treatment with BCB does not further decrease the SASP in STING KO fibroblasts.

Bar graph depicts the levels of IL-6 **(A)** and IL-8 **(B)** secreted into the media by proliferating and senescent Empty Vector and the STING deficient cell lines which have been treated with either DMSO (control) or BCB (2.5µM) 10 days post-X-ray irradiation, n=6 independent experiments. Bar graph data is shown as mean, error bars represent the standard error of the mean, statistical significance was determined using a one-way ANOVA.

5.3. Pharmacological inhibition of cGAS using RU.521 inhibits the SASP but does not rescue the cell cycle arrest.

Following our confirmation that cells lacking STING no longer exhibited a SASP we wanted to understand whether a recently identified small molecule (RU.521) which targets cGAS also impacted on the SASP. RU.521 was recently demonstrated to bind to the active site of cGAS where it could effectively block cGAS-STING activation following exposure to dsDNA (Vincent *et al.*, 2017). In the context of senescence, we therefore wanted to test whether RU.521 could effectively prevent the inflammatory response that occurs in response to cytosolic mtDNA and nuclear DNA. As expected the development of senescence promoted an increase in the secretion of IL-6, IL-8 and IP-10 ($p<0.0001$ for IL-6 and IL-8, $p<0.05$ for IP-10). Following the treatment of senescent cells with RU.521, there was a non-significant decrease in the secretion of IL-6, IL-8 and IP-10 with the 1µM concentration. However, Treatment with 2.5µM promoted a significant decrease in the secretion of each of the cytokines compared to the untreated senescent cells ($p<0.0001$ for IL-6 and IL-8, $p<0.001$ for IP-10). Higher concentration (5uM) did not further decrease the SASP, suggesting that 2.5 is the optimal concentration (Figures 5.7A, B and C). It should be noted that we still need to verify if RU521 is acting on this pathway during senescence, by measuring for instance IRF3 phosphorylation or by using STING KO cells.

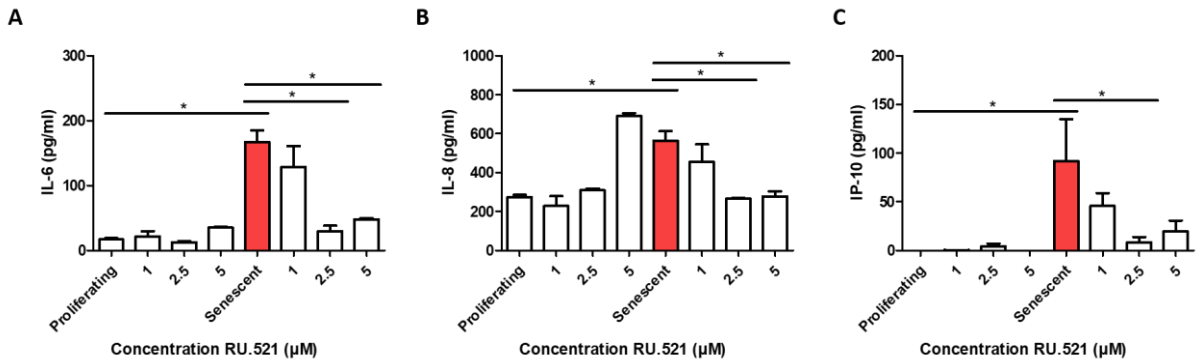

Figure 5.7 – The small molecule cGAS inhibitor RU.521 suppresses the SASP.

Proliferating and stress-induced senescent cells (20Gy irradiation) were maintained with RU.521 or a DMSO control for 10 days following the induction of senescence. The SASP was then assessed by ELISA. **(A, B and C)** Bar graph depicts the levels of IL-6 **(A)**, IL-8 **(B)** and IP-10 **(C)** secreted into the media by proliferating and senescent cells, n=4 independent experiments. *This experiment was performed in collaboration with MRes student Sophia Quigley*. Bar graph data is shown as mean, error bars represent the standard error of the mean, statistical significance was determined using a one-way ANOVA.

In addition to the SASP we wanted to characterise further the effects of RU.521 on the development of the senescence phenotype. First SA-β-Gal was measured (Figures 5.8A and B). I found that following the induction of senescence there was an increase in the percentage of SA-β-Gal positive cells ($p<0.0001$), however, senescent cells treated with RU.521 displayed a trend towards a reduction in the number of SA-β-Gal positive cells (however, not statistically significant). In the proliferating cells, RU.521 also promoted an increase in the number of positive SA-β-Gal cells, however this was non-significant (Figure 5.8B). Next, the marker of proliferation Ki67 was assessed (Figure 5.8C and D). We found that for proliferating cells there was no difference when treated with RU.521 compared to the DMSO control with approximately 50% of control cells being positive and 40% of RU.521 treated cells being positive for Ki67. In the senescent cells there was a significant decrease in the expression of Ki67 compared to their proliferating counterparts with only 2% of cells positive for Ki67 ($p<0.0001$). Similarly, senescent cells treated with RU.521 had no rescue in the loss of proliferation as they also displayed a very low level of Ki67 positive cells (4%).

The effect of RU.521 on the cyclin-dependent kinase inhibitor p21 was also measured. In proliferating cells treated with RU.521 there was no difference between those treated with DMSO alone. Following the development of senescence there was a significant increase in the number of p21 positive cells with 90% of cells being positive ($p<0.0001$). Following the treatment of senescent cells with RU.521 there was a small decrease in the number of p21 positive cells with 78% being positive, however this decrease is not significant (Figure 5.8E)

The marker γH2AX is a reliable marker of the DDR associated with senescence. We found that treatment of proliferating cells with RU.521 did not impact on the mean number of γH2AX foci per cell (approximately 1 per cell). Following the development of senescence there was a significant increase in the mean number of γH2AX foci per cell (2.7 per cell, $p<0.0001$). Culture of senescent cells with RU.521 lead to a small decrease in the mean number of γH2AX (2.1 per cell), however this was not significant (Figure 5.8F).

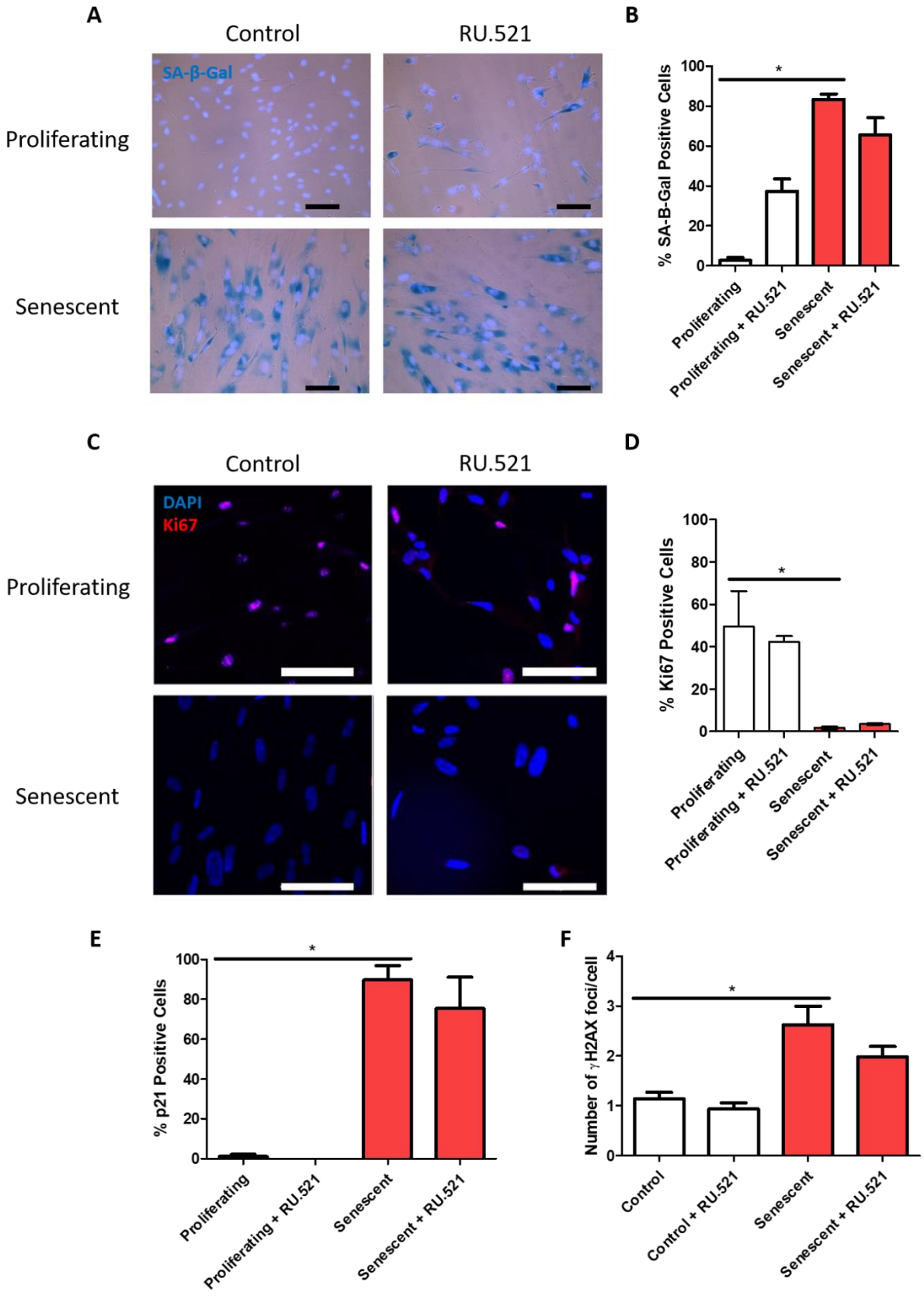

Figure 5.8 – RU.521 does not prevent the cell cycle arrest features of cellular senescence.

Proliferating and stress-induced senescent cells (20Gy irradiation) were maintained with RU.521 (2.5μM) or a DMSO control for 10 days following the induction of senescence. Markers of senescence were then assessed. **(A)** Representative images of SA-β-Gal staining in proliferating and senescent cells treated with RU.521 or a DMSO control, images acquired using bright field microscopy and a 40x objective. **(B)** Bar graph represents the quantification of the percentage of SA-β-Gal positive cells for proliferating (white bars) and senescent cells (red bars) treated with RU.521 or a DMSO control. **(C)** Representative immunofluorescent images of Ki67 and DAPI staining in proliferating and senescent cells treated with RU.521 or a DMSO control, images acquired using bright field microscopy and a 40x objective. **(D)** Bar graph represents the quantification of the percentage of Ki67 positive cells for proliferating (white bars) and senescent cells (red bars) treated with RU.521 or a DMSO control. **(E)** Bar graph represents the quantification of the percentage of p21 positive cells for proliferating (white bars) and senescent cells (red bars) treated with RU.521 or a DMSO control. **(F)** Bar graph represents the quantification of the mean number of γH2AX foci per cell for proliferating (white bars) and senescent cells (red bars) treated with RU.521 or a DMSO control. *These experiments were performed in collaboration with MRes student Sophia Quigley*. Bar graph data is shown as mean, error bars represent the standard error of the mean, n=4 independent experiments. Statistical significance was determined using a one-way ANOVA.

5.4. Pharmacological inhibition of cGAS using anti-malarial drugs inhibits the SASP but does not rescue the cell cycle arrest.

Prior to the development of RU.521 the only other compounds identified which had inhibitory activity against cGAS were a group of anti-malarial drugs. It was discovered that this family of drugs could interfere with the interaction of cGAS and double stranded DNA. Specifically, quinacrine dihydrochloride and 9-amino-6-chloro-2-methoxyacridine (ACMA) were demonstrated to have a good inhibitory efficiency and prevented IFN-β expression in response to double stranded DNA (An *et al.*, 2015). Furthermore, these drugs are already used in the clinic and from a safety perspective they are well tolerated. Therefore, it was of interest to understand whether the findings of cGAS inhibition using RU.521 could be achieved using the anti-malarial drugs quinacrine dihydrochloride and ACMA.

First the two compounds were assessed for their capacity to inhibit the SASP in MRC5 human fibroblasts. Quinacrine dihydrochloride was assessed at 1-10μM. Proliferating cells display low levels of secreted IL-6, IL-8 and IP-10, as such, treatment with quinacrine dihydrochloride at each of the concentrations did not have an effect on proliferating cells. Following the development of stress-induced senescence there was a statistical increase in each of the cytokines for the control senescent cells; IL-6, IL-8 and IP-10 (<0.0001 for each) (Figures 5.9A-C). Treatment of senescent cells with quinacrine dihydrochloride at 1μM had no effect on the level of IL-6, IL-8 and IP-10 secreted by senescent cells. Treatment with Quinacrine dihydrochloride at 5μM provoked a significant decrease in the secretion of IL-6, IL-8 and IP-10 (<0.01 for IL-6 and <0.001 for IL-8 and IP-10). Treatment with quinacrine dihydrochloride at 10μM had the most pronounced effect on reducing the SASP. There was a significant reduction in the secretion of IL-6, IL-8 and IP-10 (<0.001 for IL-6 and <0.0001 for IL-8 and IP-10 (Figures 5.9A, B and C).

ACMA was assessed at 1μM. Proliferating cells display low levels of secreted IL-6, IL-8 and IP-10, as such, treatment with ACMA did not have an effect on proliferating cells. Following the development of stress-induced senescence there was a statistical increase in each of the cytokines for the control senescent cells; IL-6, IL-8 and IP-10 (<0.0001 for each). Treatment with ACMA at 1μM provoked a significant decrease in the secretion of IL-6, IL-8 and IP-10 <0.001 for IL-6, IL-8 and IP-10, Figures 5.9 D, E and F).

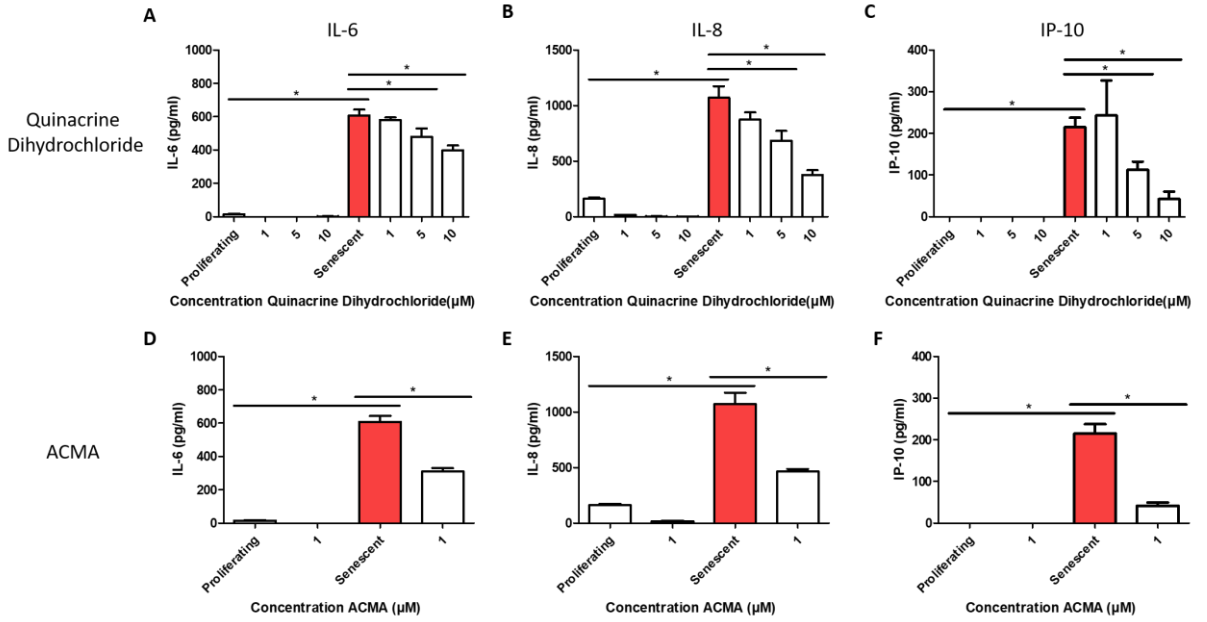

Figure 5.9 – The anti-malarial drugs quinacrine dihydrochloride and ACMA suppress the SASP.

Proliferating and stress-induced senescent cells (20Gy irradiation) were maintained with quinacrine dihydrochloride (1-10μM), ACMA (1μM) or a DMSO control for 10 days following the induction of senescence. The SASP was then assessed by ELISA. **(A, B and C)** Bar graph depicts the levels of IL-6 **(A)**, IL-8 **(B)** and IP-10 **(C)** secreted into the media by proliferating and senescent cells treated with either a DMSO control or quinacrine dihydrochloride 1-10μM, n=4 independent experiments. **(D, E and F)** Bar graph depicts the levels of IL-6 **(D)**, IL-8 **(E)** and IP-10 **(F)** secreted into the media by proliferating and senescent cells treated with either a DMSO control or ACMA 1μM, n=4 independent experiments. *These experiments were performed in collaboration with the undergraduate student Tom Kidder*. Bar graph data is shown as mean, error bars represent the standard error of the mean, statistical significance was determined using a one-way ANOVA.

Next, other markers of senescence and the cell cycle arrest were measured following treatment with quinacrine dihydrochloride. First, SA-β-Gal was measured. Treatment of proliferating cells with quinacrine dihydrochloride provoked a small non-significant increase in the number of SA-β-Gal positive cells. Following the induction of senescence there was a significant increase in the number of positive cells ($p<0.0001$). Treatment of senescent cells with quinacrine dihydrochloride lead to a small decrease in the number of positive cells, however this was not significant (Figure 5.10A).

Next, γH2AX was measured. Treatment of proliferating cells with quinacrine dihydrochloride did not have an impact on the mean number of γH2AX per cell. Senescent cells displayed a 3.5 fold increase in the number of foci ($p<0.001$), interestingly, senescent cells treated with quinacrine dihydrochloride had a significant decrease in the mean number of γH2AX foci (from 3.5 to 2.2 foci per cell, Figure 5.10B).

In addition the markers of the cell cycle Ki67 and p21 were measured. Ki67 was present in approximately 40% of proliferating cells, treatment of proliferating cells with quinacrine dihydrochloride had no effect on the number of Ki67 positive cells. Following the induction of senescence there was a decrease to only 1% of cells being positive for Ki67 ($p<0.001$). Similarly treatment of senescent cells with quinacrine dihydrochloride did not increase the number of Ki67 positive cells compared to senescent control cells (Figure 5.10C). For p21, there was no difference in the level of p21 cells in proliferating control and quinacrine dihydrochloride treated cells. In senescent cells, there was an increase to 97% of cells being positive for p21 ($p<0.0001$). Treatment of senescent cells with quinacrine dihydrochloride did not reduce the number of p21 positive cells compared to senescent control cells (Figure 5.10D).

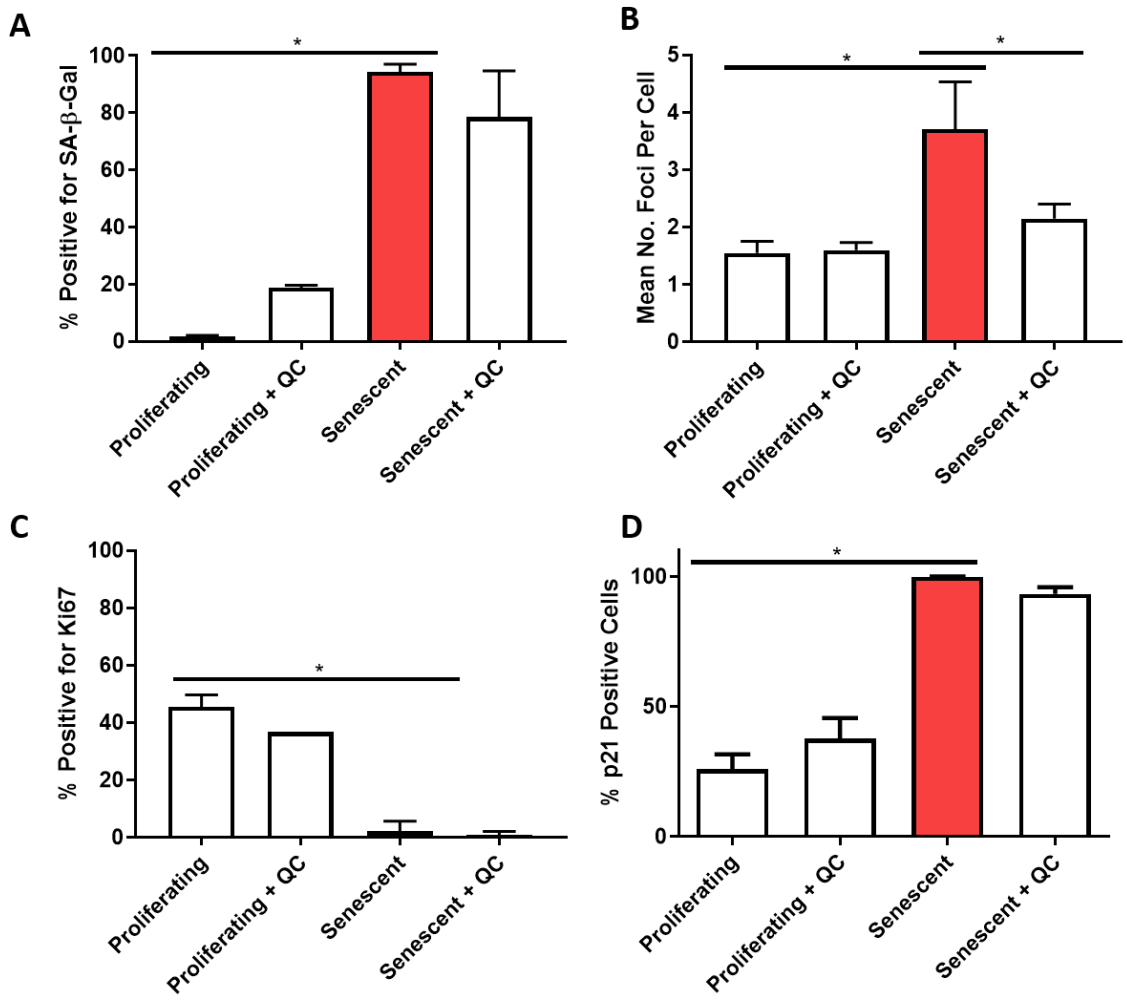

Figure 5.10 – The anti-malarial drug quinacrine dihydrochloride does not rescue the cell cycle arrest.

Proliferating and stress-induced senescent cells (20Gy irradiation) were maintained with quinacrine dihydrochloride (5μM) or a DMSO control for 10 days following the induction of senescence. Markers of senescence were then assessed. **(A)** Bar graph represents the quantification of the percentage of SA-β-Gal positive cells for proliferating (white bars) and senescent cells (red bars) treated with quinacrine dihydrochloride or a DMSO control. **(B)** Bar graph represents the quantification of the mean number of γH2AX foci per cell for proliferating (white bars) and senescent cells (red bars) treated with quinacrine dihydrochloride or a DMSO control. **(C)** Bar graph represents the quantification of the percentage of Ki67 positive cells for proliferating (white bars) and senescent cells (red bars) treated with quinacrine dihydrochloride or a DMSO control. **(D)** Bar graph represents the quantification of the percentage of p21 positive cells for proliferating (white bars) and senescent cells (red bars) treated with quinacrine dihydrochloride or a DMSO control. *These experiments were performed in collaboration with undergraduate student Tom Kidder*. Bar graph data is shown as mean, error bars represent the standard error of the mean, n=4 independent experiments. Statistical significance was determined using a one-way ANOVA.

The anti-malarial drug ACMA was also assessed for its effect on the cell cycle arrest features of the senescence phenotype. First, SA-β-Gal was assessed as a robust marker of senescence. Following the development of senescence there was a significant increase in the percentage of cells positive for SA-β-Gal from 1% of proliferating cells positive to 92% of senescent cells being positive ($p<0.0001$). Following the maintenance of senescent cells with ACMA there was a significant decrease in the number of positive cells to 28% ($p<0.05$, Figure 5.11A).

Second, the number of γH2AX foci per cell were measured to assess the effect of ACMA on DNA damage. Following the development of senescence the mean number of γH2AX foci increases from an average of 1.6 foci per cell to 3.6 foci per cell ($p<0.001$). Treatment of senescent cells with ACAM produced a very small decrease in the mean number of γH2AX foci, however this was not significant (Figure 5.11B).

To understand whether ACMA affects the cell cycle arrest, the proliferation marker Ki67 was assessed. It was present in 44% of the proliferating cells, this reduced to 1% of cells being positive in senescent cells ($p<0.0001$). Treatment of senescent cells with ACMA did not promote an increase in the number of Ki67 positive cells in comparison to untreated senescent cells (Figure 5.11C).

Finally, the cyclin dependent kinase inhibitor p21 was measured. The development of senescence caused a significant increase in the number of p21 positive cells from 22% of proliferating cells to 98% in senescent cells ($p<0.0001$). Senescent cells cultured with ACMA displayed a small decrease in the number of p21 positive cells to 83%, however, this was not significant (Figure 5.11D).

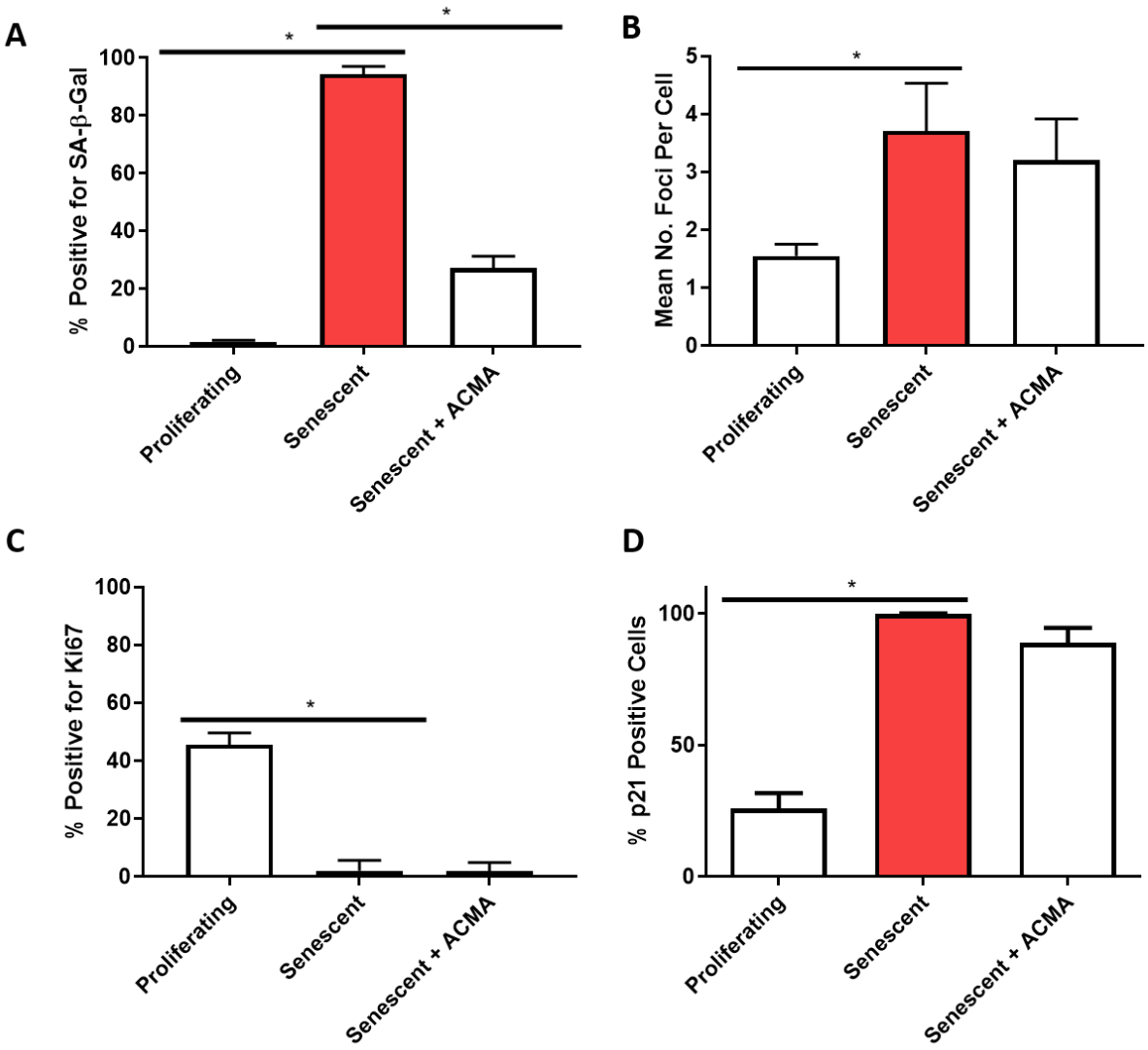

Figure 5.11 – The anti-malarial drug ACMA does not rescue the cell cycle arrest.

Proliferating and stress-induced senescent cells (20Gy irradiation) were maintained with ACMA (1μM) or a DMSO control for 10 days following the induction of senescence. Markers of senescence were then assessed. **(A)** Bar graph represents the quantification of the percentage of SA-β-Gal positive cells for proliferating (white bars) and senescent cells (red bars) treated with ACMA or a DMSO control. **(B)** Bar graph represents the quantification of the mean number of γH2AX foci per cell for proliferating (white bars) and senescent cells (red bars) treated with ACMA or a DMSO control. **(C)** Bar graph represents the quantification of the percentage of Ki67 positive cells for proliferating (white bars) and senescent cells (red bars) treated with ACMA or a DMSO control. **(D)** Bar graph represents the quantification of the percentage of p21 positive cells for proliferating (white bars) and senescent cells (red bars) treated with ACMA or a DMSO control. *These experiments were performed in collaboration with undergraduate student Tom Kidder*. Bar graph data is shown as mean, error bars represent the standard error of the mean, n=4 independent experiments. Statistical significance was determined using a one-way ANOVA.

Earlier in this study the pro-inflammatory response was reduced in STING^{CRISPR} cells following the transfection of mtDNA, however, it was not completely reduced. Therefore it was postulated that other pathways may be involved in the response to mtDNA in senescent cells.

Therefore, I assessed the NLRP3 inflammasome, which has been previously implicated in OIS and recognised as having the capacity to mount an inflammatory response to mtDNA (Nakahira *et al.*, 2011; Acosta *et al.*, 2013). First, the total protein level of the NLRP3 inflammasome was measured by western blot, interestingly, there appeared to be a slight decrease in senescent cells however this was not statistically different (Figure 5.12A and B). It is possible that the NLRP3 inflammasome is active and this is not associated with overall changes in protein level. Its activation is associated with cleavage of caspase 1, therefore the levels of cleaved caspase-1 were assessed. Analysis of the total protein levels of caspase 1 measured by pro-caspase 1 revealed that there was a significant 3-fold increase in the levels found in senescent cells ($p=0.0216$) (Figure 5.12C and D). Indeed, there was also a 3-fold increase in the levels of cleaved-caspase 1 in senescent cells when compared to proliferating cells ($p=0.0012$) (Figure 5.12C and E). The cleavage of caspase 1 promotes an inflammatory response by promoting the maturation of IL-1β through cleavage to cleaved IL-1β, which then leads to secretion of IL-1β and IL-18 (Jo *et al.*, 2016). Interestingly, despite cleaved-caspase 1 being present there was no detectable cleavage of IL-1β in senescent MRC5 fibroblasts (Figure 3.18F). Furthermore, as inflammasome activation is associated with secretion of IL-18, I measured the levels of secreted IL-18 in proliferating and senescent cells. The levels of IL-18 were very low, bordering on the detectable limit with no differences between proliferating and senescent cells (Figure 5.12G).

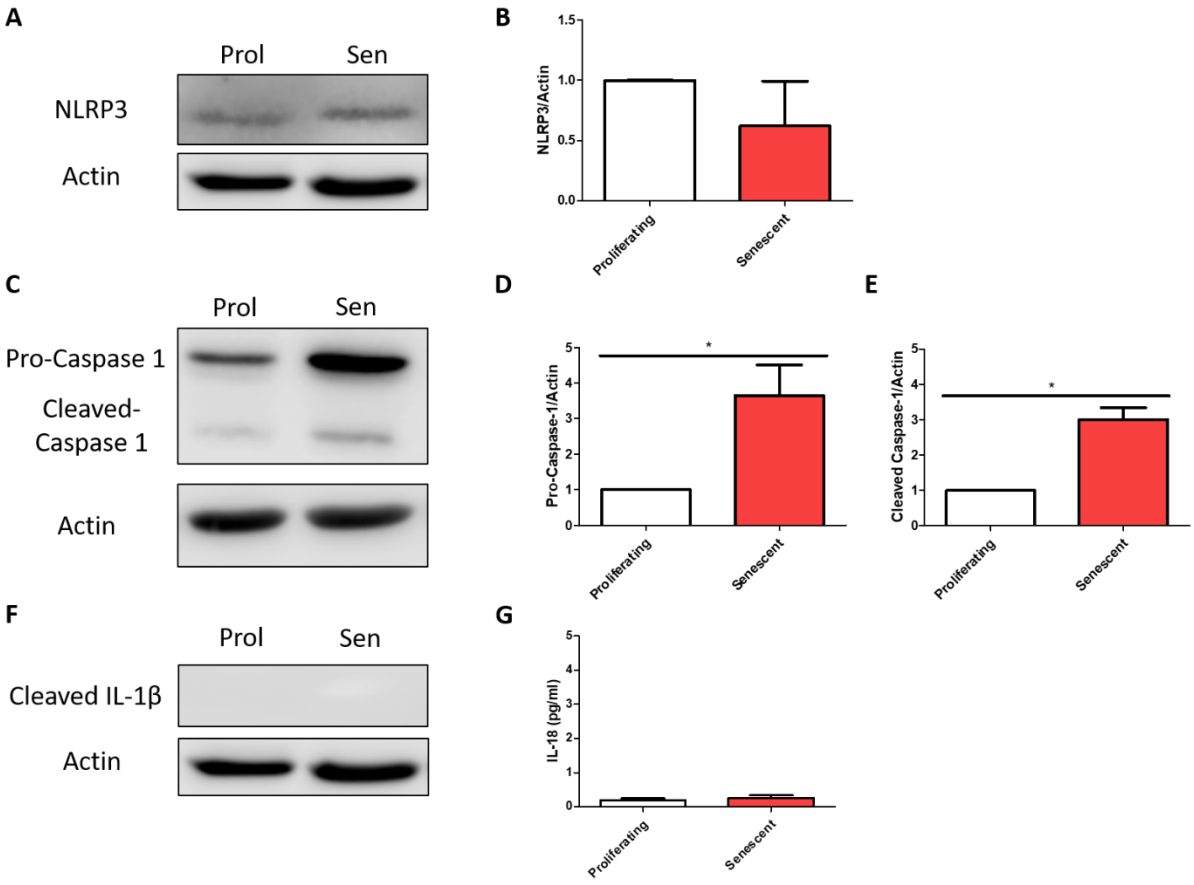

Figure 5.12 – Characterisation of the NLRP3 inflammasome in senescence.

MRC5 fibroblasts were analysed 10 days post induction of stress induced senescence (20Gy, irradiation). **(A)** Representative western blot of total level of NLRP3 in proliferating and senescent fibroblasts. **(B)** Bar graph depicting the protein level of NLRP3 normalised to β-actin in proliferating (white bar) and senescent cells (red bar), n=4 independent experiments. **(C)** Representative western blot of pro-caspase 1 and cleaved-caspase 1 in proliferating and senescent fibroblasts. **(D)** Bar graph depicting the protein level of pro-caspase 1 normalised to β-actin in proliferating (white bar) and senescent cells (red bar), n=4 independent experiments. **(E)** Bar graph depicting the protein level of pro-caspase 1 normalised to β-actin in proliferating (white bar) and senescent cells (red bar), n=4 independent experiments. **(F)** Representative western blot of cleaved –IL-1β in proliferating (white bar) and senescent cells (red bar), n=4 independent experiments. **(G)** Bar graph depicts the levels of IL-18 (pg/ml) secreted by proliferating (white bar) and senescent cells (red bar) as measured by cytokine array, n=6 independent experiments. Bar graph data is shown as mean, error bars represent the standard error of the mean, statistical significance was determined using a two-tailed unpaired t-test.

It has been reported that TLR9 can provoke a pro-inflammatory response to unmethylated double stranded DNA CpG motifs which are found within the genome of bacteria and viruses, as well as DNA that arises following cellular damage (Mouchess *et al.*, 2011). In addition, it has been identified that TLR9 can induce an inflammatory response to mtDNA through p38 MAPK and NF-κB (Bao *et al.*, 2016). Therefore we hypothesised that if TLR9 was responsible for the inflammatory response to mtDNA its expression would be upregulated in senescent cells. We measured the total protein level of TLR9 by Western Blot and found that senescent cells displayed a non-significant 1.4-fold increase in the expression of TLR9 (Figures 5.12A and B).

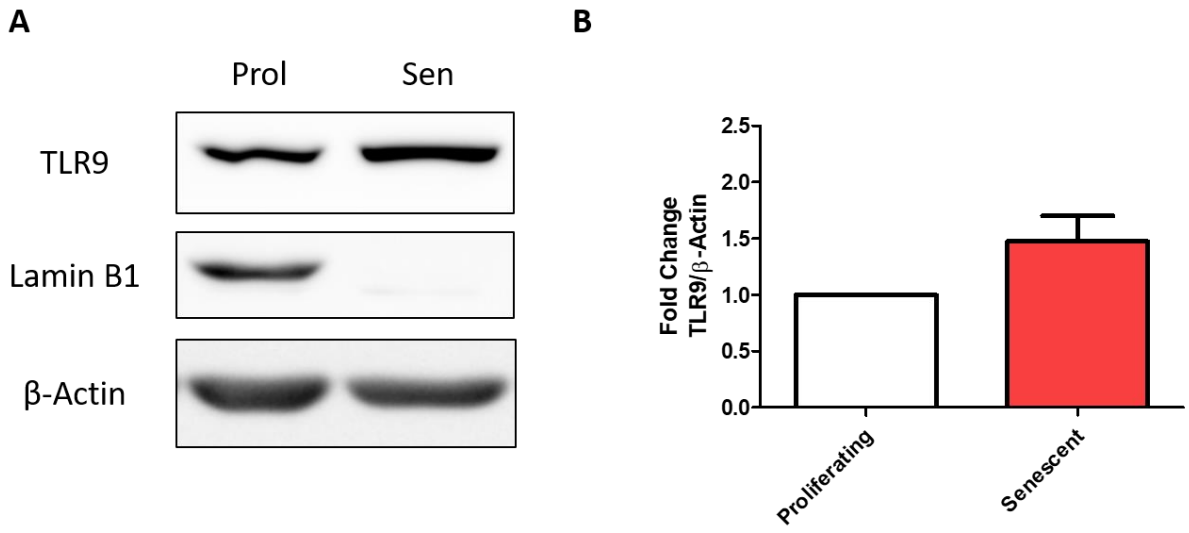

Figure 5.13 - The expression of TLR9 is unchanged in senescent cells.

MRC5 fibroblasts were analysed 10 days post induction of stress induced senescence (20Gy, irradiation). **(A)** Representative western blot of total level of TLR9 in proliferating and senescent fibroblasts. **(B)** Bar graph depicting the protein level of TLR9 normalised to β-actin in proliferating (white bar) and senescent cells (red bar), n=3 independent experiments. Bar graph data is shown as mean, error bars represent the standard error of the mean, statistical significance was determined using a two-tailed unpaired t-test.

5.5. Discussion

Earlier in this study it has been demonstrated that mtDNA is present in the cytosol of senescent cells. Whilst here it becomes available to the innate immune system to launch a pro-inflammatory response. In this part of the study we aimed to understand mechanistically how mtDNA mediates this response and whether pharmacological interventions can prevent the SASP. Specifically, our data indicates that the pro-inflammatory response which transpires in response to mtDNA ensues as a consequence of recognition by the DNA sensor cGAS. Furthermore, we show that pharmacological inhibitors of cGAS can alleviate the SASP without removing the cell cycle arrest aspect of senescence.

I investigated the potential of the NLRP3 inflammasome as a candidate for the mtDNA-associated SASP observed during senescence. It has previously been reported that the NLRP3 inflammasome is active and contributes to the SASP in OIS and senescent endothelial vascular cells (Acosta *et al.*, 2013; Yin *et al.*, 2017; Wiggins *et al.*, 2019). First, we assessed the total level of NLRP3 and found this to be unchanged between proliferating and senescent cells. However, it is possible that NLRP3 could be active with no observable change in overall protein levels. In order to further characterise the NLRP3 inflammasome, the cleavage of caspase 1 was assessed. It is known that during activation caspase 1 undergoes autocatalytic activation to cleaved caspase 1. The role of cleaved caspase 1 is then to cleave pro-IL-1β to the mature form IL-1β, which promotes its secretion and that of IL-18 (Jo *et al.*, 2016). We found that senescent cells had enhanced levels of cleaved caspase 1, however this was not associated with cleavage of IL-1β or secretion of IL-18 which both occur downstream of NLRP3 inflammasome activation. However, at this stage it is unclear what role cleaved caspase 1 is undertaking during senescence and therefore warrants further investigation. Although, in the previous chapter I found that inhibition of caspase 1 had no effect on the secretion of IL-6 or IL-8. Furthermore, cleaved IL-1β is a feature of other models of senescence such as OIS (Acosta *et al.*, 2013). Therefore it is plausible that the inflammasome not being active may be a phenomenon that is unique to MRC5 human fibroblasts, as such further investigation is required. Together, these data suggest that the NLRP3 inflammasome is not active in stress-induced senescence of MRC5 fibroblasts. However, at this stage these findings should be considered preliminary as further work is still required to confirm this notion. Therefore, it is important to assess whether the genetic removal or knockdown of NLRP3 has an effect on SASP regulation. Similarly, it would be interesting to observe whether NLRP3 deficient cells display an altered inflammatory response to the transfection of mtDNA in MRC5 human fibroblasts and other cell lines.

Next we assessed the potential of TLR9 as being an inducer of the SASP in response to cytosolic mtDNA. It has been reported that TLR9 can recognise mtDNA and stimulate the upregulation of IFN1 genes (Uematsu and Akira, 2007; Bao *et al.*, 2016). It was found that senescent cells displayed a small non-significant increase in the total protein level of TLR9. Although interesting, this finding does not allow us to determine whether TLR9 is being activated during senescence. Furthermore, it is known that TLR9 activation culminates in signalling to NF-κB, which is activated by a number of other stimuli during senescence (Uematsu and Akira, 2007; Chien *et al.*, 2011; Kang *et al.*, 2015; Wiley *et al.*, 2016). As such, it is challenging to dissect the role of TLR9 in senescence. Furthermore, a recent study investigating the role of TLRs in senescence found that during OIS there was no observable upregulation of the TLR9 gene (Hari *et al.*, 2018). As such, the data in this study on TLR9 is not sufficient to draw any conclusions regarding its role in regulating the SASP in response to mtDNA. Therefore, to further clarify this relationship future work should examine whether the genetic removal or pharmacological inhibition of TLR9 in senescent cells has an effect on the SASP. In addition, it would be of interest to genetically or pharmacologically modulate BAX/BAK pores to prevent mtDNA release and assess whether this has an effect on the protein level of TLR9. Similarly, it would be useful to generate cells deficient for both STING and TLR9 and assess whether this leads to a further decrease in the SASP. Together, these experiments would give us a clearer idea of the role of TLR9 during senescence.

In addition, to characterising the NLRP3 inflammasome and TLR9 we assessed the cGAS-STING axis. It has been published previously that cGAS can recognise mtDNA and mount an inflammatory response through NF-κB and IFN1 genes (West *et al.*, 2015). We observed that senescent cells expressing cGAS-GFP reporter system displayed co-localisation with cytosolic TFAM. This complements findings by *West et al*, who demonstrated that cGAS colocalises with mtDNA (West *et al.*, 2015). In addition, we demonstrated that downstream of cGAS-STING activation senescent cells display an increased level of phosphorylated IRF-3, this phosphorylation is diminished in senescent cells which have had mtDNA release blocked using BCB. To further address the importance of the cGAS-STING axis signalling in response to cytosolic mtDNA we generated STING deficient cells and transfected mtDNA into them. We found that STING deficient cells had a significantly diminished secretion of IL-6 and IL-8 following transfection of mtDNA compared to their STING proficient counterparts. Finally, we observed that in the absence of STING senescent cells had a dramatically reduced SASP. These findings corroborate previous studies which have demonstrated that cGAS or STING deficient

fibroblasts, MEFs and mice have a reduced SASP response (Dou *et al.*, 2017; Gluck *et al.*, 2017; Yang *et al.*, 2017). Earlier in this study, I found that the mtDNA release and associated pro-inflammatory response was dependent on BAX and BAK pores, consistently, it was shown that the BAX inhibitor BCB could decrease the SASP. Therefore, I questioned whether treatment of STING deficient cells with BCB would have an additional effect at decreasing the SASP. I found that BCB had no further effect at reducing the SASP in STING deficient cells. This suggests that the mechanism by which BCB and STING lead to SASP reduction are potentially interlinked, which in this model of stress-induced senescence is BAX/BAK mediated mtDNA release and subsequent detection by the cGAS-STING axis leading to pro-inflammatory signalling. Collectively, these findings provide convincing evidence that the cGAS-STING axis is active during senescence in response to cytosolic mtDNA. However, there are some considerations which need to be taken into account.

First, senescent STING deficient cells displayed an almost complete reduction in the SASP, whereas when mtDNA was transfected into STING deficient cells there was approximately a 50% reduction in the secretion of IL-6 and IL-8. This suggests that during stress-induced senescence the SASP is predominantly being regulated by cGAS-STING, however, the transfection of mtDNA is likely activating another innate immune pathway and not solely cGAS-STING. It is likely that in our experiment of transfecting mtDNA, the level of DNA transfected is above physiological levels of mtDNA observed in the cytosol of senescent cells and may be activating the TLR9 or NLRP3 pathway alongside the cGAS-STING axis. To further dissect the pathways active it would be interesting experimentally to transfect mtDNA into cells that are deficient for both STING and TLR9 or NLRP3 and examine the resulting inflammatory response. Another point of consideration is that a recent study demonstrated that genetic manipulation of a gene can trigger compensatory upregulation of related genes to allow the cell to continue to function adequately (Rossi *et al.*, 2015). In this context, it is conceivable that STING deficient cells could upregulate TLR9 and NLRP3 DNA sensing mechanisms. Conversely, as cGAS (which is responsible for DNA sensing) is still functional in these cells and it is the signalling network that is impaired by STING knockout, it is unlikely that this is the case. However, it would still be interesting to assess the activity of TLR9 and NLRP3 activity in this setting.

Interestingly, the amount of IL-6 and IL-8 produced by senescent cells and proliferating cells transfected with mtDNA is comparable. It is important to consider that work in the field has pinpointed the role of nuclear derived CCFs being recognised by cGAS-STING during

senescence (Dou *et al.*, 2017; Gluck *et al.*, 2017). This indicates that as both CCFs and mtDNA are contributing to the SASP it is likely that the notion of transfecting more mtDNA into the cells than is observed physiologically in senescent cells is applicable. Conversely, earlier in our study BAX and BAK deficient cells displayed an almost complete ablation of the SASP, suggesting that mtDNA is the key determinant of the SASP rather than a dual contribution from CCFs. In further support of this notion, the percentage of cells positive for CCFs is relatively low in our model of stress-induced senescence (13.5%), whereas in published studies where CCFs have been implicated as drivers of the SASP the percentage of cells is much higher (approximately 30% in MEFs, 40% in IMR90s and 60% in BJs) (Dou *et al.*, 2017). Moreover, the studies investigating CCFs have been predominantly performed in OIS or senescence induced by genotoxic agents such as palbociclib or etoposide (Dou *et al.*, 2017; Gluck *et al.*, 2017). We also found that senescent BAX and BAK deficient cells with a significantly decreased SASP displayed the same percentage of cells containing CCFs as senescent Empty Vector control cells. To put our data into context these findings support the idea that in our model of stress-induced senescent cells mtDNA plays a more significant role in driving the SASP than CCFs. However, further investigation is still required to clarify this relationship as it is likely CCFs are more important in the SASP regulation of other cell types such as IMR90s where they are observed at a higher frequency.

Following these observations we were interested in investigating the origin of CCFs more closely. The formation of CCFs has been associated with the loss of Lamin B1, a protein responsible for maintaining nuclear integrity (Ivanov *et al.*, 2013; Dou *et al.*, 2017; Gluck *et al.*, 2017). Following the induction of stress-induced senescence we observed a complete loss of Lamin B1, furthermore, in cells expressing cGAS-GFP we saw clear co-localisation of cGAS with CCFs. This complements published findings where live-cell imaging demonstrates that CCFs "bud off" from the nucleus due to the loss of Lamin B1 and subsequently being detected by cGAS (Dou *et al.*, 2017; Gluck *et al.*, 2017).

In our study, I observed that the percentage of MRC5 human fibroblasts harbouring CCFs was relatively low, I therefore speculated that some CCFs may in fact be of mitochondrial origin as earlier work in this study has implicated mtDNA as an important regulator of the SASP. Classically, CCFs have been identified by labelling with DAPI, γH2AX and Histone H3 (generally considered to be specific to nuclear DNA). Often just DAPI and γH2AX are used to identify CCFs. It is known that DAPI labels all double stranded DNA, therefore it is possible that some CCFs may not be nuclear DNA but in fact be misidentified as mtDNA (Dou *et al.*,

2017; Gluck *et al.*, 2017). Therefore we assessed cGAS co-localization with TFAM and DAPI signals in the cytoplasm of senescent cells. We found that 50% of cGAS positive cytosolic DNA fragments were positive for both TFAM and DAPI. This suggests that 50% of these cytosolic DNA fragments CCFs are potentially of mitochondrial origin rather than the nucleus. Furthermore, when we analysed senescent BAX/BAK deficient cells which do not release mtDNA to the cytoplasm we did not see any differences in the percentage of cells harbouring CCFs, however the mean number of CCFs per cell was reduced by 43% (though non-significant). This fits with our earlier observation of 50% of cytosolic nuclear DNA being TFAM positive and potentially of mitochondrial origin as these would no longer be released in BAX/BAK deficient cells, and therefore we would expect to see a reduction in the mean number of CCFs per cell. An important consideration is that the TFAM antibody used could potentially inadvertently bind to double stranded nuclear DNA fragments found in the cytoplasm. Another key limitation, is that the size of the cytoplasmic DNA fragments has not been taken into account. It is likely that as mtDNA is only 16,569 base pairs it would appear particularly small as a punctate DNA foci (as seen in earlier staining's in this study). Therefore, it would be interesting to characterise whether DNA which has been labelled positively for DAPI, DNA, TFAM and cGAS is largely restricted to smaller fragments of DNA rather than larger ones which are feasibly more likely to have budded from the nucleus. Similarly, as the cells in this analysis were not labelled for a mitochondrial marker, it cannot be ruled out that DNA which is positively labelled for DAPI, DNA, TFAM and cGAS is not still within the mitochondria. Therefore, hypothetically, cGAS could plausibly have access to the mtDNA labelled by TFAM if the mitochondria were damaged in some way. With this in mind, they would not be CCFs and skew the analysis that some CCFs are of mitochondrial origin. Therefore, a strategy to further dissect these findings would be to use ChIP-sequencing to determine the relative interactions between cGAS and nuclear/mtDNA. At this stage, these observations are relatively preliminary but they do highlight the plausibility that some cytosolic DNA may be mtDNA rather than nuclear DNA.

It has also been reported that DNA damage enhances the formation of CCFs/cytosolic nuclear DNA (Lan *et al.*, 2014; Hartlova *et al.*, 2015). Characteristically, these CCFs are generally always positive for the DNA damage marker γH2AX (Dou *et al.*, 2017; Gluck *et al.*, 2017; Yang *et al.*, 2017). With that in mind, although technically demanding to investigate, it would be important to understand whether cytosolic mtDNA is also associated with DNA damage. Following on from this it would be interesting to explore whether stress-induced senescence

promotes damaged mitochondria and whether the level of damage correlates with mtDNA release.

We observed that fibroblasts deficient for STING had a completely reduced SASP when induced to become senescent, complementing the findings of others who have genetically manipulated this pathway (Dou *et al.*, 2017; Gluck *et al.*, 2017). It is known that the activation of STING mediates the upregulation of NF-κB and interferon genes through TBK1 and IRF3 (Chen *et al.*, 2016). NF-κB is considered a master regulator of the SASP and it has been demonstrated that a number of senescence related pathways feed into NF-κB signalling, for example, the stabilisation of GATA4 and activity of p38MAPK mediated by the DDR have also been implicated with NF-κB activation (Chien *et al.*, 2011; Kang *et al.*, 2015; Wiley *et al.*, 2016). Furthermore, NF-κB is an integral part of the innate immune system and has a myriad of roles in regulating the response to infections (Hayden and Ghosh, 2008). Previous studies have demonstrated beneficial effects on both senescence and overall health span during ageing by targeting NF- κB signalling (Tilstra *et al.*, 2012; Correia-Melo *et al.*, 2019). However, we postulate that the inhibition of cGAS further upstream of NF- κB may be a more promising strategy as it has the potential to preserve NF- κB function in response to infections in healthy cells but prevent its SASP promoting effects in senescent cells. Thus, we wanted to address the question of whether pharmacological targeting of cGAS could suppress the SASP.

In the context of senescence, to our knowledge no study has assessed pharmacological inhibitors of cGAS. The first identified inhibitors are derivatives of anti-malarial drugs, therefore we set out to test quinacrine dihydrochloride and ACMA (An *et al.*, 2015). Following the discovery of these inhibitors a group of small molecule specific inhibitor of cGAS were developed, therefore we also tested one of these compounds; RU.521 (Vincent *et al.*, 2017). We found that in stress-induced senescent cells RU.521 (2.5μM) could robustly decrease the secretion of IL-6, IL-8 and IP-10 to comparable levels with proliferating cells. Similarly, both quinacrine dihydrochloride and ACMA led to a substantial suppression of IL-6, IL-8 and IP-10 secretion by senescent cells. Interestingly, the decrease was not as strong as that observed in senescent cells treated with RU.521 as the level of secretion for the three cytokines was higher than proliferating control cells. One possible explanation for this observation is that the small molecule RU.521 is believed to act as a non-competitive inhibitor and therefore acts very efficiently to completely prevent activation of cGAS (Vincent *et al.*, 2017). The anti-malarial drugs on the other hand act by preventing the interaction between cGAS and double stranded DNA, interestingly, the mechanism of action occurs due to non-specific interactions with

nucleic acids rather than direct association and interference of cGAS and its enzymatic activity (An *et al.*, 2015). As such, it is possible that the anti-malarial drugs to not bind to all of the available DNA substrate and therefore do not fully prevent the inflammatory response. Therefore it seems plausible to speculate that cGAS is inhibited to a greater extent by RU.521 than the two anti-malarial drugs which could explain why RU.521 is more effective at suppressing the SASP. Another possible explanation is that cGAS knockdown was recently demonstrated to lead to a reduction in caspase 5 protein levels. Caspase 5 was shown to be essential for the cleavage of IL-1α and subsequent interferon response during senescence (Wiggins *et al.*, 2019). As such, RU.521 could hypothetically be more efficacious than the anti-malarial drugs at diminishing the SASP as it is reducing IL-1α cleavage by reducing the expression of caspase 5 as well as blocking the detection of mtDNA.

Early work indicated that anti-malarial drugs structurally are similar to the active site of cGAS, however, it is now been demonstrated that their effects are predominantly attributed to their interference with double stranded DNA which occurs by binding of the drug to DNA. This binding prevents the DNA from acting as a ligand to cGAS (Kuznik *et al.*, 2011; An *et al.*, 2015). It has also been shown that this binding also inhibits interactions between DNA and TLRs, including TLR9 (Kuznik *et al.*, 2011). Anti-malarial drugs which inhibit both cGAS and TLRs do not exert as complete a reduction in the SASP as RU.521 and genetic depletion of STING, these findings therefore support the notion that the cGAS-STING axis is responsible for the inflammatory response to mtDNA in senescent cells rather than TLR9. Although, as discussed previously it is possible that the observed effect is ascribed to the anti-malarial drugs incompletely acting on the available double stranded DNA substrate itself rather than inhibiting the cGAS/TLRs directly.

In the literature the role of cGAS in senescence is conflicting. In the study by *Dou et al* it was demonstrated that both cGAS and STING deficient human fibroblasts induced to become senescent via stress or oncogene activation no longer displayed a SASP but still underwent the cell cycle arrest as measured by p16 expression. *In vivo*, they demonstrated that following the induction of senescence via irradiation STING KO mice displayed a diminished SASP but cells were still positive for p21 (Dou *et al.*, 2017). *Gluck et al* found that cGAS was an important regulator of the SASP, however they also demonstrated that cGAS is important for the cell cycle arrest. Under normal culturing conditions cGAS KO MEFs were more resistant to premature senescence compared to cGAS proficient MEFs, in addition they did not present upregulation of p16, SA-β-Gal and various senescence associated genes which were observed

in proficient MEFs following the induction of senescence. Furthermore, they demonstrated that following oxidative stress cGAS deficient WI-38 human fibroblasts cells displayed increased markers of proliferation and a reduced level of SA-β-Gal positive cells compared to cGAS competent controls. Moreover, following the establishment of stress-induced senescence the silencing of cGAS led to a reduction in the expression of p16. *In vivo* they found that cGAS and STING deficient mice did not display p16 whereas WT mice did following the induction of senescence via irradiation (Gluck *et al.*, 2017). Similarly, another study found that cGAS deficient MEFs and human cells were resistant to the induction of senescence by DNA damage (etoposide and irradiation) (Yang *et al.*, 2017). Of further interest it has been shown that in OIS the genetic removal of IFN1 downstream of cGAS leads to a bypass of the senescence phenotype, moreover, the reintroduction of IFN1 leads to the induction of senescence (Katlinskaya *et al.*, 2016). Therefore we were curious to investigate whether the inhibition of cGAS using either RU.521 or the anti-malarial drugs would have an impact on the development of stress-induced senescence in human MRC5 fibroblasts.

We found that following the induction of stress-induced senescence cells maintained in culture with RU.521 there was a significant increase in the number of cells positive for p21, SA-β-Gal and the mean number of γH2AX foci, there was also a complete loss of the proliferation marker Ki67. For each of these markers there was no significant difference between the control senescent cells and those treated with RU.521. Similarly, we found for the anti-malarial drugs that fibroblasts still underwent the cell cycle arrest following irradiation as evidenced by expression of p21 and loss of Ki67. Interestingly, senescent cells maintained with quinacrine dihydrochloride had a reduced level of DNA damage as measured by γH2AX. This is an unusual finding as it has been reported that quinacrine dihydrochloride can intercalate into DNA and inhibit DNA repair (Popanda and Thielmann, 1992). However, it has also been shown that quinacrine (of which quinacrine dihydrochloride is derived from) promotes antioxidant defences, furthermore, another antimalarial drug from the same family of drugs; chloroquine also has been shown to have antioxidant effects (Farombi *et al.*, 2003; Turnbull *et al.*, 2003). In this scenario, it may be that quinacrine dihydrochloride is boosting anti-oxidant defences and therefore is preventing some ROS mediated DNA damage which occurs during senescence. There is also some evidence that DNA damage could contribute to cGAS activation, a recent proteomic study discovered that following the induction of DNA damage cGAS is associated with a multi-subunit ribonuclear complex which contains the DNA repair proteins DNA-protein kinase (Morchikh *et al.*, 2017). It is possible that the reduced levels of DNA damage associated

with quinacrine dihydrochloride are responsible for a reduction in the activation of cGAS and as such reduced stimulation of NF-κB/IFN-1 genes. Of further consideration, it has also been shown that DNA damage is responsible for provoking the release of CCFs/micronuclei and self DNA from the nucleus which can trigger cGAS activation (Lan *et al.*, 2014; Hartlova *et al.*, 2015). It would be of interest to investigate whether maintaining cells with quinacrine dihydrochloride has an impact on the number of CCFs. It is possible that this decrease in DNA damage is contributing in part to a reduction in the SASP by reducing the number of CCFs.

Another interesting observation was that of senescent cells which were maintained with ACMA, these cells displayed a reduced number of SA-β-Gal positive cells. The expression of SA-β-Gal is associated with the increased expression of the lysosomal β-galactosidase protein (Lee *et al.*, 2006). It has also been shown that SA-β-Gal staining clusters at sites of autophagy vacuoles which utilise lysosomes to clear and recycle cellular debris (Gerland *et al.*, 2003). There is evidence that anti-malarial drugs inhibit autophagy, therefore, it could be that ACMA is reducing autophagic activity which is leading to a reduced amount of lysosomes and therefore less labelling of lysosomal β-galactosidase protein by SA-β-Gal staining (Golden *et al.*, 2015). In addition, it has been demonstrated that quinacrine dihydrochloride is also inhibitor of autophagy (Golden *et al.*, 2015). Furthermore, in senescent cells maintained with quinacrine dihydrochloride there is a small but non-significant decrease in the number of SA-β-Gal positive cells, although purely speculative, this could be because quinacrine dihydrochloride is inhibiting autophagy to a lower extent than ACMA. Taken together, it is plausible that a reduction in autophagy is responsible for the reduced number of SA-β-Gal positive cells in senescent cells cultured with ACMA.

Our findings complement the work by *Dou et al* as we demonstrated that inhibition of cGAS using either RU.521 or the antimalarial drugs depleted the SASP but did not impair the cell cycle arrest (Dou *et al.*, 2017). This is in contrast to the studies by *Gluck et al* and *Yang et al* which demonstrated that cGAS has a regulatory role in implementing the cell cycle arrest and the SASP (Gluck *et al.*, 2017; Yang *et al.*, 2017). A potential explanation of the differences observed could be attributed to the cell lines used, both our work and that of *Dou et al* was performed in human lung fibroblasts (IMR90 and MRC5 fibroblasts) whereas the work performed by *Gluck et al* and *Yang et al* was predominantly performed in MEFs (Dou *et al.*, 2017; Gluck *et al.*, 2017; Yang *et al.*, 2017). As such it may be that the role of cGAS varies between mice and humans. In support of this idea *Yang et al* demonstrated that cGAS deficient BJ human foreskin fibroblasts lacked expression of SASP related genes and SA-β-Gal

following irradiation but there was still evidence of p21 upregulation (Yang *et al.*, 2017). However, *Katlinskaya et al* found that suppression of IFN1 downstream of cGAS could override the senescence phenotype in OIS IMR90 cells (Katlinskaya *et al.*, 2016). This therefore lends strength to the idea that at least in human cells the effects of cGAS on cell cycle regulation are most likely attributed to paracrine effects of the SASP which can reinforce and induce senescence in neighbouring cells (Acosta *et al.*, 2008; Nelson *et al.*, 2012; Acosta *et al.*, 2013; Dou *et al.*, 2017).

Nevertheless, if cGAS has an independent role in implementing the cell cycle arrest it would not be expected that the anti-malarial drugs would have an impact as these drugs bind to double stranded DNA and prevent cGAS from recognising it rather than directly inhibiting cGAS. As such it would be expected that cGAS would still be free to undertake its additional roles in the implementation of senescence. However, we also did not observe an impact on the cell cycle arrest with the small molecule inhibitor RU.521 which non-competitively inhibits the active DNA binding site of cGAS. This suggests that either cGAS does not have an independent role in implementing the cell cycle arrest or alternatively it can prevent cellular proliferation without requiring its DNA binding active site. Our findings with those of *Dou et al*, suggest that the predominant role of cGAS in human fibroblasts is in modulating the SASP but not the cell cycle arrest (Dou *et al.*, 2017).

This highlights particular promise of using RU.521 or anti-malarial drugs as senostatic drugs to alleviate the SASP without preventing the cell cycle arrest. Moreover, the anti-malarial drugs are already in use in the clinics with a relatively good safety profile. The data in this chapter supports a preliminary case for repurposing of these drugs as a potential strategy for ameliorating inflammation in senescence associated diseases. Although attention must be paid as direct inhibition of either cGAS or STING could exacerbate the susceptibility of individuals to infectious diseases. With that in mind, administration of these agents would need to be carried out in a manner which does not compromise immune function.

6. Chapter 6: Conclusions

Work over the past decades has demonstrated that senescent cells accumulate in a variety of tissues with age and at sites of chronic diseases (Dimri *et al.*, 1995; Krishnamurthy *et al.*, 2004; Herbig *et al.*, 2006; Hewitt *et al.*, 2012; Waaijer *et al.*, 2012). More recently, it has been established that senescent cells can drive to a certain extent ageing and age-related pathologies (Baker *et al.*, 2011; Baker *et al.*, 2016). Mitochondria have been implicated in both ageing and the development of the senescent phenotype for some time, however, it is only recently that they have been identified as being an essential mediator of the SASP (Correia-Melo *et al.*, 2016; Wiley *et al.*, 2016; Chapman *et al.*, 2019). Work in our lab recently conducted a proof of principle experiment to determine the extent that mitochondria are required for senescence. They generated mitochondrial-depleted senescent cells and discovered that they no longer displayed a SASP but still undergo an irreversible cell cycle arrest (Correia-Melo *et al.*, 2016). This work led us to propose that mitochondria may be highly promising targets for anti-senescence therapies and that by targeting them we may be able to suppress the detrimental SASP known to contribute to aging, while maintaining the tumour suppressor capabilities of senescent cells. However, mechanistically it is still not known how mitochondria regulate the SASP. For that reason, I aimed in this thesis to investigate the role of mitochondrial apoptosis in the regulation of the senescent phenotype, particularly the role of mtDNA release and caspase activation.

In this study, corroborating the findings of others I found that mitochondria in senescent cells display signs of dysfunction such as exacerbated ROS production, enlarged networks and a reduced mitochondrial membrane potential (Yoon *et al.*, 2006; Passos *et al.*, 2007; Passos *et al.*, 2010; Correia-Melo *et al.*, 2016). For the first time, this thesis demonstrated that senescent cells can be characterised by the presence of cytosolic DNA which is of mitochondrial origin. Moreover, I found that the release of mtDNA is dependent on the capacity for a cell to form BAX and BAK pores as cells deficient for BAX and BAK no longer released mtDNA when they became senescent. Previous work has highlighted the role of mtDNA as a particularly potent immunostimulatory molecule (Nakahira *et al.*, 2011; West *et al.*, 2015; Bao *et al.*, 2016). Indeed, I found that the transfection of mtDNA into human fibroblasts promoted a robust inflammatory response. In the context of senescence, a reduced level of cytosolic mtDNA as observed in BAX and BAK deficient cells was associated with a strong reduction in the SASP. Despite lacking a SASP, BAX and BAK deficient cells did not have an impaired induction of the cell cycle arrest as measured by the expression of p16, p21 and Ki67. This strengthens the

findings that mitochondria are essential for the pro-ageing features of senescence (pro-inflammatory and pro-oxidant) but not for implementation of the cell cycle arrest (Correia-Melo *et al.*, 2016).

The observation that mtDNA is the molecule responsible for the SASP highlighted a therapeutic window that could be exploited. As the release of mtDNA is dependent on the proteins BAX and BAK I decided to test whether two inhibitors (BIPv5 and BCB) which target these proteins can ameliorate the SASP. I found that both of these inhibitors could reduce the secretion of IL-6 and IL-8 which are both key constituents of the SASP. Furthermore, comprehensive characterisation of the SASP in cells where BAX and BAK had been abrogated genetically revealed that an array of pro-inflammatory cytokines and chemokines were downregulated during senescence. These findings are of particular interest to the clinic as they highlight a strategy to alleviate the detrimental aspects of senescence without compromising the tumour suppressive effects of the cell cycle arrest. Building on these observations, it was shown *in vivo* that mice which harbour BAX and BAK deficient livers did not display an upregulation of SASP related genes following low grade irradiation which induces senescence. This highlights that the importance of BAX and BAK in SASP regulation is also evident *in vivo*. As such, it will be both interesting and important to establish whether the two inhibitors can replicate these beneficial effects in an *in vivo* context.

Next, I investigated mechanisms which could trigger the release of mtDNA via BAX and BAK. Recent work has implicated a process whereby a subset of mitochondria are permeabilised in the absence of cell death, leading to cytochrome c release and the induction of DNA damage (Ichim *et al.*, 2015). The implementation of DNA damage and absence of cell death are key distinguishing features of senescence, therefore I investigated the potential of miMOMP as a feature of senescence. Indeed, I found evidence that senescent cells display limited mitochondrial outer membrane permeabilisation as measured by colocalisation of cytochrome c and TOM20. Cytochrome c release also occurs via BAX and BAK pores (Tait and Green, 2010). Supporting this it was observed that when BAX and BAK deficient cells become senescent they do not display reduced colocalisation of cytochrome c and TOM20. In addition, it was shown that the pharmacological induction of miMOMP using ABT737 promoted a senescence like-phenotype, complementing previous findings that demonstrated ABT737 mediated induction of senescence in cancer cells (Song *et al.*, 2011). These findings highlight that miMOMP is both a feature of senescence as well as an inducer. Of further interest, we

found that the induction of miMOMP using ABT737 was associated with promoting mtDNA release.

The observation that ABT737 can induce a senescent-like phenotype is of particular interest as drugs within this family are currently being explored as senolytic therapies (Chang *et al.*, 2016; Yosef *et al.*, 2016b; Walaszczyk *et al.*, 2019). This study found that ABT737 treatment was associated with DNA damage and the secretion of IL-6 and IL-8 *in vitro*. These observations suggest that senolytics from this family may have a detrimental effect on healthy cells, this therefore highlights the need for further research to understand the effects of ABT737 on healthy tissue *in vivo*.

A number of the miMOMP associated effects (increased levels of γH2AX, p21, SA-β-Gal and the secretion of IL-6 and IL-8) were dependent on caspase activity. Although caspase 1 and 5 have been previously been identified as mediating the SASP, other caspases have not been investigated (Acosta *et al.*, 2013; Wiggins *et al.*, 2019). This prompted us to investigate whether caspases have a role in regulation of the senescence phenotype. It was discovered that specifically there is sub-lethal caspase 3 activity in senescent cells, preliminary work in this study suggests that its inhibition leads to a reduction in the DDR (γH2AX and 53BP1) as well as a partial reduction in the SASP. However, this work only assessed the role of caspases 1-4 in SASP regulation, therefore future work should seek to further understand the role of caspase 3 and elucidate the contribution of other caspases to the senescence phenotype.

In addition, this study also set out to understand mechanistically how cytosolic mtDNA can promote a pro-inflammatory response during senescence. Whilst exploring the roles of caspases in senescence I observed that there was evidence of caspase 1 cleavage. Caspase 1 cleavage has been associated with activation of the inflammasome in response to mtDNA (Nakahira *et al.*, 2011; Shimada *et al.*, 2012; Shalini *et al.*, 2015). Furthermore, caspase 1 and the inflammasome have been implicated in modulating the SASP in OIS (Acosta *et al.*, 2013). In this study, despite there being cleavage of caspase 1 there was no evidence of NLRP3 activation, as measured by the cleavage of IL-1β and the secretion of IL-18. It has been reported that TLR9 can also mount an inflammatory response to mtDNA (Bao *et al.*, 2016). Our work found that there was not a difference in overall protein levels between proliferating and senescent cells. Previous work has also demonstrated that TLR9 is not upregulated in OIS (Hari *et al.*, 2018). However, at this stage more data is required in order to confidently determine whether TLR9 is involved in the response to mtDNA during senescence.

The cGAS-STING pathway has been previously implicated in senescence. Specifically, it acts as part of the innate immune system which recognises nuclear fragments of DNA referred to as CCFs, following recognition, it promotes an inflammatory response through NF-κB and IFN-1 genes (Ivanov *et al.*, 2013; Dou *et al.*, 2017; Gluck *et al.*, 2017; Yang *et al.*, 2017). The cGAS-STING axis can also induce inflammation in response to mtDNA (West *et al.*, 2015). In stress-induced senescence this study observed that the phosphorylation of IRF3 which is downstream of cGAS-STING signalling was increased in senescent cells. Moreover, when treated with the BAX channel blocker BCB to prevent mtDNA release the phosphorylation of IRF3 was reduced. Furthermore, senescent cells expressing a GFP reporter system on cGAS displayed colocalisation of cGAS with TFAM. It was also observed that STING deficient cells displayed a reduced SASP following the induction of senescence and also had a reduced pro-inflammatory response following the transfection of mtDNA. Collectively these data demonstrate that the cGAS-STING axis is responsible for the SASP which occurs in response to mtDNA released during senescence. However, at this stage the contribution of TLR9 cannot be ruled out as silencing of STING does not completely prevent the response to mtDNA transfection.

Following the identification that cGAS-STING contributes to the SASP in response to mtDNA I wanted to assess whether this pathway could be targeted pharmacologically. Previous studies investigating the cGAS-STING axis in SASP regulation have utilised genetic silencing of cGAS and STING to determine their role. However, a number of anti-malarial drugs and a specific small molecule inhibitor have been recently identified which can inhibit the activity of cGAS (An *et al.*, 2015; Vincent *et al.*, 2017). I found that each of the inhibitors RU.521, ACMA and quinacrine dihydrochloride which target cGAS activity could ameliorate the SASP in stress-induced senescence. Interestingly, these drugs did not prevent the cell cycle arrest as measured by p21 and Ki67. Similar, to the BAX and BAK inhibitors these drugs show promise as potential senostatic therapies.

Collectively, we have shown that during senescence mtDNA escapes into the cytosol via BAX and BAK. Whilst here it can act as a profound inflammatory molecule where it is responsible for the SASP through cGAS-STING activation. The SASP has been associated with detrimental effects due to its role in paracrine-induced senescence as well as creating a microenvironment that is prone to tumour progression (Coppe *et al.*, 2010; Nelson *et al.*, 2012; Acosta *et al.*, 2013). Utilising this knowledge we have identified two putative targets for suppression of the SASP without impacting on the cell cycle arrest aspects of senescence. First, through the inhibition of

BAX and BAK to prevent mtDNA release and secondly by targeting cGAS which is responsible for identification of mtDNA downstream of its release. Cellular senescence has been identified as a driver of ageing and multiple age-related pathologies and indeed clinical trials are currently underway to assess the potential benefits of senolytics (Baker *et al.*, 2011; Baker *et al.*, 2016; Kirkland *et al.*, 2017; Justice *et al.*, 2019). It is therefore of significant interest to understand the biological mechanisms which underpin senescence and the associated SASP. As such, these findings are of particular interest to the clinic and may therefore be beneficial as a senostatic therapy for alleviating the detrimental effects associated with the accumulation of senescent cells and associated inflammation.

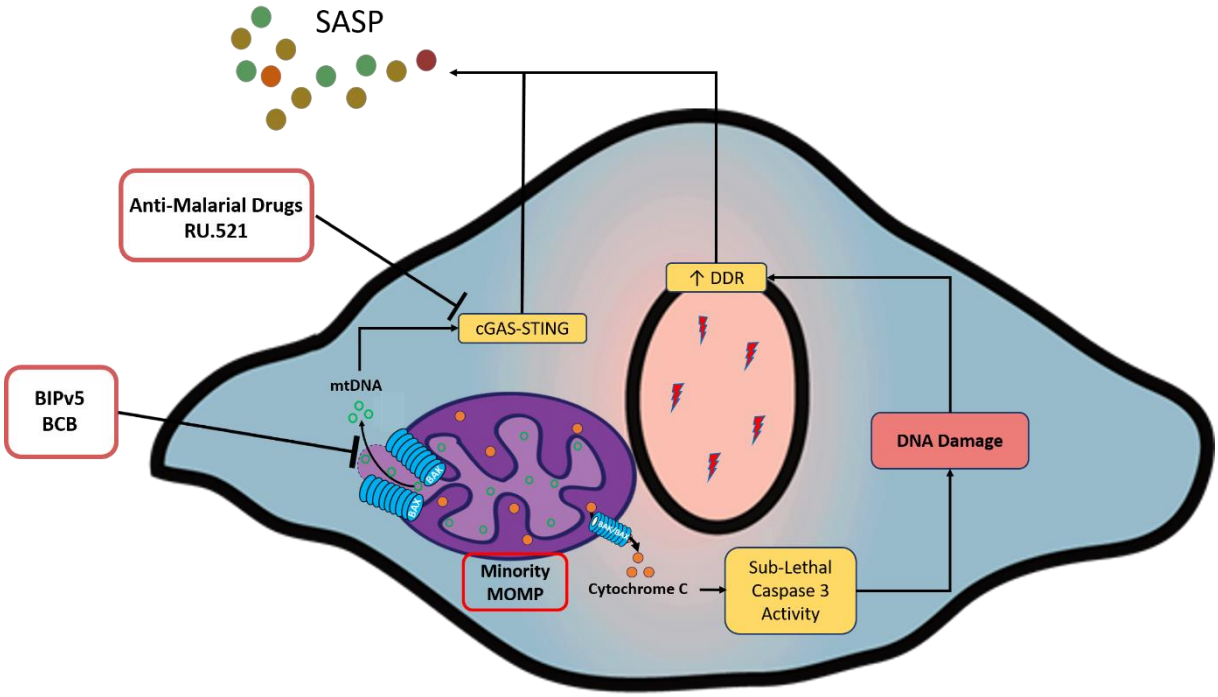

Figure 6.1 – Summary of the relationship between mitochondria and the SASP during cellular senescence.

During senescence it was discovered that mtDNA is being released through BAX and BAK pores into the cytosol where it is recognised by cGAS which provokes the SASP. Blockage of BAX and BAK pores using BIPv5 and BCB can prevent mtDNA release and the subsequent SASP. Similarly, targeting of cGAS using anti-malarial drugs or RU.521 can inhibit the SASP. It was also discovered that senescent cells display evidence of miMOMP where cytochrome c is also being released though BAX and BAK pores. The release of cytochrome C is associated with promoting caspase 3 activity during senescence which promotes DNA damage. This contributes to the DDR which can exacerbate the SASP.

7. References

Acosta, J.C., Banito, A., Wuestefeld, T., Georgilis, A., Janich, P., Morton, J.P., Athineos, D., Kang, T.W., Lasitschka, F., Andrulis, M., Pascual, G., Morris, K.J., Khan, S., Jin, H., Dharmalingam, G., Snijders, A.P., Carroll, T., Capper, D., Pritchard, C., Inman, G.J., Longerich, T., Sansom, O.J., Benitah, S.A., Zender, L. and Gil, J. (2013) 'A complex secretory program orchestrated by the inflammasome controls paracrine senescence', *Nat Cell Biol*, 15(8), pp. 978-90.

Acosta, J.C., O'Loghlen, A., Banito, A., Guijarro, M.V., Augert, A., Raguz, S., Fumagalli, M., Da Costa, M., Brown, C., Popov, N., Takatsu, Y., Melamed, J., d'Adda di Fagagna, F., Bernard, D., Hernando, E. and Gil, J. (2008) 'Chemokine signaling via the CXCR2 receptor reinforces senescence', *Cell*, 133(6), pp. 1006-18.

Ahmad, T., Sundar, I.K., Lerner, C.A., Gerloff, J., Tormos, A.M., Yao, H. and Rahman, I. (2015) 'Impaired mitophagy leads to cigarette smoke stress-induced cellular senescence: implications for chronic obstructive pulmonary disease', *Faseb j*, 29(7), pp. 2912-29.

Alcorta, D.A., Xiong, Y., Phelps, D., Hannon, G., Beach, D. and Barrett, J.C. (1996) 'Involvement of the cyclin-dependent kinase inhibitor p16 (INK4a) in replicative senescence of normal human fibroblasts', *Proc Natl Acad Sci U S A*, 93(24), pp. 13742-7.

Amano, H., Chaudhury, A., Rodriguez-Aguayo, C., Lu, L., Akhanov, V., Catic, A., Popov, Y.V., Verdin, E., Johnson, H., Stossi, F., Sinclair, D.A., Nakamaru-Ogiso, E., Lopez-Berestein, G., Chang, J.T., Neilson, J.R., Meeker, A., Finegold, M., Baur, J.A. and Sahin, E. (2019) 'Telomere Dysfunction Induces Sirtuin Repression that Drives Telomere-Dependent Disease', *Cell Metab*.

An, J., Woodward, J.J., Sasaki, T., Minie, M. and Elkon, K.B. (2015) 'Cutting edge: Antimalarial drugs inhibit IFN-beta production through blockade of cyclic GMP-AMP synthase-DNA interaction', *J Immunol*, 194(9), pp. 4089-93.

Anderson, R., Lagnado, A., Maggiorani, D., Walaszczyk, A., Dookun, E., Chapman, J., Birch, J., Salmonowicz, H., Ogrodnik, M., Jurk, D., Proctor, C., Correia-Melo, C., Victorelli, S., Fielder, E., Berlinguer-Palmini, R., Owens, A., Greaves, L.C., Kolsky, K.L., Parini, A., Douin-Echinard, V., LeBrasseur, N.K., Arthur, H.M., Tual-Chalot, S., Schafer, M.J., Roos, C.M., Miller, J.D., Robertson, N., Mann, J., Adams, P.D., Tchkonia, T., Kirkland, J.L., Mialet-Perez, J., Richardson, G.D. and Passos, J.F. (2019) 'Length-independent telomere damage drives post-mitotic cardiomyocyte senescence', *Embo j*, 38(5).

Anwar, M., Kasper, A., Steck, A.R. and Schier, J.G. (2017) 'Bongkrekic Acid-a Review of a Lesser-Known Mitochondrial Toxin', *J Med Toxicol*, 13(2), pp. 173-179.

Arivazhagan, P., Mizutani, E., Fujii, M. and Ayusawa, D. (2004) 'Cardiolipin induces premature senescence in normal human fibroblasts', *Biochem Biophys Res Commun*, 323(3), pp. 739-42.

Baar, M.P., Brandt, R.M.C., Putavet, D.A., Klein, J.D.D., Derks, K.W.J., Bourgeois, B.R.M., Stryeck, S., Rijksen, Y., van Willigenburg, H., Feijtel, D.A., van der Pluijm, I., Essers, J., van Cappellen, W.A., van, I.W.F., Houtsmuller, A.B., Pothof, J., de Bruin, R.W.F., Madl, T., Hoeijmakers, J.H.J., Campisi, J. and de Keizer, P.L.J. (2017) 'Targeted Apoptosis of Senescent Cells Restores Tissue Homeostasis in Response to Chemotoxicity and Aging', *Cell*, 169(1), pp. 132-147.e16.

Baker, D.J., Childs, B.G., Durik, M., Wijers, M.E., Sieben, C.J., Zhong, J., Saltness, R.A., Jeganathan, K.B., Verzosa, G.C., Pezeshki, A., Khazaie, K., Miller, J.D. and van Deursen, J.M. (2016) 'Naturally occurring p16(Ink4a)-positive cells shorten healthy lifespan', *Nature*, 530(7589), pp. 184-9.

Baker, D.J., Perez-Terzic, C., Jin, F., Pitel, K.S., Niederlander, N.J., Jeganathan, K., Yamada, S., Reyes, S., Rowe, L., Hiddinga, H.J., Eberhardt, N.L., Terzic, A. and van Deursen, J.M.

(2008) 'Opposing roles for p16Ink4a and p19Arf in senescence and ageing caused by BubR1 insufficiency', *Nat Cell Biol*, 10(7), pp. 825-36.
Baker, D.J., Wijshake, T., Tchkonia, T., LeBrasseur, N.K., Childs, B.G., van de Sluis, B., Kirkland, J.L. and van Deursen, J.M. (2011) 'Clearance of p16Ink4a-positive senescent cells delays ageing-associated disorders', *Nature*, 479(7372), pp. 232-6.
Banin, S., Moyal, L., Shieh, S., Taya, Y., Anderson, C.W., Chessa, L., Smorodinsky, N.I., Prives, C., Reiss, Y., Shiloh, Y. and Ziv, Y. (1998) 'Enhanced phosphorylation of p53 by ATM in response to DNA damage', *Science*, 281(5383), pp. 1674-7.
Bao, W., Xia, H., Liang, Y., Ye, Y., Lu, Y., Xu, X., Duan, A., He, J., Chen, Z., Wu, Y., Wang, X., Zheng, C., Liu, Z. and Shi, S. (2016) 'Toll-like Receptor 9 Can be Activated by Endogenous Mitochondrial DNA to Induce Podocyte Apoptosis', *Sci Rep*, 6, p. 22579.
Bartkova, J., Rezaei, N., Liontos, M., Karakaidos, P., Kletsas, D., Issaeva, N., Vassiliou, L.V., Kolettas, E., Niforou, K., Zoumpourlis, V.C., Takaoka, M., Nakagawa, H., Tort, F., Fugger, K., Johansson, F., Sehested, M., Andersen, C.L., Dyrskjot, L., Orntoft, T., Lukas, J., Kittas, C., Helleday, T., Halazonetis, T.D., Bartek, J. and Gorgoulis, V.G. (2006) 'Oncogene-induced senescence is part of the tumorigenesis barrier imposed by DNA damage checkpoints', *Nature*, 444(7119), pp. 633-7.
Bayreuther, K., Rodemann, H.P., Hommel, R., Dittmann, K., Albiez, M. and Francz, P.I. (1988) 'Human skin fibroblasts in vitro differentiate along a terminal cell lineage', *Proceedings of the National Academy of Sciences of the United States of America*, 85(14), pp. 5112-5116.
Beausejour, C.M., Krtolica, A., Galimi, F., Narita, M., Lowe, S.W., Yaswen, P. and Campisi, J. (2003) 'Reversal of human cellular senescence: roles of the p53 and p16 pathways', *Embo j*, 22(16), pp. 4212-22.
Berry, D.C., Jiang, Y., Arpke, R.W., Close, E.L., Uchida, A., Reading, D., Berglund, E.D., Kyba, M. and Graff, J.M. (2017) 'Cellular Aging Contributes to Failure of Cold-Induced Beige Adipocyte Formation in Old Mice and Humans', *Cell metabolism*, 25(1), pp. 166-181.
Bhat, R., Crowe, E.P., Bitto, A., Moh, M., Katsetos, C.D., Garcia, F.U., Johnson, F.B., Trojanowski, J.Q., Sell, C. and Torres, C. (2012) 'Astrocyte senescence as a component of Alzheimer's disease', *PLoS One*, 7(9), p. e45069.
Birch, J., Anderson, R.K., Correia-Melo, C., Jurk, D., Hewitt, G., Marques, F.M., Green, N.J., Moisey, E., Birrell, M.A., Belvisi, M.G., Black, F., Taylor, J.J., Fisher, A.J., De Soyza, A. and Passos, J.F. (2015) 'DNA damage response at telomeres contributes to lung aging and chronic obstructive pulmonary disease', *Am J Physiol Lung Cell Mol Physiol*, 309(10), pp. L1124-37.
Birch, J. and Passos, J.F. (2017) 'Targeting the SASP to combat ageing: Mitochondria as possible intracellular allies?', *Bioessays*, 39(5).
Birket, M.J., Orr, A.L., Gerencser, A.A., Madden, D.T., Vitelli, C., Swistowski, A., Brand, M.D. and Zeng, X. (2011) 'A reduction in ATP demand and mitochondrial activity with neural differentiation of human embryonic stem cells', *J Cell Sci*, 124(Pt 3), pp. 348-58.
Blackburn, E.H. (1991) 'Structure and function of telomeres', *Nature*, 350(6319), pp. 569-73.
Blackburn, E.H., Epel, E.S. and Lin, J. (2015) 'Human telomere biology: A contributory and interactive factor in aging, disease risks, and protection', *Science*, 350(6265), pp. 1193-8.
Bodnar, A.G., Ouellette, M., Frolkis, M., Holt, S.E., Chiu, C.P., Morin, G.B., Harley, C.B., Shay, J.W., Lichtsteiner, S. and Wright, W.E. (1998) 'Extension of life-span by introduction of telomerase into normal human cells', *Science*, 279(5349), pp. 349-52.
Bombarde, O., Boby, C., Gomez, D., Frit, P., Giraud-Panis, M.J., Gilson, E., Salles, B. and Calsou, P. (2010) 'TRF2/RAP1 and DNA-PK mediate a double protection against joining at telomeric ends', *Embo j*, 29(9), pp. 1573-84.
Bombrun, A., Gerber, P., Casi, G., Terradillos, O., Antonsson, B. and Halazy, S. (2003) '3,6-dibromocarbazole piperazine derivatives of 2-propanol as first inhibitors of cytochrome c release via Bax channel modulation', *J Med Chem*, 46(21), pp. 4365-8.

Boohaker, R.J., Zhang, G., Carlson, A.L., Nemec, K.N. and Khaled, A.R. (2011) 'BAX supports the mitochondrial network, promoting bioenergetics in nonapoptotic cells', *American journal of physiology. Cell physiology*, 300(6), pp. C1466-C1478.
Bordet, T., Berna, P., Abitbol, J.-L. and Pruss, R.M. (2010) 'Olesoxime (TRO19622): A Novel Mitochondrial-Targeted Neuroprotective Compound', *Pharmaceuticals (Basel, Switzerland)*, 3(2), pp. 345-368.
Bossy-Wetzel, E. and Green, D.R. (1999) 'Caspases induce cytochrome c release from mitochondria by activating cytosolic factors', *J Biol Chem*, 274(25), pp. 17484-90.
Braidy, N., Guillemin, G.J., Mansour, H., Chan-Ling, T., Poljak, A. and Grant, R. (2011) 'Age related changes in NAD+ metabolism oxidative stress and Sirt1 activity in wistar rats', *PLoS One*, 6(4), p. e19194.
Brand, M.D. (2005) 'The efficiency and plasticity of mitochondrial energy transduction', *Biochem Soc Trans*, 33(Pt 5), pp. 897-904.
Brighton, P.J., Maruyama, Y., Fishwick, K., Vrljicak, P., Tewary, S., Fujihara, R., Muter, J., Lucas, E.S., Yamada, T., Woods, L., Lucciola, R., Hou Lee, Y., Takeda, S., Ott, S., Hemberger, M., Quenby, S. and Brosens, J.J. (2017) 'Clearance of senescent decidual cells by uterine natural killer cells in cycling human endometrium', *Elife*, 6.
Briston, T., Roberts, M., Lewis, S., Powney, B., J, M.S., Szabadkai, G. and Duchen, M.R. (2017) 'Mitochondrial permeability transition pore: sensitivity to opening and mechanistic dependence on substrate availability', *Sci Rep*, 7(1), p. 10492.
Brookes, S., Rowe, J., Ruas, M., Llanos, S., Clark, P.A., Lomax, M., James, M.C., Vatcheva, R., Bates, S., Vousden, K.H., Parry, D., Gruis, N., Smit, N., Bergman, W. and Peters, G. (2002) 'INK4a-deficient human diploid fibroblasts are resistant to RAS-induced senescence', *Embo j*, 21(12), pp. 2936-45.
Brown, J.P., Wei, W. and Sedivy, J.M. (1997) 'Bypass of senescence after disruption of p21CIP1/WAF1 gene in normal diploid human fibroblasts', *Science*, 277(5327), pp. 831-4.
Brugarolas, J., Chandrasekaran, C., Gordon, J.I., Beach, D., Jacks, T. and Hannon, G.J. (1995) 'Radiation-induced cell cycle arrest compromised by p21 deficiency', *Nature*, 377(6549), pp. 552-7.
Bussian, T.J., Aziz, A., Meyer, C.F., Swenson, B.L., van Deursen, J.M. and Baker, D.J. (2018) 'Clearance of senescent glial cells prevents tau-dependent pathology and cognitive decline', *Nature*, 562(7728), pp. 578-582.
Campisi, J. and d'Adda di Fagagna, F. (2007) 'Cellular senescence: when bad things happen to good cells', *Nat Rev Mol Cell Biol*, 8(9), pp. 729-40.
Certo, M., Del Gaizo Moore, V., Nishino, M., Wei, G., Korsmeyer, S., Armstrong, S.A. and Letai, A. (2006) 'Mitochondria primed by death signals determine cellular addiction to antiapoptotic BCL-2 family members', *Cancer Cell*, 9(5), pp. 351-65.
Chandra, T., Ewels, P.A., Schoenfelder, S., Furlan-Magaril, M., Wingett, S.W., Kirschner, K., Thuret, J.Y., Andrews, S., Fraser, P. and Reik, W. (2015) 'Global reorganization of the nuclear landscape in senescent cells', *Cell Rep*, 10(4), pp. 471-83.
Chang, J., Wang, Y., Shao, L., Laberge, R.M., Demaria, M., Campisi, J., Janakiraman, K., Sharpless, N.E., Ding, S., Feng, W., Luo, Y., Wang, X., Aykin-Burns, N., Krager, K., Ponnappan, U., Hauer-Jensen, M., Meng, A. and Zhou, D. (2016) 'Clearance of senescent cells by ABT263 rejuvenates aged hematopoietic stem cells in mice', *Nat Med*, 22(1), pp. 78-83.
Chapman, J., Fielder, E. and Passos, J.F. (2019) 'Mitochondrial dysfunction and cell senescence: deciphering a complex relationship', *FEBS Lett*.
Chaturvedi, V., Qin, J.Z., Denning, M.F., Choubey, D., Diaz, M.O. and Nickoloff, B.J. (1999) 'Apoptosis in proliferating, senescent, and immortalized keratinocytes', *J Biol Chem*, 274(33), pp. 23358-67.

Chehab, N.H., Malikzay, A., Appel, M. and Halazonetis, T.D. (2000) 'Chk2/hCds1 functions as a DNA damage checkpoint in G(1) by stabilizing p53', *Genes Dev*, 14(3), pp. 278-88.
Chen, J.H., Stoeber, K., Kingsbury, S., Ozanne, S.E., Williams, G.H. and Hales, C.N. (2004a) 'Loss of proliferative capacity and induction of senescence in oxidatively stressed human fibroblasts', *J Biol Chem*, 279(47), pp. 49439-46.
Chen, Q. and Ames, B.N. (1994) 'Senescence-like growth arrest induced by hydrogen peroxide in human diploid fibroblast F65 cells', *Proc Natl Acad Sci U S A*, 91(10), pp. 4130-4.
Chen, Q., Fischer, A., Reagan, J.D., Yan, L.J. and Ames, B.N. (1995a) 'Oxidative DNA damage and senescence of human diploid fibroblast cells', *Proceedings of the National Academy of Sciences of the United States of America*, 92(10), pp. 4337-4341.
Chen, Q., Fischer, A., Reagan, J.D., Yan, L.J. and Ames, B.N. (1995b) 'Oxidative DNA damage and senescence of human diploid fibroblast cells', *Proc Natl Acad Sci U S A*, 92(10), pp. 4337-41.
Chen, Q., Sun, L. and Chen, Z.J. (2016) 'Regulation and function of the cGAS-STING pathway of cytosolic DNA sensing', *Nat Immunol*, 17(10), pp. 1142-9.
Chen, Q.M., Liu, J. and Merrett, J.B. (2000) 'Apoptosis or senescence-like growth arrest: influence of cell-cycle position, p53, p21 and bax in H2O2 response of normal human fibroblasts', *Biochem J*, 347(Pt 2), pp. 543-51.
Chen, X., Liang, H., Van Remmen, H., Vijg, J. and Richardson, A. (2004b) 'Catalase transgenic mice: characterization and sensitivity to oxidative stress', *Arch Biochem Biophys*, 422(2), pp. 197-210.
Chien, Y., Scuoppo, C., Wang, X., Fang, X., Balgley, B., Bolden, J.E., Premsrirut, P., Luo, W., Chicas, A., Lee, C.S., Kogan, S.C. and Lowe, S.W. (2011) 'Control of the senescence-associated secretory phenotype by NF-κB promotes senescence and enhances chemosensitivity', *Genes & development*, 25(20), pp. 2125-2136.
Childs, B.G., Baker, D.J., Wijshake, T., Conover, C.A., Campisi, J. and van Deursen, J.M. (2016) 'Senescent intimal foam cells are deleterious at all stages of atherosclerosis', *Science*, 354(6311), pp. 472-477.
Chini, C., Hogan, K.A., Warner, G.M., Tarrago, M.G., Peclat, T.R., Tchkonia, T., Kirkland, J.L. and Chini, E. (2019) 'The NADase CD38 is induced by factors secreted from senescent cells providing a potential link between senescence and age-related cellular NAD(+) decline', *Biochem Biophys Res Commun*, 513(2), pp. 486-493.
Coppe, J.P., Desprez, P.Y., Krtolica, A. and Campisi, J. (2010) 'The senescence-associated secretory phenotype: the dark side of tumor suppression', *Annu Rev Pathol*, 5, pp. 99-118.
Coppe, J.P., Patil, C.K., Rodier, F., Sun, Y., Munoz, D.P., Goldstein, J., Nelson, P.S., Desprez, P.Y. and Campisi, J. (2008) 'Senescence-associated secretory phenotypes reveal cell-nonautonomous functions of oncogenic RAS and the p53 tumor suppressor', *PLoS Biol*, 6(12), pp. 2853-68.
Cordero, M.D., Williams, M.R. and Ryffel, B. (2018) 'AMP-Activated Protein Kinase Regulation of the NLRP3 Inflammasome during Aging', *Trends Endocrinol Metab*, 29(1), pp. 8-17.
Correia-Melo, C., Birch, J., Fielder, E., Rahmatika, D., Taylor, J., Chapman, J., Lagnado, A., Carroll, B.M., Miwa, S., Richardson, G., Jurk, D., Oakley, F., Mann, J., Mann, D.A., Korolchuk, V.I. and Passos, J.F. (2019) 'Rapamycin improves healthspan but not inflammaging in nfkappab1(-/-) mice', *Aging Cell*, 18(1), p. e12882.
Correia-Melo, C., Ichim, G., Tait, S.W. and Passos, J.F. (2017) 'Depletion of mitochondria in mammalian cells through enforced mitophagy', *Nat Protoc*, 12(1), pp. 183-194.
Correia-Melo, C., Marques, F.D., Anderson, R., Hewitt, G., Hewitt, R., Cole, J., Carroll, B.M., Miwa, S., Birch, J., Merz, A., Rushton, M.D., Charles, M., Jurk, D., Tait, S.W., Czapiewski, R., Greaves, L., Nelson, G., Bohlooly, Y.M., Rodriguez-Cuenca, S., Vidal-Puig, A., Mann, D.,

Saretzki, G., Quarato, G., Green, D.R., Adams, P.D., von Zglinicki, T., Korolchuk, V.I. and Passos, J.F. (2016) 'Mitochondria are required for pro-ageing features of the senescent phenotype', *Embo j*, 35(7), pp. 724-42.
Cortez, D., Guntuku, S., Qin, J. and Elledge, S.J. (2001) 'ATR and ATRIP: partners in checkpoint signaling', *Science*, 294(5547), pp. 1713-6.
d'Adda di Fagagna, F. (2008) 'Living on a break: cellular senescence as a DNA-damage response', *Nat Rev Cancer*, 8(7), pp. 512-22.
d'Adda di Fagagna, F., Reaper, P.M., Clay-Farrace, L., Fiegler, H., Carr, P., Von Zglinicki, T., Saretzki, G., Carter, N.P. and Jackson, S.P. (2003) 'A DNA damage checkpoint response in telomere-initiated senescence', *Nature*, 426(6963), pp. 194-8.
Dalle Pezze, P., Nelson, G., Otten, E.G., Korolchuk, V.I., Kirkwood, T.B., von Zglinicki, T. and Shanley, D.P. (2014) 'Dynamic modelling of pathways to cellular senescence reveals strategies for targeted interventions', *PLoS Comput Biol*, 10(8), p. e1003728.
De Cecco, M., Ito, T., Petrashen, A.P., Elias, A.E., Skvir, N.J., Criscione, S.W., Caligiana, A., Brocculi, G., Adney, E.M., Boeke, J.D., Le, O., Beausejour, C., Ambati, J., Ambati, K., Simon, M., Seluanov, A., Gorbunova, V., Slagboom, P.E., Helfand, S.L., Neretti, N. and Sedivy, J.M. (2019) 'L1 drives IFN in senescent cells and promotes age-associated inflammation', *Nature*, 566(7742), pp. 73-78.
de Lange, T. (2005) 'Shelterin: the protein complex that shapes and safeguards human telomeres', *Genes Dev*, 19(18), pp. 2100-10.
Debacq-Chainiaux, F., Boilan, E., Dedessus Le Moutier, J., Weemaels, G. and Toussaint, O. (2010) 'p38(MAPK) in the senescence of human and murine fibroblasts', *Adv Exp Med Biol*, 694, pp. 126-37.
Debacq-Chainiaux, F., Borlon, C., Pascal, T., Royer, V., Eliaers, F., Ninane, N., Carrard, G., Friguet, B., de Longueville, F., Boffe, S., Remacle, J. and Toussaint, O. (2005) 'Repeated exposure of human skin fibroblasts to UVB at subcytotoxic level triggers premature senescence through the TGF-beta1 signaling pathway', *J Cell Sci*, 118(Pt 4), pp. 743-58.
Demaria, M., Ohtani, N., Youssef, S.A., Rodier, F., Toussaint, W., Mitchell, J.R., Laberge, R.M., Vijg, J., Van Steeg, H., Dolle, M.E., Hoeijmakers, J.H., de Bruin, A., Hara, E. and Campisi, J. (2014) 'An essential role for senescent cells in optimal wound healing through secretion of PDGF-AA', *Dev Cell*, 31(6), pp. 722-33.
Detmer, S.A. and Chan, D.C. (2007) 'Functions and dysfunctions of mitochondrial dynamics', *Nat Rev Mol Cell Biol*, 8(11), pp. 870-9.
Di Leonardo, A., Linke, S.P., Clarkin, K. and Wahl, G.M. (1994) 'DNA damage triggers a prolonged p53-dependent G1 arrest and long-term induction of Cip1 in normal human fibroblasts', *Genes Dev*, 8(21), pp. 2540-51.
Di Micco, R., Fumagalli, M., Cicalese, A., Piccinin, S., Gasparini, P., Luise, C., Schurra, C., Garre, M., Nuciforo, P.G., Bensimon, A., Maestro, R., Pelicci, P.G. and d'Adda di Fagagna, F. (2006) 'Oncogene-induced senescence is a DNA damage response triggered by DNA hyper-replication', *Nature*, 444(7119), pp. 638-42.
Dimri, G.P., Lee, X., Basile, G., Acosta, M., Scott, G., Roskelley, C., Medrano, E.E., Linskens, M., Rubelj, I., Pereira-Smith, O. and et al. (1995) 'A biomarker that identifies senescent human cells in culture and in aging skin in vivo', *Proc Natl Acad Sci U S A*, 92(20), pp. 9363-7.
Dirac, A.M. and Bernards, R. (2003) 'Reversal of senescence in mouse fibroblasts through lentiviral suppression of p53', *J Biol Chem*, 278(14), pp. 11731-4.
Dou, Z., Ghosh, K., Vizioli, M.G., Zhu, J., Sen, P., Wangensteen, K.J., Simithy, J., Lan, Y., Lin, Y., Zhou, Z., Capell, B.C., Xu, C., Xu, M., Kieckhaefer, J.E., Jiang, T., Shoshkes-Carmel, M., Tanim, K., Barber, G.N., Seykora, J.T., Millar, S.E., Kaestner, K.H., Garcia, B.A., Adams, P.D. and Berger, S.L. (2017) 'Cytoplasmic chromatin triggers inflammation in senescence and cancer', *Nature*, 550(7676), pp. 402-406.

Dou, Z., Xu, C., Donahue, G., Shimi, T., Pan, J.A., Zhu, J., Ivanov, A., Capell, B.C., Drake, A.M., Shah, P.P., Catanzaro, J.M., Ricketts, M.D., Lamark, T., Adam, S.A., Marmorstein, R., Zong, W.X., Johansen, T., Goldman, R.D., Adams, P.D. and Berger, S.L. (2015) 'Autophagy mediates degradation of nuclear lamina', *Nature*, 527(7576), pp. 105-9.

Dussmann, H., Rehm, M., Concannon, C.G., Anguissola, S., Wurstle, M., Kacmar, S., Voller, P., Huber, H.J. and Prehn, J.H. (2010) 'Single-cell quantification of Bax activation and mathematical modelling suggest pore formation on minimal mitochondrial Bax accumulation', *Cell Death Differ*, 17(2), pp. 278-90.

Edlich, F., Banerjee, S., Suzuki, M., Cleland, M.M., Arnoult, D., Wang, C., Neutzner, A., Tjandra, N. and Youle, R.J. (2011) 'Bcl-x(L) retrotranslocates Bax from the mitochondria into the cytosol', *Cell*, 145(1), pp. 104-16.

Efeyan, A., Ortega-Molina, A., Velasco-Miguel, S., Herranz, D., Vassilev, L.T. and Serrano, M. (2007) 'Induction of p53-dependent senescence by the MDM2 antagonist nutlin-3a in mouse cells of fibroblast origin', *Cancer Res*, 67(15), pp. 7350-7.

Efimova, E.V., Mauceri, H.J., Golden, D.W., Labay, E., Bindokas, V.P., Darga, T.E., Chakraborty, C., Barreto-Andrade, J.C., Crawley, C., Sutton, H.G., Kron, S.J. and Weichselbaum, R.R. (2010) 'Poly(ADP-ribose) polymerase inhibitor induces accelerated senescence in irradiated breast cancer cells and tumors', *Cancer research*, 70(15), pp. 6277-6282.

Egashira, M., Hirota, Y., Shimizu-Hirota, R., Saito-Fujita, T., Haraguchi, H., Matsumoto, L., Matsuo, M., Hiraoka, T., Tanaka, T., Akaeda, S., Takehisa, C., Saito-Kanatani, M., Maeda, K.I., Fujii, T. and Osuga, Y. (2017) 'F4/80+ Macrophages Contribute to Clearance of Senescent Cells in the Mouse Postpartum Uterus', *Endocrinology*, 158(7), pp. 2344-2353.

Elmore, S. (2007) 'Apoptosis: a review of programmed cell death', *Toxicologic pathology*, 35(4), pp. 495-516.

Fadok, V.A., de Cathelineau, A., Daleke, D.L., Henson, P.M. and Bratton, D.L. (2001) 'Loss of phospholipid asymmetry and surface exposure of phosphatidylserine is required for phagocytosis of apoptotic cells by macrophages and fibroblasts', *J Biol Chem*, 276(2), pp. 1071-7.

Falck, J., Coates, J. and Jackson, S.P. (2005) 'Conserved modes of recruitment of ATM, ATR and DNA-PKcs to sites of DNA damage', *Nature*, 434(7033), pp. 605-11.

Farombi, E.O., Shyntum, Y.Y. and Emerole, G.O. (2003) 'Influence of chloroquine treatment and Plasmodium falciparum malaria infection on some enzymatic and non-enzymatic antioxidant defense indices in humans', *Drug Chem Toxicol*, 26(1), pp. 59-71.

Farr, J.N., Fraser, D.G., Wang, H., Jaehn, K., Ogrodnik, M.B., Weivoda, M.M., Drake, M.T., Tchkonia, T., LeBrasseur, N.K., Kirkland, J.L., Bonewald, L.F., Pignolo, R.J., Monroe, D.G. and Khosla, S. (2016) 'Identification of Senescent Cells in the Bone Microenvironment', *J Bone Miner Res*, 31(11), pp. 1920-1929.

Farr, J.N., Xu, M., Weivoda, M.M., Monroe, D.G., Fraser, D.G., Onken, J.L., Negley, B.A., Sfeir, J.G., Ogrodnik, M.B., Hachfeld, C.M., LeBrasseur, N.K., Drake, M.T., Pignolo, R.J., Pirtskhalava, T., Tchkonia, T., Oursler, M.J., Kirkland, J.L. and Khosla, S. (2017) 'Targeting cellular senescence prevents age-related bone loss in mice', *Nat Med*, 23(9), pp. 1072-1079.

Faulds, D., Goa, K.L. and Benfield, P. (1993) 'Cyclosporin. A review of its pharmacodynamic and pharmacokinetic properties, and therapeutic use in immunoregulatory disorders', *Drugs*, 45(6), pp. 953-1040.

Feng, Z., Hu, W., Teresky, A.K., Hernando, E., Cordon-Cardo, C. and Levine, A.J. (2007) 'Declining p53 function in the aging process: a possible mechanism for the increased tumor incidence in older populations', *Proc Natl Acad Sci U S A*, 104(42), pp. 16633-8.

Ferguson, M., Mockett, R.J., Shen, Y., Orr, W.C. and Sohal, R.S. (2005) 'Age-associated decline in mitochondrial respiration and electron transport in Drosophila melanogaster', *Biochem J*, 390(Pt 2), pp. 501-11.
Ferrer, P.E., Frederick, P., Gulbis, J.M., Dewson, G. and Kluck, R.M. (2012) 'Translocation of a Bak C-terminus mutant from cytosol to mitochondria to mediate cytochrome C release: implications for Bak and Bax apoptotic function', *PLoS One*, 7(3), p. e31510.
Freund, A., Laberge, R.-M., Demaria, M. and Campisi, J. (2012) 'Lamin B1 loss is a senescence-associated biomarker', *Molecular biology of the cell*, 23(11), pp. 2066-2075.
Freund, A., Patil, C.K. and Campisi, J. (2011) 'p38MAPK is a novel DNA damage response-independent regulator of the senescence-associated secretory phenotype', *Embo j*, 30(8), pp. 1536-48.
Fuhrmann-Stroissnigg, H., Ling, Y.Y., Zhao, J., McGowan, S.J., Zhu, Y., Brooks, R.W., Grassi, D., Gregg, S.Q., Stripay, J.L., Dorronsoro, A., Corbo, L., Tang, P., Bukata, C., Ring, N., Giacca, M., Li, X., Tchkonia, T., Kirkland, J.L., Niedernhofer, L.J. and Robbins, P.D. (2017) 'Identification of HSP90 inhibitors as a novel class of senolytics', *Nat Commun*, 8(1), p. 422.
Fumagalli, M., Rossiello, F., Clerici, M., Barozzi, S., Cittaro, D., Kaplunov, J.M., Bucci, G., Dobreva, M., Matti, V., Beausejour, C.M., Herbig, U., Longhese, M.P. and d'Adda di Fagagna, F. (2012) 'Telomeric DNA damage is irreparable and causes persistent DNA-damage-response activation', *Nat Cell Biol*, 14(4), pp. 355-65.
Gao, Z., Shao, Y. and Jiang, X. (2005) 'Essential roles of the Bcl-2 family of proteins in caspase-2-induced apoptosis', *J Biol Chem*, 280(46), pp. 38271-5.
Garrido, C., Galluzzi, L., Brunet, M., Puig, P.E., Didelot, C. and Kroemer, G. (2006) 'Mechanisms of cytochrome c release from mitochondria', *Cell Death Differ*, 13(9), pp. 1423-33.
Gavathiotis, E., Reyna, D.E., Davis, M.L., Bird, G.H. and Walensky, L.D. (2010) 'BH3-triggered structural reorganization drives the activation of proapoptotic BAX', *Mol Cell*, 40(3), pp. 481-92.
Genova, M.L. and Lenaz, G. (2014) 'Functional role of mitochondrial respiratory supercomplexes', *Biochim Biophys Acta*, 1837(4), pp. 427-43.
Gerland, L.M., Peyrol, S., Lallemand, C., Branche, R., Magaud, J.P. and Ffrench, M. (2003) 'Association of increased autophagic inclusions labeled for beta-galactosidase with fibroblastic aging', *Exp Gerontol*, 38(8), pp. 887-95.
Giampazolias, E., Zunino, B., Dhayade, S., Bock, F., Cloix, C., Cao, K., Roca, A., Lopez, J., Ichim, G., Proïcs, E., Rubio-Patiño, C., Fort, L., Yatim, N., Woodham, E., Orozco, S., Taraborrelli, L., Peltzer, N., Lecis, D., Machesky, L., Walczak, H., Albert, M.L., Milling, S., Oberst, A., Ricci, J.-E., Ryan, K.M., Blyth, K. and Tait, S.W.G. (2017) 'Mitochondrial permeabilization engages NF-κB-dependent anti-tumour activity under caspase deficiency', *Nature cell biology*, 19(9), pp. 1116-1129.
Gire, V., Roux, P., Wynford-Thomas, D., Brondello, J.M. and Dulic, V. (2004) 'DNA damage checkpoint kinase Chk2 triggers replicative senescence', *Embo j*, 23(13), pp. 2554-63.
Gluck, S., Guey, B., Gulen, M.F., Wolter, K., Kang, T.W., Schmacke, N.A., Bridgeman, A., Rehwinkel, J., Zender, L. and Ablasser, A. (2017) 'Innate immune sensing of cytosolic chromatin fragments through cGAS promotes senescence', *Nat Cell Biol*, 19(9), pp. 1061-1070.
Golden, E.B., Cho, H.Y., Hofman, F.M., Louie, S.G., Schonthal, A.H. and Chen, T.C. (2015) 'Quinoline-based antimalarial drugs: a novel class of autophagy inhibitors', *Neurosurg Focus*, 38(3), p. E12.
Gomes, A.P., Price, N.L., Ling, A.J., Moslehi, J.J., Montgomery, M.K., Rajman, L., White, J.P., Teodoro, J.S., Wrann, C.D., Hubbard, B.P., Mercken, E.M., Palmeira, C.M., de Cabo, R., Rolo, A.P., Turner, N., Bell, E.L. and Sinclair, D.A. (2013) 'Declining NAD(+) induces a

pseudohypoxic state disrupting nuclear-mitochondrial communication during aging', *Cell*, 155(7), pp. 1624-38.
Gorgoulis, V.G. and Halazonetis, T.D. (2010) 'Oncogene-induced senescence: the bright and dark side of the response', *Curr Opin Cell Biol*, 22(6), pp. 816-27.
Grabowska, W., Sikora, E. and Bielak-Zmijewska, A. (2017) 'Sirtuins, a promising target in slowing down the ageing process', *Biogerontology*, 18(4), pp. 447-476.
Grazioli, S. and Pugin, J. (2018) 'Mitochondrial Damage-Associated Molecular Patterns: From Inflammatory Signaling to Human Diseases', *Frontiers in immunology*, 9, pp. 832-832.
Grewal, S.I. and Jia, S. (2007) 'Heterochromatin revisited', *Nat Rev Genet*, 8(1), pp. 35-46.
Griffith, J.D., Comeau, L., Rosenfield, S., Stansel, R.M., Bianchi, A., Moss, H. and de Lange, T. (1999) 'Mammalian telomeres end in a large duplex loop', *Cell*, 97(4), pp. 503-14.
Gustafsson, C.M., Falkenberg, M. and Larsson, N.G. (2016) 'Maintenance and Expression of Mammalian Mitochondrial DNA', *Annu Rev Biochem*, 85, pp. 133-60.
Halestrap, A.P. (2009) 'What is the mitochondrial permeability transition pore?', *J Mol Cell Cardiol*, 46(6), pp. 821-31.
Halestrap, A.P., Connern, C.P., Griffiths, E.J. and Kerr, P.M. (1997) 'Cyclosporin A binding to mitochondrial cyclophilin inhibits the permeability transition pore and protects hearts from ischaemia/reperfusion injury', *Mol Cell Biochem*, 174(1-2), pp. 167-72.
Hamilton, M.L., Van Remmen, H., Drake, J.A., Yang, H., Guo, Z.M., Kewitt, K., Walter, C.A. and Richardson, A. (2001) 'Does oxidative damage to DNA increase with age?', *Proc Natl Acad Sci U S A*, 98(18), pp. 10469-74.
Hari, P., Millar, F.R., Tarrats, N., Birch, J., Rink, C.J., Fernández-Duran, I., Muir, M., Finch, A.J., Brunton, V.G., Passos, J.F., Morton, J.P., Boulter, L. and Acosta, J.C. (2018) 'The innate immune sensor Toll-like receptor 2 controls the senescence-associated secretory phenotype', *bioRxiv*, p. 466755.
Harley, C.B., Futcher, A.B. and Greider, C.W. (1990) 'Telomeres shorten during ageing of human fibroblasts', *Nature*, 345(6274), pp. 458-60.
Harman, D. (1972) 'The biologic clock: the mitochondria?', *J Am Geriatr Soc*, 20(4), pp. 145-7.
Harrison, D.E., Strong, R., Sharp, Z.D., Nelson, J.F., Astle, C.M., Flurkey, K., Nadon, N.L., Wilkinson, J.E., Frenkel, K., Carter, C.S., Pahor, M., Javors, M.A., Fernandez, E. and Miller, R.A. (2009) 'Rapamycin fed late in life extends lifespan in genetically heterogeneous mice', *Nature*, 460(7253), pp. 392-395.
Hartlova, A., Erttmann, S.F., Raffi, F.A., Schmalz, A.M., Resch, U., Anugula, S., Lienenklaus, S., Nilsson, L.M., Kroger, A., Nilsson, J.A., Ek, T., Weiss, S. and Gekara, N.O. (2015) 'DNA damage primes the type I interferon system via the cytosolic DNA sensor STING to promote anti-microbial innate immunity', *Immunity*, 42(2), pp. 332-343.
Hashimoto, M., Asai, A., Kawagishi, H., Mikawa, R., Iwashita, Y., Kanayama, K., Sugimoto, K., Sato, T., Maruyama, M. and Sugimoto, M. (2016) 'Elimination of p19(ARF)-expressing cells enhances pulmonary function in mice', *JCI Insight*, 1(12), p. e87732.
Hayden, M.S. and Ghosh, S. (2008) 'Shared principles in NF-kappaB signaling', *Cell*, 132(3), pp. 344-62.
Hayflick, L. (1965) 'The Limited In Vitro Lifetime Of Human Diploid Cell Strains', *Exp Cell Res*, 37, pp. 614-36.
Hepple, R.T. (2016) 'Impact of aging on mitochondrial function in cardiac and skeletal muscle', *Free Radic Biol Med*, 98, pp. 177-186.
Herbig, U., Ferreira, M., Condel, L., Carey, D. and Sedivy, J.M. (2006) 'Cellular senescence in aging primates', *Science*, 311(5765), p. 1257.

Herbig, U., Jobling, W.A., Chen, B.P., Chen, D.J. and Sedivy, J.M. (2004) 'Telomere shortening triggers senescence of human cells through a pathway involving ATM, p53, and p21(CIP1), but not p16(INK4a)', *Mol Cell*, 14(4), pp. 501-13.
Herranz, N., Gallage, S., Mellone, M., Wuestefeld, T., Klotz, S., Hanley, C.J., Raguz, S., Acosta, J.C., Innes, A.J., Banito, A., Georgilis, A., Montoya, A., Wolter, K., Dharmalingam, G., Faull, P., Carroll, T., Martinez-Barbera, J.P., Cutillas, P., Reisinger, F., Heikenwalder, M., Miller, R.A., Withers, D., Zender, L., Thomas, G.J. and Gil, J. (2015) 'mTOR regulates MAPKAPK2 translation to control the senescence-associated secretory phenotype', *Nat Cell Biol*, 17(9), pp. 1205-17.
Hewitt, G., Jurk, D., Marques, F.D.M., Correia-Melo, C., Hardy, T., Gackowska, A., Anderson, R., Taschuk, M., Mann, J. and Passos, J.F. (2012) 'Telomeres are favoured targets of a persistent DNA damage response in ageing and stress-induced senescence', *Nat Commun*, 3, p. 708.
Hoffmann, J., Haendeler, J., Aicher, A., Rossig, L., Vasa, M., Zeiher, A.M. and Dimmeler, S. (2001) 'Aging enhances the sensitivity of endothelial cells toward apoptotic stimuli: important role of nitric oxide', *Circ Res*, 89(8), pp. 709-15.
Houssaini, A., Breau, M., Kebe, K., Abid, S., Marcos, E., Lipskaia, L., Rideau, D., Parpaleix, A., Huang, J., Amsellem, V., Vienney, N., Validire, P., Maitre, B., Attwe, A., Lukas, C., Vindrieux, D., Boczkowski, J., Derumeaux, G., Pende, M., Bernard, D., Meiners, S. and Adnot, S. (2018) 'mTOR pathway activation drives lung cell senescence and emphysema', *JCI insight*, 3(3), p. e93203.
Hubackova, S., Davidova, E., Rohlenova, K., Stursa, J., Werner, L., Andera, L., Dong, L., Terp, M.G., Hodny, Z., Ditzel, H.J., Rohlena, J. and Neuzil, J. (2019) 'Selective elimination of senescent cells by mitochondrial targeting is regulated by ANT2', *Cell Death Differ*, 26(2), pp. 276-290.
Huyen, Y., Zgheib, O., Ditullio, R.A., Jr., Gorgoulis, V.G., Zacharatos, P., Petty, T.J., Sheston, E.A., Mellert, H.S., Stavridi, E.S. and Halazonetis, T.D. (2004) 'Methylated lysine 79 of histone H3 targets 53BP1 to DNA double-strand breaks', *Nature*, 432(7015), pp. 406-11.
Ichim, G., Lopez, J., Ahmed, S.U., Muthalagu, N., Giampazolias, E., Delgado, M.E., Haller, M., Riley, J.S., Mason, S.M., Athineos, D., Parsons, M.J., van de Kooij, B., Bouchier-Hayes, L., Chalmers, A.J., Rooswinkel, R.W., Oberst, A., Blyth, K., Rehm, M., Murphy, D.J. and Tait, S.W. (2015) 'Limited mitochondrial permeabilization causes DNA damage and genomic instability in the absence of cell death', *Mol Cell*, 57(5), pp. 860-72.
Itahana, K., Campisi, J. and Dimri, G.P. (2004) 'Mechanisms of cellular senescence in human and mouse cells', *Biogerontology*, 5(1), pp. 1-10.
Ito, T., Teo, Y.V., Evans, S.A., Neretti, N. and Sedivy, J.M. (2018) 'Regulation of Cellular Senescence by Polycomb Chromatin Modifiers through Distinct DNA Damage- and Histone Methylation-Dependent Pathways', *Cell Rep*, 22(13), pp. 3480-3492.
Ivanov, A., Pawlikowski, J., Manoharan, I., van Tuyn, J., Nelson, D.M., Rai, T.S., Shah, P.P., Hewitt, G., Korolchuk, V.I., Passos, J.F., Wu, H., Berger, S.L. and Adams, P.D. (2013) 'Lysosome-mediated processing of chromatin in senescence', *J Cell Biol*, 202(1), pp. 129-43.
Jacobs, J.J. and de Lange, T. (2004) 'Significant role for p16INK4a in p53-independent telomere-directed senescence', *Curr Biol*, 14(24), pp. 2302-8.
Jacobs, J.J., Kieboom, K., Marino, S., DePinho, R.A. and van Lohuizen, M. (1999) 'The oncogene and Polycomb-group gene bmi-1 regulates cell proliferation and senescence through the ink4a locus', *Nature*, 397(6715), pp. 164-8.
Jendrach, M., Pohl, S., Voth, M., Kowald, A., Hammerstein, P. and Bereiter-Hahn, J. (2005) 'Morpho-dynamic changes of mitochondria during ageing of human endothelial cells', *Mech Ageing Dev*, 126(6-7), pp. 813-21.

Jennings, P., Koppelstaetter, C., Aydin, S., Abberger, T., Wolf, A.M., Mayer, G. and Pfaller, W. (2007) 'Cyclosporine A induces senescence in renal tubular epithelial cells', *Am J Physiol Renal Physiol*, 293(3), pp. F831-8.
Jeon, O.H., Kim, C., Laberge, R.M., Demaria, M., Rathod, S., Vasserot, A.P., Chung, J.W., Kim, D.H., Poon, Y., David, N., Baker, D.J., van Deursen, J.M., Campisi, J. and Elisseeff, J.H. (2017) 'Local clearance of senescent cells attenuates the development of post-traumatic osteoarthritis and creates a pro-regenerative environment', *Nat Med*.
Jeyapalan, J.C., Ferreira, M., Sedivy, J.M. and Herbig, U. (2007) 'Accumulation of senescent cells in mitotic tissue of aging primates', *Mech Ageing Dev*, 128(1), pp. 36-44.
Jiang, P., Du, W., Mancuso, A., Wellen, K.E. and Yang, X. (2013) 'Reciprocal regulation of p53 and malic enzymes modulates metabolism and senescence', *Nature*, 493(7434), pp. 689-93.
Jo, E.-K., Kim, J.K., Shin, D.-M. and Sasakawa, C. (2016) 'Molecular mechanisms regulating NLRP3 inflammasome activation', *Cellular & molecular immunology*, 13(2), pp. 148-159.
Jurk, D., Wang, C., Miwa, S., Maddick, M., Korolchuk, V., Tsolou, A., Gonos, E.S., Thrasivoulou, C., Saffrey, M.J., Cameron, K. and von Zglinicki, T. (2012) 'Postmitotic neurons develop a p21-dependent senescence-like phenotype driven by a DNA damage response', *Aging Cell*, 11(6), pp. 996-1004.
Jurk, D., Wilson, C., Passos, J.F., Oakley, F., Correia-Melo, C., Greaves, L., Saretzki, G., Fox, C., Lawless, C., Anderson, R., Hewitt, G., Pender, S.L., Fullard, N., Nelson, G., Mann, J., van de Sluis, B., Mann, D.A. and von Zglinicki, T. (2014) 'Chronic inflammation induces telomere dysfunction and accelerates ageing in mice', *Nat Commun*, 2, p. 4172.
Justice, J.N., Nambiar, A.M., Tchkonia, T., LeBrasseur, N.K., Pascual, R., Hashmi, S.K., Prata, L., Masternak, M.M., Kritchevsky, S.B., Musi, N. and Kirkland, J.L. (2019) 'Senolytics in idiopathic pulmonary fibrosis: Results from a first-in-human, open-label, pilot study', *EBioMedicine*, 40, pp. 554-563.
Kaefer, A., Yang, J., Noertersheuser, P., Mensing, S., Humerickhouse, R., Awni, W. and Xiong, H. (2014) 'Mechanism-based pharmacokinetic/pharmacodynamic meta-analysis of navitoclax (ABT-263) induced thrombocytopenia', *Cancer Chemother Pharmacol*, 74(3), pp. 593-602.
Kang, C., Xu, Q., Martin, T.D., Li, M.Z., Demaria, M., Aron, L., Lu, T., Yankner, B.A., Campisi, J. and Elledge, S.J. (2015) 'The DNA damage response induces inflammation and senescence by inhibiting autophagy of GATA4', *Science*, 349(6255), p. aaa5612.
Kang, H.R., Cho, S.J., Lee, C.G., Homer, R.J. and Elias, J.A. (2007) 'Transforming growth factor (TGF)-beta1 stimulates pulmonary fibrosis and inflammation via a Bax-dependent, bid-activated pathway that involves matrix metalloproteinase-12', *J Biol Chem*, 282(10), pp. 7723-32.
Kang, H.T., Lee, H.I. and Hwang, E.S. (2006) 'Nicotinamide extends replicative lifespan of human cells', *Aging Cell*, 5(5), pp. 423-36.
Kang, H.T., Lee, K.B., Kim, S.Y., Choi, H.R. and Park, S.C. (2011a) 'Autophagy impairment induces premature senescence in primary human fibroblasts', *PLoS One*, 6(8), p. e23367.
Kang, T.-B., Ben-Moshe, T., Varfolomeev, E.E., Pewzner-Jung, Y., Yogev, N., Jurewicz, A., Waisman, A., Brenner, O., Haffner, R., Gustafsson, E., Ramakrishnan, P., Lapidot, T. and Wallach, D. (2004) 'Caspase-8 Serves Both Apoptotic and Nonapoptotic Roles', *The Journal of Immunology*, 173(5), pp. 2976-2984.
Kang, T.W., Yevsa, T., Woller, N., Hoenicke, L., Wuestefeld, T., Dauch, D., Hohmeyer, A., Gereke, M., Rudalska, R., Potapova, A., Iken, M., Vucur, M., Weiss, S., Heikenwalder, M., Khan, S., Gil, J., Bruder, D., Manns, M., Schirmacher, P., Tacke, F., Ott, M., Luedde, T., Longerich, T., Kubicka, S. and Zender, L. (2011b) 'Senescence surveillance of pre-malignant hepatocytes limits liver cancer development', *Nature*, 479(7374), pp. 547-51.

Karbowski, M., Lee, Y.J., Gaume, B., Jeong, S.Y., Frank, S., Nechushtan, A., Santel, A., Fuller, M., Smith, C.L. and Youle, R.J. (2002) 'Spatial and temporal association of Bax with mitochondrial fission sites, Drp1, and Mfn2 during apoptosis', *J Cell Biol*, 159(6), pp. 931-8.
Karimian, A., Ahmadi, Y. and Yousefi, B. (2016) 'Multiple functions of p21 in cell cycle, apoptosis and transcriptional regulation after DNA damage', *DNA Repair (Amst)*, 42, pp. 63-71.
Katlinskaya, Y.V., Katlinski, K.V., Yu, Q., Ortiz, A., Beiting, D.P., Brice, A., Davar, D., Sanders, C., Kirkwood, J.M., Rui, H., Xu, X., Koumenis, C., Diehl, J.A. and Fuchs, S.Y. (2016) 'Suppression of Type I Interferon Signaling Overcomes Oncogene-Induced Senescence and Mediates Melanoma Development and Progression', *Cell Rep*, 15(1), pp. 171-180.
Kayo, T., Allison, D.B., Weindruch, R. and Prolla, T.A. (2001) 'Influences of aging and caloric restriction on the transcriptional profile of skeletal muscle from rhesus monkeys', *Proc Natl Acad Sci U S A*, 98(9), pp. 5093-8.
Khanna, A.K. (2009) 'Enhanced susceptibility of cyclin kinase inhibitor p21 knockout mice to high fat diet induced atherosclerosis', *J Biomed Sci*, 16, p. 66.
Kim, S.J., Mehta, H.H., Wan, J., Kuehnemann, C., Chen, J., Hu, J.F., Hoffman, A.R. and Cohen, P. (2018) 'Mitochondrial peptides modulate mitochondrial function during cellular senescence', *Aging (Albany NY)*, 10(6), pp. 1239-1256.
Kim, W.Y. and Sharpless, N.E. (2006) 'The regulation of INK4/ARF in cancer and aging', *Cell*, 127(2), pp. 265-75.
Kirkland, J.L., Tchkonia, T., Zhu, Y., Niedernhofer, L.J. and Robbins, P.D. (2017) 'The Clinical Potential of Senolytic Drugs', *J Am Geriatr Soc*, 65(10), pp. 2297-2301.
Ko, J.H., Yoon, S.O., Lee, H.J. and Oh, J.Y. (2017) 'Rapamycin regulates macrophage activation by inhibiting NLRP3 inflammasome-p38 MAPK-NFkappaB pathways in autophagy- and p62-dependent manners', *Oncotarget*, 8(25), pp. 40817-40831.
Kosar, M., Bartkova, J., Hubackova, S., Hodny, Z., Lukas, J. and Bartek, J. (2011) 'Senescence-associated heterochromatin foci are dispensable for cellular senescence, occur in a cell type- and insult-dependent manner and follow expression of p16(ink4a)', *Cell Cycle*, 10(3), pp. 457-68.
Kothakota, S., Azuma, T., Reinhard, C., Klippel, A., Tang, J., Chu, K., McGarry, T.J., Kirschner, M.W., Koths, K., Kwiatkowski, D.J. and Williams, L.T. (1997) 'Caspase-3-generated fragment of gelsolin: effector of morphological change in apoptosis', *Science*, 278(5336), pp. 294-8.
Krimpenfort, P., Quon, K.C., Mooi, W.J., Loonstra, A. and Berns, A. (2001) 'Loss of p16Ink4a confers susceptibility to metastatic melanoma in mice', *Nature*, 413(6851), pp. 83-6.
Krishnamurthy, J., Torrice, C., Ramsey, M.R., Kovalev, G.I., Al-Regaiey, K., Su, L. and Sharpless, N.E. (2004) 'Ink4a/Arf expression is a biomarker of aging', *J Clin Invest*, 114(9), pp. 1299-307.
Krizhanovsky, V., Yon, M., Dickins, R.A., Hearn, S., Simon, J., Miething, C., Yee, H., Zender, L. and Lowe, S.W. (2008) 'Senescence of activated stellate cells limits liver fibrosis', *Cell*, 134(4), pp. 657-67.
Krtolica, A., Parrinello, S., Lockett, S., Desprez, P.Y. and Campisi, J. (2001) 'Senescent fibroblasts promote epithelial cell growth and tumorigenesis: a link between cancer and aging', *Proc Natl Acad Sci U S A*, 98(21), pp. 12072-7.
Kruk, P.A., Rampino, N.J. and Bohr, V.A. (1995) 'DNA damage and repair in telomeres: relation to aging', *Proceedings of the National Academy of Sciences of the United States of America*, 92(1), pp. 258-262.
Kuilman, T., Michaloglou, C., Vredeveld, L.C., Douma, S., van Doorn, R., Desmet, C.J., Aarden, L.A., Mooi, W.J. and Peeper, D.S. (2008) 'Oncogene-induced senescence relayed by an interleukin-dependent inflammatory network', *Cell*, 133(6), pp. 1019-31.

Kuzelova, K., Grebenova, D. and Brodska, B. (2011) 'Dose-dependent effects of the caspase inhibitor Q-VD-OPh on different apoptosis-related processes', *J Cell Biochem*, 112(11), pp. 3334-42.
Kuznik, A., Bencina, M., Svajger, U., Jeras, M., Rozman, B. and Jerala, R. (2011) 'Mechanism of endosomal TLR inhibition by antimalarial drugs and imidazoquinolines', *J Immunol*, 186(8), pp. 4794-804.
Lan, Y.Y., Londono, D., Bouley, R., Rooney, M.S. and Hacohen, N. (2014) 'Dnase2a deficiency uncovers lysosomal clearance of damaged nuclear DNA via autophagy', *Cell Rep*, 9(1), pp. 180-192.
Lawless, C., Wang, C., Jurk, D., Merz, A., Zglinicki, T. and Passos, J.F. (2010) 'Quantitative assessment of markers for cell senescence', *Exp Gerontol*, 45(10), pp. 772-8.
Lee, A.C., Fenster, B.E., Ito, H., Takeda, K., Bae, N.S., Hirai, T., Yu, Z.X., Ferrans, V.J., Howard, B.H. and Finkel, T. (1999) 'Ras proteins induce senescence by altering the intracellular levels of reactive oxygen species', *J Biol Chem*, 274(12), pp. 7936-40.
Lee, B.Y., Han, J.A., Im, J.S., Morrone, A., Johung, K., Goodwin, E.C., Kleijer, W.J., DiMaio, D. and Hwang, E.S. (2006) 'Senescence-associated beta-galactosidase is lysosomal beta-galactosidase', *Aging Cell*, 5(2), pp. 187-95.
Lee, S., Jeong, S.Y., Lim, W.C., Kim, S., Park, Y.Y., Sun, X., Youle, R.J. and Cho, H. (2007) 'Mitochondrial fission and fusion mediators, hFis1 and OPA1, modulate cellular senescence', *J Biol Chem*, 282(31), pp. 22977-83.
Lee, S.M., Dho, S.H., Ju, S.K., Maeng, J.S., Kim, J.Y. and Kwon, K.S. (2012) 'Cytosolic malate dehydrogenase regulates senescence in human fibroblasts', *Biogerontology*, 13(5), pp. 525-36.
Leifer, C.A., Kennedy, M.N., Mazzoni, A., Lee, C., Kruhlak, M.J. and Segal, D.M. (2004) 'TLR9 is localized in the endoplasmic reticulum prior to stimulation', *Journal of immunology (Baltimore, Md. : 1950)*, 173(2), pp. 1179-1183.
Lemasters, J.J. and Holmuhamedov, E. (2006) 'Voltage-dependent anion channel (VDAC) as mitochondrial governator--thinking outside the box', *Biochim Biophys Acta*, 1762(2), pp. 181-90.
Lesniewski, L.A., Seals, D.R., Walker, A.E., Henson, G.D., Blimline, M.W., Trott, D.W., Bosshardt, G.C., LaRocca, T.J., Lawson, B.R., Zigler, M.C. and Donato, A.J. (2017) 'Dietary rapamycin supplementation reverses age-related vascular dysfunction and oxidative stress, while modulating nutrient-sensing, cell cycle, and senescence pathways', *Aging cell*, 16(1), pp. 17-26.
Lewis-McDougall, F.C., Ruchaya, P.J., Domenjo-Vila, E., Shin Teoh, T., Prata, L., Cottle, B.J., Clark, J.E., Punjabi, P.P., Awad, W., Torella, D., Tchkonia, T., Kirkland, J.L. and Ellison-Hughes, G.M. (2019) 'Aged-senescent cells contribute to impaired heart regeneration', *Aging Cell*, 18(3), p. e12931.
Li, A., Zhang, S., Li, J., Liu, K., Huang, F. and Liu, B. (2016) 'Metformin and resveratrol inhibit Drp1-mediated mitochondrial fission and prevent ER stress-associated NLRP3 inflammasome activation in the adipose tissue of diabetic mice', *Mol Cell Endocrinol*, 434, pp. 36-47.
Li, P., Nijhawan, D., Budihardjo, I., Srinivasula, S.M., Ahmad, M., Alnemri, E.S. and Wang, X. (1997) 'Cytochrome c and dATP-dependent formation of Apaf-1/caspase-9 complex initiates an apoptotic protease cascade', *Cell*, 91(4), pp. 479-89.
Li, T. and Chen, Z.J. (2018) 'The cGAS–cGAMP–STING pathway connects DNA damage to inflammation, senescence, and cancer', *The Journal of Experimental Medicine*, 215(5), pp. 1287-1299.
Little, J.P., Simtchouk, S., Schindler, S.M., Villanueva, E.B., Gill, N.E., Walker, D.G., Wolthers, K.R. and Klegeris, A. (2014) 'Mitochondrial transcription factor A (Tfam) is a pro-inflammatory extracellular signaling molecule recognized by brain microglia', *Mol Cell Neurosci*, 60, pp. 88-96.

Liu, L., Trimarchi, J.R., Smith, P.J. and Keefe, D.L. (2002) 'Mitochondrial dysfunction leads to telomere attrition and genomic instability', *Aging Cell*, 1(1), pp. 40-6.
Liu, S., Cai, X., Wu, J., Cong, Q., Chen, X., Li, T., Du, F., Ren, J., Wu, Y.T., Grishin, N.V. and Chen, Z.J. (2015) 'Phosphorylation of innate immune adaptor proteins MAVS, STING, and TRIF induces IRF3 activation', *Science*, 347(6227), p. aaa2630.
Llambi, F., Moldoveanu, T., Tait, S.W., Bouchier-Hayes, L., Temirov, J., McCormick, L.L., Dillon, C.P. and Green, D.R. (2011) 'A unified model of mammalian BCL-2 protein family interactions at the mitochondria', *Mol Cell*, 44(4), pp. 517-31.
Lopez-Otin, C., Blasco, M.A., Partridge, L., Serrano, M. and Kroemer, G. (2013) 'The hallmarks of aging', *Cell*, 153(6), pp. 1194-217.
Luo, Y., Zou, P., Zou, J., Wang, J., Zhou, D. and Liu, L. (2011) 'Autophagy regulates ROS-induced cellular senescence via p21 in a p38 MAPKalpha dependent manner', *Exp Gerontol*, 46(11), pp. 860-7.
Macip, S., Igarashi, M., Fang, L., Chen, A., Pan, Z.Q., Lee, S.W. and Aaronson, S.A. (2002) 'Inhibition of p21-mediated ROS accumulation can rescue p21-induced senescence', *Embo j*, 21(9), pp. 2180-8.
Mai, S., Klinkenberg, M., Auburger, G., Bereiter-Hahn, J. and Jendrach, M. (2010) 'Decreased expression of Drp1 and Fis1 mediates mitochondrial elongation in senescent cells and enhances resistance to oxidative stress through PINK1', *J Cell Sci*, 123(Pt 6), pp. 917-26.
Mailand, N., Falck, J., Lukas, C., Syljuasen, R.G., Welcker, M., Bartek, J. and Lukas, J. (2000) 'Rapid destruction of human Cdc25A in response to DNA damage', *Science*, 288(5470), pp. 1425-9.
Makhov, P., Golovine, K., Teper, E., Kutikov, A., Mehrazin, R., Corcoran, A., Tulin, A., Uzzo, R.G. and Kolenko, V.M. (2014) 'Piperlongumine promotes autophagy via inhibition of Akt/mTOR signalling and mediates cancer cell death', *Br J Cancer*, 110(4), pp. 899-907.
Manzella, N., Santin, Y., Maggiorani, D., Martini, H., Douin-Echinard, V., Passos, J.F., Lezoualc'h, F., Binda, C., Parini, A. and Mialet-Perez, J. (2018) 'Monoamine oxidase-A is a novel driver of stress-induced premature senescence through inhibition of parkin-mediated mitophagy', *Aging Cell*, 17(5), p. e12811.
Marechal, A. and Zou, L. (2013) 'DNA damage sensing by the ATM and ATR kinases', *Cold Spring Harb Perspect Biol*, 5(9).
Martinon, F. and Tschopp, J. (2004) 'Inflammatory caspases: linking an intracellular innate immune system to autoinflammatory diseases', *Cell*, 117(5), pp. 561-74.
Matarrese, P., Straface, E., Pietraforte, D., Gambardella, L., Vona, R., Maccaglia, A., Minetti, M. and Malorni, W. (2005) 'Peroxynitrite induces senescence and apoptosis of red blood cells through the activation of aspartyl and cysteinyl proteases', *Faseb j*, 19(3), pp. 416-8.
McArthur, K., Whitehead, L.W., Heddleston, J.M., Li, L., Padman, B.S., Oorschot, V., Geoghegan, N.D., Chappaz, S., Davidson, S., San Chin, H., Lane, R.M., Dramicanin, M., Saunders, T.L., Sugiana, C., Lessene, R., Osellame, L.D., Chew, T.L., Dewson, G., Lazarou, M., Ramm, G., Lessene, G., Ryan, M.T., Rogers, K.L., van Delft, M.F. and Kile, B.T. (2018) 'BAK/BAX macropores facilitate mitochondrial herniation and mtDNA efflux during apoptosis', *Science*, 359(6378).
McCarroll, S.A., Murphy, C.T., Zou, S., Pletcher, S.D., Chin, C.S., Jan, Y.N., Kenyon, C., Bargmann, C.I. and Li, H. (2004) 'Comparing genomic expression patterns across species identifies shared transcriptional profile in aging', *Nat Genet*, 36(2), pp. 197-204.
McCarthy, D.A., Clark, R.R., Bartling, T.R., Trebak, M. and Melendez, J.A. (2013) 'Redox control of the senescence regulator interleukin-1alpha and the secretory phenotype', *J Biol Chem*, 288(45), pp. 32149-59.

Mehta, I.S., Figgitt, M., Clements, C.S., Kill, I.R. and Bridger, J.M. (2007) 'Alterations to nuclear architecture and genome behavior in senescent cells', *Ann N Y Acad Sci*, 1100, pp. 250-63.
Melk, A., Schmidt, B.M., Takeuchi, O., Sawitzki, B., Rayner, D.C. and Halloran, P.F. (2004) 'Expression of p16INK4a and other cell cycle regulator and senescence associated genes in aging human kidney', *Kidney Int*, 65(2), pp. 510-20.
Menck, C.F. and Munford, V. (2014) 'DNA repair diseases: What do they tell us about cancer and aging?', *Genetics and molecular biology*, 37(1 Suppl), pp. 220-233.
Meng, A., Wang, Y., Van Zant, G. and Zhou, D. (2003) 'Ionizing radiation and busulfan induce premature senescence in murine bone marrow hematopoietic cells', *Cancer Res*, 63(17), pp. 5414-9.
Mercer, J., Figg, N., Stoneman, V., Braganza, D. and Bennett, M.R. (2005) 'Endogenous p53 protects vascular smooth muscle cells from apoptosis and reduces atherosclerosis in ApoE knockout mice', *Circ Res*, 96(6), pp. 667-74.
Mhaidat, N.M., Zhang, X.D., Allen, J., Avery-Kiejda, K.A., Scott, R.J. and Hersey, P. (2007) 'Temozolomide induces senescence but not apoptosis in human melanoma cells', *British journal of cancer*, 97(9), pp. 1225-1233.
Mihaylova, M.M. and Shaw, R.J. (2011) 'The AMPK signalling pathway coordinates cell growth, autophagy and metabolism', *Nat Cell Biol*, 13(9), pp. 1016-23.
Mikhailov, V., Mikhailova, M., Degenhardt, K., Venkatachalam, M.A., White, E. and Saikumar, P. (2003) 'Association of Bax and Bak homo-oligomers in mitochondria. Bax requirement for Bak reorganization and cytochrome c release', *J Biol Chem*, 278(7), pp. 5367-76.
Mizuno, S., Bogaard, H.J., Kraskauskas, D., Alhussaini, A., Gomez-Arroyo, J., Voelkel, N.F. and Ishizaki, T. (2011) 'p53 Gene deficiency promotes hypoxia-induced pulmonary hypertension and vascular remodeling in mice', *Am J Physiol Lung Cell Mol Physiol*, 300(5), pp. L753-61.
Moiseeva, O., Bourdeau, V., Roux, A., Deschenes-Simard, X. and Ferbeyre, G. (2009) 'Mitochondrial dysfunction contributes to oncogene-induced senescence', *Mol Cell Biol*, 29(16), pp. 4495-507.
Moiseeva, O., Mallette, F.A., Mukhopadhyay, U.K., Moores, A. and Ferbeyre, G. (2006) 'DNA damage signaling and p53-dependent senescence after prolonged beta-interferon stimulation', *Mol Biol Cell*, 17(4), pp. 1583-92.
Montecino-Rodriguez, E., Berent-Maoz, B. and Dorshkind, K. (2013) 'Causes, consequences, and reversal of immune system aging', *J Clin Invest*, 123(3), pp. 958-65.
Montessuit, S., Somasekharan, S.P., Terrones, O., Lucken-Ardjomande, S., Herzig, S., Schwarzenbacher, R., Manstein, D.J., Bossy-Wetzel, E., Basanez, G., Meda, P. and Martinou, J.C. (2010) 'Membrane remodeling induced by the dynamin-related protein Drp1 stimulates Bax oligomerization', *Cell*, 142(6), pp. 889-901.
Morchikh, M., Cribier, A., Raffel, R., Amraoui, S., Cau, J., Severac, D., Dubois, E., Schwartz, O., Bennasser, Y. and Benkirane, M. (2017) 'HEXIM1 and NEAT1 Long Non-coding RNA Form a Multi-subunit Complex that Regulates DNA-Mediated Innate Immune Response', *Mol Cell*, 67(3), pp. 387-399.e5.
Mouchess, M.L., Arpaia, N., Souza, G., Barbalat, R., Ewald, S.E., Lau, L. and Barton, G.M. (2011) 'Transmembrane mutations in Toll-like receptor 9 bypass the requirement for ectodomain proteolysis and induce fatal inflammation', *Immunity*, 35(5), pp. 721-32.
Mouraret, N., Marcos, E., Abid, S., Gary-Bobo, G., Saker, M., Houssaini, A., Dubois-Rande, J.L., Boyer, L., Boczkowski, J., Derumeaux, G., Amsellem, V. and Adnot, S. (2013) 'Activation of lung p53 by Nutlin-3a prevents and reverses experimental pulmonary hypertension', *Circulation*, 127(16), pp. 1664-76.

Muller, F.L., Lustgarten, M.S., Jang, Y., Richardson, A. and Van Remmen, H. (2007) 'Trends in oxidative aging theories', *Free Radic Biol Med*, 43(4), pp. 477-503.
Munoz-Espin, D., Canamero, M., Maraver, A., Gomez-Lopez, G., Contreras, J., Murillo-Cuesta, S., Rodriguez-Baeza, A., Varela-Nieto, I., Ruberte, J., Collado, M. and Serrano, M. (2013) 'Programmed cell senescence during mammalian embryonic development', *Cell*, 155(5), pp. 1104-18.
Munoz-Espin, D., Rovira, M., Galiana, I., Gimenez, C., Lozano-Torres, B., Paez-Ribes, M., Llanos, S., Chaib, S., Munoz-Martin, M., Ucero, A.C., Garaulet, G., Mulero, F., Dann, S.G., VanArsdale, T., Shields, D.J., Bernardos, A., Murguia, J.R., Martinez-Manez, R. and Serrano, M. (2018) 'A versatile drug delivery system targeting senescent cells', *EMBO Mol Med*, 10(9).
Muñoz-Espín, D. and Serrano, M. (2014) 'Cellular senescence: from physiology to pathology', *Nature Reviews Molecular Cell Biology*, 15, p. 482.
Murray-Zmijewski, F., Slee, E.A. and Lu, X. (2008) 'A complex barcode underlies the heterogeneous response of p53 to stress', *Nat Rev Mol Cell Biol*, 9(9), pp. 702-12.
Musi, N., Valentine, J.M., Sickora, K.R., Baeuerle, E., Thompson, C.S., Shen, Q. and Orr, M.E. (2018) 'Tau protein aggregation is associated with cellular senescence in the brain', *Aging Cell*, 17(6), p. e12840.
Nacarelli, T., Lau, L., Fukumoto, T., Zundell, J., Fatkhutdinov, N., Wu, S., Aird, K.M., Iwasaki, O., Kossenkov, A.V., Schultz, D., Noma, K.I., Baur, J.A., Schug, Z., Tang, H.Y., Speicher, D.W., David, G. and Zhang, R. (2019) 'NAD(+) metabolism governs the proinflammatory senescence-associated secretome', *Nat Cell Biol*, 21(3), pp. 397-407.
Nakahira, K., Haspel, J.A., Rathinam, V.A., Lee, S.J., Dolinay, T., Lam, H.C., Englert, J.A., Rabinovitch, M., Cernadas, M., Kim, H.P., Fitzgerald, K.A., Ryter, S.W. and Choi, A.M. (2011) 'Autophagy proteins regulate innate immune responses by inhibiting the release of mitochondrial DNA mediated by the NALP3 inflammasome', *Nat Immunol*, 12(3), pp. 222-30.
Narita, M., Narita, M., Krizhanovsky, V., Nunez, S., Chicas, A., Hearn, S.A., Myers, M.P. and Lowe, S.W. (2006) 'A novel role for high-mobility group a proteins in cellular senescence and heterochromatin formation', *Cell*, 126(3), pp. 503-14.
Narita, M., Nunez, S., Heard, E., Narita, M., Lin, A.W., Hearn, S.A., Spector, D.L., Hannon, G.J. and Lowe, S.W. (2003) 'Rb-mediated heterochromatin formation and silencing of E2F target genes during cellular senescence', *Cell*, 113(6), pp. 703-16.
Narita, M., Young, A.R., Arakawa, S., Samarajiwa, S.A., Nakashima, T., Yoshida, S., Hong, S., Berry, L.S., Reichelt, S., Ferreira, M., Tavare, S., Inoki, K., Shimizu, S. and Narita, M. (2011) 'Spatial coupling of mTOR and autophagy augments secretory phenotypes', *Science*, 332(6032), pp. 966-70.
Nelson, G., Kucheryavenko, O., Wordsworth, J. and von Zglinicki, T. (2018) 'The senescent bystander effect is caused by ROS-activated NF-κB signalling', *Mechanisms of ageing and development*, 170, pp. 30-36.
Nelson, G., Wordsworth, J., Wang, C., Jurk, D., Lawless, C., Martin-Ruiz, C. and von Zglinicki, T. (2012) 'A senescent cell bystander effect: senescence-induced senescence', *Aging Cell*, 11(2), pp. 345-9.
Nicholls, D.G. (2004) 'Mitochondrial membrane potential and aging', *Aging Cell*, 3(1), pp. 35-40.
Nunnari, J. and Suomalainen, A. (2012) 'Mitochondria: in sickness and in health', *Cell*, 148(6), pp. 1145-59.
Odell, A., Askham, J., Whibley, C. and Hollstein, M. (2010) 'How to become immortal: let MEFs count the ways', *Aging*, 2(3), pp. 160-165.
Ogrodnik, M., Miwa, S., Tchkonia, T., Tiniakos, D., Wilson, C.L., Lahat, A., Day, C.P., Burt, A., Palmer, A., Anstee, Q.M., Grellscheid, S.N., Hoeijmakers, J.H.J., Barnhoorn, S., Mann,

D.A., Bird, T.G., Vermeij, W.P., Kirkland, J.L., Passos, J.F., von Zglinicki, T. and Jurk, D. (2017) 'Cellular senescence drives age-dependent hepatic steatosis', *Nat Commun*, 8, p. 15691.
Ogrodnik, M., Zhu, Y., Langhi, L.G.P., Tchkonia, T., Kruger, P., Fielder, E., Victorelli, S., Ruswhandi, R.A., Giorgadze, N., Pirtskhalava, T., Podgorni, O., Enikolopov, G., Johnson, K.O., Xu, M., Inman, C., Palmer, A.K., Schafer, M., Weigl, M., Ikeno, Y., Burns, T.C., Passos, J.F., von Zglinicki, T., Kirkland, J.L. and Jurk, D. (2019) 'Obesity-Induced Cellular Senescence Drives Anxiety and Impairs Neurogenesis', *Cell Metab*.
Oliver, C.N., Ahn, B.W., Moerman, E.J., Goldstein, S. and Stadtman, E.R. (1987) 'Age-related changes in oxidized proteins', *J Biol Chem*, 262(12), pp. 5488-91.
Olovnikov, A.M. (1971) '[Principle of marginotomy in template synthesis of polynucleotides]', *Dokl Akad Nauk SSSR*, 201(6), pp. 1496-9.
Ovadya, Y., Landsberger, T., Leins, H., Vadai, E., Gal, H., Biran, A., Yosef, R., Sagiv, A., Agrawal, A., Shapira, A., Windheim, J., Tsoory, M., Schirmbeck, R., Amit, I., Geiger, H. and Krizhanovsky, V. (2018) 'Impaired immune surveillance accelerates accumulation of senescent cells and aging', *Nat Commun*, 9(1), p. 5435.
Packer, L. and Fuehr, K. (1977) 'Low oxygen concentration extends the lifespan of cultured human diploid cells', *Nature*, 267(5610), pp. 423-5.
Palmer, A.K., Xu, M., Zhu, Y., Pirtskhalava, T., Weivoda, M.M., Hachfeld, C.M., Prata, L.G., van Dijk, T.H., Verkade, E., Casaclang-Verzosa, G., Johnson, K.O., Cubro, H., Doornebal, E.J., Ogrodnik, M., Jurk, D., Jensen, M.D., Chini, E.N., Miller, J.D., Matveyenko, A., Stout, M.B., Schafer, M.J., White, T.A., Hickson, L.J., Demaria, M., Garovic, V., Grande, J., Arriaga, E.A., Kuipers, F., von Zglinicki, T., LeBrasseur, N.K., Campisi, J., Tchkonia, T. and Kirkland, J.L. (2019) 'Targeting senescent cells alleviates obesity-induced metabolic dysfunction', *Aging Cell*, p. e12950.
Panel, M., Ghaleb, B. and Morin, D. (2018) 'Mitochondria and aging: A role for the mitochondrial transition pore?', *Aging cell*, 17(4), pp. e12793-e12793.
Pang, J.H. and Chen, K.Y. (1994) 'Global change of gene expression at late G1/S boundary may occur in human IMR-90 diploid fibroblasts during senescence', *J Cell Physiol*, 160(3), pp. 531-8.
Pang, Y.P., Dai, H., Smith, A., Meng, X.W., Schneider, P.A. and Kaufmann, S.H. (2012) 'Bak Conformational Changes Induced by Ligand Binding: Insight into BH3 Domain Binding and Bak Homo-Oligomerization', *Sci Rep*, 2, p. 257.
Pantoja, C. and Serrano, M. (1999) 'Murine fibroblasts lacking p21 undergo senescence and are resistant to transformation by oncogenic Ras', *Oncogene*, 18(35), pp. 4974-82.
Park, Y.Y., Lee, S., Karbowski, M., Neutzner, A., Youle, R.J. and Cho, H. (2010) 'Loss of MARCH5 mitochondrial E3 ubiquitin ligase induces cellular senescence through dynamin-related protein 1 and mitofusin 1', *J Cell Sci*, 123(Pt 4), pp. 619-26.
Passos, J.F., Nelson, G., Wang, C., Richter, T., Simillion, C., Proctor, C.J., Miwa, S., Olijslagers, S., Hallinan, J., Wipat, A., Saretzki, G., Rudolph, K.L., Kirkwood, T.B. and von Zglinicki, T. (2010) 'Feedback between p21 and reactive oxygen production is necessary for cell senescence', *Mol Syst Biol*, 6, p. 347.
Passos, J.F., Saretzki, G., Ahmed, S., Nelson, G., Richter, T., Peters, H., Wappler, I., Birket, M.J., Harold, G., Schaeuble, K., Birch-Machin, M.A., Kirkwood, T.B. and von Zglinicki, T. (2007) 'Mitochondrial dysfunction accounts for the stochastic heterogeneity in telomere-dependent senescence', *PLoS Biol*, 5(5), p. e110.
Patrushev, M., Kasymov, V., Patrusheva, V., Ushakova, T., Gogvadze, V. and Gaziev, A. (2004) 'Mitochondrial permeability transition triggers the release of mtDNA fragments', *Cell Mol Life Sci*, 61(24), pp. 3100-3.

Perrott, K.M., Wiley, C.D., Desprez, P.Y. and Campisi, J. (2017) 'Apigenin suppresses the senescence-associated secretory phenotype and paracrine effects on breast cancer cells', *Geroscience*, 39(2), pp. 161-173.
Petersen, S., Saretzki, G. and von Zglinicki, T. (1998) 'Preferential accumulation of single-stranded regions in telomeres of human fibroblasts', *Exp Cell Res*, 239(1), pp. 152-60.
Pinti, M., Cevenini, E., Nasi, M., De Biasi, S., Salvioli, S., Monti, D., Benatti, S., Gibellini, L., Cotichini, R., Stazi, M.A., Trenti, T., Franceschi, C. and Cossarizza, A. (2014) 'Circulating mitochondrial DNA increases with age and is a familiar trait: Implications for "inflamm-aging"', *Eur J Immunol*, 44(5), pp. 1552-62.
Pitiyage, G.N., Slijepcevic, P., Gabrani, A., Chianea, Y.G., Lim, K.P., Prime, S.S., Tilakaratne, W.M., Fortune, F. and Parkinson, E.K. (2011) 'Senescent mesenchymal cells accumulate in human fibrosis by a telomere-independent mechanism and ameliorate fibrosis through matrix metalloproteinases', *J Pathol*, 223(5), pp. 604-17.
Popanda, O. and Thielmann, H.W. (1992) 'The function of DNA topoisomerases in UV-induced DNA excision repair: studies with specific inhibitors in permeabilized human fibroblasts', *Carcinogenesis*, 13(12), pp. 2321-8.
Probin, V., Wang, Y., Bai, A. and Zhou, D. (2006) 'Busulfan selectively induces cellular senescence but not apoptosis in WI38 fibroblasts via a p53-independent but extracellular signal-regulated kinase-p38 mitogen-activated protein kinase-dependent mechanism', *J Pharmacol Exp Ther*, 319(2), pp. 551-60.
Purvis, J.E., Karhohs, K.W., Mock, C., Batchelor, E., Loewer, A. and Lahav, G. (2012) 'p53 dynamics control cell fate', *Science*, 336(6087), pp. 1440-4.
Ramsey, M.R. and Sharpless, N.E. (2006) 'ROS as a tumour suppressor?', *Nat Cell Biol*, 8(11), pp. 1213-5.
Rasola, A. and Bernardi, P. (2011) 'Mitochondrial permeability transition in Ca(2+)-dependent apoptosis and necrosis', *Cell Calcium*, 50(3), pp. 222-33.
Rayess, H., Wang, M.B. and Srivatsan, E.S. (2012) 'Cellular senescence and tumor suppressor gene p16', *Int J Cancer*, 130(8), pp. 1715-25.
Reed, J.C. (2006) 'Proapoptotic multidomain Bcl-2/Bax-family proteins: mechanisms, physiological roles, and therapeutic opportunities', *Cell Death Differ*, 13(8), pp. 1378-86.
Ricci, J.E., Munoz-Pinedo, C., Fitzgerald, P., Bailly-Maitre, B., Perkins, G.A., Yadava, N., Scheffler, I.E., Ellisman, M.H. and Green, D.R. (2004) 'Disruption of mitochondrial function during apoptosis is mediated by caspase cleavage of the p75 subunit of complex I of the electron transport chain', *Cell*, 117(6), pp. 773-86.
Riley, J.S., Quarato, G., Cloix, C., Lopez, J., O'Prey, J., Pearson, M., Chapman, J., Sesaki, H., Carlin, L.M., Passos, J.F., Wheeler, A.P., Oberst, A., Ryan, K.M. and Tait, S.W. (2018) 'Mitochondrial inner membrane permeabilisation enables mtDNA release during apoptosis', *The EMBO journal*, 37(17), p. e99238.
Ritschka, B., Storer, M., Mas, A., Heinzmann, F., Ortells, M.C., Morton, J.P., Sansom, O.J., Zender, L. and Keyes, W.M. (2017) 'The senescence-associated secretory phenotype induces cellular plasticity and tissue regeneration', *Genes Dev*, 31(2), pp. 172-183.
Robles, S.J. and Adami, G.R. (1998) 'Agents that cause DNA double strand breaks lead to p16INK4a enrichment and the premature senescence of normal fibroblasts', *Oncogene*, 16(9), pp. 1113-23.
Rodier, F., Coppe, J.P., Patil, C.K., Hoeijmakers, W.A., Munoz, D.P., Raza, S.R., Freund, A., Campeau, E., Davalos, A.R. and Campisi, J. (2009) 'Persistent DNA damage signalling triggers senescence-associated inflammatory cytokine secretion', *Nat Cell Biol*, 11(8), pp. 973-9.
Rodriguez-Vilarrupla, A., Diaz, C., Canela, N., Rahn, H.P., Bachs, O. and Agell, N. (2002) 'Identification of the nuclear localization signal of p21(cip1) and consequences of its mutation on cell proliferation', *FEBS Lett*, 531(2), pp. 319-23.

Rogakou, E.P., Boon, C., Redon, C. and Bonner, W.M. (1999) 'Megabase chromatin domains involved in DNA double-strand breaks in vivo', *J Cell Biol*, 146(5), pp. 905-16.
Rongvaux, A., Jackson, R., Harman, C.C., Li, T., West, A.P., de Zoete, M.R., Wu, Y., Yordy, B., Lakhani, S.A., Kuan, C.Y., Taniguchi, T., Shadel, G.S., Chen, Z.J., Iwasaki, A. and Flavell, R.A. (2014) 'Apoptotic caspases prevent the induction of type I interferons by mitochondrial DNA', *Cell*, 159(7), pp. 1563-77.
Roos, C.M., Zhang, B., Palmer, A.K., Ogrodnik, M.B., Pirtskhalava, T., Thalji, N.M., Hagler, M., Jurk, D., Smith, L.A., Casaclang-Verzosa, G., Zhu, Y., Schafer, M.J., Tchkonia, T., Kirkland, J.L. and Miller, J.D. (2016a) 'Chronic senolytic treatment alleviates established vasomotor dysfunction in aged or atherosclerotic mice', *Aging Cell*.
Roos, C.M., Zhang, B., Palmer, A.K., Ogrodnik, M.B., Pirtskhalava, T., Thalji, N.M., Hagler, M., Jurk, D., Smith, L.A., Casaclang-Verzosa, G., Zhu, Y., Schafer, M.J., Tchkonia, T., Kirkland, J.L. and Miller, J.D. (2016b) 'Chronic senolytic treatment alleviates established vasomotor dysfunction in aged or atherosclerotic mice', *Aging Cell*, 15(5), pp. 973-7.
Roper, J.M., Mazzatti, D.J., Watkins, R.H., Maniscalco, W.M., Keng, P.C. and O'Reilly, M.A. (2004) 'In vivo exposure to hyperoxia induces DNA damage in a population of alveolar type II epithelial cells', *Am J Physiol Lung Cell Mol Physiol*, 286(5), pp. L1045-54.
Rossi, A., Kontarakis, Z., Gerri, C., Nolte, H., Holper, S., Kruger, M. and Stainier, D.Y. (2015) 'Genetic compensation induced by deleterious mutations but not gene knockdowns', *Nature*, 524(7564), pp. 230-3.
Ryu, C., Sun, H., Gulati, M., Herazo-Maya, J.D., Chen, Y., Osafo-Addo, A., Brandsdorfer, C., Winkler, J., Blaul, C., Faunce, J., Pan, H., Woolard, T., Tzouvelekis, A., Antin-Ozerkis, D.E., Puchalski, J.T., Slade, M., Gonzalez, A.L., Bogenhagen, D.F., Kirillov, V., Feghali-Bostwick, C., Gibson, K., Lindell, K., Herzog, R.I., Dela Cruz, C.S., Mehal, W., Kaminski, N., Herzog, E.L. and Trujillo, G. (2017) 'Extracellular Mitochondrial DNA Is Generated by Fibroblasts and Predicts Death in Idiopathic Pulmonary Fibrosis', *Am J Respir Crit Care Med*, 196(12), pp. 1571-1581.
Sadaie, M., Salama, R., Carroll, T., Tomimatsu, K., Chandra, T., Young, A.R., Narita, M., Perez-Mancera, P.A., Bennett, D.C., Chong, H., Kimura, H. and Narita, M. (2013) 'Redistribution of the Lamin B1 genomic binding profile affects rearrangement of heterochromatic domains and SAHF formation during senescence', *Genes Dev*, 27(16), pp. 1800-8.
Sage, J., Mulligan, G.J., Attardi, L.D., Miller, A., Chen, S., Williams, B., Theodorou, E. and Jacks, T. (2000) 'Targeted disruption of the three Rb-related genes leads to loss of G(1) control and immortalization', *Genes Dev*, 14(23), pp. 3037-50.
Sakahira, H., Enari, M. and Nagata, S. (1998) 'Cleavage of CAD inhibitor in CAD activation and DNA degradation during apoptosis', *Nature*, 391(6662), pp. 96-9.
Sanders, Y.Y., Liu, H., Zhang, X., Hecker, L., Bernard, K., Desai, L., Liu, G. and Thannickal, V.J. (2013) 'Histone modifications in senescence-associated resistance to apoptosis by oxidative stress', *Redox Biol*, 1, pp. 8-16.
Saretzki, G., Murphy, M.P. and von Zglinicki, T. (2003) 'MitoQ counteracts telomere shortening and elongates lifespan of fibroblasts under mild oxidative stress', *Aging Cell*, 2(2), pp. 141-3.
Sawada, M., Hayes, P. and Matsuyama, S. (2003) 'Cytoprotective membrane-permeable peptides designed from the Bax-binding domain of Ku70', *Nat Cell Biol*, 5(4), pp. 352-7.
Schafer, M.J., White, T.A., Iijima, K., Haak, A.J., Ligresti, G., Atkinson, E.J., Oberg, A.L., Birch, J., Salmonowicz, H., Zhu, Y., Mazula, D.L., Brooks, R.W., Fuhrmann-Stroissnigg, H., Pirtskhalava, T., Prakash, Y.S., Tchkonia, T., Robbins, P.D., Aubry, M.C., Passos, J.F., Kirkland, J.L., Tschumperlin, D.J., Kita, H. and LeBrasseur, N.K. (2017) 'Cellular senescence mediates fibrotic pulmonary disease', *Nat Commun*, 8, p. 14532.

Schellenberg, B., Wang, P., Keeble, J.A., Rodriguez-Enriquez, R., Walker, S., Owens, T.W., Foster, F., Tanianis-Hughes, J., Brennan, K., Streuli, C.H. and Gilmore, A.P. (2013) 'Bax exists in a dynamic equilibrium between the cytosol and mitochondria to control apoptotic priming', *Mol Cell*, 49(5), pp. 959-71.
Sciaky, D., Brazer, W., Center, D.M., Cruikshank, W.W. and Smith, T.J. (2000) 'Cultured human fibroblasts express constitutive IL-16 mRNA: cytokine induction of active IL-16 protein synthesis through a caspase-3-dependent mechanism', *J Immunol*, 164(7), pp. 3806-14.
Senturk, S., Mumcuoglu, M., Gursoy-Yuzugullu, O., Cingoz, B., Akcali, K.C. and Ozturk, M. (2010) 'Transforming growth factor-beta induces senescence in hepatocellular carcinoma cells and inhibits tumor growth', *Hepatology*, 52(3), pp. 966-74.
Serra, V., von Zglinicki, T., Lorenz, M. and Saretzki, G. (2003) 'Extracellular superoxide dismutase is a major antioxidant in human fibroblasts and slows telomere shortening', *J Biol Chem*, 278(9), pp. 6824-30.
Serrano, M., Lin, A.W., McCurrach, M.E., Beach, D. and Lowe, S.W. (1997) 'Oncogenic ras provokes premature cell senescence associated with accumulation of p53 and p16INK4a', *Cell*, 88(5), pp. 593-602.
Seshadri, T. and Campisi, J. (1990) 'Repression of c-fos transcription and an altered genetic program in senescent human fibroblasts', *Science*, 247(4939), pp. 205-9.
Severino, J., Allen, R.G., Balin, S., Balin, A. and Cristofalo, V.J. (2000) 'Is beta-galactosidase staining a marker of senescence in vitro and in vivo?', *Exp Cell Res*, 257(1), pp. 162-71.
Shalini, S., Dorstyn, L., Dawar, S. and Kumar, S. (2015) 'Old, new and emerging functions of caspases', *Cell death and differentiation*, 22(4), pp. 526-539.
Shelton, D.N., Chang, E., Whittier, P.S., Choi, D. and Funk, W.D. (1999) 'Microarray analysis of replicative senescence', *Curr Biol*, 9(17), pp. 939-45.
Shimada, K., Crother, T.R., Karlin, J., Dagvadorj, J., Chiba, N., Chen, S., Ramanujan, V.K., Wolf, A.J., Vergnes, L., Ojcius, D.M., Rentsendorj, A., Vargas, M., Guerrero, C., Wang, Y., Fitzgerald, K.A., Underhill, D.M., Town, T. and Arditi, M. (2012) 'Oxidized mitochondrial DNA activates the NLRP3 inflammasome during apoptosis', *Immunity*, 36(3), pp. 401-14.
Silzer, T., Barber, R., Sun, J., Pathak, G., Johnson, L., O'Bryant, S. and Phillips, N. (2019) 'Circulating mitochondrial DNA: New indices of type 2 diabetes-related cognitive impairment in Mexican Americans', *PLoS One*, 14(3), p. e0213527.
Sodhi, K., Nichols, A., Mallick, A., Klug, R.L., Liu, J., Wang, X., Srikanthan, K., Goguet-Rubio, P., Nawab, A., Pratt, R., Lilly, M.N., Sanabria, J.R., Xie, Z., Abraham, N.G. and Shapiro, J.I. (2018) 'The Na/K-ATPase Oxidant Amplification Loop Regulates Aging', *Scientific reports*, 8(1), pp. 9721-9721.
Song, J.H., Kandasamy, K., Zemskova, M., Lin, Y.-W. and Kraft, A.S. (2011) 'The BH3 mimetic ABT-737 induces cancer cell senescence', *Cancer research*, 71(2), pp. 506-515.
Spallarossa, P., Altieri, P., Barisione, C., Passalacqua, M., Aloi, C., Fugazza, G., Frassoni, F., Podesta, M., Canepa, M., Ghigliotti, G. and Brunelli, C. (2010) 'p38 MAPK and JNK antagonistically control senescence and cytoplasmic p16INK4A expression in doxorubicin-treated endothelial progenitor cells', *PLoS One*, 5(12), p. e15583.
Stein, G.H., Drullinger, L.F., Robetorye, R.S., Pereira-Smith, O.M. and Smith, J.R. (1991) 'Senescent cells fail to express cdc2, cycA, and cycB in response to mitogen stimulation', *Proc Natl Acad Sci U S A*, 88(24), pp. 11012-6.
Stein, G.H., Drullinger, L.F., Soulard, A. and Dulic, V. (1999) 'Differential roles for cyclin-dependent kinase inhibitors p21 and p16 in the mechanisms of senescence and differentiation in human fibroblasts', *Mol Cell Biol*, 19(3), pp. 2109-17.
Stockl, P., Hutter, E., Zwerschke, W. and Jansen-Durr, P. (2006) 'Sustained inhibition of oxidative phosphorylation impairs cell proliferation and induces premature senescence in human fibroblasts', *Exp Gerontol*, 41(7), pp. 674-82.

Stockl, P., Zankl, C., Hutter, E., Unterluggauer, H., Laun, P., Heeren, G., Bogengruber, E., Herndler-Brandstetter, D., Breitenbach, M. and Jansen-Durr, P. (2007) 'Partial uncoupling of oxidative phosphorylation induces premature senescence in human fibroblasts and yeast mother cells', *Free Radic Biol Med*, 43(6), pp. 947-58.
Suzuki, K., Yanagihara, T., Yokoyama, T., Maeyama, T., Ogata-Suetsugu, S., Arimura-Omori, M., Mikumo, H., Hamada, N., Harada, E., Kuwano, K., Harada, T. and Nakanishi, Y. (2017) 'Bax-inhibiting peptide attenuates bleomycin-induced lung injury in mice', *Biol Open*, 6(12), pp. 1869-1875.
Tait, S.W. and Green, D.R. (2010) 'Mitochondria and cell death: outer membrane permeabilization and beyond', *Nat Rev Mol Cell Biol*, 11(9), pp. 621-32.
Tait, S.W., Oberst, A., Quarato, G., Milasta, S., Haller, M., Wang, R., Karvela, M., Ichim, G., Yatim, N., Albert, M.L., Kidd, G., Wakefield, R., Frase, S., Krautwald, S., Linkermann, A. and Green, D.R. (2013) 'Widespread mitochondrial depletion via mitophagy does not compromise necroptosis', *Cell Rep*, 5(4), pp. 878-85.
Takahashi, A., Loo, T.M., Okada, R., Kamachi, F., Watanabe, Y., Wakita, M., Watanabe, S., Kawamoto, S., Miyata, K., Barber, G.N., Ohtani, N. and Hara, E. (2018) 'Downregulation of cytoplasmic DNases is implicated in cytoplasmic DNA accumulation and SASP in senescent cells', *Nat Commun*, 9(1), p. 1249.
Tanaka, Y. and Chen, Z.J. (2012) 'STING specifies IRF3 phosphorylation by TBK1 in the cytosolic DNA signaling pathway', *Sci Signal*, 5(214), p. ra20.
Tarrago, M.G., Chini, C.C.S., Kanamori, K.S., Warner, G.M., Caride, A., de Oliveira, G.C., Rud, M., Samani, A., Hein, K.Z., Huang, R., Jurk, D., Cho, D.S., Boslett, J.J., Miller, J.D., Zweier, J.L., Passos, J.F., Doles, J.D., Becherer, D.J. and Chini, E.N. (2018) 'A Potent and Specific CD38 Inhibitor Ameliorates Age-Related Metabolic Dysfunction by Reversing Tissue NAD(+) Decline', *Cell Metab*, 27(5), pp. 1081-1095.e10.
Taylor, R.C., Cullen, S.P. and Martin, S.J. (2008) 'Apoptosis: controlled demolition at the cellular level', *Nat Rev Mol Cell Biol*, 9(3), pp. 231-41.
Tibbetts, R.S., Brumbaugh, K.M., Williams, J.M., Sarkaria, J.N., Cliby, W.A., Shieh, S.Y., Taya, Y., Prives, C. and Abraham, R.T. (1999) 'A role for ATR in the DNA damage-induced phosphorylation of p53', *Genes Dev*, 13(2), pp. 152-7.
Tilstra, J.S., Robinson, A.R., Wang, J., Gregg, S.Q., Clauson, C.L., Reay, D.P., Nasto, L.A., St Croix, C.M., Usas, A., Vo, N., Huard, J., Clemens, P.R., Stolz, D.B., Guttridge, D.C., Watkins, S.C., Garinis, G.A., Wang, Y., Niedernhofer, L.J. and Robbins, P.D. (2012) 'NF-κB inhibition delays DNA damage-induced senescence and aging in mice', *The Journal of clinical investigation*, 122(7), pp. 2601-2612.
Trojer, P. and Reinberg, D. (2007) 'Facultative heterochromatin: is there a distinctive molecular signature?', *Mol Cell*, 28(1), pp. 1-13.
Tse, C., Shoemaker, A.R., Adickes, J., Anderson, M.G., Chen, J., Jin, S., Johnson, E.F., Marsh, K.C., Mitten, M.J., Nimmer, P., Roberts, L., Tahir, S.K., Xiao, Y., Yang, X., Zhang, H., Fesik, S., Rosenberg, S.H. and Elmore, S.W. (2008) 'ABT-263: a potent and orally bioavailable Bcl-2 family inhibitor', *Cancer Res*, 68(9), pp. 3421-8.
Turnbull, S., Tabner, B.J., Brown, D.R. and Allsop, D. (2003) 'Quinacrine acts as an antioxidant and reduces the toxicity of the prion peptide PrP106-126', *Neuroreport*, 14(13), pp. 1743-5.
Uematsu, S. and Akira, S. (2007) 'Toll-like receptors and Type I interferons', *J Biol Chem*, 282(21), pp. 15319-23.
van de Ven, R.A.H., Santos, D. and Haigis, M.C. (2017) 'Mitochondrial Sirtuins and Molecular Mechanisms of Aging', *Trends Mol Med*, 23(4), pp. 320-331.
van der Veer, E., Ho, C., O'Neil, C., Barbosa, N., Scott, R., Cregan, S.P. and Pickering, J.G. (2007) 'Extension of human cell lifespan by nicotinamide phosphoribosyltransferase', *J Biol Chem*, 282(15), pp. 10841-5.

Vincent, J., Adura, C., Gao, P., Luz, A., Lama, L., Asano, Y., Okamoto, R., Imaeda, T., Aida, J., Rothamel, K., Gogakos, T., Steinberg, J., Reasoner, S., Aso, K., Tuschl, T., Patel, D.J., Glickman, J.F. and Ascano, M. (2017) 'Small molecule inhibition of cGAS reduces interferon expression in primary macrophages from autoimmune mice', *Nat Commun*, 8(1), p. 750.
von Zglinicki, T. (2002) 'Oxidative stress shortens telomeres', *Trends Biochem Sci*, 27(7), pp. 339-44.
von Zglinicki, T., Saretzki, G., Docke, W. and Lotze, C. (1995) 'Mild hyperoxia shortens telomeres and inhibits proliferation of fibroblasts: a model for senescence?', *Exp Cell Res*, 220(1), pp. 186-93.
Waaijer, M.E., Parish, W.E., Strongitharm, B.H., van Heemst, D., Slagboom, P.E., de Craen, A.J., Sedivy, J.M., Westendorp, R.G., Gunn, D.A. and Maier, A.B. (2012) 'The number of p16INK4a positive cells in human skin reflects biological age', *Aging Cell*, 11(4), pp. 722-5.
Waga, S., Hannon, G.J., Beach, D. and Stillman, B. (1994) 'The p21 inhibitor of cyclin-dependent kinases controls DNA replication by interaction with PCNA', *Nature*, 369(6481), pp. 574-8.
Walaszczyk, A., Dookun, E., Redgrave, R., Tual-Chalot, S., Victorelli, S., Spyridopoulos, I., Owens, A., Arthur, H.M., Passos, J.F. and Richardson, G.D. (2019) 'Pharmacological clearance of senescent cells improves survival and recovery in aged mice following acute myocardial infarction', *Aging Cell*, p. e12945.
Wan, M., Hua, X., Su, J., Thiagarajan, D., Frostegard, A.G., Haeggstrom, J.Z. and Frostegard, J. (2014) 'Oxidized but not native cardiolipin has pro-inflammatory effects, which are inhibited by Annexin A5', *Atherosclerosis*, 235(2), pp. 592-8.
Wang, C., Jurk, D., Maddick, M., Nelson, G., Martin-Ruiz, C. and von Zglinicki, T. (2009) 'DNA damage response and cellular senescence in tissues of aging mice', *Aging Cell*, 8(3), pp. 311-23.
Wang, E. (1995) 'Senescent human fibroblasts resist programmed cell death, and failure to suppress bcl2 is involved', *Cancer Res*, 55(11), pp. 2284-92.
Wang, W., Yang, X., Lopez de Silanes, I., Carling, D. and Gorospe, M. (2003) 'Increased AMP:ATP ratio and AMP-activated protein kinase activity during cellular senescence linked to reduced HuR function', *J Biol Chem*, 278(29), pp. 27016-23.
Wang, Z., Deng, Z., Dahmane, N., Tsai, K., Wang, P., Williams, D.R., Kossenkov, A.V., Showe, L.C., Zhang, R., Huang, Q., Conejo-Garcia, J.R. and Lieberman, P.M. (2015) 'Telomeric repeat-containing RNA (TERRA) constitutes a nucleoprotein component of extracellular inflammatory exosomes', *Proc Natl Acad Sci U S A*, 112(46), pp. E6293-300.
Watson, J.D. (1972) 'Origin of concatemeric T7 DNA', *Nat New Biol*, 239(94), pp. 197-201.
Waugh, D.J. and Wilson, C. (2008) 'The interleukin-8 pathway in cancer', *Clin Cancer Res*, 14(21), pp. 6735-41.
Wei, W., Herbig, U., Wei, S., Dutriaux, A. and Sedivy, J.M. (2003a) 'Loss of retinoblastoma but not p16 function allows bypass of replicative senescence in human fibroblasts', *EMBO Rep*, 4(11), pp. 1061-6.
Wei, W., Jobling, W.A., Chen, W., Hahn, W.C. and Sedivy, J.M. (2003b) 'Abolition of cyclin-dependent kinase inhibitor p16Ink4a and p21Cip1/Waf1 functions permits Ras-induced anchorage-independent growth in telomerase-immortalized human fibroblasts', *Mol Cell Biol*, 23(8), pp. 2859-70.
Wei, W. and Sedivy, J.M. (1999) 'Differentiation between senescence (M1) and crisis (M2) in human fibroblast cultures', *Exp Cell Res*, 253(2), pp. 519-22.
Weiss, R.S., Matsuoka, S., Elledge, S.J. and Leder, P. (2002) 'Hus1 acts upstream of chk1 in a mammalian DNA damage response pathway', *Curr Biol*, 12(1), pp. 73-7.
West, A.P., Khoury-Hanold, W., Staron, M., Tal, M.C., Pineda, C.M., Lang, S.M., Bestwick, M., Duguay, B.A., Raimundo, N., MacDuff, D.A., Kaech, S.M., Smiley, J.R., Means, R.E.,

Iwasaki, A. and Shadel, G.S. (2015) 'Mitochondrial DNA stress primes the antiviral innate immune response', *Nature*, 520(7548), pp. 553-7.
Westphal, D., Dewson, G., Czabotar, P.E. and Kluck, R.M. (2011) 'Molecular biology of Bax and Bak activation and action', *Biochim Biophys Acta*, 1813(4), pp. 521-31.
White, M.J., McArthur, K., Metcalf, D., Lane, R.M., Cambier, J.C., Herold, M.J., van Delft, M.F., Bedoui, S., Lessene, G., Ritchie, M.E., Huang, D.C. and Kile, B.T. (2014) 'Apoptotic caspases suppress mtDNA-induced STING-mediated type I IFN production', *Cell*, 159(7), pp. 1549-62.
Wiel, C., Lallet-Daher, H., Gitenay, D., Gras, B., Le Calve, B., Augert, A., Ferrand, M., Prevarskaya, N., Simonnet, H., Vindrieux, D. and Bernard, D. (2014) 'Endoplasmic reticulum calcium release through ITPR2 channels leads to mitochondrial calcium accumulation and senescence', *Nat Commun*, 5, p. 3792.
Wiggins, K.A., Parry, A.J., Cassidy, L.D., Humphry, M., Webster, S.J., Goodall, J.C., Narita, M. and Clarke, M.C.H. (2019) 'IL-1alpha cleavage by inflammatory caspases of the noncanonical inflammasome controls the senescence-associated secretory phenotype', *Aging Cell*, 18(3), p. e12946.
Wiley, C.D., Velarde, M.C., Lecot, P., Liu, S., Sarnoski, E.A., Freund, A., Shirakawa, K., Lim, H.W., Davis, S.S., Ramanathan, A., Gerencser, A.A., Verdin, E. and Campisi, J. (2016) 'Mitochondrial Dysfunction Induces Senescence with a Distinct Secretory Phenotype', *Cell Metab*, 23(2), pp. 303-14.
Wilkins, H.M., Weidling, I.W., Ji, Y. and Swerdlow, R.H. (2017) 'Mitochondria-Derived Damage-Associated Molecular Patterns in Neurodegeneration', *Frontiers in immunology*, 8, pp. 508-508.
Williams, G.C. (1957) 'Pleiotropy, Natural Selection, and the Evolution of Senescence', *Evolution*, 11(4), pp. 398-411.
Woo, M., Hakem, R., Furlonger, C., Hakem, A., Duncan, G.S., Sasaki, T., Bouchard, D., Lu, L., Wu, G.E., Paige, C.J. and Mak, T.W. (2003) 'Caspase-3 regulates cell cycle in B cells: a consequence of substrate specificity', *Nat Immunol*, 4(10), pp. 1016-22.
Wu, B., Ni, H., Li, J., Zhuang, X., Zhang, J., Qi, Z., Chen, Q., Wen, Z., Shi, H., Luo, X. and Jin, B. (2017) 'The Impact of Circulating Mitochondrial DNA on Cardiomyocyte Apoptosis and Myocardial Injury After TLR4 Activation in Experimental Autoimmune Myocarditis', *Cell Physiol Biochem*, 42(2), pp. 713-728.
Wu, J., Niu, J., Li, X., Wang, X., Guo, Z. and Zhang, F. (2014) 'TGF-β1 induces senescence of bone marrow mesenchymal stem cells via increase of mitochondrial ROS production', *BMC developmental biology*, 14, pp. 21-21.
Wu, M., Neilson, A., Swift, A.L., Moran, R., Tamagnine, J., Parslow, D., Armistead, S., Lemire, K., Orrell, J., Teich, J., Chomicz, S. and Ferrick, D.A. (2007) 'Multiparameter metabolic analysis reveals a close link between attenuated mitochondrial bioenergetic function and enhanced glycolysis dependency in human tumor cells', *Am J Physiol Cell Physiol*, 292(1), pp. C125-36.
Xiong, Y., Hannon, G.J., Zhang, H., Casso, D., Kobayashi, R. and Beach, D. (1993) 'p21 is a universal inhibitor of cyclin kinases', *Nature*, 366(6456), pp. 701-4.
Xu, M., Palmer, A.K., Ding, H., Weivoda, M.M., Pirtskhalava, T., White, T.A., Sepe, A., Johnson, K.O., Stout, M.B., Giorgadze, N., Jensen, M.D., LeBrasseur, N.K., Tchkonia, T. and Kirkland, J.L. (2015a) 'Targeting senescent cells enhances adipogenesis and metabolic function in old age', *Elife*, 4, p. e12997.
Xu, M., Pirtskhalava, T., Farr, J.N., Weigand, B.M., Palmer, A.K., Weivoda, M.M., Inman, C.L., Ogrodnik, M.B., Hachfeld, C.M., Fraser, D.G., Onken, J.L., Johnson, K.O., Verzosa, G.C., Langhi, L.G.P., Weigl, M., Giorgadze, N., LeBrasseur, N.K., Miller, J.D., Jurk, D., Singh, R.J., Allison, D.B., Ejima, K., Hubbard, G.B., Ikeno, Y., Cubro, H., Garovic, V.D., Hou, X.,

Weroha, S.J., Robbins, P.D., Niedernhofer, L.J., Khosla, S., Tchkonia, T. and Kirkland, J.L. (2018) 'Senolytics improve physical function and increase lifespan in old age', *Nat Med*, 24(8), pp. 1246-1256.
Xu, M., Tchkonia, T., Ding, H., Ogrodnik, M., Lubbers, E.R., Pirtskhalava, T., White, T.A., Johnson, K.O., Stout, M.B., Mezera, V., Giorgadze, N., Jensen, M.D., LeBrasseur, N.K. and Kirkland, J.L. (2015b) 'JAK inhibition alleviates the cellular senescence-associated secretory phenotype and frailty in old age', *Proceedings of the National Academy of Sciences of the United States of America*, 112(46), pp. E6301-E6310.
Yanai, H., Shteinberg, A., Porat, Z., Budovsky, A., Braiman, A., Ziesche, R. and Fraifeld, V.E. (2015) 'Cellular senescence-like features of lung fibroblasts derived from idiopathic pulmonary fibrosis patients', *Aging (Albany NY)*, 7(9), pp. 664-72.
Yang, H., Wang, H., Ren, J., Chen, Q. and Chen, Z.J. (2017) 'cGAS is essential for cellular senescence', *Proceedings of the National Academy of Sciences*, 114(23), pp. E4612-E4620.
Ye, X., Zerlanko, B., Zhang, R., Somaiah, N., Lipinski, M., Salomoni, P. and Adams, P.D. (2007) 'Definition of pRB- and p53-dependent and -independent steps in HIRA/ASF1a-mediated formation of senescence-associated heterochromatin foci', *Mol Cell Biol*, 27(7), pp. 2452-65.
Yeo, E.J., Hwang, Y.C., Kang, C.M., Choy, H.E. and Park, S.C. (2000) 'Reduction of UV-induced cell death in the human senescent fibroblasts', *Mol Cells*, 10(4), pp. 415-22.
Yin, Y., Zhou, Z., Liu, W., Chang, Q., Sun, G. and Dai, Y. (2017) 'Vascular endothelial cells senescence is associated with NOD-like receptor family pyrin domain-containing 3 (NLRP3) inflammasome activation via reactive oxygen species (ROS)/thioredoxin-interacting protein (TXNIP) pathway', *Int J Biochem Cell Biol*, 84, pp. 22-34.
Yoon, Y.S., Byun, H.O., Cho, H., Kim, B.K. and Yoon, G. (2003) 'Complex II defect via down-regulation of iron-sulfur subunit induces mitochondrial dysfunction and cell cycle delay in iron chelation-induced senescence-associated growth arrest', *J Biol Chem*, 278(51), pp. 51577-86.
Yoon, Y.S., Yoon, D.S., Lim, I.K., Yoon, S.H., Chung, H.Y., Rojo, M., Malka, F., Jou, M.J., Martinou, J.C. and Yoon, G. (2006) 'Formation of elongated giant mitochondria in DFO-induced cellular senescence: involvement of enhanced fusion process through modulation of Fis1', *J Cell Physiol*, 209(2), pp. 468-80.
Yosef, R., Pilpel, N., Papismadov, N., Gal, H., Ovadya, Y., Vadai, E., Miller, S., Porat, Z., Ben-Dor, S. and Krizhanovsky, V. (2017) 'p21 maintains senescent cell viability under persistent DNA damage response by restraining JNK and caspase signaling', *Embo j*, 36(15), pp. 2280-2295.
Yosef, R., Pilpel, N., Tokarsky-Amiel, R., Biran, A., Ovadya, Y., Cohen, S., Vadai, E., Dassa, L., Shahar, E., Condiotti, R., Ben-Porath, I. and Krizhanovsky, V. (2016a) 'Directed elimination of senescent cells by inhibition of BCL-W and BCL-XL', *Nature Communications*, 7, p. 11190.
Yosef, R., Pilpel, N., Tokarsky-Amiel, R., Biran, A., Ovadya, Y., Cohen, S., Vadai, E., Dassa, L., Shahar, E., Condiotti, R., Ben-Porath, I. and Krizhanovsky, V. (2016b) 'Directed elimination of senescent cells by inhibition of BCL-W and BCL-XL', *Nat Commun*, 7, p. 11190.
Yoshimoto, S., Loo, T.M., Atarashi, K., Kanda, H., Sato, S., Oyadomari, S., Iwakura, Y., Oshima, K., Morita, H., Hattori, M., Honda, K., Ishikawa, Y., Hara, E. and Ohtani, N. (2013) 'Obesity-induced gut microbial metabolite promotes liver cancer through senescence secretome', *Nature*, 499(7456), pp. 97-101.
Youm, Y.-H., Grant, R.W., McCabe, L.R., Albarado, D.C., Nguyen, K.Y., Ravussin, A., Pistell, P., Newman, S., Carter, R., Laque, A., Münzberg, H., Rosen, C.J., Ingram, D.K., Salbaum, J.M. and Dixit, V.D. (2013) 'Canonical Nlrp3 inflammasome links systemic low-grade inflammation to functional decline in aging', *Cell metabolism*, 18(4), pp. 519-532.

Young, A.R.J., Narita, M., Ferreira, M., Kirschner, K., Sadaie, M., Darot, J.F.J., Tavaré, S., Arakawa, S., Shimizu, S., Watt, F.M. and Narita, M. (2009) 'Autophagy mediates the mitotic senescence transition', *Genes & development*, 23(7), pp. 798-803.
Zaffagnini, G. and Martens, S. (2016) 'Mechanisms of Selective Autophagy', *Journal of molecular biology*, 428(9 Pt A), pp. 1714-1724.
Zhang, J., Patel, J.M. and Block, E.R. (2002) 'Enhanced apoptosis in prolonged cultures of senescent porcine pulmonary artery endothelial cells', *Mech Ageing Dev*, 123(6), pp. 613-25.
Zhang, P., Kishimoto, Y., Grammatikakis, I., Gottimukkala, K., Cutler, R.G., Zhang, S., Abdelmohsen, K., Bohr, V.A., Misra Sen, J., Gorospe, M. and Mattson, M.P. (2019) 'Senolytic therapy alleviates Abeta-associated oligodendrocyte progenitor cell senescence and cognitive deficits in an Alzheimer's disease model', *Nat Neurosci*, 22(5), pp. 719-728.
Zhang, R., Poustovoitov, M.V., Ye, X., Santos, H.A., Chen, W., Daganzo, S.M., Erzberger, J.P., Serebriiskii, I.G., Canutescu, A.A., Dunbrack, R.L., Pehrson, J.R., Berger, J.M., Kaufman, P.D. and Adams, P.D. (2005) 'Formation of MacroH2A-containing senescence-associated heterochromatin foci and senescence driven by ASF1a and HIRA', *Dev Cell*, 8(1), pp. 19-30.
Zhang, Y.-W., Shi, J., Li, Y.-J. and Wei, L. (2009) 'Cardiomyocyte death in doxorubicin-induced cardiotoxicity', *Archivum immunologiae et therapiae experimentalis*, 57(6), pp. 435-445.
Zhang, Y., Center, D.M., Wu, D.M., Cruikshank, W.W., Yuan, J., Andrews, D.W. and Kornfeld, H. (1998) 'Processing and activation of pro-interleukin-16 by caspase-3', *J Biol Chem*, 273(2), pp. 1144-9.
Zhu, F., Li, Y., Zhang, J., Piao, C., Liu, T., Li, H.H. and Du, J. (2013) 'Senescent cardiac fibroblast is critical for cardiac fibrosis after myocardial infarction', *PLoS One*, 8(9), p. e74535.
Zhu, H., Ren, S., Bitler, B.G., Aird, K.M., Tu, Z., Skordalakes, E., Zhu, Y., Yan, J., Sun, Y. and Zhang, R. (2015a) 'SPOP E3 Ubiquitin Ligase Adaptor Promotes Cellular Senescence by Degrading the SENP7 deSUMOylase', *Cell Rep*, 13(6), pp. 1183-1193.
Zhu, J., Woods, D., McMahon, M. and Bishop, J.M. (1998) 'Senescence of human fibroblasts induced by oncogenic Raf', *Genes & development*, 12(19), pp. 2997-3007.
Zhu, Y., Doornebal, E.J., Pirtskhalava, T., Giorgadze, N., Wentworth, M., Fuhrmann-Stroissnigg, H., Niedernhofer, L.J., Robbins, P.D., Tchkonia, T. and Kirkland, J.L. (2017) 'New agents that target senescent cells: the flavone, fisetin, and the BCL-XL inhibitors, A1331852 and A1155463', *Aging (Albany NY)*, 9(3), pp. 955-963.
Zhu, Y., Tchkonia, T., Fuhrmann-Stroissnigg, H., Dai, H.M., Ling, Y.Y., Stout, M.B., Pirtskhalava, T., Giorgadze, N., Johnson, K.O., Giles, C.B., Wren, J.D., Niedernhofer, L.J., Robbins, P.D. and Kirkland, J.L. (2016) 'Identification of a novel senolytic agent, navitoclax, targeting the Bcl-2 family of anti-apoptotic factors', *Aging Cell*, 15(3), pp. 428-35.
Zhu, Y., Tchkonia, T., Pirtskhalava, T., Gower, A.C., Ding, H., Giorgadze, N., Palmer, A.K., Ikeno, Y., Hubbard, G.B., Lenburg, M., O'Hara, S.P., LaRusso, N.F., Miller, J.D., Roos, C.M., Verzosa, G.C., LeBrasseur, N.K., Wren, J.D., Farr, J.N., Khosla, S., Stout, M.B., McGowan, S.J., Fuhrmann-Stroissnigg, H., Gurkar, A.U., Zhao, J., Colangelo, D., Dorronsoro, A., Ling, Y.Y., Barghouthy, A.S., Navarro, D.C., Sano, T., Robbins, P.D., Niedernhofer, L.J. and Kirkland, J.L. (2015b) 'The Achilles' heel of senescent cells: from transcriptome to senolytic drugs', *Aging Cell*, 14(4), pp. 644-58.
Zilfou, J.T. and Lowe, S.W. (2009) 'Tumor suppressive functions of p53', *Cold Spring Harb Perspect Biol*, 1(5), p. a001883.
Zwerschke, W., Mazurek, S., Stockl, P., Hutter, E., Eigenbrodt, E. and Jansen-Durr, P. (2003) 'Metabolic analysis of senescent human fibroblasts reveals a role for AMP in cellular senescence', *Biochem J*, 376(Pt 2), pp. 403-11.